



Ranchi University Journal of SCIENCE and TECHNOLOGY

RUJOST



Ranchi University
Ranchi - 834001, Jharkhand
India



Ranchi University Journal of Science & Technology

(RUJOST : ISSN 2319-4227)

A biannual, peer reviewed, referred **Ranchi University Journal of Science & Technology** published by Ranchi University, Ranchi, Jharkhand, India, every January & July

PATRON

Prof. (Dr) Ramesh Kumar Pandey
Hon'ble Vice Chancellor, Ranchi University, Ranchi

CO-PATRON

Prof. (Dr) Kamini Kumar
Hon'ble Pro. Vice Chancellor, Ranchi University, Ranchi

MANAGING EDITOR

Dr. P.K. Verma
Dean, Students Welfare, Ranchi University, Ranchi

CHIEF EDITOR

Prof. Mahendra Prasad
Dean, Faculty of Science, Ranchi University, Ranchi

EXECUTIVE EDITORS

Prof. S. K. Sinha
Head, Univ. Dept. of Botany, Ranchi University, Ranchi
Prof. A.K. Srivastava
Dept. of Botany, R.U. Ranchi, Ex. Dean, Faculty of Science
Prof. Ashok Kumar Choudhary
Univ. Dept. of Botany, Ranchi University, Ranchi
Prof. Jyoti Kumar
Univ. Dept. of Botany, Ranchi University, Ranchi
Prof. Hanuman Prasad Sharma
Uni. Dept. of Botany, Ranchi University, Ranchi
Prof. Rajesh Kumar
Head, Univ. Dept. of Chemistry, Ranchi University, Ranchi
Prof. Sanjay Mishra
Univ. Dept. of Chemistry, Ranchi University, Ranchi
Dr. Uday Kumar
Head, Univ. Dept. of Geology, Ranchi University, Ranchi
Prof. Deepak Kumar Bhattacharya
Univ. Dept. of Geology, Ranchi University, Ranchi
Prof. B. K. Chakravarty
Dean & Prof. in MME Dept. NIFFT, Ranchi

Dr. Smita Dey
Head, Univ. Dept. of Mathematics Ranchi University, Ranchi
Prof. M. M. P. Singh
Univ. Dept. of Mathematics, Ranchi University, Ranchi
Prof. Anil Kumar Mahto
Univ. Dept. of Mathematics, Ranchi University, Ranchi
Dr. A. K. Akhoury
Head, Univ. Dept. of Physics, Ranchi University, Ranchi
Dr. Sanjay Dey
Univ. Dept. of Physics, Ranchi University, Ranchi
Dr. A. Kapoor
Univ. Dept. of Physics, Ranchi University, Ranchi
Prof. Amitabh Hore
Former Head, Univ. Dept. of Zoology, Ranchi University, Ranchi
Prof. Bishwaroop Mukherjee
Head, Univ. Dept. of Zoology, Ranchi University, Ranchi
Dr. Suhasini Besra
Univ. Dept. of Zoology, Ranchi University, Ranchi

EDITORIAL BOARD

Dr. R.K. Jha
Univ. Dept. of Botany, Ranchi University, Ranchi
Prof. Mahmood Alam
Univ. Dept. of Chemistry, Ranchi University, Ranchi
Dr. S.M. Shamim
Univ. Dept. of Zoology, Ranchi University, Ranchi
Dr. Anand Murari Tiwary
Univ. Dept. of Geology, Ranchi University, Ranchi
Dr. B.R. Jha
Univ. Dept. of Geology, Ranchi University, Ranchi
Dr. C.S.P. Lugun
Univ. Dept. of Mathematics, Ranchi University, Ranchi

Dr. R.A. Mahto
Univ. Dept. of Mathematics Ranchi University, Ranchi
Dr. Sudha Singh
Univ. Dept. of Physics, Ranchi University, Ranchi
Dr. Arun Kumar
Univ. Dept. of Physics, Ranchi University, Ranchi
Dr. Abhijeet Dutta
Univ. Dept. of Zoology, Ranchi University, Ranchi
Dr. S. Nehar
Univ. Dept. of Zoology, Ranchi University, Ranchi

EDITORIAL ADVISORY BOARD

Prof. K.K. Nag
Former V.C, Ranchi, Vinoba Bhawe & Tilika Majhi University
Prof. Kunul Kadir
Pro. V.C, Dept. of Botany, V.B.U, Hazaribagh
Prof. G.D. Mishra
Ex. H.O.D & Dean, Dept. of Chemistry
Prof. S.P. Singh
Ex. V.C, Dept. of Geology
Prof. J.N. Prasad
Ex. H.O.D, Dept. of Physics
Prof. A.A. Khan
Ex. V.C, Dept. of Physics

Prof. M.P. Singh
Ex. V.C, Dept. of Zoology
Prof. M.P. Sinha
V.C, Dept. of Zoology, S.K.M.U
Prof. R.K. Jha
Head Medicine, RIMS, Ranchi
Prof. S.N. Singh
V.C, N.P. University, Medininagar
Prof. Partha Pratim Chattopadhyay
Director NIFFT, Ranchi
Prof. Bijay Singh
Pro. V.C, N.P. University, Medininagar

RUJOST

ISSN : 2319-4227

Ranchi University Journal of
Science and Technology

A Biannual peer reviewed refereed journal of Science & Technology published by Ranchi University, Ranchi every January & July

Vol. 4

No. 2(ii)

July-2017

ISSN : 2319-4227

Cheif Editor

Prof. (Dr.) Mahendra Prasad



RANCHI UNIVERSITY
Ranchi- 834008, Jharkhand, India

RANCHI UNIVERSITY, RANCHI

Chief Editor : Prof. (Dr.) Mahendra Prasad

No part of this publication may be reproduced or transmitted in any form by means, electronics or mechanical, including photocopy, recording or any information storage and retrieval system, without permission in writing from the copyright owners.

DISCLAIMER

The authors are solely responsible for the contents of the papers compiled in this volume. The Publishers or editors do not take any responsibility for the same in any manner. Errors, if any, are purely unintentional and readers are requested to communicate such errors to the editors or publishers to avoid discrepancies in future.

Publisher



RANCHI UNIVERSITY

Ranchi- 834008, Jharkhand, India

Tel: +91- 9431389253

E-mail : pkv_rujost@yahoo.com

Website : www.ranchiuniversity.ac.in

From Editors Desk:

It is a matter of great pleasure that our prestigious University Science Journal, **RUJOST (Ranchi University Journal of Science and Technology, ISSN: 2319-4227), Vol 4, No-2(ii) July, 2018 issue** is being brought to you as a result continuous exercise of the editorial team & office of the Dean, Faculty of Science, Ranchi University, Ranchi. As a matter of fact this Journal is a biannual in nature published every January & July but due to some constraints the issue is being released a little delayed for which we sincerely regret and apologise.

The Journal mainly covers the research articles of all the six science University Departments- Botany, Chemistry, Geology, Mathematics, Physics & Zoology with the acronym **BCGMPZ** but is slated to cover the articles of allied branches of science like Engineering, Medical, Ayurveda, Yoga, Meditation along with Transcendental medicine but despite of our repeated call from these branches, no article could be received under the section of technology which is the second important flank of the publication. This is a good challenge for the coming team of publication headed by the onroll Dean of Faculty of Science of Ranchi University.

The journal is also now online to enhance the domain of its readers as well as in the process of enlistment in the UGC for which the application has already been transmitted in the month of May 2017. The motivation for such quality up gradation of the publication is entirely due to constant inspiration and guidelines from **Honorable Chancellor of Universities of Jharkhand, Smt. Draupadi Murmu**, as well as **Honorable Vice Chancellor, Prof. Ramesh Kr. Pandey & Pro Vice Chancellor, Prof. Kamini Kumar** who are themselves devoted researchers of repute and outstanding scientist of Life science, specially the plant science, having hundreds of publications to their credit and realize the need and importance of research paper and the journal.

The layout of the cover page having the hexagons symbolizes six different University Science Departments- **BCGMPZ**, which gets established as the copyright front page design of RUJOST which should be maintained in future as the first look identity of the Journal.

This journal has already made a big headway by entering into its fourth ending year (July, 2017) of continuous publication and is successful in propelling many research initiatives for the socio-economic uplift of the state of Jharkhand. It is intended to make this journal a guiding resource to all the research activities for the development of our Nation and State.

Chief Editor,

Prof. (Dr.) Mahendra Prasad,
Dean, Faculty of Science,
Professor & Former Head,
University Department of Zoology,
Ranchi University, Ranchi, Jharkhand

Managing Editor,

Dr. P. K. Verma,
Dean of Students Welfare &
Associate Professor,
University Department of Geology,
Ranchi University, Ranchi, Jharkhand

Ranchi University

Journal of Science and Technology (RUJOST)

The Ranchi University Journal of Science and Technology (RUJOST) is a medium to provide up to date information on all scientific investigations together with their applications. The journal includes full length and mini reviews, original articles and scientific reports to the Chief Editor. The Journal hopes to attract the most important and highly innovative papers from the current research from academia, research communities, most importantly from young investigators and students. RUJOST features scholarly articles in rapidly moving science and technology related research areas like Botany, Zoology, Agriculture, Ethno botany, Microbiology, Genetics, Molecular Biology, Bio-Technology, Bio-Chemistry, Geology, Physics, Mathematics, Bio-Informatics, Pharmacology, Chemistry, Physiology, and other sciences, which will be published subject to acceptability after referee and editorial assessment.

Professors/ Academicians/ Scientists/ Researchers/ Engineers/ Scholars/ Students can send their papers directly to:

Chief Editor

Prof.(Dr.) Mahendra Prasad

Professor, Department of Zoology,
Dean, Faculty of Science, Ranchi University,
Ranchi, Jharkhand, INDIA
+91-9431389253
mahendraprasadmset.resh@yahoo.com

For all other Enquiries

Managing Editor

Dr. P.K.Verma

Associate Professor, Department of Geology, R.U
Dean Students Welfare , R.U., Ranchi
Ranchi, Jharkhand, INDIA
+ 91-9431715160
pkv_rujost@yahoo.com



Contents

BOTANY

1. Cytological studies on three species of *Aloe* collected from Ranchi, Jharkhand
Unnita Mahato & Kamini Kumar 1-6
2. Effect of organic liquids and inorganic inputs on population and species diversity of rhizosphere mycoflora in wheat fields of fields of Gopalganj district of Bihar
Basant Narain Singh & Amarendra Kumar Jha 7-12
3. Comparative cytological studies of two varieties of *Lens culinaris*
Surabhi Joshi & Kamini Kumar 13-16
4. Study on some non-heterocystous cyanobacteria from Ranchi, Jharkhand, India
Chhaya Thakur & Radha Sahu 17-22
5. Studies on stomatal frequency and pollen analysis in *Zephyranthes candida* (Lindl.) Herb
Sameer Gunjan Lakra & Kamini Kumar 23-28
6. Antidiabetic efficacy of leaf extract of *Annona squamosa* L.
Manju Sinku & H. P. Sharma 29-34
7. Comparative karyological studies of two varieties of *Zea mays* L. collected from Ranchi, Jharkhand, India
Sagufta Ismat & Kamini Kumar 35-38
8. A report on karyomorphological and stomatal studies of three varieties of *Triticum vulgare* (Vill.)
Sneha Singh & Kamini Kumar 39-44
9. Certain endangered and threatened ethnobotanically important plants of Ranchi district, Jharkhand
Arpan Anjan, Malti Kerketta & Cynthia Khalkho 45-48
10. Apical shoot elongation of *Lawsonia inermis* L. through tissue culture in plane medium
Nazra Paiker & Kunul Kandir 49-50

CHEMISTRY

11. Electro organic synthesis of Schiff bases as chelating reagents.
Shreya Gorai & M. Alam 51-54
12. Oxidation of phenyl hydrazine by ditertiarybutyl chromate in non-aqueous media
Richa Kumari 55-58
13. Synthesis of heteropoly complexes containing Al^{3+} and Ce^{4+} and cations
Ranjeeta Sharma, Alok Kumar Thakur, G. S. Tiwari & Rajesh Kumar 59-64

GEOLOGY

14. Classification and rank determination of pundi area, west bokaro coalfield, district- Ramgarh, Jharkhand, India
Bacha Ram Jha, Chanchal Lakra & M. L. Banra 65-70

15. Clean coal technology in environmental amelioration: A case study from north karanpura coalfields, Jharkhand
Uday Kumar, R. P Singh, Debashree P. Singh & Anubha Tigga 71-76
16. Effects of rain water harvesting induced artificial recharge on the ground water in the areas of Palamu
Shweta Mishra, P. K. Verma & Uday Kumar 77-82
17. Evaluation of fluoride contamination in ground water in hard rocks terrains in and around Chukru - Chianki areas, Palamau, Jharkhand, India
Vijay Pandey, P. K. Verma & Uday Kumar 83-96
18. Comparative study of change in soil composition due to the biomass generation through Chakriya Vikas Pranali Project - A case study of Tandwa, district Palamu
Shyam Lal Singh, P. K. Verma & Shweta Mishra 97-102

MATHEMATICS

19. Evaluation of portfolio performance
Mrinalini Smita & Anita Mehta 103-106
20. New approach for dual simplex method to solve linear programming models
Rahidas Kumar & Sahdeo Mahto 107-112

PHYSICS

21. Grain-size and dielectric properties of perovskite structure lead-free potassium-sodium-niobate ($K_{0.5}Na_{0.5}NbO_3$) ceramics
Anurag Mishra & J. P Sharma 113-118
22. Diffractionless propagation of elliptic gaussian laser beams in disordered ferroelectrics
Binay Prakash Akhouri, Pradeep Kumar Gupta, Rajesh Kumar & Sumit Kaur 119-122
23. Study of high energy radiotherapy beams and analysis of its characteristics in water
Sudha Singh & Payal Raina 123-128
24. Exact dynamics for a two-level atom interacting with intensity dependent single-mode quantized cavity field in a Kerr medium
Sudha Singh & Arun Kumar 129-134
25. Optical phonon and collective charge fluctuation induced superconductivity in $Mg_{1-x}Al_xB_2$ and $Mg(B_{1-y}C_y)_2$
Roopam Sharma, Namita Singh, Dinesh Varshney & R. Khenata 135-142

ZOOLOGY

26. Effect of dietary chitosan extracted from carapace of freshwater crab *Sartoriana spinigera* on food intake of albino rats
Shiny E. C. Kachhap & Suhasini Besra 143-146
27. Biochemical composition of leg muscle of freshwater edible crab *Sartoriana spinigera* with special reference to glucose
Kumari Neetu & Suhasini Besra 147-150
28. Biochemical properties of stress secretion of freshwater snail *Bellamya bengalensis* (Jousseaume, 1886) with reference to body size
Kanchan & Suhasini Besra 151-154



Cytological studies on three species of *Aloe* collected from Ranchi, Jharkhand

Unnita Mahato* & Kamini Kumar

Department of Botany, Ranchi University, Ranchi, Jharkhand, India

*Corresponding author : Phone : 9905232802 , E-mail : unnitamahato6@gmail.com

Abstract: *Aloe*, commonly known as 'Burn Plant' or 'Medicinal Aloe', has many therapeutic values and for aesthetic value, its different species are widely cultivated throughout the world. The present findings provide cytological studies on three different species of *Aloe* of Ranchi including karyomorphological studies, mitotic index and stomatal index.

Paper History:

Received

7th May 2017

Revised

12th June 2017

Peer reviewed

20th June 2017

Accepted

1st July 2017

Keywords: *Aloe*, Karyomorphological studies, Mitotic index, Stomatal index.

INTRODUCTION

Aloe is known as 'Lily of Desert by Arabs', 'Nature's gift plant' of immortality and medicine plant.¹ In Hindi it is known as 'Ghreetkumari'. The APG IV system (2016) places the genus in the family Asphodelaceae, sub family Asphodeloideae.² *Aloe* is perennial evergreen, monocot, Crassulacean Acid Metabolism (CAM) plant, characterized with succulent leaves, inflorescence in branches and liliiform flowers.³ *Aloe* contains a mixture of glycosides collectively known as Aloin, is the active constitute of drug. As the plants contain lupeol and salicylic acid which increases blood flow in the wounded areas and stimulates fibroblast cells, responsible for healing.⁴ *Aloe* is also used for classroom material for chromosome preparations for the smaller no of chromosomes and their larger size.

MATERIALS & METHODS

Three different species of *Aloe* were collected from the local nurseries of Ranchi (Jharkhand), those are:

- Aloe barbadensis* Mill.
- Aloe plicatilis*
- Aloe abyssinica* Lam.

Potted clones of three concerned species of *Aloe* rooted readily in fine compost and sand mixture. Rooted apices of about 5mm length were excised, pretreated with PDB i.e. par dichlorobenzene for 6 hrs at 15°C, fixed in 1:3 acetoalcohol and after 24 hrs transferred to preservative- 70% ethanol. Squash preparations were made by warming the root tips in 2% aceto-carmin, 2% aceto-orcin and N-HCL with few drops of ferric chloride for 45 minutes. Photomicrographs of well separated chromosome plates of metaphase stages were taken. Fixed roots are stained with 2% aceto-carmin, cutoff in a drop of 45% acetic acid macerated and squashed for pollen mitosis study. The mitotic index (M.I.) of concerned three species of *Aloe* is calculated using the following formula:

$$\text{Mitotic Index (M.I.)} = \frac{\text{Total no of dividing cell}}{\text{Total no of cell observed}} \times 100$$

Stomatal studies done by usual method of peeling of epidermis from fresh leaves. Peeling of epidermis was done at apex, middle and base portion of dorsal and ventral surface of the leaves. The materials were stained with aqueous saffranin and mounted in glycerin. The formula for determining the stomatal index (S.I.):

$$S.I. = \frac{\text{Total no. of stomata}}{\text{Total no. of epidermal cells} + \text{Total no. of stomata}} \times 100$$

Where S.I = Stomatal Index.

Statistical data was obtained from mean, standard deviation, standard error.

RESULT

a) The karyomorphological data have been depicted in table.1 and fig.1 to 6 and 10 and 11. The concerned three species showed symmetry in chromosome no $2n=2x=14$.

Table-1: Karyomorphological data of three species of *Aloe*

Sl. No.	Species	Chromosome pair	Length in micron (μ)		Chromosome length	Arm ratio LA/SA	Classification
			Long arm	Short arm			
1	<i>Aloe barbadensis</i> Mill.	L ₁	9.05	2.65	11.70	3.41	nsm(+)
		L ₂	9.00	2.50	11.50	3.60	nsm(+)
		L ₃	8.00	2.50	10.5	3.20	nsm(-)
		L ₄	7.10	2.70	9.80	2.62	nsm(-)
		S ₁	2.70	1.30	4.00	2.07	nsm(-)
		S ₂	2.50	1.20	3.70	2.08	nsm(-)
		S ₃	1.30	0.55	1.85	2.36	nsm(-)
					TLC = 53.05		
2.	<i>Aloe plicatilis</i>	L ₁	10.00	2.10	12.10	4.76	nst(-)
		L ₂	10.00	2.05	12.05	4.87	nst(-)
		L ₃	7.50	1.25	8.75	6.00	nst(-)
		L ₄	6.80	2.25	9.05	3.02	nsm(+)
		S ₁	2.50	1.05	3.55	2.38	nsm(-)
		S ₂	2.50	1.20	3.70	2.08	nsm(-)
		S ₃	2.50	2.25	4.75	1.11	nm
					TLC = 53.95		
3.	<i>Aloe abyssinica</i> Lam.	L ₁	7.95	2.30	10.25	3.45	nsm(+)
		L ₂	7.05	2.30	9.35	3.06	nsm(+)
		L ₃	6.15	2.30	8.45	3.67	nsm(-)
		L ₄	5.75	2.50	8.25	2.30	nsm(-)
		S ₁	3.30	1.80	5.10	1.83	nsm(-)
		S ₂	2.50	1.10	3.60	2.27	nsm(-)
		S ₃	2.25	1.00	3.25	2.25	nsm(-)
					TLC = 48.25		

Karyotype Formula:

1) *Aloe barbadensis* Mill.

$$2n = 2x = 14 = 8L + 6S = 3L \{nsm (+) + 1L \{nsm (-)\} + 3S \{nsm (-)\}$$

2) *Aloe plicatilis*

$$2n = 2x = 14 = 8L + 6S = 3L \{nst (-) + 1L \{nsm (+)\} + 2S nsm (-)\} + 1Snm$$

3) *Aloe abyssinica* Lam.

$$2n = 2x = 14 = 8L + 6S = 2L \{nsm (+) + 2L \{nsm (-)\} + 3S \{nsm (-)\}$$

b) In Table 2 the data of mitotic index have been depicted:

c) **Stomatal index:** The type of stomata has observed in three species of *Aloe* is **paracytic** in nature. As the *Aloe*

are CAM plants, maximum stomata are found in closed condition during observation i.e. in day time. Fig 7 to 9 are showing the stomata of the three experimental species. The Table 3 is showing the stomatal indexes of concerned three species of *Aloe*.

Table-2: Mitotic indexes of three species of *Aloe*

Sl.No.	Name of Species	Mitotic Index
1	<i>Aloe barbadensis</i> Mill.	46.31
2	<i>Aloe plicatilis</i>	72.5
3	<i>Aloe abyssinica</i> Lam.	78.64

Table-3: Stomatal index of three species of *Aloe*

Plant Species	Dorsal			Ventral		
	Apex	Middle	Base	Apex	Middle	Base
1) <i>Aloe barbadensis</i> Mill.	8.08 ± 0.26	7.92 ± 0.097	5.58 ± 0.62	8.99 ± 1.10	5.00 ± 0.04	5.35 ± 0.76
2) <i>Aloe plicatilis</i>	8.45 ± 0.46	6.16 ± 0.06	5.37 ± 0.66	7.13 ± 0.43	4.53 ± 0.39	4.12 ± 0.63
3) <i>Aloe abyssinica</i> Lam.	8.65 ± 0.38	6.08 ± 0.43	8.78 ± 0.99	8.71 ± 0.42	5.76 ± 0.26	5.12 ± 0.55



Fig.: 1-*Aloe barbadensis* Mill.



Fig.: 3- *Aloe plicatilis*

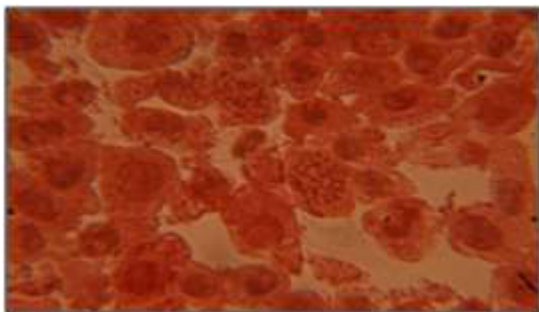


Fig.: 2-Mitotic metaphase chromosomes of *Aloe barbadensis* Mill.

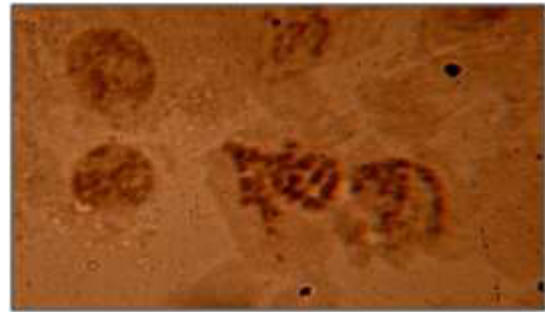


Fig.: 4- Mitotic metaphase chromosomes of *Aloe plicatilis*



Fig.:5- *Aloe abyssinica* Lam.

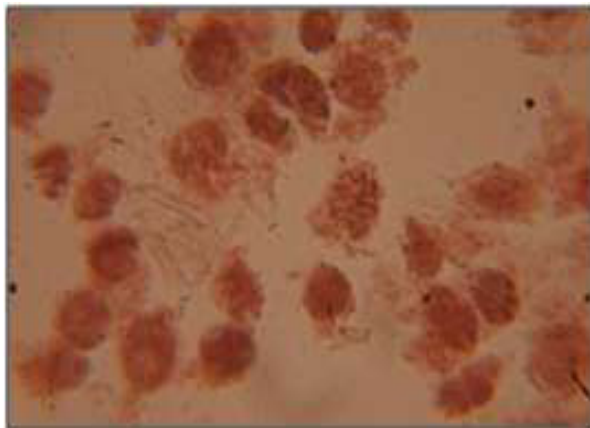


Fig.:6-Mitotic metaphase chromosomse of *Aloe abyssinica* Lam.



Fig.:7- Stomata of *Aloe barbadensis* Mill.



Fig.:8- Stomata of *Aloe plicatilis*



Fig.:9- Stomata of *Aloe abyssinica* Lam.

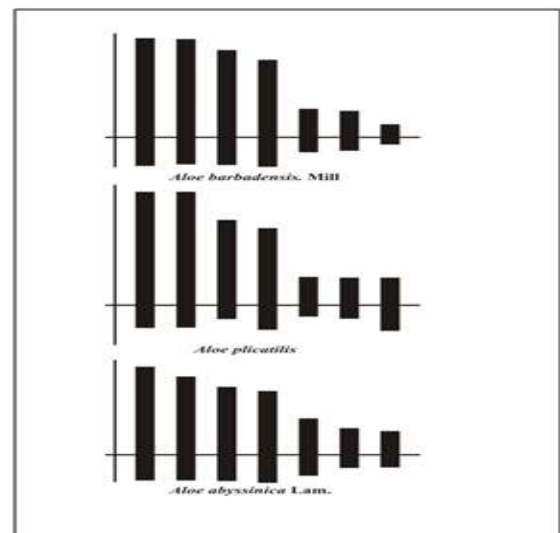


Fig.: 10- Idiograms of three species of *Aloe*

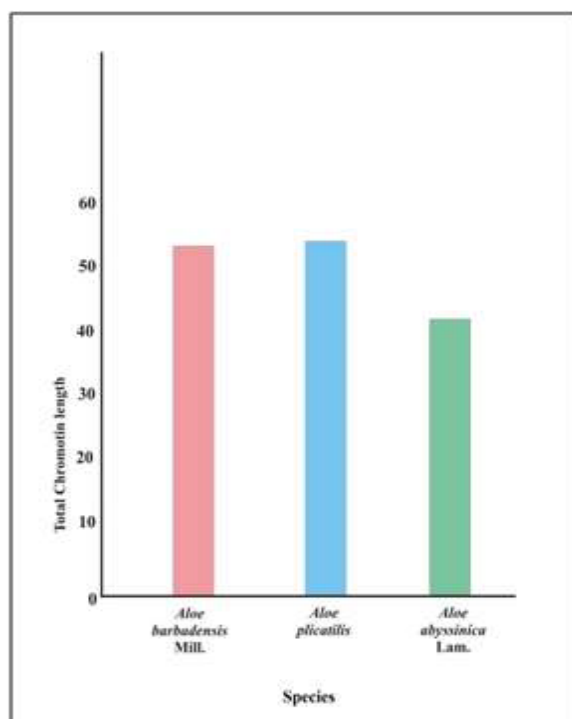


Fig.:11- Comparative histogram of three species of *Aloe*

DISCUSSION

In the present investigation all 3 species of *Aloe* are maintaining the equal diploid chromosome number i.e. $n=7$ i.e. $2n=2x=14$. Where 8 chromosomes are long and 6 are short, showing that those species are highly asymmetric and with bimodal karyotype.⁶⁻⁸ Asymmetrical karyotypes are considered advanced than symmetrical karyotypes.⁹ According to the evaluation of centromeric position, *Aloe plicatilis* was found to be the most asymmetric, among the three experimental *Aloe* species. *Aloe plicatilis* and *Aloe abyssinica* Mill., are showing symmetrical mitotic index. The concerned species are showing symmetrical distribution of stomata.

CONCLUSION

Three of the experimental species of *Aloe* are comprised atypical bimodal karyotype, with asymmetric nature, which reflects their advancement.

ACKNOWLEDGEMENT

I would like to express my sincere gratitude to my guide Dr. (Mrs.) Kamini Kumar and special thanks to the faculty member of our department of Botany, Ranchi University, Ranchi, Dr. Anjani Kumar Srivastava.

REFERENCES

1. Gunjan Kumari and Roy Bijoy Krishna (2010). Karyotype studies in dominant species of *Aloe* from eastern India. *Caryologia*, Vol. 63(1), pp. 41-49.
2. Stevens, P. F. (2001) (onwards) "Asphodelaceae", Angiosperm Phylogeny, retrieved 2016-06-09.
3. Jahan Bushreen, Vahidy Ahasana, Saeed Rafat and Mirbahar Ameer Ahmed (2014). Karyological studies in ten different populations of desert Lily *Aloe vera* from Pakistan. *Pak.J.Bot.* Vol. 46(5), pp.1731-1734.
4. Cruzzell, J. Z. (1986). Readers remedies for pressure sores *Aloe vera*. *American Journal of Nursing*. pp. 923.
5. Sapre, A. B. (1978). Karyotype of *Aloe barbadensis* Mill. : a reinvestigation. *Cytologia*, Vol. 43, pp. 237-241.
6. Darlington, C. D. (1963). *Chromosome Botany and the origin of cultivated plants*. George Allen and Unwin Ltd., London.
7. Stebbins, G. L. (1971). *Chromosomal evolution in higher plants*. Edward Arnold Ltd., London.
8. Adamas, S. P., Leitch, I.J., Bennette, M.D., Chase, M.W. and Leitch, A.R. (2000). Ribosomal DNA evolution and phylogeny in *Aloe* (Asphodelaceae). *Am.J.Bot.* Vol 87(11), pp. 1578-1583.
9. Levitsky, G. A. (1931). The Karyotype in systematic. *Bulletin of Applied Botany, Genetics and Plant breeding*, Vol 27, pp. 19-174.



Effect of organic liquids and inorganic inputs on population and species diversity of rhizosphere mycoflora in Wheat fields of Gopalganj district of Bihar

Basant Narain Singh^{a*} and Amarendra Kumar Jha^b

^{a*}Dr. Shukla Singh (SS) School, Khairatia (Malikana) Gopalganj, Bihar, India

^bDepartment of Botany, Jai Prakash University, Chapra, Bihar, India

*Corresponding author : Phone : 9430219611, E-mail : bnsingh.botany@gmail.com

Abstract : In present investigation an experiment was conducted in a wheat field during 2010-2013, to study the effect of various liquid organic inputs and inorganic inputs on rhizosphere mycoflora population and species diversity. The soil rhizosphere mycoflora population and diversity was studied by using serial dilution technique. Result observed that application of organic liquid bio-booster like farm yard manure, Beejamruth and Jeevamruth enhances rhizosphere mycoflora population and species diversity in organic field. The application of inorganic inputs lowers the rhizosphere mycoflora population and species diversity compare to organic field of wheat. The total 30 mycoflora species were isolated and identified from rhizosphere of organic field and a total 24 mycoflora species from rhizosphere of inorganic field. The isolated mycoflora species belongs to genera *Aspergillus*, *Penicillium*, *Trichoderma*, *Fusarium*, *Rhizopus* and *Cladosporium* in both organic and inorganic field. The *Acremonium* sp., *Tichoderma pseudokonigii*, *Glomus* sp., *Cladosporium herbarum* and *Curvularia lunata* are found in rhizosphere of organic field. Overall result shows organic bio-booster like farm yard manure, Beejamruth and Jeevamruth increases mycoflora diversity which helpful for maintenance of soil fertility for sustainable development.

Paper History:

Received

5th May 2017

Revised

28th June 2017

Peer reviewed

30th June 2017

Accepted

1st July 2017

Keywords: Wheat, Rhizosphere, Mycoflora, Diversity, Organic and Inorganic inputs

INTRODUCTION

Soil is an important panorama for wide range of microflora which includes fungi, bacteria and actinomycetes. Microflora increases nutrient content of soil via decomposition of crop residues, mineralization and immobilization of nutrients, biological nitrogen fixation and bioturbation. Rhizosphere is a zone of soil which directly influenced by root secretions and associated soil microorganisms. It is observed that rhizosphere having greater microbial activity. The changes in rhizosphere microbes depends on type of plant, age of plant, soil physico-chemical parameters, nature of root exudation, type of agricultural inputs mainly fertilizers and different environmental conditions. In modern agriculture there is indiscriminate use of inorganic fertilizer to increase the

production. But various results revealed that over use of chemical fertilizers has been shown to have a direct effect on the composition of the soil microbial community (Doran *et al.*, 1996). The lower fungal diversity may be due to there are many disturbances such as irrigation, fertilizer and agricultural practices (Yadav, 2014). It is Reported that application of Chemical fertilizer (Urea) @ 300 kg per ha to wheat field decreases the microbial population (Kumar *et al.*, 2010). The application of commonly used herbicides on non-target soil of maize field resulted in decreases in microbial counts (Ayansina and Oso, 2006). Inorganic treatment lowers the microbial population (Kapoor *et al.*, 2015). It is found that 1% of the pesticides applied may contact the target organisms and remainder moves into the soil, thereby soil flora and fauna may be adversely affected (Misra and Mani, 1994).

To minimize the adverse impact of chemical fertilizer now a day's farmers using various organic inputs for sustainable and eco-friendly development. Various comparative research on soil microflora population under different organic and inorganic inputs applied field revealed that addition of organic manure as an organic fertilizer rich in bacterial diversity, fungal diversity and other number of microorganisms compared to inorganic field (Ishaq and Khan, 2011). It is recorded that highest fungal population in treatment of FYM 40.6X 10⁴ g-l compared to urea treatment 38.8X10⁴ g -l (Raindra *et al.*, 2010). Organic fertilizers to soybean variety increases the microbial population compared to NPK and control (Das and Dkhar, 2010). 10-26% increase in microbial biomass under organic management was reported (Fraser *et al.*, 1994). The liquid boosters contain beneficial microorganism's mostly lactic acid bacteria, yeast, actinomycets, photosynthetic bacteria, nitrogen fixers, phosphorus solublisers and fungi (Sreenivasa *et al.*, 2010)). The present investigation was carried out to study the effect of organic inputs (FYM, Jeevamruth and Beejamruth) and inorganic inputs on soil rhizosphere mycoflora population and species diversity in Wheat field.

MATERIALS & METHODS

Agricultural fields at Gopalganj district of Bihar were selected for the study of rhizosphere mycoflora populations and species diversity under the influence of organic and inorganic inputs applied field of wheat during 2016 wheat crop. The selected experimental organic field was supplied with farm yard manure and organic liquid booster like Jeevamruth and Beejamruth (Palekar, 2006). The Jeevamruth applied to field crop and Beejamruth applied to seed. The inorganic field supplied with regular chemical fertilizers.

The rhizosphere soil samples were collected from organic and inorganic crop fields of Wheat crop by digging out soil around the rhizosphere area up to 20 cm from plant to a dimension of 15 cm height and 7 cm diameter. The five samples were collected from sampling site from each selected crop field and mixed together into a single. These soil samples were collected in sterile polythene bags and brought to the laboratory.

The rhizosphere fungi were enumerated by Serial dilution method (Waksman, 1992). The collected

rhizosphere soil samples from both the organic and inorganic inputs applied field were used for preparation of different serial Dilutions such as 10⁻², 10⁻³, 10⁻⁴, and 10⁻⁵. Then transferred 1 ml aliquots from each dilution were used to isolate fungi on Martins Rose Bengal Agar Medium, potato dextrose agar and Czapek's Dox Agar. One percent streptomycin solution was added to the medium before pouring into petriplates for preventing bacterial growth and plates were kept for incubation at 28 °C for 4-7 days for fungi. After 6 days of incubation the different colonies were counted from different organic and inorganic soil plates.

The quantitative analysis of fungal population was studied at 10⁻³ dilution. The percentage contribution of each colony forming units (CFU) of different fungal isolate was calculated by using the formula. Mean plate count X dilution factor **CFU/ g dry soil** = dry weight of soil Total no. of CFU of an individual species X 100 **Percentage contribution** = Total no. of CFU of all species

The individual colonies of fungi were selected based on morphology and purified by inoculation on PDA and Czapek's- Dox agar plates which were incubated for 7–14 days at 28°C. Further slants were prepared and incubated at 28°C for 7 to 10 days.

The fungal morphology were studied macroscopically by observing colony features (Colour and Texture) and microscopically by staining with lacto phenol cotton blue and observe under compound microscope for the conidia, conidiophores and arrangement of spores . The microphotograph was taken for isolated species by using Magnus camera. The fungi were identified with the help of literature identification of the species (Nagamani *et al.*, 2006).

RESULTS & OBSERVATIONS

The results on rhizosphere mycoflora population and species diversity in organic and inorganic field shows there is increase in rhizosphere mycoflora population and species diversity in organic inputs applied field compared to inorganic inputs applied field. The rhizosphere mycoflora population was more in organic field of crop plants during the 2015-2017 (Table.1).

In organic field rhizosphere Population of fungi ranged from 36.4×10⁻³ to 54.3×10⁻³CFU/g of soil during 2010-13. (Fig.1). In inorganic field rhizosphere Population

Singh & Jha: Effect of organic liquids and inorganic inputs on population and species diversity of rhizosphere mycoflora in Wheat fields of Gopalganj district Bihar

Table 1. Rhizosphere mycoflora (x10⁻³ CFU/ g soil) in organic and inorganic wheat fields.

Sl. No.	Months	Organic field 2015-16	Organic field 2016-17	Inorganic field 2015-16	Inorganic field 2016-17
1	Nov	39.01	42.40	32.60	29.60
2	Dec	45.60	49.20	36.00	32.80
3	Jan	48.80	47.20	31.20	36.80
4	Feb	38.40	39.20	26.00	24.80
5	March	43.20	42.38	30.20	25.20
	Average	43.03	44.06	31.08	29.84
	SD	±4.34	± 4.02	±3.44	±5.10

of fungi 20.5×10⁻³ to 36.8×10⁻³CFU/g of soil. (Fig.2). Application of panchagavya and beejamrutha treatment increases rhizosphere microbial population of maize (Shubha *et al.*, 2014). Application of FYM (5 t/ha) to soybean field had significantly increased the fungi 22.21 and 27.25 CFUx10³/g (Meena and Ghasolia, 2013). Inorganic fertilizer to crop field significantly lowers the rhizosphere microbial population and diversity (Nelson and Mele, 2006). The soil bacterial, fungal, actinomycetes and N fixing bacteria were more in organic fields than inorganic field (Padmavathy and Poyyamoli, 2011). The results on soil rhizosphere mycoflora species colonies and percentage contribution in organic field of Wheat during 2015-17 are presented in table 2. The results on soil rhizosphere mycoflora species colonies and percentage contribution

in inorganic field of Wheat during 2015-17 are presented in table 3.

Overall diversity indicated that rhizosphere of organic field shows more species diversity i.e. 26 mycoflora species in organic field and 17 species in inorganic field during 2015- 2017. The identified dominant rhizosphere mycoflora species belongs to genera *Aspergillus*, *Penicillium*, *Trichoderma*, *Fusarium*, *Rhizopus* and *Cladosporium* in organic and inorganic field. While genera like *Botrytis*, *Nigrospora*, *Sclerotium* and *Humicola* are least population diversity.

The *Acremonium* sp., *Tichoderma pseudokonigii*, *Glomus* sp., *Cladosporium herbarum* and *Curvularia lunata* are found in rhizosphere of organic field. It is observed that changes in frequency of mycoflora in

Table 2. Average Monthly variation of rhizosphere mycoflora in organic wheat field during 2015-2017.

Mycoflora Species	Nov	Dec	Jan	Feb	Mar	Total colonies	Percentage
<i>Aspergillus sps</i>	26	36	33	29	38	162	53.11
<i>Pencillium sps</i>	10	17	05	05	15	57	18.68
<i>Rhizopus sps</i>	05	04	02	01	00	12	3.93
<i>Trichoderma sps</i>	09	12	06	05	03	35	11.47
<i>Botrytis ceneria</i>	03	02	00	02	04	11	3.60
<i>Cladosporium herbarum</i>	00	03	00	03	07	13	4.26
<i>Fusarium oxysporum</i>	02	04	02	00	00	08	2.62
<i>Nigrospora sphaerica</i>	00	04	01	02	00	07	2.29
Total colonies	55	82	49	47	67	305	100

Table 3. Average Monthly variation of rhizosphere mycoflora in Inorganic wheat field during 2015-2017

Mycoflora Species	Nov	Dec	Jan	Feb	Mar	Total colonies	Percentage
<i>Aspergillus sps</i>	14	16	13	09	18	70	48.95
<i>Pencillium sps</i>	08	12	02	02	10	34	23.77
<i>Rhizopus sps</i>	03	02	03	02	01	11	7.69
<i>Trichoderma sps</i>	06	04	03	02	01	16	11.18
<i>Botrytis ceneria</i>	02	02	00	02	00	06	4.19
<i>Alternaria solani</i>	03	02	04	02	00	11	7.69
<i>Humicola grisea</i>	02	00	00	00	00	02	1.39
<i>Mycelia sterilea</i>	02	00	00	00	01	03	2.09
Total colonies	40	28	25	19	31	143	100

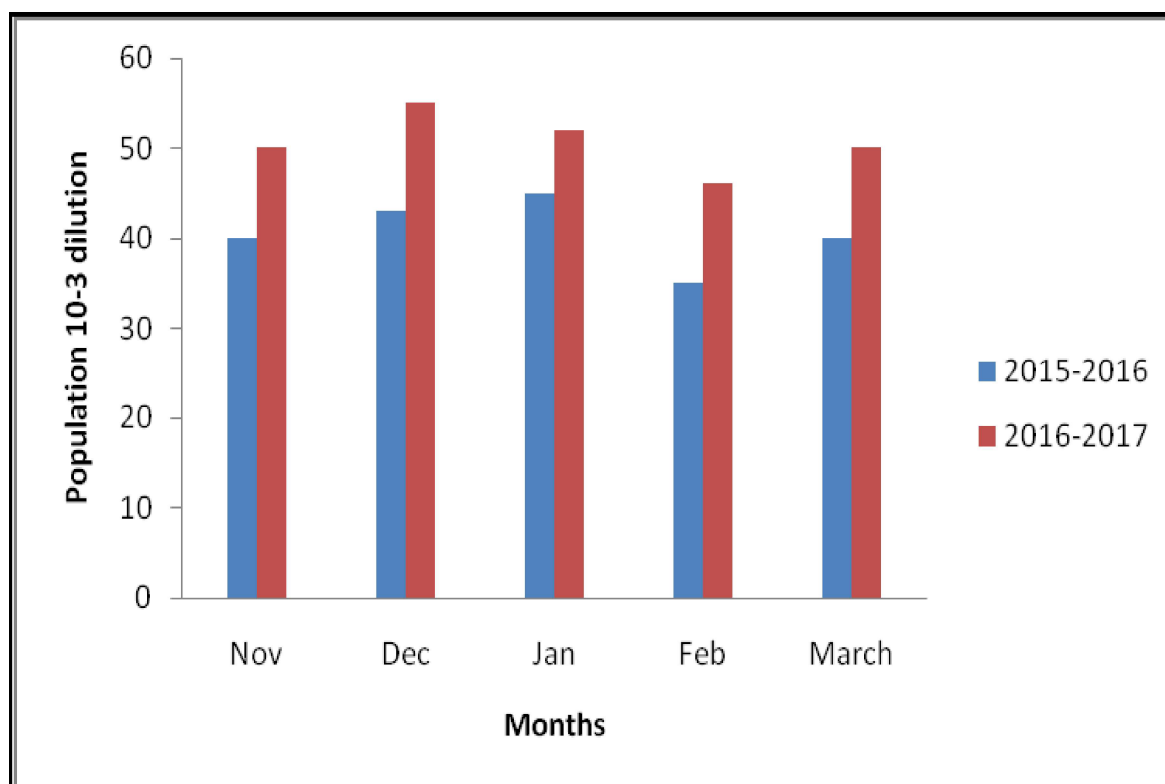


Figure 1. Rhizosphere mycoflora population in organic wheat field.

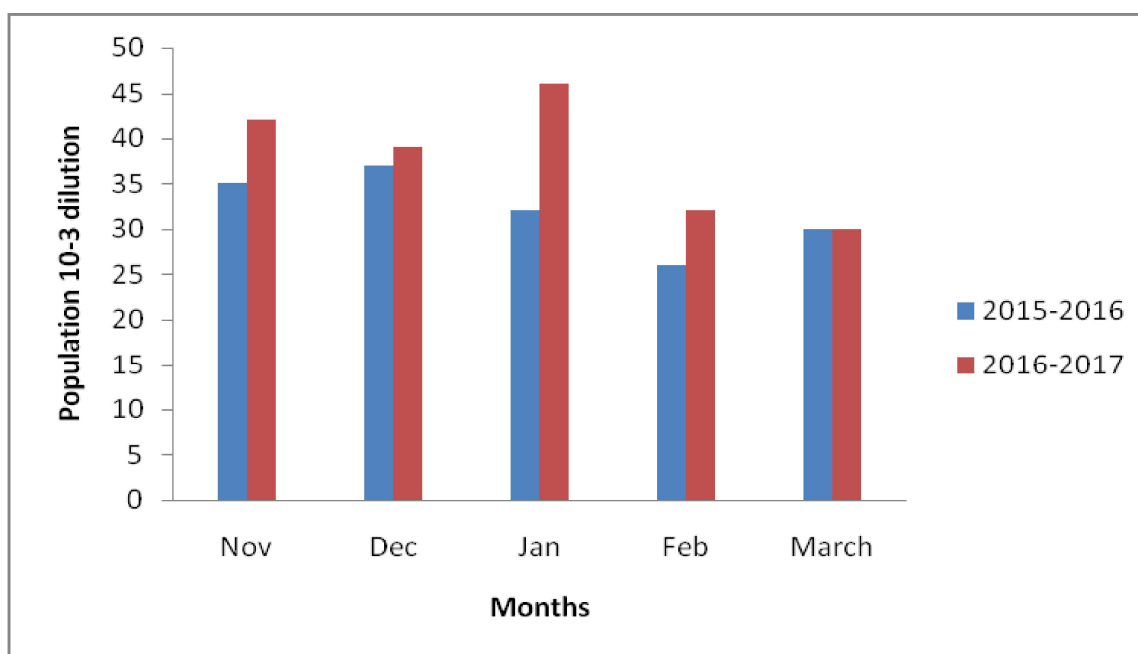


Figure 2. Rhizosphere mycoflora population in Inorganic wheat field.

agricultural fields are due to several factors like temperature, humidity, vegetation, organic and inorganic materials, soil type and texture (Gaddeyya *et al.*, 2012). The different fertilization changes in soil microfungi communities and fungal activities in agricultural soils (Rezacova *et al.*, 2007). It is observed that long-term effects of organic matter inputs on different cropping systems in a 10-year-old experiment enhances microbial activity (Chirinda *et al.*, 2008). Overall results revealed that there is monthly and yearly variation in rhizosphere total colonies and species diversity in organic and inorganic field of wheat. The organic field shows more rhizosphere population and species diversity compared to inorganic field.

CONCLUSION

The organic liquid bio-booster contains microbial load and soil nutrient which results increase in microbial population. The organic inputs like farm yard manure, Jeevamruth and Beejamruth increases the soil beneficial mycoflora population and species diversity compared to inorganic inputs applied field which adversely affect mycoflora diversity. The Increase in soil mycoflora diversity enhances nutrient availability to crop ultimately

increases growth and yield of crop plants. From this result we can conclude that organic liquid manure can be used as a bio-booster for increase in microbial population and species diversity for sustainable eco-friendly development.

REFERENCES

1. Ayansina A. D. V. and Oso, B. A. (2006). *Effect of two commonly used herbicides on soil microflora at two different concentrations. African Journal of Biotechnology*, 5 (2):129-132
2. Chirinda, N., Olesen, J.E. and Porter, J.R. (2008). *Effects of organic matter input on soil microbial properties and crop yields in conventional and organic cropping systems. 16th IFOAM Organic World Congress, Modena, Italy, June 16-20, 2008.*
3. Das, B.B. and Dkhar, M.S. (2010). *Rhizosphere Microflora of Soybean as affected by organic amendments in Meghalaya. NeBio*, 1(4):1-7.
4. Doran, J.W., Sarrantonio, M. and Liebig, M.A. (1996). *Soil health and sustainability. Advance in Agronomy*. 56:1-54.

5. Fraser, P.M., Haynes, R.J. and Williams, P.H. (1994). *Effects of pasture improvement and intensive cultivation on microbial biomass, enzyme activities and composition and size of earthworm population. Biol. Fertil. Soils*, 17: 185-190.
6. Gaddeyya, G., Shiny, P., Niharika, B.P. and Ratna, K. P. K. (2012). *Isolation and identification of soil mycoflora in different crop fields at Salur Mandal. Advances in Applied Science Research*, 3 (4):2020-2026.
7. Ishaq Fouzia and Khan Amir. (2011). *Isolation, Identification and Comparative Study of Fungal and Bacterial Strains Found in Organic and Inorganic Soils of Different Agricultural Fields. Recent Research in Science and Technology*, 3(11): 30-36.
8. Kapoor, T., Ramesh, C., Chauhan, S., Sambyal M., Raashee, A. and Natasha, S. (2015). *Impact of Different Farming Systems on the Soil Quality under Sub Humid agro-ecosystem of Zone-II of Himachal Pradesh. The 2nd Int Conf on Bio-resource and Stress Management during 7-10th Jan 2015 at PJTSAU, Rajendranagar, Hyderabad, India.*
9. Kumar, V., Chandra, A. and Singh, G. (2010). *Efficacy of fly-ash based bio-fertilizers vs. chemical fertilizers in wheat (Triticum aestivum). International Journal of Engineering, Science and Technology*, 2(7):31-35.
10. Meena, S. and Ghasolia R. P. (2013). *Effect of phosphate solubilizers and FYM on microbial Population of soybean field [Glycine max (L.) Merrill]. The Bioscan*, 8(3): 965-968.
11. Misra, S. G. and Mani, D. (1994). *Agricultural Pollution, Vol. I. Asish Publishing House, 8/81, Punjabi Bagh, New Delhi-110026.*
12. Nelson, D.R. and Mele, P.M. (2006). *Subtle changes in rhizosphere microbial community structure in response to increased boron and sodium chloride concentrations. Soil Biology & Biochemistry*, 39: 340-351.
13. Raindra, K., Seweta, S., Manisha, S. and Asha, S. (2010). *Effect of organic amendments on soil mycoflora. Asian Journal of Plant Pathology*, 4(2):73-81.
14. Rezacova, V., Baldrian P., Hrselova H., Larsen, J. and Gryndler, M. (2007). *Influence of mineral and organic fertilization on soil fungi, enzyme activities and humic substances in long term field experiment. Folia Microbiol*, 52 (4):415-422.
15. Waksman, S. A. (1992). *A method for counting the numbers of fungi in the soil. J. Bot.* 7:339-341.
16. Yadav, A.M. (2014). *Comparative study of Mycoflora of Paddy field soil in Bhandara District. Int. J. of Life Sciences, Special Issue A2:59-61.*



Comparative cytological studies of two varieties of *Lens culinaris*

Surabhi Joshi* & Kamini Kumar

Department of Botany, Ranchi University, Ranchi, Jharkhand, India

*Corresponding author : Phone : 9835815439 , E-mail : joshisurabhi603@gmail.com

Abstract: Lentil (*Lens culinaris*; Medikus) is the most ancient cultivated crops among the legumes. Diploid set of chromosomes were recorded with $2n=2x=14$, in both the species.

Paper History:

Received

8th May 2017

Revised

2nd June 2017

Peer reviewed

20th June 2017

Accepted

3rd July 2017

Keywords: Chromosome, Diploid, Karyotype, Lentil.

INTRODUCTION

Lens culinaris (Lentil) belongs to the family Fabaceae. It is indigenous to south western Asia and the Mediterranean region. There is an archaeological evidence of lentil dated back to 7500-6500 BC. It is commonly used for human nutrition animal feed and soil fertility. It is a diploid species $2n=14$ ¹. The plant was given the scientific name *Lens culinaris* in 1787 by Medikus, a German botanist and physician. Lentils are very good source of cholesterol lowering fibers. They also help to manage blood sugar. Lentil also provides excellent source of six important minerals, two vitamin B and proteins. Research studies have shown that lentil helps to prevent digestive disorders like irritable bowel syndrome and diverticulosis.

MATERIALS & METHODS

The seeds of lentil RL-12-53 and RL-12-56 were collected from Birsa Agricultural University, Kanke Ranchi Jharkhand. The healthy seeds were soaked in petriplate.

When young root apices about 1-2 cm long were excised between 2:00 to 2:30 pm. The root apices were pre-treated for 4 hours in paradichlorobenzene. The root apices were washed and transferred to 1:3 aceto alcohol (Carnoy's fluid) for 24 hours; after 24 hours the root apices were transferred to 70% alcohol for preservation. The slides were prepared in 2% acetocarmine stain by squash technique. Photographs of metaphase chromosome plates of 2 varieties were taken and data were analysed.

RESULT & DISCUSSION

The Lentil (*Lens culinaris*) Medik L. showed a diploid no. of chromosomes i.e. $2n=2x=14$ ². Both the varieties i.e. RL-12-53 and RL-12-56 showed $2n=14$. The total chromatin length (TCL) of RL-12-53 was shorter i.e.; $3.49\mu^3$. While RL-12-56 showed 3.51μ which was larger. The variety RL-12-53 consists of 2nm and 5m chromosomes and variety RL-12-56 had 1nm and 6m chromosome. The maximum numbers of met centric

chromosome were found in both the species⁴. There was no telocentric chromosome found in both the species. Maximum no. of metacentric chromosome was recorded in RL-12-56 and considered as a most primitive, whereas RL-12-53 had only metacentric chromosome which were considered as most advanced species⁵.

Table-1: Cytological data of two varieties of *Lens culinaris* L.

Varieties of <i>Lens culinaris</i>	Chrom No	Arm Length (μ)		T.L(μ)	LA/SA arm ratio	Classification
		Long arm	Short arm			
Var. RL-12-56	1.	0.40±0.08	0.30±0.00	0.70±0.08	1.33±0.28	nm
	2.	0.30±0.00	0.30±0.00	0.60±0.00	1.00±0.00	m
	3.	0.30±0.00	0.30±0.00	0.60±0.00	1.00±0.00	m
	4.	0.29±0.00	0.29±0.00	0.58±0.01	1.00±0.00	m
	5.	0.22±0.03	0.22±0.03	0.44±0.06	1.00±0.00	m
	6.	0.15±0.00	0.15±0.00	0.30±0.00	1.00±0.00	m
	7.	0.14±0.00	0.14±0.00	0.29±0.00	1.00±0.00	m
TCL(μ)				3.51±0.15		
Var. RL-12-53	1.	0.40±0.08	0.30±0.00	0.70±0.00	1.30±0.28	nm
	2.	0.30±0.00	0.30±0.00	0.60±0.00	1.00±0.00	m
	3.	0.29±0.00	0.29±0.00	0.58±0.17	1.00±0.0	m
	4.	0.29±0.00	0.26±0.03	0.55±0.04	1.16±0.00	nm
	5.	0.22±0.03	0.22±0.03	0.44±0.06	1.00±0.00	m
	6.	0.16±0.00	0.16±0.00	0.32±0.01	1.00±0.00	m
	7.	0.15±0.00	0.15±0.00	0.30±0.00	1.00±0.00	m
TCL(μ)				3.49±0.20		



Fig. 1: Seeds of *Lens culinaris* var. RL-12-56

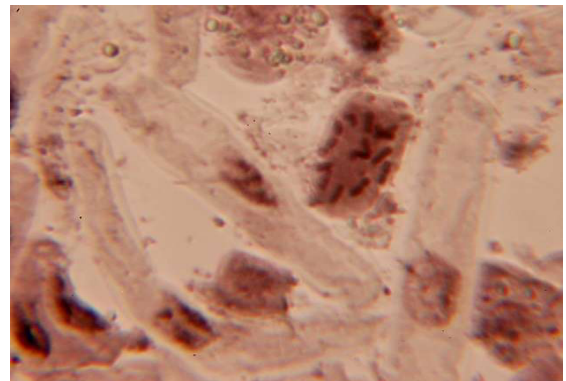


Fig. 2: Mitotic metaphase chromosome of var. RL-12-56



Fig. 3: Seeds of *Lens culinaris* var. RL-12-53

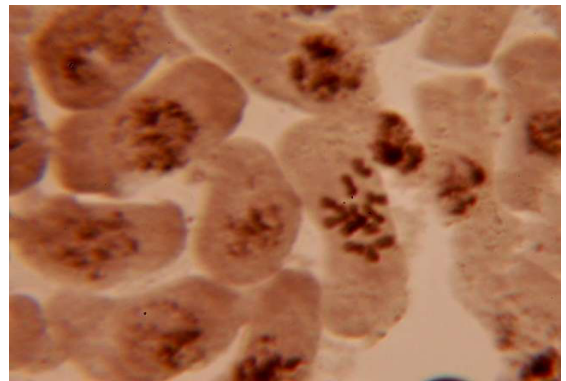


Fig. 4: Mitotic metaphase chromosome of var. RL-12-53

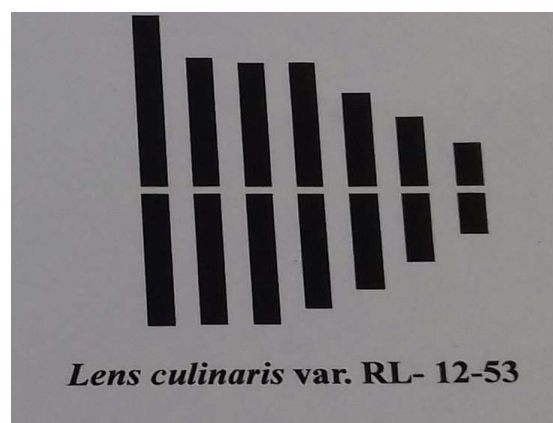


Fig: Ideogram of two varieties of *Lens culinaris*.

CONCLUSION

Lens culinaris; (Medik) of family Fabaceae was various medicinally important properties and is highly nutritious. Both the varieties were recorded with 14 chromosomes in diploid condition. Variety RL-12-53 has symmetrical nature in ideogram and only with metacentric chromosomes showed the advanced feature and considered as advance than variety RL-12-56.

ACKNOWLEDGEMENT

I express my sincere gratitude to Dr. Sashi Kumar Sinha, Head of Department, University Department of Botany, Ranchi University Ranchi, for providing the laboratory facilities.

REFERENCES

1. Abraham Z. and P. N. Prasad, 1983. A system of chromosome classification and nomenclature. *Cytologia*.48:95-101.
2. Kumar Upendra and S.S.N.Sinha, 1992. Karyotypic Analysis in some varieties of *Lens culinaris*. *Cytologia* 57:295-301.
3. Gupta P. K., S. Kumar, B. S. Tyagi and S. K. Sharma, 1999. Chromosome interchange in Lentil (*Lens culinaris*). *Cytologia*. 64(1):387-394.
4. Levan A., Fredga K. and Sandberg A. A. 1964. Nomenclature for centromeric position on chromosomes. *Hereditas* 52:201-220.
5. Stebbins G. L. 1971. Chromosomal Evolution in Higher Plants. Edward Arnold Ltd. London.



Study on some non-heterocystous cyanobacteria from Ranchi, Jharkhand, India

Chhaya Thakur* & Radha Sahu

Department of Botany, Ranchi University, Ranchi, Jharkhand, India

*Corresponding author : Phone : 9430114622 , E-mail : chhaya.thakur90@gmail.com

Abstract: Some non-heterocystous cyanobacteria may temporally separate nitrogen fixation and photosynthesis by fixing nitrogen during night. An intensive study of some non-heterocystous cyanobacteria have been made from various unusual habitats such as tree-bark, exposed and submerged rocks, hydrophytic twig, epizoic on snail, barren land soil, paddy fields etc. at many places in Ranchi district. The present communication records species of genera *Aphanathece*, *Gloeotheca*, *Gloeocapsa*, *Synechococcus*, *Spirulina*, *Oscillatoria*, *Phormidium*, *Microcoleus*, and *Lyngbya*. Among these the genus *Spirulina* is of commercial importance due to its overall nutritional qualities such as high protein content, pigments, medicinal value, whereas *Oscillatorialimosa*, *O.chalybea*, *Microcoleus chthonoplastes*, *Lyngbyamajuscula*, *L.aestuarii*, *Phormidium*, *Gloeotheca*, *Synechococcus* are known for their ability to fix atmospheric nitrogen. The genus *Oscillatoria* is most dominant.

Paper History:

Received

12th May 2017

Revised

11th June 2017

Peer reviewed

23rd June 2017

Accepted

11th July 2017

Keywords: Cyanobacteria, non-heterocystous, trichome, various habitats.

INTRODUCTION

Cyanobacteria constitute the largest, most diverse and widely distributed group performing oxygenic photosynthesis. They are of considerable importance as primary producers of organic matter and pioneer colonizers of land.¹ Their ability to grow in extremities of the environment and desiccation tolerance is well established.² Influences of cyanobacteria on soil properties have been reported by many workers such as water holding capacity and aeration status of the soil increased due to algal inoculation.^{3,4} The specialized cell wall, viscous protoplasm and mucilaginous sheath are the characteristic features of cyanobacteria. The mucilage sheath can quickly absorb moisture from humid atmosphere and increases the water holding capacity of cyanobacteria which enhance their desiccation tolerance capacity. Moreover, through mucilaginous covering they firmly hold the soil particle and hence check the soil erosion.

The mucilaginous and fragile thalli of *Aphanathece*

form a compact grey substratum firmly holding the soil particles together which checks the soil erosion.⁵ One of the most important event the diazotrophy has also been carried by non-heterocystous forms under anaerobic conditions although *Gloeocapsa* is an aerobic nitrogen fixer.⁶ *Microcoleus* and *Lyngbya* fix nitrogen towards end of the day and during night.⁷ The species *Lyngbya majuscula* has the property of immune modulation, pharmaceutical and nutrition.⁸ The non-heterocystous *Spirulina* is of commercial importance due to its overall nutritional qualities such as high protein content (60% to 70% of dry weight), low fat, high vitamins content (particularly B₁₂), iron, calcium, magnesium, beta-carotene, cyanin as well as its content of the essential fatty acid gammalinolic acid.^{9,10}

So far many works have been done on *Oscillatoria* in different regions like in cultivated soil in Ranchi and Andhra Pradesh^{11, 12} and lower Gangetic plains of West Bengal.¹³ The species of *Lyngbya* have also well studied.^{14,15}

MATERIALS AND METHODS

Study Area:

Ranchi is the capital of Jharkhand state situated in the Chhotanagpur plateau at the longitude 84° 20' to 85° 54' East and the latitude 22° to 23° 15' North, and about 629 m above the sea level. The tropical deciduous forest of the state is full of natural wealth which support the luxuriant growth of microalgae specially cyanobacteria in this area.

Sampling spot:

Repeated and regular collections of sample were made from various habitats in many places such as Itki, Ratu, Ormanjhi, Kanke, Hatia, Bundu, Namkum etc. in Ranchi. The samples were found growing on moist soil, rocky surfaces, tree-bark, sandy bricks, shell of snail, hydrophytic plants, bare and cultivated fields.

Collection and analysis of cyanobacterial sample:

The green scum on moist soil, tree trunk, mile stone, and rocks was scrapped with the help of sterile scalpel. All samples were collected in plastic bottles, polythene bags etc. The collected specimens were thoroughly washed with tap water taking care of the quality of the specimens. Temporary slides were prepared using methylene blue and chloro-zinc iodine and studied under the standard research microscope. Camera Lucida diagrams, micrometric measurements were taken. Identifications were made with the help of standard keys, monographs, literatures, research papers and various standard journals.^{16, 17, 18} Collected specimens have been also preserved in 4% formalin for further references.



Fig 1 : Map showing various sampling spots in Ranchi

RESULT

Systematic Enumeration:-

Table 1:

Family- Chroococcaceae

Genus- *Aphanothece* Nag.

1. *A. microscopia* Nag.

Cells oblong cylindrical, 2.1-3.4μ broad, 3.2-6.9μ long.

Habitat- growing on snail, Kanke dam.

Genus- *Gloeotheca* Nag.

2. *G. samoensis* Wille

Cells ellipsoidal, 3.2-4.2 broad, 4.6-7.5 long.

Habitat- growing on muddy soil, Khijri.

Genus- *Gloeocapsa* Kuetzing

3. *G. nigrescens* Nag. Cells spherical, 11.5-14.8μ in diameter

Habitat- growing on surface of earthen flower pot, Ormanjhi.

Genus- *Synechococcus* Nag.

4. *Synechococcus aeruginosus* Nag.

Cells cylindrical, 9.9-11.6μ broad and 16.5-19.8 μ long, pale blue- green in colour.

Habitat- Growing on moist barren soil in a field, Ratu,

Thakur & Sahu: Study on some non-heterocystous cyanobacteria from Ranchi,
Jharkhand, India

Plate- 1

Family- Oscillatoriaceae

Genus- *Spirulina* Turpin Em Gardner

5. *Spirulina major* Kuetz. Ex Gomont
Trich. 1.6- 1.9 μ broad, regularly spirally coiled;
spirals 2.6- 3.5 μ broad and 3.5- 5.5 μ distant.
Habitat- Attached with submerged river rock,
Panchghagh.
6. *S. laxissima* West, G.S. f. *major* f. nov.
Trich. 1.6 μ broad; spirals not close, 7 μ broad
and 14.8- 18.8 μ distant from each other.
Habitat - Growing along sewage drain, Panchvati,
Rly colony.
7. *S. gigantean* Schmidle
Trich. 3.3- 4.5 μ broad; spirals 13.2- 16.5 μ broad
and 13.2- 19.8 μ distant.
Habitat - Growing on moist soil at Harmuriver,
Harmu.

Genus- *Oscillatoria* Vaucher

8. *O. limosa* Ag. ex Gomont
Trich. 13.2 μ broad, cells 3.3-4.6 μ long
Habitat - Attached with stone wall, Ratu.
9. *O. chlorina* Kuetz. ex. Gomont
Trich. 6.2-7.5 μ broad, cells 3.9-5.9 μ long
Habitat- Growing on moist sandy soil, Ranchi Hill.
10. *O. chalybea* (Mertens) Gomont var. *insularia*
Gardner
Trich. 6-7 μ broad, cells 1.7-4.6 μ long
Habitat- Moist soil in barren field, Itki.
11. *O. rubescens* DC ex. Gomont
Trich. 5-7 μ broad, cells 2.9-4.6 μ long
Habitat- damp barren soil, Hatia.
12. *O. amoena* (Kuetz) Gomont
Trich. 3.6-6.6 μ broad, cells 2-5.2 μ long
Habitat- Moist soil of sewage, Bundu.
13. *O. willei* Gardnerem. Drouet
Trich. 3.3-3.6 μ broad, cells 3.3-7.6 μ long
Habitat- Moist sandy soil, Tagore hill.
14. *O. tenuis* Ag. ex. Gomont
Trich. 6.2 μ broad, cells 2.6-5.3 μ long
Habitat- Moist barren soil, Ratu.
15. *O. terebriformis* Ag. ex. Gomont
Trich. 4-6 μ broad, cells 3-6.6 μ long
Habitat- Moist soil of barren field, Bundu.

16. *O. perornata* Skuja Trich.
4.6-6 μ broad, cells 1.9-3.3 μ long
Habitat- Moist soil of well, Itki
17. *O. proscidea* Gomont
Trich. 5-7 μ broad
Habitat- Wet exposed rock Namkom.
18. *O. proteus* Skuja
Trich. 4.6-6 μ broad, cells 2.3-3.3 μ long
Habitat- Damp soil, Hatia.
19. *O. Formosa* Bory ex. Gomont
Trich. 4.2-5.2 μ broad, cells 3.1-5 μ long
Habitat- Exposed rock, Kanke.
20. *O. acuta* Bruhl et Biswas, orth. Mut. Geitler
Trich. 3.5-4 μ broad, cells 2.5-3.4 μ long
Habitat- Exposed rock, Kanke.
21. *O. sbbrevis* Schmidle
Trich. 4.6 μ broad, cells 1.6-2.5 μ long
Habitat- Moist soil of paddy field, Piska.
22. *O. curviceps* Ag. ex. Gomont var. *angusta* Ghose
Trich. 4-5.5 μ broad, cells 1.5-2 μ long
Habitat- Moist soil of paddy field, Ratu.
23. *O. raoi* De Toni, J.
Trich. 6-6.6 μ broad, cells 3-5 μ long
Habitat- Moist sandy bricks, Tagore hill.
24. *O. laete-virens* (Crouan) Gomont
Trich. 2.5-5 μ broad, cells 2.7-4 μ long
Habitat- Moist soil, Dhurwa.
25. *O. agardhii* Gomont
Trich. 4.9-6.6 μ broad, cells 3-5 μ long
Habitat- Attached to stone wall, Ratu.
26. *O. corallina* (Kuetz) Gomont
Trich. 3-6 μ broad, cells 2-3.5 μ long
Habitat- Moist soil of well, Hatia.

Genus- *Phormidium* Kuetz.

27. *P. retzii* (Ag.) Gomont Filament 6.6- 9.9 μ broad,
cells 3.3- 6.6 μ long.
Habitat- Soil of paddy field, Morabadi.

Genus- *Microcoleus* Desmazieres

28. *M. chthonoplastes* Thuret ex. Gomont Trich. 3.3-
4 μ broad, cells 3.3-6.6 μ long.
Habitat- Moist soil of barren land, Ratu.

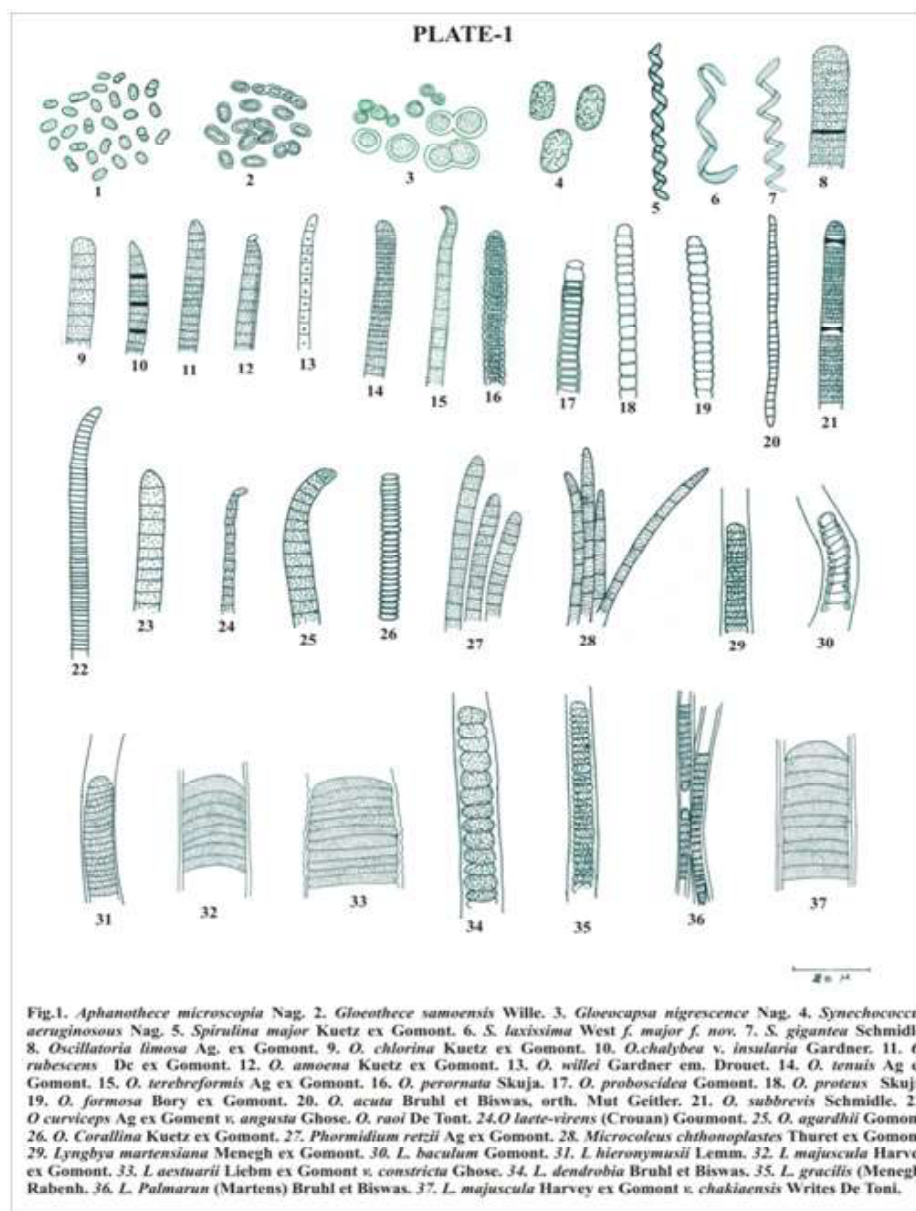
Genus- *Lyngbya* Ag.

29. *L. martensiana* Menegh. Ex. Gomont
Trich. 5-6.6 μ broad, cells 1.8-3 μ long.

- Habitat- Submerged rocky surface, Namkum.
30. *L. baculum* Gomont
Trich. 6.6-10 μ broad, cells 2.5-5 μ long
Habitat- Exposed rocky surface, Namkum.
31. *L. hieronymusii* Lemm.
Filament 13-14 μ broad, trich. 10-12.5 μ broad, cells 2.9-4 μ long
Habitat- Moist soil, Tagore hill.
32. *L. majuscula* Harvey ex. Gomont
Filament 46.2 μ broad, trich. 40-43 μ broad, cells 3.3-6.9 μ long
Habitat- Moist soil in paddy field, Ratu.
33. *L. aestuarii* Liebm. Ex. Gomont var. *constricta* Ghose
Filament 57-75 μ broad, trich. 37-52 μ broad, cells 6-12 μ long
Habitat- Moist soil of paddy field, Ratu.
34. *L. dendrobia* Bruhl et. Biswas
Filament 9.9-11 μ broad, trich. 7.2-9 μ broad, cells 4-7 μ long
Habitat- Tree-bark, Tupudana.
35. *L. gracilis* (Menegh.) Rabenh.
Filament 7-8.3 μ broad, trich. 5-6.3 μ broad, cells 2-3.3 μ long
Habitat- Moist soil, Ormanjhi.
36. *L. palmarum* (Martens) Bruhl et Biswas
Filament 10-15 μ broad, trich. 6-9 μ broad, cells 6-9 μ long.
Habitat- Tree- bark, Bundu.
37. *L. majuscula* Harvey ex. Gomont var. *chakiaensis* writes J. De Toni
Filament 36 μ broad, trich. 33 μ broad, cells 6.6-9.9 μ long
Habitat- Hydrophytic twig, Jonhewaterfall.

Table 1: Some non- heterocystous members of class Cyanophyceae.

Order	Family	Genus	Species
Chroococcales	Chroococcaceae	<i>Aphanothece</i>	<i>A. microscopia</i>
		<i>Gloeothece</i>	<i>G. samoensis</i>
		<i>Gloeocapsa</i>	<i>G. nigrescence</i>
		<i>Synechococcus</i>	<i>S. aeruginosus</i>
Nostocales	Oscillatoriaceae	<i>Spirulina</i>	<i>S. major</i> , <i>S. laxissima</i> f. <i>major</i> , <i>S. gigantean</i>
		<i>Oscillatoria</i>	<i>O. limosa</i> , <i>O. chlorine</i> , <i>O. chalybea</i> var. <i>insularia</i> , <i>O. rubescens</i> , <i>O. amoena</i> , <i>O. willei</i> , <i>O. tenuis</i> , <i>O. terebriformis</i> , <i>O. perornata</i> , <i>O. proboscidea</i> , <i>O. proteus</i> , <i>O. formosa</i> , <i>O. acuta</i> , <i>O. subbrevis</i> , <i>O. curviceps</i> var. <i>angusta</i> , <i>O. raoi</i> , <i>O. laete-virens</i> , <i>O. agardhii</i> , <i>O. corallina</i> ,
		<i>Phormidium</i>	<i>P. retzii</i>
		<i>Microcoleus</i>	<i>M. chthonoplastes</i>
		<i>Lyngbya</i>	<i>L. martensiana</i> , <i>L. baculum</i> , <i>L. hieronymusii</i> , <i>L. majuscula</i> , <i>L. aestuarii</i> var. <i>constricta</i> , <i>L. dendrobia</i> , <i>L. gracilis</i> , <i>L. palmarum</i> , <i>L. majuscula</i> var. <i>chakiaensis</i>



DISCUSSION

It is well established that the cyanobacteria have the capacity to fix atmospheric nitrogen. Some non-heterocystous species like *Microcoleus*, *Oscillatoria*, *Lyngbya* photosynthesis during most of the day and fix nitrogen towards end of the day and during night. Nitrogen fixing cyanobacteria are often used for reclaiming usar soil. Their regular inoculation in rice fields could be reduce intensive nitrogen fertilizer input and enhance the crop productivity.¹⁹ Further, they are important source of novel bioactive secondary metabolites which show interesting

and exciting biological activities including antimicrobial, anticancer, anti-HIV, antibacterial, antifungal, anti-inflammatory, antimalarial, antiprotozoal, anti-tuberculosis, antiviral and anti-tumour activities. Species of *Oscillatoria* contain antioxidant compounds. Pigment phycocyanin from *Spirulina*, *Phormidium* can be used as natural colorant in cosmetic and food industry.^{20,21} Phycocyanin being nontoxic, odourless and slightly sweet is used in eye shadow, eyeliner, lipsticks, candy, ice-creams, dairy products and soft drinks. Moreover, dyes are components of diagnostic kits.²²

CONCLUSION

The state Jharkhand is gifted with vast cyanobacterial diversity in various habitats. Cyanobacteria are most suitable microalgae on earth because they are able to grow in adverse and harsh extreme conditions. The cultivation of cyanobacteria is very economic as they need simple inorganic salts for growth and they multiply rapidly, therefore large scale biomass production is possible within a very short time. In current scenario cyanobacteria are beneficial in various ways, so it is necessary to conserve them and to do more systematic work on their potential and application for benefit of human as well as other organisms. The efforts should be made to utilize the potential of cyanobacteria in divergent aspects for the betterment of poor ethnic population of the state.

ACKNOWLEDGEMENT

We are thankful to the University Department of Botany, Ranchi University, Ranchi for cooperation during this research work.

REFERENCES

1. Das, S. C, Mandal B. and Mandal, L.N.(1991), *Plant Soil* **138** pp. 75-84.
2. Goyal, S. K.(1997), *Phykos* **36** pp.1-12.
3. Marathe, K.V.(1972), *The taxonomy and biology of blue-green algae*, (ed) Desikachary TV. University of Madras Press. Madras pp. 328-331.
4. Subhashini, D. and Kaushik, B. D.(1981), *Aust J Soil Res* **19** pp. 361-367.
5. Singh, R. N.(1961), *Role of blue-green algae in nitrogen economy of Indian agriculture*, ICAR, New Delhi .
6. Wyatt, J.T. and Silvey, J.K.G.(1969), *Science* **165**, pp. 908-909.
7. Swarnalakshmi, K., Dolly Wattal Dhar and Singh, P. K.(2006), *Proc Indian NatnSciAcad* **72** No.3 pp. 167-178.
8. Singh, S., Kate, B. N. and Banerjee, U. C.(2005), *Critical reviews in Biotechnology* **25**: pp. 73-95.
9. Srivastava, P. and Gajraj, R.S.(1996), *Recent advances in Biotechnology*. (eds.)
10. Srivastava, P. and Sharma, A.(2002), *Algological Research in India*. Ed. N. Anand, BSMPS, pub., Dehra Dun, India, pp. 337-343.
11. Columba, S. (1996), *Ph.D. thesis R.U. Ranchi*.
12. Raj Kumari, N. B.(2006), *Algal Taxonomy*. Vol. II. APC Pub. New Delhi, pp. 587-620.
13. Sen, C. R. and Gupta, D. (1998), *Phykos* **37**(1&2): pp. 89-93.
14. Shakuntala, J. (1990), *Indian Bot. Repr.* **9** (1): pp. 27-29.
15. Ray, S.(2006), *Cyanobacteria*, New Age International (P) Limited Publishers.
16. Prescott, G.W. (1951), *Inst. Sci. Bull.*, **31**: 946.
17. Desikachary, T. V.(1959), *Cyanophyta, Monograph*, ICAR, New Delhi.
18. Adhikari, S. P.(2002), *Algological Research in India*, pp. 143-164.
19. Anonymous.(1996), *Final Technical Report, DBT, Govt. of India*, New Delhi, pp. 144.
20. Subramanian, G. (1998), *Proceedings of the International Symposium on Cyanobacterial Biotechnology*. Oxford and IBH Pub.Co.Pvt. Ltd., New Delhi. pp. 281-286.
21. Venkataraman, L.V. (2002), *Algological Research in India*, pp. 7-27.
22. Curtin, M.E. (1985), *Biotechnology* **3**, pp.34-37



Studies on stomatal frequency and pollen analysis in *Zephyranthes candida* (Lindl.) Herb

Sameer Gunjan Lakra* & Kamini Kumar

Department of Botany, Ranchi University, Ranchi, Jharkhand, India

*Corresponding author : Phone : 9122609874 , E-mail : gunjansmeer5@gmail.com

Abstract : *Zephyranthes candida* (Lindl.) Herb. belongs to the family Liliaceae. The present study includes shape, size and frequency of stomata as well as shape, size of pollen grains along with its fertility and sterility percentage rate. The maximum number of stomata was observed on the adaxial surface of the leaf in apex portion. The longest stomata observed in the base portion of the leaf. The plant was recorded with high pollen fertility rate.

Paper History:

Received

5th May 2017

Revised

23rd June 2017

Peer reviewed

28th June 2017

Accepted

21st July 2017

Keywords: Frequency, Pollen, Stomata, *Zephyranthes candida* (Lindl.) Herb.

INTRODUCTION

Zephyranthes candida (Lindl.) Herb. is an ornamental, perennial herbaceous plant which comes under family Liliaceae. It is commonly known as rain-lily. *Zephyranthes* is native to Florida and is considered as primary centre of origin¹. The plant generally bears bulb or tubers. Flowers are white in color and leaves are green and linear. It has many medicinal properties. It relieves insomnia, used as a headache remedy, lower the fever, improves liver function etc.

The present investigation, on *Zephyranthes candida* (Lindl.) Herb., was carried out to determine the shape, size and frequency of stomata and shape, size of pollen and its fertility and sterility rate.

MATERIALS & METHODS

Zephyranthes candida (Lindl.) Herb. was collected from Mandar locality, Ranchi, Jharkhand. The locality is

30 Kms away from the Ranchi main town. Following studies has been carried out on the selected plant:

Stomatal studies:

Fresh leaves were collected for stomatal studies. They were scratched with sharp razor, stained with safranin and mounted with glycerin. It was observed under microscope and shape and number of stomata was recorded. 10 readings were recorded from both the adaxial and abaxial surface of the leaves in apex, middle and base portion. Length and width of stomata were also recorded.

$$\text{Stomatal Index} = \frac{\text{Number of stomata per unit area}}{\text{Number of stomata per unit area} + \text{Number of epidermal cell per unit area}} \times 100$$

Pollen studies:

Fresh flowers were used for the pollen studies. The anthers were excised from the flower and warmed in 2% acetocarmine to calculate the pollen fertility and sterility

rate. Stained anthers were teased in slide and observed under microscope. Stained pollens were considered as fertile. It was calculated by following formula-

$$\text{Percentage Pollen Fertility} = \frac{\text{Total number of fertile pollens}}{\text{Total number of pollen studied}} \times 100$$

$$\text{Percentage Pollen Sterility} = \frac{\text{Total number of sterile pollens}}{\text{Total number of pollen studied}} \times 100$$

Shape of the pollens grains of flowers were determined by using the technique of Erdman (1952)². It was calculated by dividing polar diameter of pollen with equatorial diameter of pollens.

RESULTS

Stomatal studies:

In this investigation, stomata observed was kidney shaped³ (Fig. 2). Stomatal Index was calculated which

showed highest number of stomata on the apex portion of adaxial surface. It was recorded with 22.95 ± 1.892 . Less number of stomata was observed in the base portion of abaxial surface i.e, 7.55 ± 0.77 (Table-1). In adaxial surface, the longest stomata were recorded in base portion with 52.8 ± 1.287 and the widest stomata were recorded in middle portion with 29.7 ± 0.788 whereas, in abaxial surface, base portion had the longest stomata i.e, 53.4 ± 0.38 and middle portion had the widest stomata 29.7 ± 0.895 (Table-2).

Pollen studies:

Pollen fertility and sterility rate of *Zephyranthes candida* (Lindl.) Herb. was examined and a high percentage of pollen fertility was recorded with 79%⁴ (Table-3). Shape of the pollen was observed as sub-prolate spheroidal with monoporate structure (Fig. 3). Pollens polar diameter was longer than its equatorial diameter (Table-4).

Table-1: Stomatal Index data of *Zephyranthes candida* (Lindl.) Herb.

Leaf Portion	Adaxial surface (μ)	Abaxial surface (μ)
Apex	22.95 ± 1.892	18.27 ± 1.529
Middle	16.29 ± 1.276	12.20 ± 0.900
Base	09.39 ± 1.380	07.55 ± 0.770

Table-2: Data related to measurement of stomata of *Zephyranthes candida* (Lindl.) Herb.

Leaf Portion	Adaxial surface		Abaxial surface	
	Length(μ)	Width(μ)	Length(μ)	Width(μ)
Apex	42.9 ± 0.435	22.5 ± 0.474	34.2 ± 1.355	14.4 ± 0.710
Middle	46.2 ± 0.629	29.7 ± 0.788	44.7 ± 0.788	29.7 ± 0.895
Base	52.8 ± 1.287	26.4 ± 1.802	53.4 ± 1.740	21.9 ± 1.345

Table-3: Percentage pollen sterility and percentage pollen fertility in *Zephyranthes candida* (Lindl.) Herb.

Sl. no.	Total number of pollen grain studied	Sterile pollens	Percentage pollen sterility	Fertile pollens	Percentage pollen fertility
1.	200	42	21	158	79

Lakra & Kumar: Studies on stomatal frequency and pollen analysis in *Zephyranthes candida* (Lindl.) Herb

Table-4: Pollen morphology of *Zephyranthes candida* (Lindl.) Herb.

Sl. no.	Polar diameter (P) μ	Equatorial diameter (E) μ	P/E	Shape
1.	61.2 ± 2.01	48.9 ± 1.27	1.26 ± 0.06	Sub-prolate spheroidal

Photograph of *Zephyranthes candida* (Lindl.) Herb. plant (Fig. 1) and photomicrographs stomata (Fig. 2) and pollens (Fig. 3).



Fig. 1

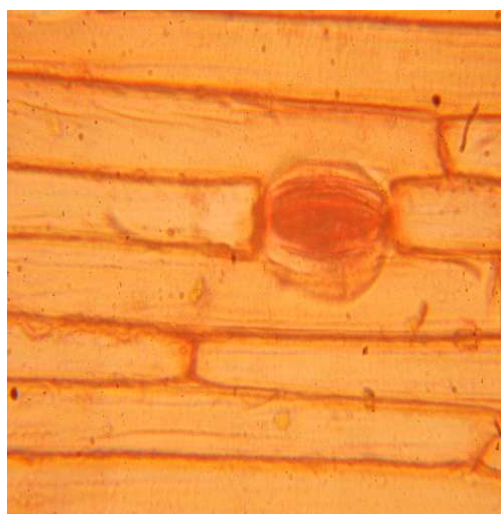


Fig. 2



Fig. 3

Fig. 4: Column graph showing the stomatal index of *Zephyranthes candida* (Lindl.) Herb.

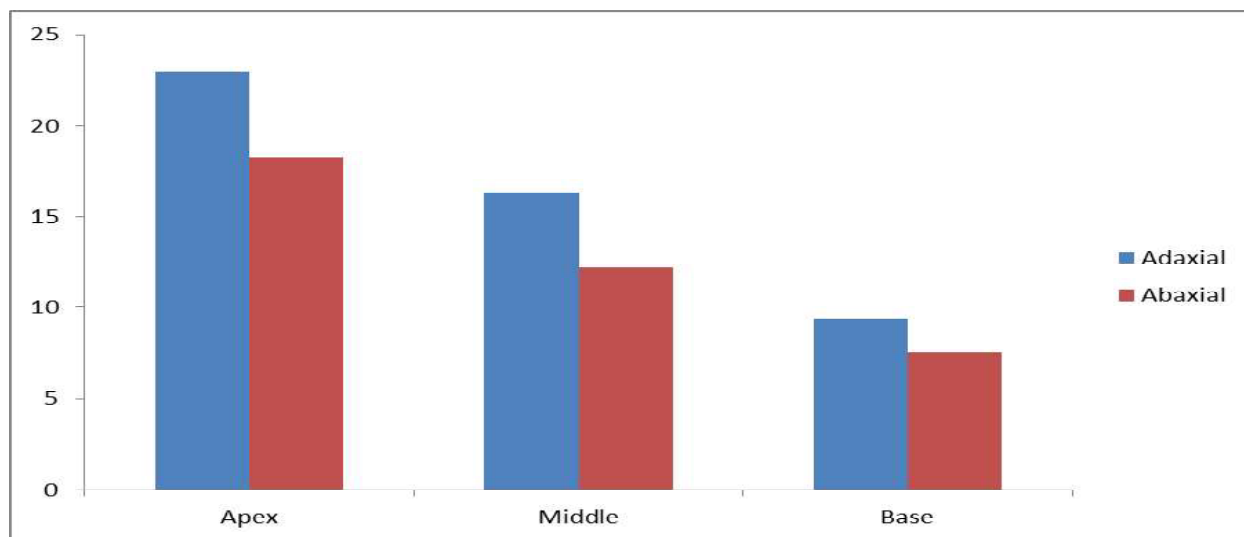


Fig. 5: Column graph showing the stomatal length and width (in μ) of *Zephyranthes candida* (Lindl.) Herb.

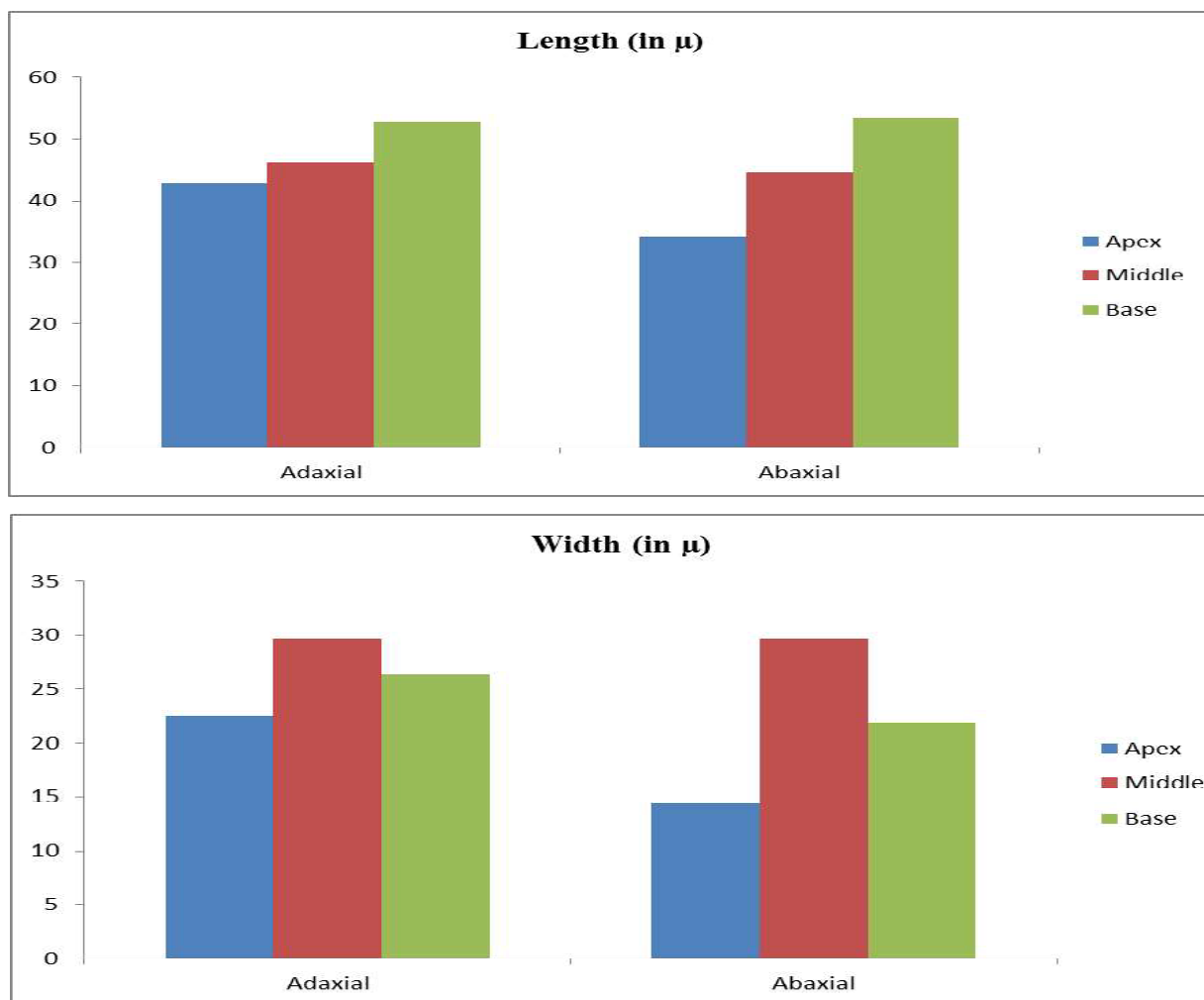
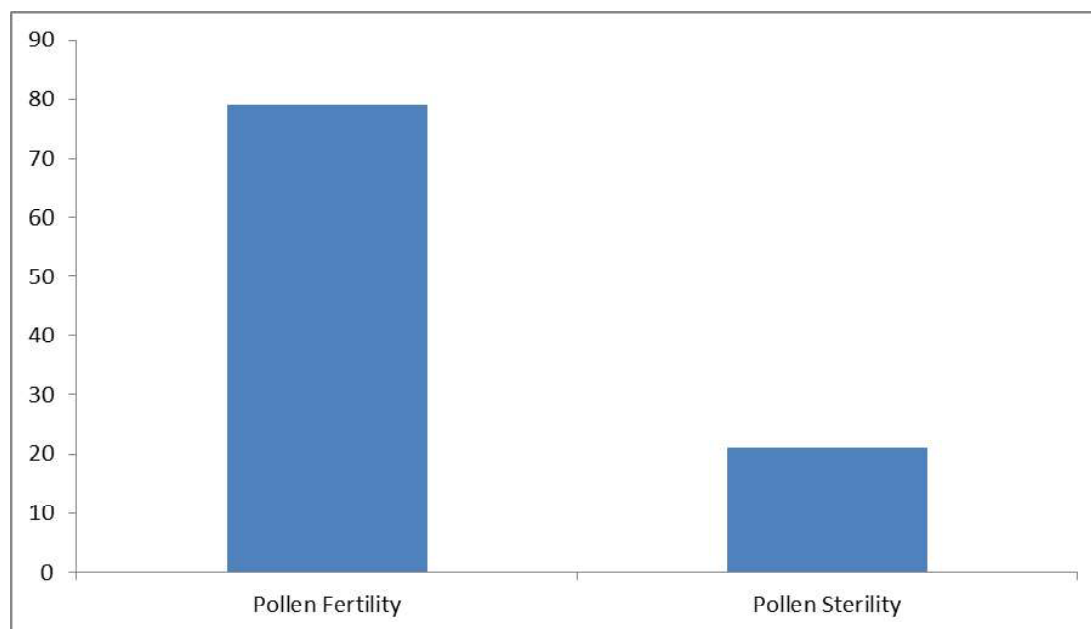


Fig. 6: Column graph showing percentage pollen fertility and percentage pollen sterility of *Zephyranthes candida* (Lindl.) Herb.



DISCUSSION

The stomata size, frequency are important parameters in selecting drought resistant genotypes. In the present finding higher stomatal frequencies were recorded on the adaxial surface. The stomata present on the adaxial surface were comparatively higher than abaxial surface which indicates a water loving nature.

Pollen studies also play an important role in modern plant taxonomy by determining its shape and size (Edeoga et al. 1996)⁵. Pollens were medium sized and its high rate of fertility showed the stability of plant. Although it is highly fertile but shows sexual incompatibility.

ACKNOWLEDGEMENT

I express my sincere gratitude to Dr. S. K. Sinha, Head, University Department of Botany, Ranchi University, Ranchi for providing the laboratory facilities.

REFERENCES

1. **Edward, F. Gilman. (1999)**, *Zephyranthes spp.* University of Florida Cooperative Extension Service Institute of Food and Agricultural Sciences, Fact Sheet FPS-621.
2. **Erdtman, G. (1952)**, Pollen morphology plant taxonomy. *Angiosperms Almqvist and Wiksell*, pp.539.
3. **Jiang, Z., Yu, J., Ma, S. and Wang, Y. (2011)**, Dynamic changes of stomatal characteristics during the flower, fruits and leaf developments of *Zephyranthes candida* (Lindl.) Herb. *African Journal of Biotechnology* Vol. 10, No. 62, pp. 13470-13475.
4. **Thoibi, D.T. and Borua, P.K. (1997)**, Meiotic behavior and pollen fertility in three species of *Zephyranthes* (Amaryllidaceae). *Biol Plant.* Vol. 35, pp. 281-282.
5. **Edeoga, H.O., Ogbebor, N.O. and Amayo, A.O. (1996)**, Pollen morphology of some Nigerian species of *Aneilema* R. Br. and *Ludevigia* L. *New Bot* Vol. 23, pp. 223-231.



Antidiabetic efficacy of leaf extract of *Annona squamosa* L.

Manju Sinku* & H. P. Sharma

Department of Botany, Ranchi University, Ranchi, Jharkhand, India

*Corresponding author : Phone :7091315749 , E-mail : sinku.manju890@rediffmail.com

Abstract : *Annona squamosa* L. (belongs to family Annonaceae) is tree in nature and is known for edible, sweet and fleshy fruits. In addition to nutritional tasty fruits the plant is widely used in traditional system of medicines in different kinds of diseases. In the present investigation attempts have been made to prove scientific validation of medicinal properties of the plant species. Two parameters were investigated i.e. phytochemical screening for the presence of secondary metabolites and antidiabetic efficacy of methanol extract. Phytochemical screening was performed adopting standard methods prescribed for different secondary metabolites. Methanol extract showed the presence of phenol, coumarin, terpenoid, saponin, betacyanin, anthocyanin and alkaloids while in aqueous extract quinone and saponin were present. Evaluation of anti-diabetic activity was done using inhibition of enzyme activity. Alpha- amylase (starch degrading enzyme) inhibition confirms anti-diabetic activity. The result shows an increase in percent of inhibition from 14.29% to 34.48 % at very low concentration of extract (360µg/µl).

Paper History:

Received

15th May 2017

Revised

18th June 2017

Peer reviewed

28th June 2017

Accepted

21st July 2017

Keywords: Diabetes, Hyperglycemia, WHO, Buffer, Methanol.

INTRODUCTION

Diabetes is a metabolic disorder of carbohydrate, fat and protein, affecting a large number of population in the world. Diabetes mellitus (DM) is not a single disorder but it is a group of metabolic disorder characterised by chronic hyperglycemia, resulting from defects in insulin secretion, insulin action, or both. The word 'diabetes' is derived from the Greek word "Diab" (meaning to pass through, referring to the cycle of heavy thirst and frequent urination); 'mellitus' is the Latin word for "sweetened with honey" (refers to the presence of sugar in the urine). According to ancient Hindu physicians, it is called 'Madhumeha' and had recorded in their observations that 'if too many ants swarm around a spot of urine, then the person have symptoms of diabetes mellitus' (Warjeet *et al.* 2011).

According to World Health Organization projection, the diabetes population is likely to increase to 300 million or more by the year 2025 (Meenakshi *et al.* 2010). The current studies in India indicate that there is an alarming

rise in prevalence of diabetes which has gone beyond epidemic form to a pandemic one. It is predicted that by 2030, India, China and the United States will have the largest number of people with diabetes (Frode *et al.* 2008). In recent year type 2 DM (T2DM), have been increasing in contrast to cases of type 1 DM. In more developed countries cure and prevention of T2DM have become important concerns. It is also expected to become a more serious problem due to shift in Western style diet. Increased thirst, increased urinary output, ketoacidosis (ketone bodies present in blood or urine), ketonemia and ketonuria are the common symptoms of diabetes mellitus, which occur due to the abnormalities in carbohydrate, fat, and protein metabolism. Diabetes is mainly attributed to the rapid rise in unhealthy life style, urbanization and aging.

Hyperglycemia which is the main symptom of diabetes mellitus generates reactive oxygen species (ROS) which cause lipid peroxidation and membrane damage. ROS plays an important role in the development of

secondary complications in diabetes mellitus such as cataract, neuropathy and nephropathy. Antioxidants protect β -cells from oxidation by inhibiting the peroxidation chain reaction and thus they play an important role in the diabetes. Plants containing natural antioxidants such as tannins, flavonoids, vitamin C and E can preserve β -cell function and prevent diabetes induced ROS formation. Polyphenols, which are classified into many groups such as flavonoids, tannins and stilbenes, have been known as health-beneficial properties, which include free radical scavenging, inhibition of hydrolytic and oxidative enzymes, anti-inflammatory action and antidiabetogenic potentiality (Patel and Kumar *et al.* 2011). Therefore, improvement of insulin resistance is expected to be an effective therapeutic strategy for improvement of T2DM as well as metabolic syndrome.

Annona squamosa L. the plant of Annonaceae family, also known as custard apple or sugar apple, is commonly found in deciduous forest. It is commonly cultivated in tropical South America but often in Central America, very frequently in Southern Mexico, West Indies. Cultivation is most extensive in India where the tree is exceedingly popular. *A.squamosa* L. ranges from 10-20 ft. (3-6 m) in height with on crown of irregular branches and zigzag twigs, leaves alternate, the fragrant flowers borne in single or in group of 2-4, fruit rarely round, oval or conical, long, ripen fruit has creamy white fragrant juice and sweet delicious flesh.

Literature of many research work proves that every part of *A.squamosa* L. possess medicinal properties (Veeramuthu *et al.* 2006). Folkloric record reveals that this plant possess wide range of biological activities such as anti-lipidemic (Kaleem *et al.*, 2006), anti-tumour (Pardhasaradhi *et al.* 2005), anti-microbial (Patel and Kumar, 2008), anti-thyroidal, anti-oxidant and anti-diabetic activity (Shirwaikar *et al.* 2005).

Its roots, barks, seeds, fruits, and even leaves, etc. are considered to treat many diseases. Roots are employed internally in depression of spirits and spinal diseases. Bark is known to be a powerful astringent (Raj Sobiya *et.al.* 2009). In Ayurveda, fruits are considered as a good tonic, enrich blood, used as expectorant, increases muscular strength, cooling, lessens burning sensation and relieves vomiting (Patel and Kumar, 2008). The seeds are said to

be abortifacient and good to destroy lice in hair in Yunani medicine. Seed yield oil and resin which acts as detergent and their powder, is mixed with gram flour, and is a good hair wash. Seeds are powerful irritant of conjunctiva and produces ulcers in eye. A leaf decoction was taken in case of dysentery (Gajalakshmi *et al.*, 2011). Brushed leaves with salt make a cataplasm to induce suppuration. They are applied for extract of guinea- worms.

Due to uniqueness of leaves property in curing of different ailments, this part was selected for

the study. The objective of the present investigation was to screen phytochemicals of *Annona squamosa* leaf and its anti-diabetic efficacy.

MATERIALS & METHODS

Plant Material

Fresh plant material i.e. leaves of *Annona squamosa* L. was collected from the Hatia area of Ranchi.

Preparation of leaf extract

Fresh plant materials i.e. leaves of *A.squamosa* L. was washed with tap water and dried in shade and the dried leaves were powdered in grinder. 10 g of powdered leaves were weighed and dissolved in 100ml of methanol in a ratio 1:10. The solution was kept for 72 hours under room temperature. Initial weight of the conical flask was taken. Filtrate was obtained after drying in hot air oven at temperature 60°C- 70°C to obtain dried material. Final weights of the flasks were taken and percentage of solubility were calculated. The material was scratched out and from it 0.036g of dried material was dissolved in 100ml methanol. Thus, the concentration (w/v) is 0.36mg/ml methanol extract.

Phytochemical Analysis

Chemical tests were done to identify phytochemicals like tannin, phenol, coumarin, quinone, glycoside, saponin, terpenoid, betacyanin, cardiac and alkaloid using standard protocol as given by Trease and Evans (1983, 1989), Sofowora (1931) (Table 1).

Enzymatic inhibition (α -amylase)

The α - amylase inhibition assay was done using different protocols developed by Sigma-Aldrich adapted from Bernfeld (1955) and Giancarlo *et al.* (2006).

The requirements for the experiment is enzyme solution (4 unit/ml) was prepared by dissolving 0.008 g

Sinku & Sharma: Antidiabetic efficacy of leaf extract of *Annona squamosa* L.

α - amylase in 100 ml cold distilled water. [0.5 unit/ml prepared by dissolving 0.001g of enzyme in 100 ml cold distilled water as referred from article α -amylase inhibitory activities of six *Salvia* species (2008)]. Starch solution (0.5% w/v) was prepared by dissolving 0.5 g of starch in 100 ml 20 mM phosphate buffer (pH 6.9) containing 6.7 mM sodium chloride. For DNSA reagent 96 mM 3, 5-dinitrosalicylic acid, 5.31 M sodium potassium tartarate dissolved in 2 M sodium hydroxide.

The experiment was performed with four replicates. In the experiment, α -amylase inhibition was observed using pre-incubation method. In this method enzyme was incubated with plant extract. In four tubes, different volume of plant extract was added *i.e.* 10 μ l, 50 μ l, 100 μ l, 200 μ l (initial concentration of plant extract is 0.36 mg/ml) and accordingly different volumes of distilled water was added and 200 μ l of the enzyme was added and

incubated for 3min at 25°C. The reaction was started by addition of 400 μ l of starch solution such that volume of mixture becomes 800 μ l. At intervals (3min) from addition of starch to each tube 100 μ l DNSA colour reagent was added and placed in water bath (85°C).

After 15 min this mixture was diluted with 900 μ l distilled water and removed from water bath. α -amylase activity was determined by measuring the absorbance of mixture at 540 nm. For control incubations, representing 100% enzyme activity were conducted in same process replacing plant extract with methanol (10 μ l, 50 μ l, 100 μ l, 200 μ l). And for blank incubations (to allow for absorbance produced by the plant extract), the enzyme solution was replaced with distilled water (200 μ l) and the same procedure was carried out as above. The absorbance (A) due to maltose generated was calculated as:

$$A_{540nm} \text{ control or plant extract} \div A_{540nm} \text{ Test} - A_{540nm} \text{ Blank}$$

$$\text{Percent (\%)} \text{ of } \alpha\text{- amylase inhibition} = \frac{A_{540nm} \text{ of control} - A_{540nm} \text{ of sample} * 100}{A_{540nm} \text{ of control}}$$

$$\text{Or \% of inhibition} = 100 - \% \text{ of reaction}$$

$$\text{Whereby \% of reaction} = (\text{mean maltose in sample} / \text{mean maltose in control}) * 100$$

Table 1-

TESTS	REQUIREMENTS	PROCEDURE	OBSERVATION
Phenol	Distilled water, 10% FeCl ₃	To 1ml of extract, 2ml distilled water followed by few drops of 10% FeCl ₃ was added	Green colour should be obtained
Coumarin	10% NaOH	To 1ml of extract, 1ml 10% NaOH was added	Yellow colour should be obtained
Quinone	Conc. H ₂ SO ₄	To 1ml of extract, 1ml conc. H ₂ SO ₄ was added	Red colour should be obtained
Glycosides	Chloroform, 10% ammonia solution	To 2ml of extract, 3ml of chloroform and 10% ammonia solution was added	Pink colour should be obtained
Saponin	Distilled water	To 2ml extract, 2ml distilled water was added and shaken in graduated cylinder for 15 min	Formation of 1cm layer of foam should be obtained
Terpenoids	Chloroform Conc. H ₂ SO ₄	To 0.5 ml of extract, 2 ml chloroform was added and conc. H ₂ SO ₄ was added carefully	Formation of red brown colour at the interface should be obtained
Anthocyanin and Betacyanin	2N NaOH	To 2 ml extract, 1 ml of 2N NaOH was added and heated for 5 min at 100°C	Yellow colour should be obtained
Alkaloid	Conc. HCl Mayer's reagent (HgCl ₂ -1.36g + KI- 5g+ H ₂ O-100 ml)	To 2 ml of extract, 2 ml conc. HCl was added. Then a few drops of Mayer's reagent was added	Green colour should be obtained

RESULTS & DISCUSSION

Phytochemical screening

Qualitative analysis of each extract shows different colour intensities which confirms presence or absence of secondary metabolites.

In methanol extract phenol, coumarin, terpenoid, betacyanin and anthocyanin and alkaloids are present whereas quinone glycoside, and saponin is absent (table2).

The observation table of phytochemical screening is given in table 2:

Table 2: Observation table of phytochemical screening

Test of phytochemical	Methanol extract
Phenol	+
Coumarin	+
Quinone	-
Glycoside	-
Saponin	-
Terpenoid	+
Betacyanin and Anthocyanin	+
Alkaloids	+

Enzymatic inhibition (α -amylase)

Methanol extract of *A.squamosa* L. showing significant differences with difference in concentration of plant extract (table no.3). It is observed that increasing volumes of plant extract i.e. 10 μ l, 50 μ l, 100 μ l and 200 μ l (hence the concentration becomes 3.6 μ g/10 μ l, 18 μ g/50 μ l, 36 μ g/100 μ l and 76 μ g/200 μ l) the inhibition of enzyme increases as follows: 14.29% > 16.7% > 33.4% > 34.48% and also can be seen by graph showing lower absorbance in plant extract than that of control (Fig 2). The observation has been recorded from the above method is as follows:

Table 3: Calculation of percent of inhibition

Sl. No.	Blank P+ Starch present Enzyme (-)	Exp. P+ Starch+Enzyme	Control Starch+Enzyme, present P (-)	Mean of Exp.	Mean of C
1.	0.23	0.02 0.01 0.03	0.05 0.05 0.06	0.02	0.05
2.	0.09	0.03 0.02 0.03	0.04 0.03 0.04	0.03	0.04
3.	0.12	0.04 0.03 0.03	0.06 0.06 0.05	0.03	0.06
4.	0.15	0.06 0.06 0.07	0.09 0.09 0.10	0.063	0.093

Sl.no.	(A) due to maltose generation C=(A) Exp- (A) blank	(A)due to maltose generation P=(A) Control- (A) blank	% of inhibition= (A _{540nm} of C- A _{540nm} of P/A _{540nm} of C) *100
1.	0.02-0.23= -0.21	0.05-0.23= -0.18	14.29 %
2.	0.03-0.09= -0.06	0.04-0.09= -0.05	16.7 %
3.	0.03-0.12= -0.09	0.06-0.12= -0.06	33.4 %
4.	0.063-0.15= -0.087	0.093-0.15= -0.057	34.48 %

Where P= plant extract, C= control, (-) = absent, (+) = present

A_{540nm} = absorbance of sample or control at 540nm

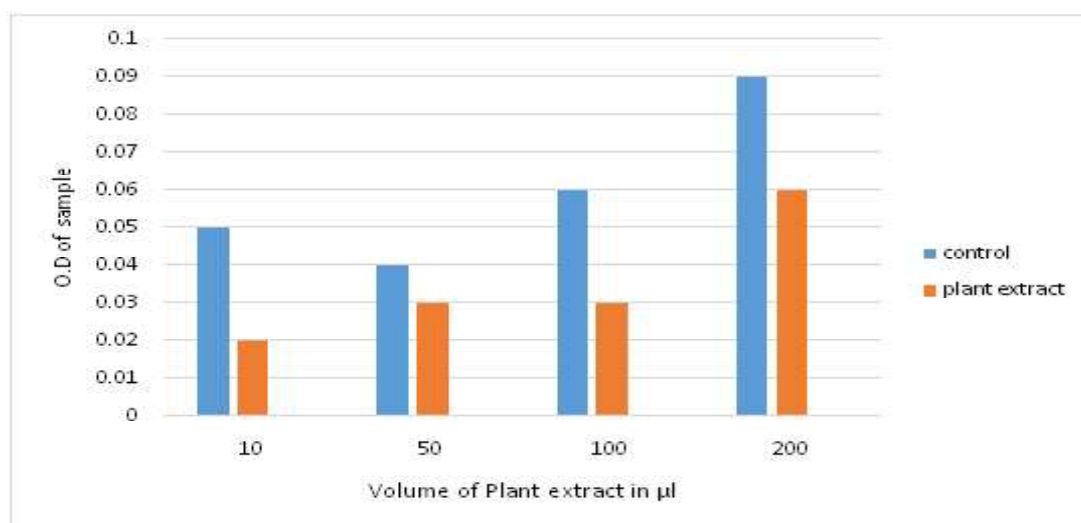


Fig 1: Absorbance of control and plant extract showing difference in O.D due to production of maltose.

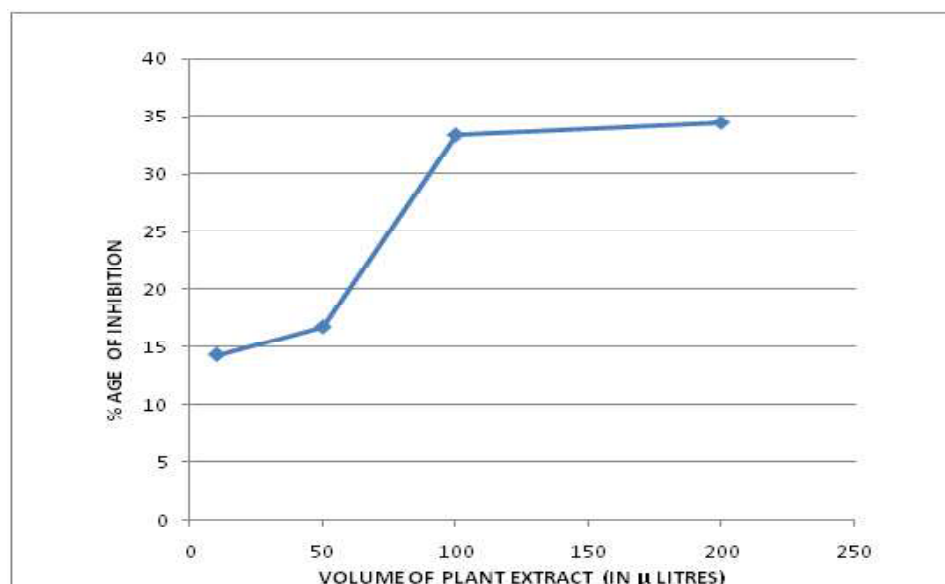


Fig 2: Showing percent of inhibition at different volume of plant extract.

In monosaccharide glucose can be readily absorbed from the gastrointestinal tract

into the blood stream after the hydrolysis of glycosidic bonds in digestible carbohydrate foods containing starch by the enzyme α -amylase and α -glucosidase. Inhibition of these enzymes reduced the high post prandial blood glucose peaks in diabetics.

The pre-incubation method gives a significant observation regarding anti-diabetic effect of *A.squamosa* L. The percent of inhibition was displayed in table 3. The assay showed that the extract contains α -amylase inhibitors

since less starch was converted to maltose as seen by lower absorbance value in the experiment. The % of inhibition as displayed in table 3 indicates increase in percent of inhibition from 14.29% to 34.48%. It can be suggested that with increase in concentration of plant extract (initial concentration 0.36 mg/ml or 0.36 µg/µl) i.e Hasenah Ali *et al.* (2006) in his paper discussed regarding some of the species eg. *Anacardiummocc identale* Linn, *Parkiaspeciosa* Hassk. *Avverhoabilimbi* Linn hexane extract which show negative values and suggested that α -amylase is activated at low concentration rather than inhibited. If this were to

occur in vivo, it would aggravate, rather than alleviate, the diabetic condition since the rate of glucose production would be increased and thereby the serum levels rise more rapidly. However it might be that an increase in the reaction product levels may be due to conformational change derived from binding of compounds to the enzyme (Kim *et al.*, 2000). Thus, further investigation is required for a better use of extract as an anti-diabetic property.

In the present study phytochemical and anti-diabetic activity of *A.squamosa* L. were confirmed with the help of many references and it can be concluded that leaf of *A.squamosa* L. can be a good source of medication without any side effect. Further research is required about its various medicinal properties.

REFERENCES

1. **Atique A, Iqbal M, Ghouse, AKM.** Use of *Annona squamosa* and *Piper nigrum* against diabetes. *Fitoterapia*.1985; 56 (3): 190-192.
2. **Filomena Conforti ,**"*In vitro* anti-oxidant effect and inhibition of α -amylase of two varieties of *Amaranthus caudatus* seeds", *Bio. Pharm. Bull.*, Vol 28(6), 1098-1102, 2005.
3. **Rajesh Kumar Gupta, Achyut Narayan Kesari, Sandhya Diwakar, Ameetabh Tyagi, Vibha Tandon, Ramesh Chandra, Geeta Watal,** "*In vivo* evaluation of antioxidant and anti lipidimicpotential of *Annona squamosa* L. aqueous extract in Type 2 diabetic model", *Journal of Ethnopharmacology*, Vol 118(1), 21-25, 2008.
4. **Bahman Nickavar, Leyla Aboulhasani and HamiderzaIzadpanah,** " α -amylase inhibitory activities of six *Salvia* species", *Iranian Journal of Pharmaceutical Research*, Vol 7(4),297-303,2008.
5. **Fröde TS, Medeiros YS.** Animal models to test drugs with potential antidiabetic activity. *J Ethnopharmacol*. Vol 115, 173–183, 2008. Patel, J.D. and Kumar, V. (2008). *Annona squamosa* L."Phytochemical analysis and antimicrobial screening", *Journal of Pharmaceutical Research* 1: 34-38.
6. **Thévenod F.** Pathophysiology of diabetes mellitus type 2: Roles of obesity, insulin resistance and β -cell dysfunction. *Front Diabetes Basel Karger*. Vol 19, 1–18, 2008.
7. **Sharma A. L., and Goray V. N. P. (2009)** "Pharmacognostical studies on the leaf of *Annona squamosa* L." *PHCOG J*, Vol I (2).
8. **Craig ME, Hattersley A, Donaghue KC.** "Definition, epidemiology and classification of diabetes in children and adolescents". *PediatrDiabetes*.Vol 10, 3–12, 2009.
9. **Rajsekhar Saha,** "Pharmacognosy and pharmacology of *Annona squamosa* L.:A review", *International Journal of Pharmacy and Life Science*, Vol2(10), 1183-1189, 2011.
10. **Neha Pandey and Dushyant Barve,** "Phytochemical and pharmacological review on *Annona squamosa* L.", *International Journal of Research in Pharmaceutical and Biomedical Sciences*, Vol 2(4), 1404-1412, 2011.
11. **Mona Agrawal, Yogesh Agrawal, Prakash Itankar, ArunPatil, Amrita Kelkar, Jayashree Vyas,** "Pharmacognostical evaluation of *Annona squamosa* L." *International Journal of Phytomedicine*, Vol 3, 480-485, 2011.
12. **Vanitha Varadharajan, Uma Devi, Kumba Janarthanan, Vijayalakshmi Krishnamurthy,** "Physicochemical, phytochemical screening and profiling of secondary metabolites of *Annona squamosa*L.leaf extract" *World Journal Of Pharmaceutical Research*, Vol 1(4), 1143-1164, 2012.
13. **Sindhu S. Nair, Vaibhavi Kavrekar and Anshu Mishra,** "*In vitro* studies on alpha amylase and alpha glucosidase inhibitory activities of selected plant extracts",*European Journal of Experimental Biology*,Vol 3 (1),128-132, 2013.



Comparative karyological studies of two varieties of *Zea mays* L. collected from Ranchi, Jharkhand, India

Sagufta Ismat* & Kamini Kumar

Department of Botany, Ranchi University, Ranchi, Jharkhand, India

*Corresponding author : Phone : 7488198187 , E-mail : saguftsmt14@gmail.com

Abstract: The seeds of *Zea mays* (L.) variety Birsa makka 1 and HQPM 1 were collected from Birsa Agricultural University, Kanke, Ranchi for comparative karyotype study. Both the varieties were reported to have diploid set of 20 chromosomes ($2n=20$) and were found to show asymmetrical karyotype.

Paper History:

Received

17th May 2017

Revised

12th June 2017

Peer reviewed

25th June 2017

Accepted

7th July 2017

Keywords: asymmetry, diploid, karyotype, *Zea mays* L.

INTRODUCTION

Maize belongs to the tribe Maydeae of the grass family Gramenae. “*Zea*” (zela) was derived from an old Greek name for a food grass. The genus *Zea* consists of four species of which *Zea mays* L. is economically important. The number of chromosomes in *Zea mays* is $2n=20$. The center of origin for *Zea mays* has been established as the Mesoamerican region, now Mexico and Central America. The word *Zea mays* comes from two languages. *Zea* comes from ancient Greek and is a generic name for cereal and grains and the meaning of *Zea* is “sustain life”. *Mays* come from the Spanish language Taino, which was spoken by aboriginal groups in the Antilles which means “life giver”. This scientific name shows the fact that plants are commonly known as “sustain life giver”. Maize is a tall, determinate, monoecious, annual plant. It produced large, narrow, opposite leaves, borne alternatively along the length of stem. In maize the sexes are partitioned into separate pistillate (ear), the female flower and staminate

(tassel), the male flower. In India, Maize is primarily a rain fed kharif crop which is sown just before monsoon starts. This crop usually grows well under temperatures varying from 22°C to 30°C . It is common grain in India.¹ To get improved cultivars cytogenetic information is necessary for selecting suitable species for agronomic and breeding program. Therefore present investigation was undertaken to study the karyological data.

MATERIALS & METHODS

Seeds of Birsa makka 1 and HQPM 1 of *Zea mays* (L.) were collected from Birsa Agricultural University, Kanke, Jharkhand and were used in this research work. Seeds were grown in the mixture of sand and vermicompost and allowed to grow in normal conditions. Newly emerged root apices of about 1-2 cm in length were excised between 12:30-1:30 am under sunlight. They were pretreated with 0.22% 8-hydroxyquinoline for 3-4 hours at 12°C temperature.² The pretreated root tips were

thoroughly washed with distilled water and fixed in fixative 1:3 acetoalcohol (Carnoy's fluid) for 24 hours. After 24 hours, root apices were rinsed properly with distilled water and transferred to 70% alcohol for preservation. The mitotic studies were performed by preparing slides in 2% Orcein solution.³ The root apices were warmed in 2% Orcein solution for about 1:15 hour. The squash

preparations were made by smearing the warmed root apices in 45% acetic acid solution.⁴ The microphotographs of well separated chromosome plates of metaphase stage were taken. The data were statistically analyzed. Karyotype analysis including ratio of long arm and short arm, total chromatin length, relative length, total form percentage, gradient index and symmetry index were calculated⁵.

Table: - 1 Karyomorphological data of two varieties of *Zea mays* L.

Variety	Chrom. No.	ARM LENGTH (μ)		CHROMOSOME LENGTH (μ)	ARM RATIO L/S	RL (μ)	F %	TCI	CLASSIFICATION
		LONG ARM	SHORT ARM						
Birsamakka1	1	2.96 ± 0.10	1.68 ± 0.09	4.64 ± 0.18	1.75 ± 0.05	100	36.20	15.143	nsm(-)
	2	2.64 ± 0.83	1.68 ± 0.09	4.32 ± 1.36	1.60 ± 0.09	94.82	36.37	14.36	nm
	3	2.32 ± 0.09	1.28 ± 0.09	3.60 ± 0.08	1.98 ± 0.25	77.58	35.56	11.75	nsm(-)
	4	2.16 ± 0.06	1.12 ± 0.05	3.28 ± 0.09	1.96 ± 0.09	70.68	34.15	10.70	nsm(-)
	5	2.00 ± 0.08	1.12 ± 0.09	3.12 ± 0.12	1.91 ± 0.17	67.25	35.89	10.19	nsm(-)
	6	1.76 ± 0.06	0.96 ± 0.06	2.72 ± 0.09	1.90 ± 0.12	58.62	35.29	8.88	nsm(-)
	7	1.60 ± 0.08	0.88 ± 0.05	2.48 ± 0.09	1.86 ± 0.13	53.45	35.48	8.09	nsm(-)
	8	1.52 ± 0.05	0.80 ± 0.00	2.32 ± 0.05	1.90 ± 0.06	50	34.48	7.57	nsm(-)
	9	1.28 ± 0.05	0.80 ± 0.00	2.08 ± 0.05	1.60 ± 0.06	44.83	38.46	6.78	nm
	10	1.20 ± 0.00	0.80 ± 0.00	2.00 ± 0.00	1.50 ± 0.00	43.1	40.00	6.53	nm
	Chrom. No.	ARM LENGTH (μ)		CHROMOSOME LENGTH (μ)	ARM RATIO L/S	RL (μ)	F %	TCI	CLASSIFICATION
		LA	SA						
HQPM1	1	3.44 ± 0.06	1.92 ± 0.09	5.36 ± 0.10	1.84 ± 0.10	100	35.80	14.90	nsm(-)
	2	3.04 ± 0.06	1.68 ± 0.09	4.72 ± 0.13	1.87 ± 0.13	88.05	35.60	13.13	nsm(-)
	3	2.72 ± 0.05	1.60 ± 0.08	4.32 ± 0.09	1.75 ± 0.10	80.59	37.04	12.01	nsm(-)
	4	2.64 ± 0.06	1.46 ± 0.12	4.10 ± 0.15	1.89 ± 0.10	76.49	35.60	11.40	nsm(-)
	5	2.32 ± 0.05	1.28 ± 0.09	3.60 ± 0.08	1.95 ± 0.18	67.16	35.56	10.01	nsm(-)
	6	2.24 ± 0.06	1.12 ± 0.09	3.36 ± 0.13	2.14 ± 0.17	62.68	33.34	9.35	nsm(-)
	7	1.92 ± 0.05	1.28 ± 0.05	3.20 ± 0.08	1.52 ± 0.05	59.7	40.00	8.90	nm
	8	1.92 ± 0.05	0.96 ± 0.06	2.89 ± 0.09	2.06 ± 0.12	53.73	27.90	9.57	nsm(-)
	9	1.52 ± 0.05	0.89 ± 0.05	2.40 ± 0.08	1.76 ± 0.09	44.96	36.92	6.70	nsm(-)
	10	1.20 ± 0.00	0.80 ± 0.00	2.00 ± 0.00	1.50 ± 0.00	37.31	40.00	5.56	nm

RL= Relative Length

F%= Form Percentage

TCI= Total Chromatin Index

Nm=Nearly median

Nsm= Nearly Sub Median

Karyotype Formula:

Birsamakka1= 3nm+7nsm(-)

HQPM 1=2nm+8nsm(-)

Table-2: Data related to Karyotype of the two varieties of *Zea mays* L.

Varieties	TCI	TF%	G.I	S.I
Birsamakka1	30.56	36.03	17.24	56.33
HQPM 1	35.95	36.13	14.93	56.58

TF%=Total Form Percentage

G.I= Gradient Index

S.I= Symmetry Index

Photographs:



Fig. 1: Mitotic metaphase chromosome of *Zea mays* L. var Birsa makka1.



Fig. 2: Mitotic metaphase chromosome of *Zea mays* L. var HQPM 1.

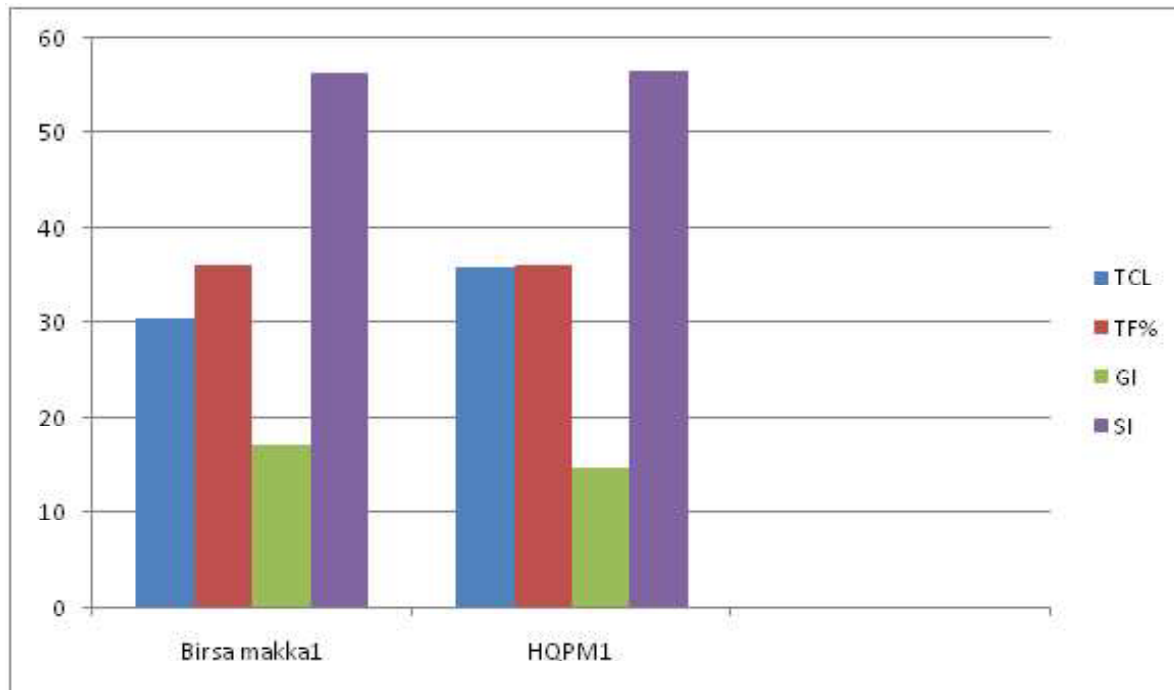


Fig-3: Column graph showing comparative Total Chromatin Length (in μ), T.F. %, G.I. value and S.I. value in different varieties of *Zea mays* L.

RESULTS

In this research, two variety of *Zea mays* L. were studied cytologically to carry out their detailed karyotype analysis. The statistical data of karyotype are presented in tables (Table-1&2) the diploid chromosome number in these two varieties of *Zea mays* L. was $2n=2x=20$. The uniformity in diploid chromosome number was observed. Both the variety of *Zea mays* L. showed $2n=20$ chromosomes. The total chromatin length (TCL) observed in Birsa makka1 is (30.56 μ) and in HQPM1 it is (35.95 μ). HQPM1 revealed maximum chromatin length and Birsa makka1 has minimum chromatin length. (Table-2) Birsa makka1 had $3nm+7nsm$ (-) chromosomes and HQPM1 had $2nm+8nsm$ (-) chromosomes. In both the varieties of *Zea mays* L. there was no telocentric chromosomes observed. The T.F % value, G.I value and S.I value has been shown in table 2. The highest T.F % value (36.13 μ) was observed in HQPM1 while the minimum was observed in Birsa makka1 which is (36.03 μ). The highest value of Gradient index (G.I) was observed in Birsa makka1 which was (17.24 μ). The highest value of symmetrical index was observed in HQPM1 (56.58 μ). (Table-2).

DISCUSSION

In both the varieties diploid chromosome count were $2n=20$.⁶ In both the varieties of *Zea mays* L. nearly median and nearly sub median chromosomes were observed which is presented in (table 1). Neither telocentric chromosome nor satellite chromosome was observed. The total chromosome length values show remarkable differences among the varieties of *Zea mays* L. This might be due to different repeated DNA sequence. Total form percentage, form percentage, Gradient index, symmetry index were observed for analytical studies of the karyotype symmetry, which indicates the nature of evolutionary process occurred among the species. In the present findings all the varieties of *Zea mays* L. have a low symmetrical index values, thus indicate the tendencies towards asymmetry. The gradient index in both the varieties of *Zea mays* L. are below 30. Therefore, they are considered highly asymmetrical as the G.I values are less than 30. Asymmetrical karyotype is considered advanced than symmetrical karyotype.⁷ The advancement has been further supported by TF% and F%. The varieties having

maximum chromatin length is considered most primitive and varieties having lowest chromatin length were considered as most advanced.⁸ In both the varieties of *Zea mays* L. it has observed that total form percentage of Birsa makka1 has value 36.03% which is lower than the HQPM1 variety having 36.13%. The gradient index was decreasing considerably. The Birsa makka 1 has value 17.24 μ which is more as compared to HQPM1 which has 14.93 μ and symmetry index of HQPM1 is more (56.58 μ) as compared to other one. All these values are depicted in table -2.

ACKNOWLEDGEMENT

I would like to express my sincere gratitude to our Head, University Department of Botany, Ranchi University, Ranchi, Jharkhand for providing the laboratory facilities.

REFERENCES

1. Series of crop specific Biology Documents "Biology of Maize".
2. Rayburn, A.L. Gold, J.R. "A procedure for obtaining mitotic chromosomes from maize". *Maydica* xxvii (1982): 113-121.
3. Chris Egbucha Kelechukwu, Aghale, Duke and Isa Hawau."Karyotype analysis in *zea mays* L. var. Everta (Popcorn) cultivated wiyhin Owerri, Southeast Nigeria". *International journal of Research in Applied, Natural and social sciences* (Impact :IJRANSS) vol 4 Issue 7 july, 2016, 127-132.
4. Filion, W. Gary and Walden, B. david (1973). "Karyotype Analysis: the detection of chromosomal alterations in the somatic karyotype of *Zea mays* L." *Chromosoma* (berl.) 41, 183-194.
5. Abraham.Z and P. Nagendra Prasad. "A system of chromosome classification and Nomenclature". *Cytologia* 48: 95-101,(1983).
6. Rhoades, M.M. and Mc Clintock, Barbara (1935). The cytogenetics of maize. *Bot. Rev.* 1: 292-325.
7. Levitsky, G.A. (1931). The karyotype in systematic Bulletin of applied Botany, Genetics and Plant Breeding.27:19-174.
8. Levan A; Fredga K. and Sandberg A.A 1964. "Nomenclature for centromeric position on chromosomes". *Hereditas* 52: 201-220.



A report on karyomorphological and stomatal studies of three varieties of *Triticum vulgare* (Vill.)

Sneha Singh* & Kamini Kumar

Department of Botany, Ranchi University, Ranchi, Jharkhand, India

*Corresponding author : Phone : 8676052661 , E-mail : snehalavis@gmail.com

Abstract: The three varieties of *Triticum vulgare* Vill. were collected from Birsa Agriculture University, Ranchi, Jharkhand for the studies on karyotype, mitotic activity and stomatal characters. The varieties were reported to show hexaploid set of 42 chromosome ($2n=6x=42$) and were asymmetrical. Each variety have different rate of mitotic activity. Graminacious type of stomata was found in these varieties of *Triticum vulgare* Vill. with variation in size and distribution.

Paper History:

Received

15th May 2017

Revised

22nd June 2017

Peer reviewed

28th June 2017

Accepted

21st July 2017

Keywords: *Triticum Vulgare* Vill. , Karyotype, Graminacious, hexaploid, Mitotic index.

INTRODUCTION

This report is based on relationship and classification of *Triticum vulgare* using comparative studies of chromosomes¹. *Triticum vulgare* Vill. or common wheat belongs to the family Poaceae (Syn.Gramineae), sub-family Pooideae and is commonly known as bread wheat (Belderak, Robert Bob; Mesdag, Hans and Donner, Dingena A.,2000) (Shewry, Petes R.,2009). It is third most produced cereal grain, originated from Levant region of the Near East cultivation began to 8000 BCE. It contains gluten (from which glutamate extract), carbohydrate, sugar, fat, fibre, protein, vitamin (B_1, B_2, B_5, B_6, B_9), minerals. Some wheat species are diploid but many are stable with polyploids with four set of chromosomes; tetraploids or six; hexaploids² (Hancock, James F.2004). Where present work is on hexaploid species (*T.vulgare* Vill.) collected from Birsa Agriculture University, Ranchi because hexaploid wheat evolved in farmer's fields. Medicinal values of wheat are antimicrobial, kidney infections, cough remedy, fertility treatment in women etc.

MATERIALS & METHODS

Source of Plant Material, collection and authentication.

The seeds of three varieties of *Triticum vulgare* Vill. were collected from Birsa Agriculture University, Ranchi, Jharkhand. The varieties of *T.vulgare* Vill. are –

1. *T.vulgare* Vill. var. HD-2967
2. *T.vulgare* Vill. var. K-307
3. *T.vulgare* Vill. var. K-9107

Seeds of each variety were germinated; the root apices of about 1-2 cm in length were excised between 1.30-2.00 pm under Sun light and were pretreated with ice cold water for 24 hours under freezing condition (Tsunewaki and Jenkins, 1980). The pretreated root tips were then thoroughly washed under distilled water and transferred to fixative 1:3 acetoalcohol (Carnoy's fluid) for 24 hours then transferred to 70% alcohol for preservation.

For Karyotype Study

Slides were prepared by 2% acetocarmine squash technique³ (Sharma, A. K. and Sharma, A. 1965). Number of chromosome, their length and position of centromere were measured in metaphase stage of cell division by the help of ocular and stage micrometer then data were statistically analyzed.

For Mitotic Study

Mitotic index is measurement of determining the percentage of cells undergoing mitosis. To measure the percentage of cells undergoing mitosis by using this formula -

$$\text{Mitotic index} = \frac{\text{Total no. of dividing cells}}{\text{Total no. of cells observed}} \times 100$$

For Stomatal Study

Fresh leaves of all three varieties of *T.vulgare* Vill. were taken for study of distribution of stomata on the upper and lower surfaces of the leaf by removing the peels of leaf by the use of Safranin (staining) and glycerene (mounting). Stomatal index were calculated by using this formula -

$$SI = \frac{\text{Total no. of stomata}}{\text{Total no. of epidermal cell} + \text{Total no. of stomata}} \times 100$$

1. Mean = $\frac{\sum x}{n}$
2. Standard deviation = $\sqrt{\frac{\sum (dx)^2}{n-1}}$
3. Standard error = $\frac{\text{standard deviation}}{\sqrt{n}}$

RESULTS

All the three varieties of *T.vulgare* bears the chromosome number $2n=6x=42$ (Murty, U.R.1973). The total chromatin length (TLC) observed in the variety HD-2967 of *T.vulgare* Vill. was 101.6μ (maximum), var. K-307 was 91.9μ and var. K-9107 was 87.4μ (minimum).

T.vulgare Vill. var. HD-2967 has 7NSM, 9NM, 2M and 3SM ; var. K-307 has 8NSM, 5NM, 2M, 1SM and 5NST; chromosomes and var. K-9107 has 6NSM, 7NM, 2M, 2SM and 4NST chromosomes.

Mitotic index of var. HD-2967 was 58.82%, var. K-307 was 58% and var. K-9107 was 59.95%.

All the three varieties of *T.vulgare* have elongated epidermal cell and dumble shaped stomata. Maximum

stomatal index was found in variety K-9107 (base, ventral surface) 27.67 ± 1.50 and minimum was found in var. HD-2967 (middle, ventral surface) 14.38 ± 2.19 .



Fig.1. Stomata of *T.vulgare* Vill. avr. HD-2967



Fig.2. Metaphase chromosome of *T.vulgare* Vill. var. HD-2967



Fig.3. Stomata of *T.vulgare* Vill. var. K-307



Fig.4. Metaphase Chromosome of *T.vulgare* Vill. var.K-307

Singh & Kumar: A report on karyomorphological and stomatal studies of three varieties of *Triticum vulgare* (Vill.)



Fig.5. Stomata of *T.vulgare* Vill var. K-9107



Fig.6: Metaphase Chromosome of *T.vulgare* Vill var. K-9107

Table.1: Stomatal index of three varieties of *T.vulgare* Vill.

Variety	Leaf surface					
	Dorsal			Ventral		
	Apex	Middle	Base	Apex	Middle	Base
var. HD-2967	25.16±2.30	20.21±0.72	24.60±1.66	26.00±2.17	14.38±2.19	16.00±1.31
var. K-307	19.70±2.04	17.31±2.08	22.30±1.53	18.45±1.70	26.92±0.78	17.53±0.90
var. K-9107	24.75±1.15	24.18±1.38	23.51±2.19	25.92±3.04	25.74±2.49	27.67±1.50

Table.2: Mitotic index of three varieties of *T.vulgare* Vill

Variety	No. of cells observed	Resting cells	Prophase	Metaphase	Anaphase	Telophase	Mitotic index
HD-2967	391	161	160	36	17	17	58.82%
K-307	412	173	154	41	25	19	58%
K-9107	432	171	182	34	26	17	59.95%

Table.3 (a): Karyomorphological data of *T.vulgare* Vill. var. HD -2967

Chrm. No.	Arm length(μ)		Total length (μ)	Arm ratio LA/SA	Classification
	Long arm	Short arm			
1	4.1	2.4	6.5	1.7	NSM
2	4	4	8	1	M
3	4	3.6	7.3	1.1	NM
4	4	2.8	6.8	1.4	NM
5	4	2.4	6.4	1.6	NM
6	4	2	6	2	NSM
7	4	1.2	5.2	3.3	NSM
8	3.6	1.2	4.8	3	SM
9	3.2	2.4	5.6	1.3	NM
10	3.2	2	5.2	1.6	NM
11	3.2	1.2	4.4	2.5	NSM
12	2.8	2.6	5.4	1	M
13	2.8	1.6	4.4	1.7	NSM
14	2.8	0.8	3.6	3.5	NSM
15	2.4	2	4.4	1.2	NM
16	2.4	1.6	4	1.5	NM
17	2.4	0.8	3.2	3	SM
18	2	1.2	3.2	1.6	NM
19	2	0.8	2.8	2.5	NSM
20	1.6	1.2	2.8	1.3	NM
21	1.2	0.4	1.6	3	SM
TLC(μ)			101.6		

Table.3(b): Karyomorphological data of *T.vulgare* Vill. var. K-307

Chrm. No.	Arm length(μ)		Total length (μ)	Arm ratio LA/SA	Classification
	Long arm	Short arm			
1	4.1	0.8	4.9	5.1	NST
2	4	4	8	1	M
3	4	2.8	6.8	1.4	NM
4	4	2.2	6.2	1.8	NSM
5	4	1.2	5.2	3.3	NSM
6	3.6	0.8	4.4	4.5	NST
7	3.2	2.4	5.6	1.3	NM
8	3.2	1.6	4.8	2	NSM
9	3.2	1.2	4.4	2.6	NSM
10	3.2	0.4	3.6	8	NST
11	2.8	2	4.8	1.4	NM
12	2.8	1.6	4.4	1.7	NSM
13	2.8	1.2	4	2.3	NSM
14	2.4	2.4	4.8	1	M
15	2.4	1.6	4	1.5	NM
16	2.4	0.8	3.2	3	SM
17	2.4	0.4	2.8	6	NST
18	2	0.8	2.8	2.5	NSM
19	2	0.4	2.4	5	NST
20	1.6	1.2	2.8	1.3	NM
21	1.6	0.4	2	4	NSM
TLC(μ)			91.9		

Table.3(c): Karyomorphological data of *T.vulgare* Vill. var. K-9107

Chrm. No.	Arm length(μ)		Total length (μ)	Arm ratio LA/SA	Classification
	Long arm	Short arm			
1	4	4	8	1	M
2	4	3.2	7.2	1.2	NM
3	4	0.8	4.8	5	NST
4	4	0.4	4.4	10	NST
5	3.6	0.8	4.4	4.5	NST
6	3.6	0.4	4	9	NST
7	3.2	1.6	4.8	2	NSM
8	3.2	1.2	4.4	2.6	NSM
9	3.2	0.8	4	4	NSM
10	2.8	2.4	5.2	1.1	NM
11	2.8	1.2	4	2.3	NSM
12	2.4	2	4.4	1.2	NM
13	2.4	1.6	4	1.5	NM
14	2.4	0.8	3.2	3	SM
15	2	2	4	1	M
16	2	1.6	3.6	1.2	NM
17	2	1.2	3.2	1.6	NM
18	2	1	3	2	NSM
19	1.6	1.2	2.8	1.3	NM
20	1.6	0.8	2.4	2	NSM
21	1.2	0.4	1.6	3	SM
TLC(μ)			87.4		

Singh & Kumar: A report on karyomorphological and stomatal studies of three varieties of *Triticum vulgare* (Vill.)

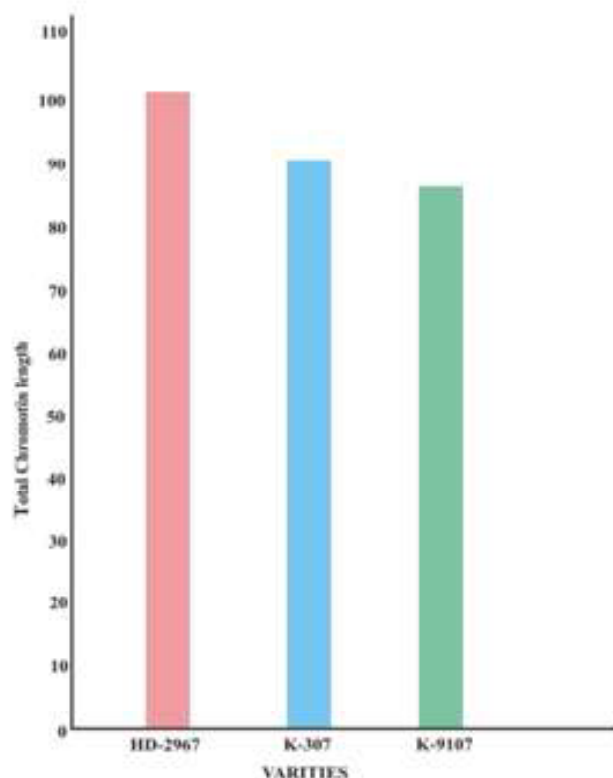


Fig.7: Histogram of three varieties of *T. vulgare* Vill.

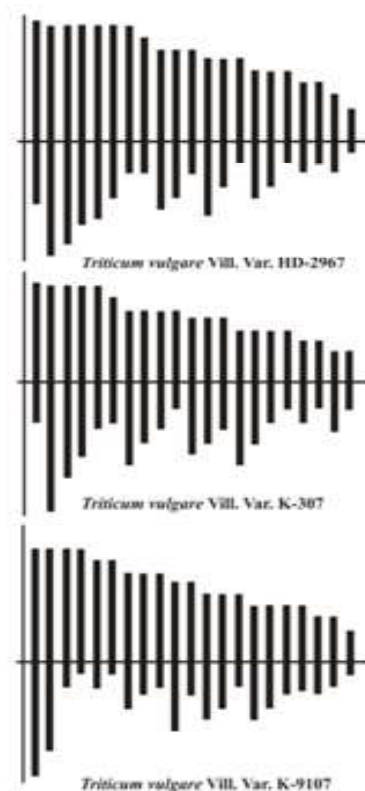


Fig.8: Ideogram of three varieties of *T.vulgare* Vill.

DISCUSSION

A simple metaphase chromosome preparation from meristematic root tip cells of wheat for karyotyping has been studied in 2010⁴. The difference in total chromatin length content may be due to chromosomal aberrations possibly due to deletion. *T.vulgare* Vill. var. HD-2967 has maximum TLC and was considered as most primitive and lowest TLC was observed in K-9107 and considered as most advanced stage (Levitsky,1931). Maximum mitotic index was observed in *T.vulgre* Vill. var. K-9107 and considering it most active and repair their injury (Urry,*et al.*2014) and minimum was var. K-307 keeping it in less active. In 2010, the variation for stomatal characteristics and water use efficiency among diploid, tetraploid and hexaploid Iranian wheat landraces⁵. No major difference between ventral surface and dorsal surface of stomatal number as wheat is monocot.

CONCLUSION

Triticum vulgare Vill. var. HD-2967 is most primitive and repair their injury at average rate. Var. K-307 is in between HD-2967 and K-9107 and repair their injury at very slow rate as compare to other two varieties. Var. K-9107 is most advanced stage and is most active for repair their injury.

ACKNOWLEDGEMENT

I would like to express my sincere gratitude to our Head, University Department of Botany, Ranchi University, Ranchi for providing the Laboratory facilities.

REFERENCES

1. Bhatia, G.S, (1938), "Cytology and Genetics of some Indian wheats.", Annals of Botany, New series Vol. 2(6), pp.335-371.

2. **Merker, A. (1973)**, “Identification of aneuploids in a line of hexaploids Triticale.”, *Hereditas*, Vol.74, pp.1-6
3. **Tsuchiya, T. (1956)**, “ An important aceto-carmin squash method, with special reference to the modified Ratten-busy’s method of making a preparation permanent”, Agronomy Department, Colorado State University, Fort Collins, Colorado, USA, pp. 71-72.
4. **Ghader and Mirzaghaderi (2010)**, “ A simple metaphase chromosome preparation from meristematic root tip cell of wheat for karyotyping or in situ hybridization”, *African Journal of Biotechnology*, Vol. 9(3). pp.314-318.
5. **Khazaei, H., Monneveux, P., Hongbo, S. (2010)**, “ Variation for stomatal characteristics and water use efficiency among diploid, tetraploid and hexaploid Iranian wheat landraces”, *Genetic Resources and crop evolution* Vol.57. pp.307.



Certain endangered and threatened ethnobotanically important plants of Ranchi district, Jharkhand

Arpan Anjan^{a*}, Malti Kerketta^b & Cynthia Khalkho^b

^{a*}I.I.T. Kharagpur

^bDepartment of Botany, Ranchi University, Ranchi, Jharkhand, India

*Corresponding author : Phone : , E-mail :

Abstract: Jharkhand came into existence as a separate state of Indian Republic on 15th November 2000. It includes the geographical territory of Chotanagpur & Santhal Paragna division of the Old Bihar State. Jharkhand Literally means “Land of Forest” and it has presently 29.61% forest area (the total area of Jharkhand is 79712 Sq. Kilometer). Ranchi is the capital and the largest district of Jharkhand. It is situated in the centre of Chotanagpur plateau of Jharkhand at an elevation of 652 meters above the sea levels approximately between 20°-23.6° North Latitude and 84.9°-85.9° East Longitude. Chotanagpur plauto the new Jharkhand where Ranchi, situated in full of forest, rivers and plants. So the people of this remote area is very much attached with forest and mountains. They love to live within nature. They behave with nature as their mother because all the necessary sources of their food, shelter and home are found in forest. So they worship some plants as God. They totally depend in forest for food cloth shelter and medicines also. Tribals dominant forest areas are playing an important role in ethnobotanical aspect in their day-to-day life.

Paper History:

Received

28th April 2017

Revised

26th June 2017

Peer reviewed

2nd July 2017

Accepted

28th June 2017

Keywords: Endangered, Ethnobotany Jharkhand.

INTRODUCTION

The plateau of Ranchi district is full of Mountains Rivers and forest. The plants are finding as pharmaceuticals cosmetics and food supplements. Even as traditional source of medicines and they continue to play pivotal rule. The world health (WHO) estimated the 80% of the population of developing countries still realise on traditional medicines. Mostly plant drugs, for their primary health care needs. Also modern pharmacopocia contains at least 25% drugs derived from plants. Many other are synthetic analogues built on prototype compounds isolated from plants. Demand for Medicinal plants is increasing in both developing and developed countries due to growing recognition of natural products, being non-toxic having no side-effects easily available at affordable prices.

Medicinal plant sector has traditionally occupied an important position in the socio-culture, spiritual and medicinal arena of rural and tribal lives of Ranchi District.

Millions of rural households use medicinal plants in self help mode. Number of ethnic people viz.-Oraon, Munda, Kharia, Ho, Santhali, Vocta etc. Tribal people have used plant species in their day-to-day life, such as food fodder medicines, vegetables, fibers and domestic purposes.

Literature reveals that certain places of Central India have been explored their ethno botanical utility (Jain 1981, Islam 1984, Brijlal and Dubey 1992, Khan & Khan 1997, Khan et. al 2000, Sukla et. al. 2001 and Sing 2002). Due to anthropogenic activity numbers of certain species are also going to be disappearing and included in the list of

endangered. Present investigation have recorded certain ethno botanically important plants and enumerated their uses in day-to-day life.

MATERIALS & METHODS

Ethnobotanical exploration were undertaken during 2000-2008 in different tribal dominant forest areas of Jharkhand. The uses of plants in different aspects of life specially medicinal purpose and causes of endangered were gathered from knowledgeable and elderly persons, because they are the only source to collect the informations about local plants name and their uses.

RESULTS & DISCUSSION

Plant species were enumerated alphabetically with family followed by their local name, habit, uses and treats to biodiversity.

Andrographis paniculata (Burm. f) Wall ex. Nees. Kalmegh

(Acanthaceae) Herbs, wild.

The plant is used for control sugar of diabetic patient, urinary trouble etc. Endangered.

Achyranthes aspera - Linn. Chirchira (Acanthaceae) Annual herbs.

Decoction of herb is useful in pneumonia, cough, kidney stone, leaf extract is used for Leprosy. A morph hallus c amp anulatus. Blume (Araceae) Herbs

It cures piles, abdominal tumours, intestinal worms and dysentery. Vegetable of tuber is useful during intestinal disorders.

Asparagus racemosus Willd (Asparagaceae) Shatawaree Climber

Satavari is powerful drug capable of improving memory power intelligence, physical strength and youthfulness. It is sweet bitter in taste. Roots are used to cure diarrhoea as well as in case chronic colic and dysentery. Tubers are refrigerant demulcent aphorodisiae, antidysentery and are useful in fever.

Ageratum conyzoides Linn. (Asteraceae) Osaaddee.

Aromatic, erect annual herb is used internally as a stimulant and tonic. Juice is a good remedy in prolapsusani. Oil applied in rheumatism, Leprosy, Skin diseases. Juice of leaves is antilithic.

Abelmoschus moschatus - Bhindi (Malvaceae) Annual herbs

Commonly known as Ladies finger. Although its different parts are used as traditional medicine and the traditional healers. It is heavy demand at national and international markets. The farmers are not growing it for the traditional healers. The healers are fulfilling their demand from wild population as well as from very small - scale cultivation.

Barteria prionitis Linn (Acanthaceae)

A much branched prikey shrub. Katsareya has antiseptic properties, its decoction is used in dropsy to wash the body. A decoction roots is used as mouth wash in toothach and paste is applied to disperse boils and glandular swelling leaves are chewed to relieve toothach.

Cissus quadrangularis Linn. (Vitaceae) Boneseter, Harkankani.

It is useful in indigestion, piles, worms and asthma. It has ability to rejoin broken bones. Juice of plant is beneficial in scurvy, Fresh shoots are applied for burns and wounds.

Centella asiatica L. Urban

(Apiaceae) Beng Sag

Centella is used as a leafy vegetables. It is most often prepared as vegetable and dal. *Centella* appears to act on the various phases of connective tissues development, which are part of the healing process and increases Keratinization which allows it to stimulate healing of ulcers, skin injuries, connective tissue and to decrease capillary fragility.

Ficus bengatensis Linn. Morace Banyan tree

An infusion of bark cures desentry nervous disorders, diarrhoea and reduces blood sugar in diabetes, Milky juice is beneficial as local application in toothache, sores and ulcers. Infusion of young buds is used in diarrhoea and descentry.

Ficus religiosa Linn. Moraceae Peepal tree.

Leaves and young shoots are purative. Bark is astringent and found efficacious in gonorrhoea, Infusion of bark given internally in scabies, ulcers and skin diseases.

Psidium guajava, Linn. Myrtaaceae Amrud

Leaves are used as astringent for bowels and wounds and ulcers, Young leaves are used as a tonic in the diseases of digestive functions. Flowers are said to cool the body and are used in bronchitis. Perukam fruit is tonic, cooling and laxative. It is good in colic and for bleediy gums.

Anjan *et. al.*: Certain endangered and threatened ethnobotanically important plants of Ranchi district, Jharkhand

Fruits and its conserve are astringent and used in diarrhoea and desentery.

Phyllanthus niruri Linn. Euphorbiaceae. Bhuee acolla. Herbs.

It is used as a diuretic in dropsical affection and other trouble of genito urinary tract. Herb is bitter, astringent, deobstruent, diuretic, febrifuge and antiseptic. Fresh root is a remedy for jaundice. Milky juice used as applications to sore. Leaves are a popular remedy against fever. Fusion of young shoots given in dysentery.

Ziziphus mauritiana Lamk. Rhamnaceae tree. Ber

Ber roots is bitter and cooling, biliousness and headache. Decoction of roots is used in fever. Fruits is mucilaginous, pectoral, styptic considered to purify blood and aid digestion.

Ethnic people of Jharkhand is well known for its heritage regarding medicinal plants growing near forest areas. The ethno medicinal values differ from species to species in composition and properties. Some plants have characteristic of quality timber, edible fruits and some are poisonous and also medicinal.

Many species are used in medicinal purposes by different tribal people and above other uses as food, fodder, fiber, timber and other purposes.

Due to different anthropogenic causes many of the specimen enumerated in the list are becoming threatened like *Centella asiatica*, *Asparagus recemosus* Vitex, *Lantana* and very rare are *Clerodendron* species.

Different measures have been adopted for conservation of these categories of species. So that it may remain protected for the benefit of the present generation. Maintaining its potential to meet the needs of the present future generation is additional priority of such ethnobotanical study.

ACKNOWLEDGEMENT

The authors are highly thankful to the Principal, Ranchi College, Ranchi & Head, University Department of Botany, Ranchi University, Ranchi for their all round encouragement & support.

REFERENCES

1. **Islam, M. 1984.** A study on the economic uses of certain wild edible vegetable of the N. Eastern region, India, *Proc. Nat. Acad. Sci.* 54(B) : 245-251.
2. **Jain, S.K. (Ed.) 1981.** Glimpses of Indian Ethnobotany, Oxford and IBH Co. New Delhi.
3. **Khan, A.A. Shukla, K.M.L. and Khan, I.M. 2000.** Enumeration of wild plants of ethnobotanical significance in Central India, *Adv. Pol. Sci.* 13(I) : 277-281.
4. **Shukla, K. M. L. Khan, A. A. Khan, Shabina and Verma, Ashok Kumar 2001,** Traditional Phytotherapy of Maikal range and Plateau of Pendra district Bilaspur (M.P.), *India Adv. Pol. Sci* 14 (I) : 11-14.



Apical shoot elongation of *Lawsonia inermis* L. through tissue culture in plane medium

Nazra Paiker* & Kunul Kandir

Department of Botany, Ranchi University, Ranchi, Jharkhand, India

*Corresponding author : Phone : 7070457082 , E-mail : nazrapaiker80@gmail.com

Abstract : Apical shoot elongation of *Lawsonia inermis* L. was carried out in MS media without any growth regulations. Small apical shoots of young plants were used as explants.

Paper History:

Received

17th April 2017

Revised

22nd April 2017

Peer reviewed

20th May 2017

Accepted

1st June 2017

Keywords: Endangered Ethnobotany Jharkhand.

INTRODUCTION

Lawsonia inermis L. belongs to the family Lythraceae. It is branched shrub or small tree. It is native of Middle East Africa. It is commonly known as Mehendi in Hindi of Egyptian Henna. The leaves of the henna plant have a red orange dye molecule Lawsone. Lawsone is a nethaquinon compound. Decoction of its leaf is used as a gargle against sore throat.¹

MATERIALS & METHODS

In the present investigation apical portion young shoots were used for experiments. The segments of apical shoots were inoculated on Ms Medicein without any phytoharmones.

OBSERVATION

Apical shoot elongation of *Lawsonia inermis* L. in plane MS medium was observed.

RESULTS & DISCUSSION

In this investigation apical shoots were cultured in plane medium. After 45 days elongation of shoots were obtained. Several attempts have been made to utilize the *in vitro* micropropagation method for rapid clonal multiplication of many tropical, subtropical and temperate fruits². Bud cultured on hormone free basal medium showed elongation, shoot elongation occurred only when cytokinin was omitted from the medicein³.

Shoot elongation of *Lawsonia inermis* L. in plane Ms medicein (without any growth hormones) in duration of sixth week in observation.

MS medium (plane)	Apical shoot elongation (in cm)					
	1st week	2nd week	3rd week	4th week	5th week	6th week
1	1.5	1.5	1.9	2.0	2.5	3.0
2	1.6	1.6	2.0	2.2	2.7	3.2
3	1.7	1.7	2.1	2.3	2.7	3.4
4	1.8	1.8	2.2	2.4	2.9	3.5
5	1.9	1.9	2.4	2.6	3.0	3.8

ACKNOWLEDGEMENT

Authors are thankful to Head, University Department of Botany, Ranchi University Ranchi for providing necessary laboratory facilities.

REFERENCES

1. Rout, G.R., Das, G., Samantaray, S. and Das, P. 2001. *In vitro* micropropagation of *Lawsonia inermis* L. (Lythraceae Int. J. Trop Bio L. Conserv. 49 : 1-7.
2. Bush, S. R., Earle, E. O. and Langhans, R. W. 1976. Plantlets from petal epidermis and shoot tips of the periclinal chimera, *Chrysanthemum morifolium* 'Indian napolis. Amer. J. Bot., 63 : 729-737.
3. Morel, G. 1971. Deviation du meristem apical de certaines orchidus. C. R. Hebd. Scances Acad. Soci. 256 : 4955-4951.



Electro organic synthesis of Schiff bases as chelating reagents

Shreya Gorai* & M. Alam

Department of Chemistry, Ranchi University, Ranchi, Jharkhand, India

*Corresponding author : Phone : 8083760470, E-mail : shreyagorai.gorai@gmail.com

Abstract: Electroorganic interaction of copper metal with salicylaldehyde and ammonia leads to the formation of chelate metal complexes. This paper covers structural features of Schiff base complexes on the basis of their elemental analysis and IR spectroscopy data.

Paper History:

Received

7th May 2017

Revised

22nd June 2017

Peer reviewed

25th June 2017

Accepted

1st July 2017

Keywords: salicylimine, salicylaldehyde, Schiff base, LiClO_4

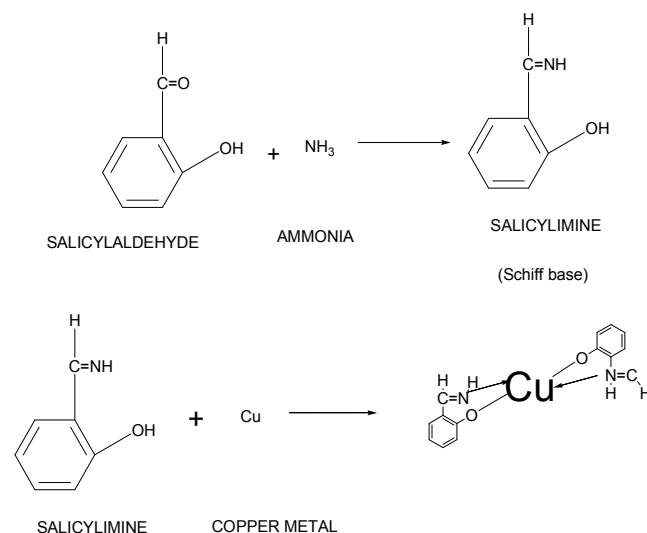
INTRODUCTION

Schiff base is considered as one of the most popular families of organic compounds which are used as synthetic intermediates as well as quite helpful in establishment of coordination chemistry¹. Hugo Schiff first introduced Schiff base². When aldehydes and ketones react with primary amines, a class of compounds is produced that contains a carbon-nitrogen double bond called imines, or Schiff bases.

Due to their Physico-chemical properties, an important role has been played by Schiff bases as chelating ligands for transition metal and for the development of coordination chemistry. Since they have flexible nature and easy proton donating property, the study of Schiff bases and their complexes

With transition metals has flourished since few decades. Schiff base ligands show a number of sites for binding that lead to higher coordination polyhedral and cause greater kinetic and thermodynamic stability.

In our present study salicylaldehyde react with ammonia to form salicylimine (Schiff base), this Schiff base shows two binding site through which it coordinate to copper metal to form chelate complex.



This above reaction is carried out in electrochemical cell. Synthesis of organic compound in electrochemical cell is known as electroorganic synthesis. Electro organic synthesis presents many advantages over classical routes such as high efficiency, lower prices of metals and high reactivity of products³.

In this method, complexes can be achieved either at a constant current or controlled potential. The synthesis of metal complexes with organic ligand is both cathodically and anodically possible either the metal or the ligand can be subject to the primary electrochemical attack^{4,5}. By applying a voltage between the electrodes, the metal is dissolved at the anode and the substrate is reduced at the cathode. The principle (Fig. 1) is standed to be an electrode process followed by a chemical reaction between both generated ions (metal ion and carbanion)^{6,7}. During this process the electrons are transferred from the cathode to the reaction mixture and from the reaction mixture to the anode and consequently allows an electrical current to flow through the cell.

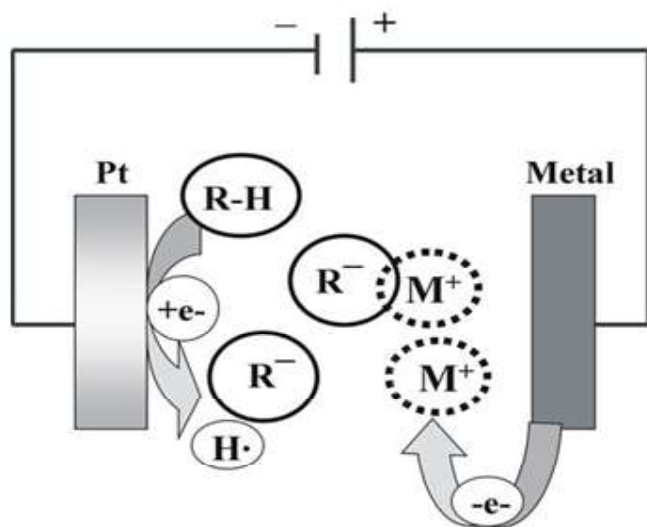


Fig - 1

If ligands possess an acidic group (OH, SH, HNR, HSe) then the dissociation of the acid takes place giving L⁻ and the solvated proton H⁺ (scheme 1) [44].

Cathode: $nHL + H^+$

Anode: $M \rightarrow M^{n+} + ne$

Complex formation: $M^{n+} + n L \rightarrow ML_n$

Scheme 1: L = LIGAND, M=METAL

In our present work of electro synthesis, we have used zinc as anode to form complexes with salicylaldehyde and ammonia. Pt electrode is used as cathode material because of its inertness in most electrolyte environments and its high oxygen over potential in aqueous media. We have carried out these electrochemical synthesis in undivided cell. Acetone and methanol were used as solvent and lithium perchlorate as electrolyte with 3v DC supply under atmospheric condition. The solids formed were isolated in the pure form and characterized on the basis of elemental analysis and FTIR spectral studies.

Chemical used: salicylaldehyde, ammonia, LiClO₄, acetone, methanol (chemical used were A.R grade)

EXPERIMENTAL METHOD

Ligand: salicylimine

0.5g LiClO₄ was dissolved in 5 ml of methanol in a 100 ml beaker. 4ml salicylaldehyde and 2ml of ammonia was added in the solution. The solution was electrolyzed using Pt as cathode and Cu as sacrificial anode under 3v DC supply. The continuation of electrolytic process was confirmed through the bubbles emerging out of Pt electrode. After 24 hrs., Green colored solution was obtained which was filtered and dark green precipitate was thus obtained. It was then washed with acetone, dried and collected as SHSN-2. The complex obtained in pure state was subjected to elemental and spectral analysis.

ELEMENTAL ANALYSIS AND RELATED DATA

Table - 1

Sample	colour	C%	H%	N%	O%	M%	Empirical formula
SHSN -2	Dark green	f: 53.33 c: 52.25	f: 3.55 c: 4.35	f: 8.164 c: 8.70	f: 12.7 c: 14.9	f: 22.3 c: 19.5	C ₁₄ H ₁₄ O ₃ N ₂ Cu

c = Calculated data, f = formulated data

Probable molecular formula: Cu (C₆H₄OCHNH)₂·H₂O

RESULTS & DISCUSSION

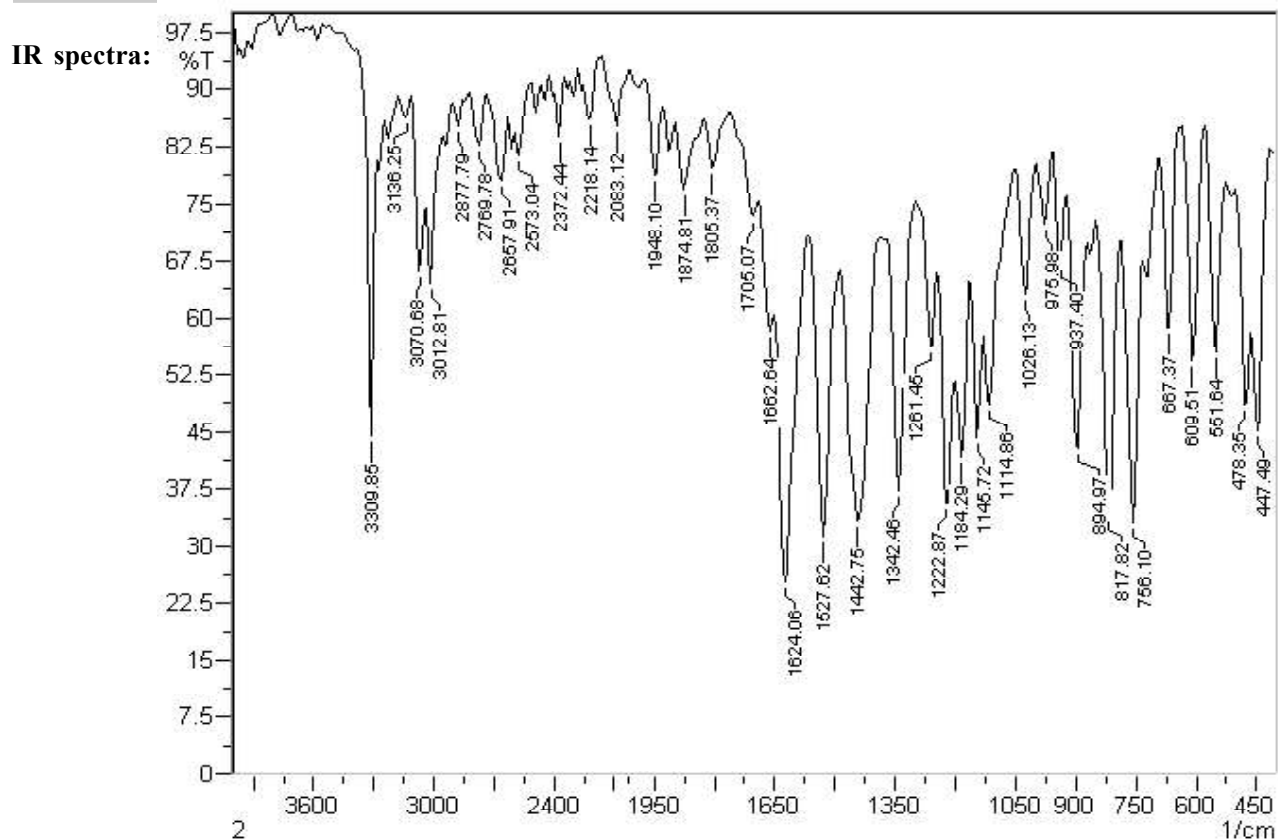


Fig - 2

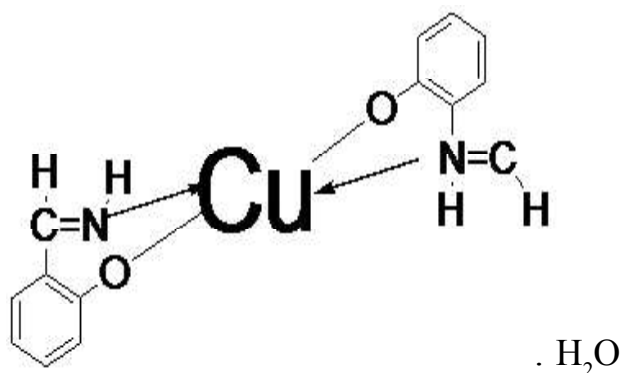
TABLE - 2

peaks	Nature of peaks	Group assignment
3309.85	sharp	-N-H Stretching
3070.68	Sharp	=C-H aromatic stretching
2877.79	Weak	overtone
2769.78	Weak	overtone
1662.64	Sharp	-C=N Imine stretching
1624.06	sharp	Aromatic stretching
1527.62	sharp	(C=O) O bonded +aromatic C=C Stretching
1442.75	sharp	C-O phenolic bending + C=C Stretching
1342.46	sharp	-C-N Stretching
1261.45	sharp	-C-O stretching
1222.87	Sharp	C-C-H in plane aromatic bending
1026.13		C-C skeletal vibration
975.98	weak	O-H out of plane bend
937.40	weak	O-H coordinated
894.97	Sharp	O- H rocking coordinated H ₂ O
817.82		
756.10	sharp	O-substituted phenyl group
667.37	sharp	M-O stretching
609.51	sharp	M-O stretching
551.64	sharp	M-O bending + M-N

The FTIR curves (fig: 1) of sample 1 contain all the peaks which are expected for the formulation. The broad band at 3309 cm⁻¹, corresponds to stretching vibration of N-H group to form coordinate bonding with metal by donation of lone pair of electron from nitrogen atom. The band at 1527 cm⁻¹ and 3070 cm⁻¹ were assigned to C=C and =C-H aromatic stretching respectively. There is a sharp band at 1662.64 cm⁻¹ confirmed the presence of -C=N stretching band. The presence of coordinated water is further confirmed by the appearance of bands in the region of 894- 937 cm⁻¹ assignable to the rocking mode of coordinated water. The appearance of band at 609 cm⁻¹ and 513 cm⁻¹ in the complex due to frequency of metal and oxygen bond (M-O). The bands at 2877 cm⁻¹ are due to C-H stretching of aldehyde group.

Proposed Formulation:

The elemental analysis and IR spectra supported the formulation shown in fig 2 and table 1 of sample SHSN-2



ACKNOWLEDGEMENT

The author is grateful to Dr. M. Alam for improvement of paper. The author is thankful to the CIF, B.I.T. Mesra for providing data of elemental analysis. This work was supported by chemistry laboratory, Department of Chemistry, Faculty of Science Ranchi University, Ranchi, Jharkhand.

REFERENCES

1. Tidwell, T. T. Hugo (ugo) Schiff, Schiff bases, and a century of β -lactam synthesis. *Angew. Chem. Int. Ed.*, **2008**, 47(6), 1016-1020.
2. Schiff, H. Mittheilungen aus dem universitatlaboratorium in pisa: Eine neue reihe organischer basen. *Justus Liebigs Annalen der Chemie*, **1864**, 131(1), 118-119.
3. Saima Q. Memon, Najma Memon, Arfana Mallah, Rubina Soomro and M.Y. Khuhawar: Schiff Bases as Chelating Reagents for Metal Ions Analysis. *Current Analytical Chemistry*, **2014**, 10, 393-417
4. <https://sundoc.bibliothek.uni-halle.de/diss-online/04/04H193/t3.pdf>
5. Garnovskin, A.D; Karisov, B. I; Direct Synthesis Of Coordination And Organometallic Compounds. 1st ed. 1999, pp 82-85
6. Davis, J.A; Hockensmith, C.M; Kukushkin, V YU; synthetic coordination chemistry: principles and practice. world scientific publishing. 1996, pp-198
7. Kumar, S; Sharma, K.L; Singh, R.K.P; Electroorganicsynthesis: a novel route of green synthesis. *Indian chem. Soc.* 2006, 86, pp 1129-1142



Oxidation of phenyl hydrazine by ditertiarybutyl chromate in non-aqueous media

Richa Kumari*

Department of Chemistry, S.S. Memorial College, Ranchi, Jharkhand, India

*Corresponding author : Phone : 8582050688 , E-mail : richa83kumar@gmail.com

Abstract: Conventional heating usually involves the use of a furnace or oil bath, which heats the walls of the reactor by convection or conduction. In the present paper we report the study of products of oxidation of Phenyl hydrazine by ditertiary butyl chromate¹⁻⁵ in few non aqueous solvents like acetonitrile, tetrahydrofuran and dioxane. The substrate solution and ditertiary butyl chromate was taken in appropriate ratio, mixed, stirred and irradiated in specified periods. The solid products of different colour and compositions so obtained were studied by elemental analysis, FTIR curves and thermogravimetric⁶⁻⁸ mass loss pattern.

Paper History:

Received

17th April 2017

Revised

12th May 2017

Peer reviewed

2nd June 2017

Accepted

12th June 2017

Keywords: Phenyl hydrazine, Ditertiarybutylchromate, Dioxane, Tetrahydrofuran

INTRODUCTION

Phenylhydrazine is the chemical compound with the formula $C_6H_5NHNH_2$. Organic chemists abbreviate the compound as $PhNHNH_2$. It is colorless to pale yellow liquid. An aryl hydrazine used in the preparation of various dyes and pharmaceutical compounds. It is used in the investigation of oligosaccharides as well as the structure of photo system II. It is soluble in alcohol. When it is exposed to air it becomes red-brown. It is slightly denser than water and slightly soluble in water. Phenylhydrazine may ignite spontaneously when in contact with oxidants such as hydrogen peroxide or nitric acid, oxides of iron or copper, or manganese, lead, copper or their alloys. Material is corrosive to tissue.

In the present work the oxidation of phenyl hydrazine was carried out by TBC in non aqueous solvent such as tetrahydrofuran (THF), dioxane and acetonitrile⁹⁻¹⁰. The oxidation of phenyl- hydrazine was carried out in different substrate: oxidant molar ratios taken were 1:1 and 1:2, 2:3. The solid products obtained after oxidation in each

case, were having different colour and composition. Precaution was taken at the time of mixing the solutions in order to avoid the reaction being violent. The products obtained were washed several times with acetone and dried. Then the dried products were powdered in a mortar and pestle and collected in air-tight glass bottles.

The products obtained in the pure states were analyzed for their elemental composition, FTIR spectrum, thermo gravimetric⁶ measurements and volumetric estimation of chromium etc. All the products obtained were found insoluble in water. It is expected that phenyl hydrazine on oxidation will give rise to different products depending on various factors such as the type of oxidant used, the extent of oxidation, the concentration of reagents, different reaction condition etc.

Table-1 give detailed information about various products formed by the oxidation of phenyl hydrazine in different molar ratios, solvent for the substrate, oxidant used, time required and mode of heating, colour of the products, solubility etc.

TABLE-1

Product Code	Solvent	Oxidant	O:S ratios	Heating condition	Colour	Solubility In water	Empirical formula
R-1	THF	TBC	1:1	No Heating	Greenish Grey	Insoluble	$\text{Cr}_3\text{C}_6\text{H}_{24}\text{O}_{15}$
R-2	THF	TBC	1:2	No Heating	Dark grey	Insoluble	$\text{Cr}_3\text{C}_6\text{H}_{24}\text{O}_{15}$
R-3	THF	TBC	2:3	No Heating	Greenish Grey	Insoluble	$\text{Cr}_4\text{C}_6\text{H}_{32}\text{O}_{22}$
R-4	Dioxane	TBC	1:1	No Heating	Light Grey	Springly Soluble	$\text{Cr}_6\text{C}_6\text{H}_{48}\text{O}_{30}$
R-5	Dioxane	TBC	1:2	No Heating	Dark grey	Insoluble	$\text{Cr}_3\text{C}_6\text{H}_{24}\text{O}_{15}$
R-6	Dioxane	TBC	2:3	No Heating	Light Grey	Insoluble	$\text{Cr}_6\text{C}_6\text{H}_{42}\text{O}_{24}$
R-7	Acetonitrile	TBC	1:1	No Heating	Dark grey	Springly Soluble	$\text{Cr}_9\text{C}_6\text{H}_{60}\text{O}_{36}$
R8	TBA	TBC	1:1	No Heating	Light Grey	Insoluble	$\text{Cr}_9\text{C}_6\text{H}_{54}\text{O}_{36}$
R-9	TBA	TBC	1:2	No Heating	Light Grey	Insoluble	$\text{Cr}_3\text{C}_6\text{H}_{36}\text{O}_{24}$
R-10	Acetonitrile	TBC	1:2	No Heating	Ash Grey	Insoluble	$\text{Cr}_3\text{C}_6\text{H}_{21}\text{O}_{15}$

Microwave assisted oxidation of Phenylhydrazine by TBC

(a) Oxidant: Substrate ratio (1:1):

The oxidant was prepared by dissolving 1g of CrO_3 in 10ml of TBA in a clean and dry beaker. In another beaker 1ml of phenyl hydrazine was accurately weighed and dissolving in 10ml of THF. The two solutions were mixed well slowly and get greenish precipitated. It was kept overnight and then washed several times with acetone, dried and collected in air-tight bottle as sample no.R-1.

(b) Oxidant: Substrate ratio (1:2):

The oxidant i.e. TBC, was prepared by dissolving 500 mg of CrO_3 in 10ml TBA in a clean beaker 1 ml of phenyl hydrazine was dissolved in 10ml of THF in another beaker. The two solutions were mixed well slowly and appear green precipitated. It was washed several times with acetone, dried and collected as sample no.R-2.

(c) Oxidant: Substrate ratio (2:3):

The oxidant was prepared by dissolving 1g of CrO_3 in 10ml of TBA in a clean and dry beaker. In another beaker 1.5 ml of phenyl hydrazine was dissolving in 10ml of THF.

The two solutions were mixed well slowly and appear green precipitated. It was kept overnight and then washed several times with acetone, dried and collected in air-tight bottle as sample no.R-3.

(d) Oxidant: Substrate ratio (1:1):

The oxidant was prepared by dissolving 1g of CrO_3 in 10ml of TBA in a clean and dry beaker. In another beaker 1 ml of phenyl hydrazine was dissolving in 10ml of dioxane. The two solutions were mixed well slowly and appear green precipitated. It was then washed several times with acetone, dried and collected in air-tight bottle as sample no.R-4.

(e) Oxidant: Substrate ratio (1:2):

The oxidant was prepared by dissolving 500 mg of CrO_3 in 10ml of TBA in a clean and dry beaker. In another beaker 1 ml of phenyl hydrazine was dissolving in 10ml of dioxane. The two solutions were mixed well slowly and appear green precipitated. It was then washed several times with acetone, dried and collected in air-tight bottle as sample no.R-5.

(f) Oxidant: Substrate ratio (2:3):

The oxidant was prepared by dissolving 1g of CrO_3 in 10ml of TBA in a clean and dry beaker. In another beaker 1.5 ml of phenyl hydrazine was dissolving in 10ml of dioxane. The two solutions were mixed well slowly and appear green precipitated. It was then washed several times with acetone, dried and collected in air-tight bottle as sample no.R-6.

(g) Oxidant: Substrate ratio (1:1):

The oxidant was prepared by dissolving 1g of CrO_3 in 10ml of TBA in a clean and dry beaker. In another beaker 1 ml of phenyl hydrazine was dissolving in 10ml of acetonitrile. The two solutions were mixed well slowly and appear green precipitated. It was kept overnight and then washed several times with acetone, dried and collected in air-tight bottle as sample no.R-7.

(h) Oxidant: Substrate ratio (2:3):

The oxidant was prepared by dissolving 1g of CrO_3 in 10ml of TBA in a clean and dry beaker. In another beaker 1 ml of phenyl hydrazine was dissolving in 10ml of TBA. The two solutions were mixed well slowly and appear green precipitated. It was then washed several times with acetone, dried and collected in air-tight bottle as sample no.R-8

(i) Oxidant: Substrate ratio (1:2):

The oxidant was prepared by dissolving 500 mg of CrO_3 in 10ml of TBA in a clean and dry beaker. In another beaker 1 ml of phenyl hydrazine was dissolving in 10ml of TBA. The two solutions were mixed well slowly and appear green precipitated. It was kept overnight and then washed several times with acetone, dried and collected in air-tight bottle as sample no.R-9.

(j) Oxidant: Substrate ratio (1:2):

The oxidant was prepared by dissolving 500 mg of CrO_3 in 10ml of TBA in a clean and dry beaker. In another beaker 1 ml of phenyl hydrazine was dissolving in 10ml of TBA. The two solutions were mixed well slowly and appear green precipitate. It was kept overnight and then washed several times with acetone, dried and collected in air-tight bottle as sample no.R-10.

RESULTS & DISCUSSION

On the basis of the parameters measured, we have been able to suggest the empirical formulation of the

compounds/complexes prepared. However, a lot more can be done as a fruitful extension of the present work. For example, the measurement of molecular masses by cryoscopic and ebullioscopic methods for soluble complexes, the measurement of their magnetic susceptibility, the measurement of optical rotation etc. will definitely tell us about the geometry of the compounds/complexes in different oxidation states of chromium.

The calculation of the oxidation states of the metal and significant atoms of the organic substrate, the time taken for their preparation by conventional and microwave methods may be helpful in the elucidation of the mechanism of the reactions involved.

Moreover, the study of solvents on the rate and yield of the product may suggest the suitable media for the reaction and thus it may help control of environmental pollution.

ACKNOWLEDGEMENT

The authors are thankful to CIF, BIT, Mesra, Ranchi and Research and Development centre, Tezpur University, Assam for their cooperation in carrying out the test and analysis of samples.

REFERENCES

1. **Anderson, R. A.** . "Chromium as an Essential Nutrient for Humans". *Regulatory Toxicology and Pharmacology* 26, **1997** .
2. **Moukarzel A .** "Chromium in parenteral nutrition: too little or too much?". *Gastroenterology* 137, **2009**.
3. **Vincent, John B.** "Chromium: Celebrating 50 years as an essential element?". *Dalton Transactions* 39, **2010**.
4. **Stearns, D. M.; W; P; W** "Chromium(III) picolinate produces chromosome damage in Chinese hamster ovary cells". *FASEB J.* 9, 1 December **1995**.
5. **Vincent, J. B.,**"Recent advances in the nutritional biochemistry of trivalent chromium". *Proceedings of the Nutrition Society* **63** (1): 41–47, **2007** .a.Thor MY, Harnack L, King D, Jasthi B, Pettit J Dec **2011**
6. **Coats, A. W.; Redfern, J. P.** "Thermogravimetric Analysis: A Review". *Analyst* **88**: 906–924, **1963**.

7. **Tikhonov, N. A.**; Arkhangelsky, I. V.; Belyaev, S. S.; Matveev, A. T. "Carbonization of polymeric nonwoven materials". *Thermochimica Acta* **486**: 66–70, **2009**.
8. "Thermogravimetric Analysis".
9. **DiBiase, S. A.**; **Beadle, J. R.**; **Gokel, G. W.**, "Synthesis of α,β -Unsaturated Nitriles from Acetonitrile: Cyclohexylideneacetonitrile and Cinnamonnitrile", *Org. Synth. ; Coll. Vol. 7*: 108.
10. **Philip Wexler**, ed. *Encyclopedia of Toxicology*, Vol. 1 (2nd ed.), Elsevier, pp. 28–30, **2005**.



Synthesis of heteropoly complexes containing Al^{3+} and Ce^{4+} and cations

Ranjeeta Sharma*, Alok Kumar Thakur, G. S. Tiwari & Rajesh Kumar

Department of Chemistry, Ranchi University, Ranchi, Jharkhand, India

*Corresponding author : Phone :8448724988 , E-mail : ranjeetasharma121982@gmail.com

Abstract: The three of heteropoly complexes were synthesised by conventional reflux method in the water bath separately by mixing Isopoly anions of Mo, V, and W. All the products isolated in solid state were crystalline in nature appeared as bright yellow in colour. The physical and chemical methods were applied to characterize all the isolated products. The IR analysis applied for identification of group frequencies also suggests the ionic nature of sodium for the isolated complexes in solid state. The thermal analysis involving DTA and TGA support the stability of complexes in the atmosphere due to the presence of large no of water of hydration. The chemical analysis suggests the ionic nature of complexes since the complexes were dissolved in warm water. The inorganic wet analysis suggests ionic nature of sodium as its cation in association with complexes. The magnetic susceptibility measurement support the paramagnetic nature of all the isolated products containing Al^{3+} and Ce^{4+} hetero cation.

Paper History:

Received

20th April 2017

Revised

2nd May 2017

Peer reviewed

28th May 2017

Accepted

20th June 2017

Key words:- Preparation, Cryoscopy, TGA & DTA thermal studies, Magnetic susceptibility and I.R.spectral studies.

INTRODUCTION

The heteropoly complexes containing isopoly anions along with hetero atoms of vanadium, molybdenum and tungsten were synthesized much earlier by Tsigidimos and co-workers,¹ in the weak acidic medium created by addition of proper amount of acetic acid into the aqueous solution of sodium tungstate, sodiummetavanadate and sodium molybdate aqueous solutions. The method of synthesis of heteropoly tungstate involves heating at reflux temperature for two and half hours of the mixture solution & as a result the bright brown coloured residue was formed in its solid state. The role of weak acidic medium is to form poly tungstate anion because in the strong acidic medium as well as in alkaline medium the poly tungstate anions will split into simple tungstate anions. The mechanism of the formation of poly tungstate anions suggested as when the proper weak acidic medium is created then the simultaneous elimination of water molecules enable to form poly oxometallate anion of the tungsten containing metal

oxygen bridge which ultimately form giant polycomplex ion having specific ionic structure depend on the number of Oxometallate Bridge formed. For example the Keggin structure² of poly oxometallates may be formed when the poly anions bears $[\text{M}_{12}\text{O}_{40}]^{n-}$ composition. Further if the composition of the poly anion changed to $[\text{M}_{18}\text{O}_{62}]^{n-}$ then the structure of the oxometallates differs.³ The synthesized triheteropoly complex collected in the form of solid residue may contain moderate to large number of water molecules as water of hydration as well as water of constitution, due to the fact that the dilute acidic medium is provided for the synthesis of the complex compound. Thus the thermal studies of the isolated complex product is important which suggest the stability of the compound which may be based on the position of the water of molecules at peripheral region as well as between the interstices of the crystalline solid and also the effect of the insertion of hetero cations into polytungstate anion. The occupation of hetero cations into the voids in the

centre of tungstate anion increases the thermal stability much effectively⁴. The thermal stability of the triheteropoly complex was determined by direct heat treatment⁵⁻¹⁴ or by dehydration methods which mainly involved differential thermal analysis and thermo gravimetric analysis¹⁵⁻¹⁶ of the synthesized complex compound. The presence of Na, Al, Ce, Mo, V, W, H and O elements have been confirmed by elemental analysis, IR, spectral analysis and thermal analysis based on TGA & DTA of the synthesized poly tungstate residue.¹⁷⁻²¹

EXPERIMENTAL

Preparation: - Preparation of the heteropolyt complex involves the mixing of an aqueous solution of 70ml of 0.36(M) sodiummolybdate mixed with 10ml of glacial acetic acid and 40ml aqueous solution of 0.65(M) Aluminium carbonate. In this mixture the step addition of 60ml aqueous solution of 0.35(M) cerium sulphate was performed sulphate with continuous stirring. After complete mixing of cerium sulphate solution, the pH of the mixture was further adjusted to 4.5 by adding about 5ml of glacial acetic acid. Now the mixture solution was refluxed for three hours. The solution was cooled and left for crystallization. After 3 days, the dark yellow coloured solid residue was obtained, which was washed with moderate concentrated alcohol and dried. The second triheteropoly complex was prepared by same method only sodium vanadate was taken instead of sodium molybdate. The solid residue was obtained. The third heteropoly complex was prepared by same method only sodium tungstate was taken instead of sodium vanadate and solid residue was obtained.

Elemental analysis: -The elemental analysis was performed on the basis of prescribed methods suggested by Vogel. The quantitative estimation of the constituent elements of the product is given below in the chart:

Elements	Percentage found			Percentage Calculated
	Exp.-1	Exp.-2	Mean	
Sodium	1.15	1.13	1.14	1.14
Aluminium	1.33	1.35	1.34	1.34
Cerium	3.48	3.44	3.46	3.46
Molybdenum	16.6	16.64	16.62	16.62
Hydrogen	7.43	7.4	7.42	7.42
Oxygen	(By difference)		70.03	70.03

As per the percentage composition of the synthesized triheteropoly complex constituent elements the proposed composition of the complex may be given as $\text{Na}_2[\text{Al}_2\text{CeMo}_7\text{O}_{27}]150\text{H}_2\text{O}$. The apparent molecular weight of the prepared complex was determined by the cryoscopic method, the apparent molecular weight found to be 4038 which is almost in accordance with the calculated molecular weight of the product 4044.

Elemental analysis of the second complex the constituent elements of the product are given below in the chart:

Elements	Percentage found			Percentage Calculated
	Exp.-1	Exp.-2	Mean	
Sodium	2.29	2.3	2.30	2.30
Aluminium	2.7	2.72	2.71	2.71
Cerium	7	7.02	7.01	7.01
Vanadium	10.21	10.23	10.22	10.22
Hydrogen	7.2	7.22	7.21	7.21
Oxygen	(By difference)		70.54	70.54

As per the percentage composition of the synthesized complex proposed composition of the complex may be given as $\text{Na}_2(\text{Al}_2\text{CeV}_4\text{O}_{16})72\text{H}_2\text{O}$. The apparent molecular weight of the prepared complex was determined by the cryoscopic method, the apparent molecular weight found to be 1991 which is almost in accordance with the calculated molecular weight of the product 1996.

Elemental analysis of the third complex the constituent elements of the product are given below in the chart:

Elements	Percentage found			Percentage Calculated
	Exp.-1	Exp.-2	Mean	
Sodium	1.04	1.02	1.03	1.03
Aluminium	1.22	1.2	1.21	1.21
Cerium	3.13	3.14	3.14	3.14
Tungsten	16.5	16.53	16.52	16.515
Hydrogen	7.7	7.73	7.72	7.72
Oxygen	(By difference)		70.38	70.38

As per the percentage composition of the synthesized triheteropoly complex constituent elements the proposed composition of the complex may be given as $\text{Na}_4(\text{Al}_2\text{CeW}_4\text{O}_{19})177\text{H}_2\text{O}$. The apparent molecular weight of the prepared complex was determined by the cryoscopic method, the apparent molecular weight found to be 4451 which is almost in accordance with the calculated molecular weight of the product 4456.

RESULTS & DISCUSSION

IR spectrum results of polytungstate residue:-
Broader peaks at 3159cm⁻¹, 2758.21cm⁻¹, 2011.51cm⁻¹, 1624.06cm⁻¹ and 1408.01cm⁻¹ are the group frequencies due to the association of water of hydration, water of crystallization frequencies. It is difficult to assign the above peaks in terms of water of hydration and water of crystallization.

Another peak 1141.36 cm⁻¹ may be assigned to W-O group frequency. 914.26 cm⁻¹ group frequency peak appears due to the presence of sodium as its ionic form. Another peak at 651.24 cm⁻¹ may be assigned to Al-O, 563.21 cm⁻¹ peak may be due to the presence of Ce=O and 501.49 cm⁻¹ group frequency appear in IR graph may be due to the presence of Ce-Mo.

The group frequency 3443 cm⁻¹, 3282.55cm⁻¹, 2079.26 cm⁻¹, 1631.78 cm⁻¹ and 1141.36 cm⁻¹ group frequency may be assigned to water of hydration and water of conjugation of the isolated product. The group frequency at 956.69 cm⁻¹ may be assigned to the Na cation associated with the product. The shifting of Na cation taken in the product may be due to the presence of different constituent element 740.67 cm⁻¹ group frequency may be assigned to V=O.

The group frequency 617.27 cm⁻¹ appears due to the presence of Al-O group and finally 536.21 cm⁻¹ group frequency may be assigned to CeO.

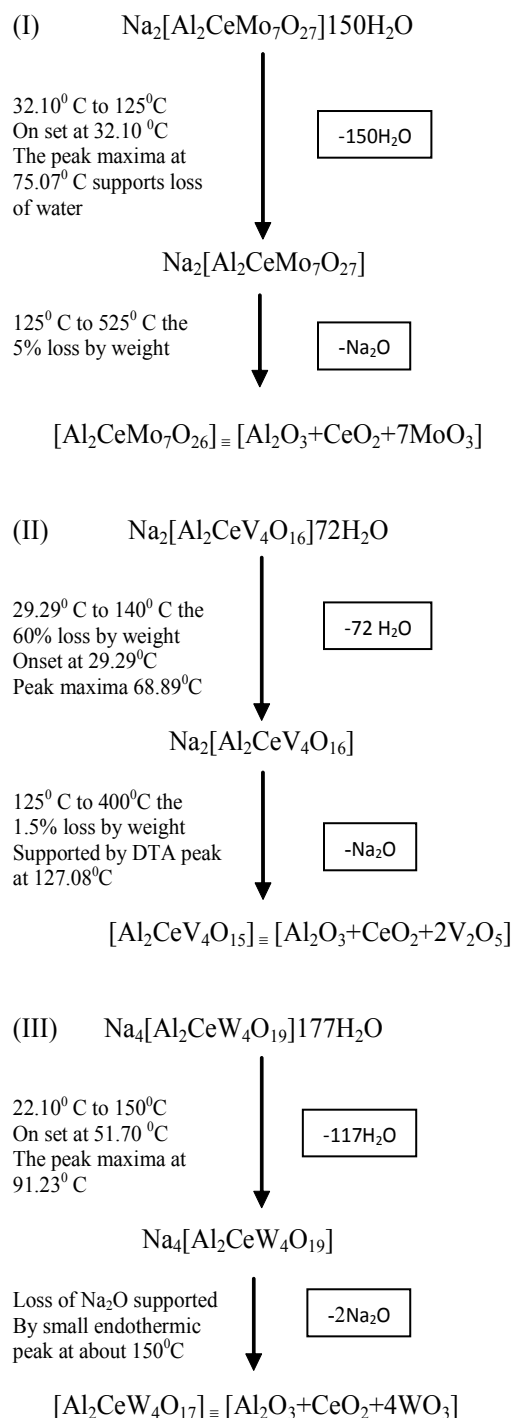
The strong broad peaks 3456.44 cm⁻¹, 3159.40cm⁻¹ indicates the association of water molecules also supported by presence of two sharp peaks at 1624.06 cm⁻¹ and 1400.32 cm⁻¹ peaks also. The appearance of 1138.00cm⁻¹ may be attributed due to the presence of W=O. The peak at 806.25 cm⁻¹ may be due to the association of Al-O and finally the 567.07 cm⁻¹ small peak may be assigned for the Ce-O group frequency.

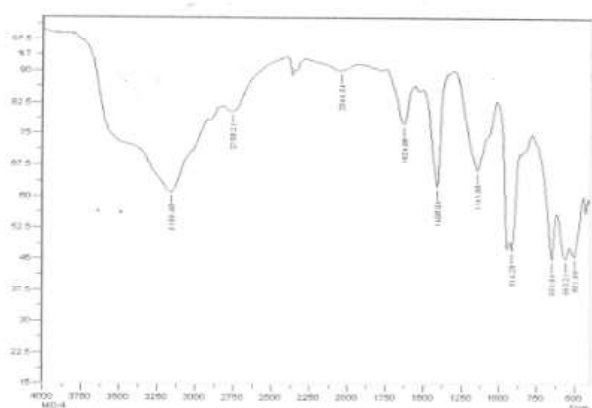
Thermal analysis involving TGA and DTA result:-

The DTA graph of the product suggest exothermal decomposition reaction for loss of water molecules and also the other minor extreme graph at 309°C and 527.72°C peak indicates the internal rearrangement of the product.

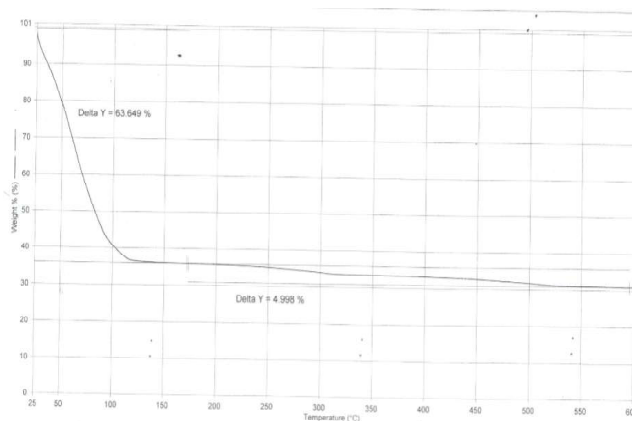
The DTA peak on set at 29.29°C and peak at 68.89°C temperature range 30°C to 140°C support the loss of water of association of the product, approx 60% by weight. Another peak at 127.08°C, onset at 108.79°C supports loss of Na₂O with further 1.5% loss by weight.

The DTA graph supports the loss of entire water molecule associated with product by the strong exothermic peak appeared at 91.23°C which onset at 51.70°C. Loss of Na₂O is supported by unnoticed small endothermic peak at about 150°C.

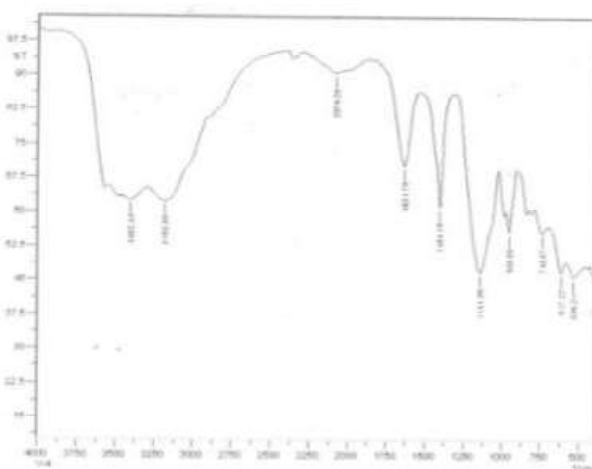




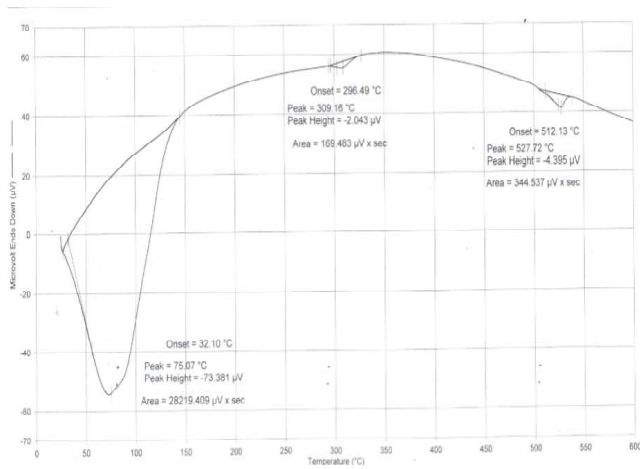
Graph1.IR of complex 1



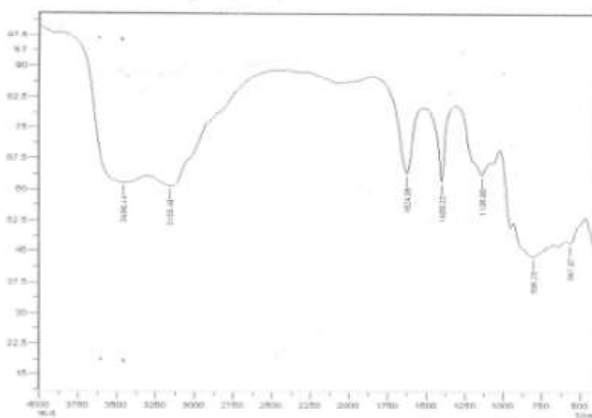
Graph 4-TGA of complex residue I



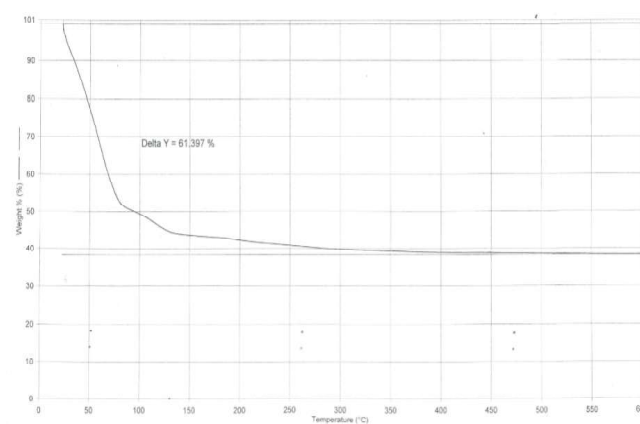
Graph2.IR of complex residue II



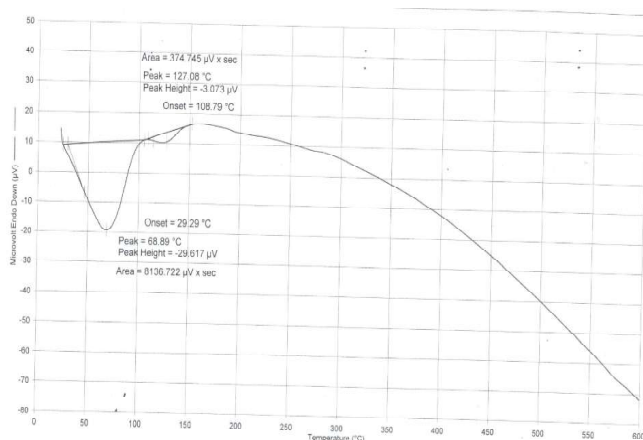
Graph 5-DTA of complex residue I



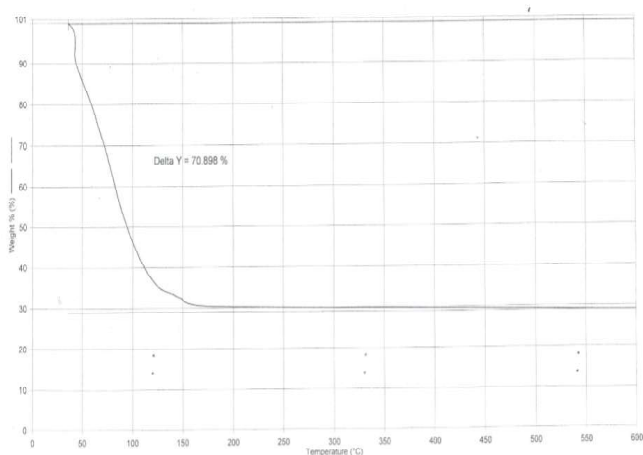
Graph3.IR of complex residue III



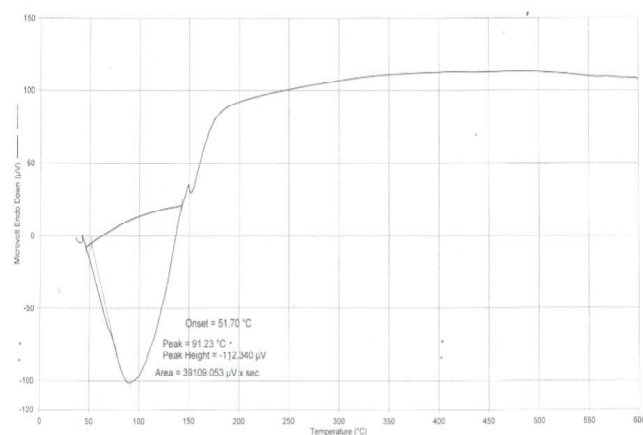
Graph 6-TGA of complex residue II



Graph 7-DTA of complex residue II



Graph 8-TGA of complex residue III



Graph 9-DTA of complex residue III

CONCLUSION

All products isolated in atmospheric condition & 9:1:1 (for isopoly molybdate anion). These products stable in air and poorly soluble in water at room temperature, however they were completely soluble in warm to boiling water. The aqueous solution of the heteropoly complex were ionic in nature containing Na⁺. The evidence of the presence of Na⁺ cations is confirmed from their IR spectral analysis in which sodium oxide IR absorption bond were observed. The presence of Na⁺ is also confirmed from the flame photometric experiment to calculate the elemental percentage of sodium element during heating in the flame photometric experiment the golden yellow flame is produced which indicate the presence of sodium. The magnetic moment determination at the room temperature suggests the strong paramagnetic nature of the isolated products. The thermal analysis of the complexes were studied on the basis of DTA & TGA curves analysis of the products, which indicates the presence of different modes of water molecules. However it is not possible to determine the H₂O molecules in terms of water of crystallization and water of constitution. The thermal analysis indicate that the thermolysis of oxometalates complexes produced by loss of water of crystallization and then subsequently the loss of water of constitution. Hence it may be concluded that the water constitution may involve in building up the structure of triheteropoly complex compound.

REFERENCES

1. **G.A.Tsigdimos**, *Heteropoly_verbindungen* (Method Chemicum) K.Niedenzu, H.Zimmer.H.(eds) Stuttgart Georg.Thiems,Veriorg,**8**,32,(**1974**)
2. **J.F.Keggin**, *nature; Proc. Royal Soc.(Lond)*, A144,75, **131**, 908(**1933**)
3. **B.Dawson**, *ActaCryst*, **6**, 113,(**1953**)
4. **Moffat, John.B.**, *Metal-Oxygen Clusters-The Surface and Catalytic Properties of Heteropoly Oxometalates*, Kluwer Academic Publishers, NewYork, Bostan, Dordrecht, London,Moscow©, p-41 (**2002**)
5. **S.F.West and RiethAud**, *L.F.J.Phys. Chem*, **59**,1069, (**1955**)
6. **E.Matijevic, M.Kerker**, *J.Am.Chem.soc*,**81**, 1307, (**1959**)

7. **A.Hegedus, M.Dvorsky**, MagrTud. Akad.Kam. Tud.Oszt Kozlemen,**11**,327,(1959)
8. **Babad Zakhryapin, A. A. Ah. Neorg**, Khim.**1**,445, 2403(1959)
9. **K. Eriks, N. F. Yannoni U. C. Agrawal, V. E. Simons and L.C.W. Baker**, Acta Cryst.,**13**,1139,(1961)
10. **D. D. Dexter, J. V. Silverton**, J.Am.Chemsoc., **90**, 3589, (1968)
11. **H.H.K. Han**, Ph.D. Thesis Boston University (1970)
12. **A. Wells**, Structural Inorganic Chem. 3rd edit., Oxford, p-451,(1962)
13. **A. Perloff.**, Inorganic Chem.,**9**,2228,9,28,(1970)
14. **H. C. Mishra, S. K. Roy and A. N. Ojha**, J. Indian Chem Soc.,**54**,307,(1978)
15. **A. Langinestra and R. Cerric**, R.Gazz,Chim, Ital.,**95**, 26(1965)
16. **E. Brukholder, V. Golub, C. J. O. Connor and Zubieta**, Inorg.Chem.**42**,6729,(2003)
17. **J.R.Ferraro**, plenumpress, New York, (Chapter V), (1971)
18. **T.Okuhara and N.Mizuno**, M. Adv. Catal, **41**, 113, (1996)
19. **J. Morizzi, M. Hobday and C. Rix**, J.Mater. Chem,**10**, 863,(2000)
20. **E. brukhlder, V. Goub, C. J. O. cornnor and J. Zubieta**, Inorg.Chem.,**42**, 6729,(2003)
21. **H. Firouzabadi and A.A. Japari, J. Iranian, Chem. Soc.** ,**2**,85,(2005)



Classification and rank determination of pundi area, west bokaro coalfield, Ramgarh, Jharkhand, India

Bacha Ram Jha^{a*}, Chanchal Lakra^a & M. L. Banra^b

^aDepartment of Geology, Ranchi University, Ranchi, Jharkhand, India

^bCSIR-Central Institute of Mining and Fuel Research, RC- Ranchi, Jharkhand, India.

*Corresponding author : Phone :9431326262 , E-mail : brjha123@gmail.com

Abstract: West Bokaro Coalfield is situated in Ramgarh district of Jharkhand state. This coalfield is separated from the North Karanpura Coalfield by a narrow stretch of metamorphic rocks and outlier of Talchir in the West. The block is covered by Survey of India Toposheet no 73E/9. It lies within latitude 23°45'52"N to 23°52'58" N and longitude 85°30'E to 35°32'37"E. The present study deals with Bore hole no. TEPE-6 in which the proximate data shows that moisture, ash, volatile matter and Fixed carbon percentage ranges from 0.6 – 1.8, 16.4 – 45.3, 10.0 – 28.3 and 33.8 – 56.6 respectively. The Fuel Ratio and Gross Calorific Value range from 1.4 – 4.3 and 8127 – 8892 respectively. The coal seams of Pundi area are high grade Bituminous –A rank coal. Hence, on the basis of proximate data we can say that they can be used for Coke Purpose.

Paper History:

Received

27th April 2017

Revised

12nd May 2017

Peer reviewed

2nd June 2017

Accepted

21st June 2017

Key words:-West Bokaro Coalfield, Pundi Area, Coal seams, Rank

INTRODUCTION

The West Bokaro Coalfield situated in Ramgarh district of Jharkhand state is the fourth coalfield in the Damodar Valley after Raniganj, Jharia and East Bokaro Coalfield. The West Bokaro Coalfield covers an area of 207 km² having a length of 16km and bears width of 11 km in the West and 3.2 km in the East. The base of the Lugu hill comprises of younger Gondwana which separates it from the East Bokaro Coalfield. This Coalfield is also separated from the North Karanpura Coalfield by a narrow stretch of metamorphic rocks in the west. (Map No.1).

Geology of the area

The Pundi Block has been named after its village name. Pundi opencast is an existing mine and it is a part of Kuju Area of Central Coalfield Limited, The mine falls within the Pundi Geological Block which is situated in the

Western part of the West Bokaro Coalfield of Jharkhand. The area is demarcated by *Northern Boundaries*: The Northern floor boundary of the quarry has been fixed along the crop. *Southern Boundaries*: The Southern surface boundary has been fixed leaving a barrier of 7.5m from Tisco Boundary. *Eastern Boundary*: the Eastern boundary of the quarry has been fixed from Bokaro River. *Western Boundaries*: The western floor boundary of the quarry has been fixed. (Map No.2).

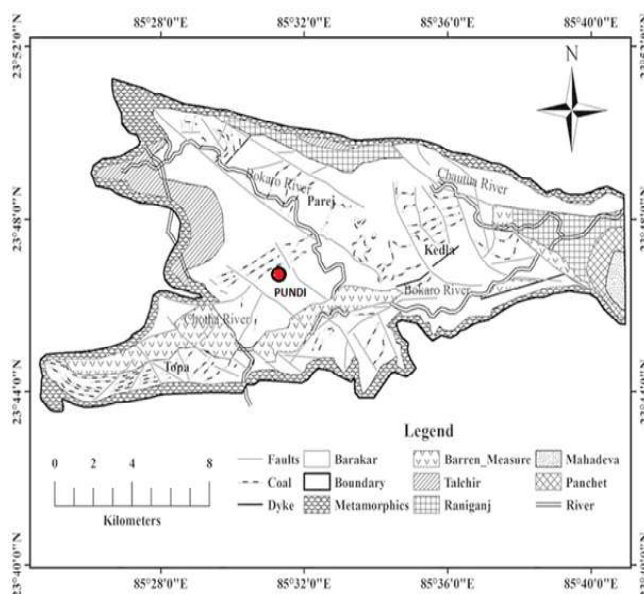
Location of the area

The block is located in the Survey of India Toposheet no 73E/9. It lies within latitude 23°45'52"N to 23°52'58" N and longitude 85°30'E to 35°32'37"E and covers an area of about 6 Sq. km.¹ The Pundi Block is connected to NH – 33 between Ranchi and Ramgarh by a 6 km weather metaled road leading from adjoining Hesagora block. The distance of this block from Ranchi and

Hazaribagh is about 60 and 40 km respectively. The nearest airport is at Ranchi whereas nearest railway station is at Ranchi Road station.



Map No.1: Map of West Bokaro Coalfield



Map No.2: Location Map of Pundi Area

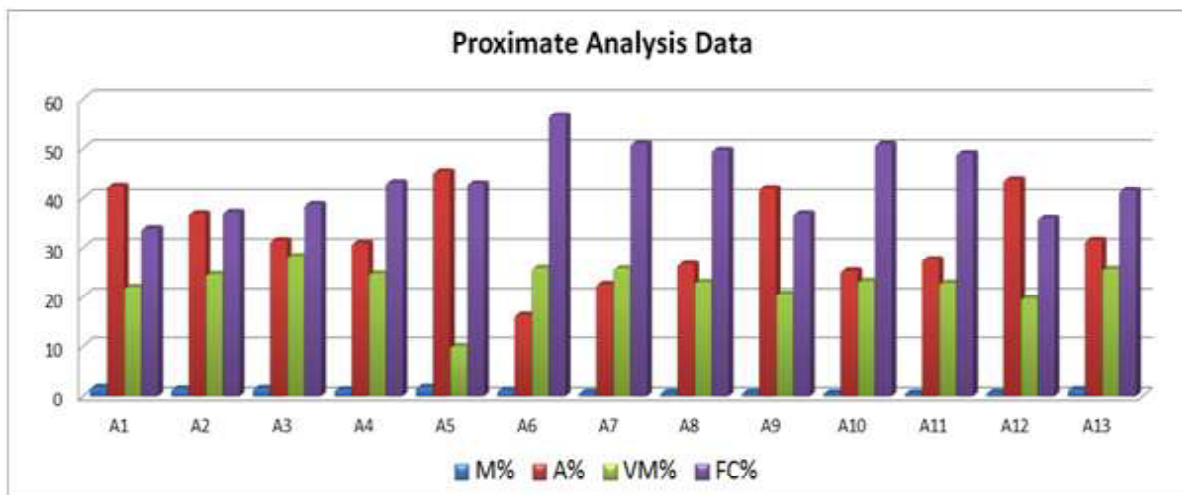
MATERIALS & METHODS

For the present chemical investigation the sample of TEPE-6 has been collected from different boreholes drilled by CMPDIL, RI – III, Ranchi through the courtesy of CSIR – Central Institute of Mining and Fuel Research (Erstwhile Central Fuel Research Institute) Unit Ranchi. Authors have selected 13 samples (A1 to A13) for detail study.^{1,2,3,4} Laboratory Scale sample preparation of Coal is done as per IS: 436 (Part I) 1964 APPENDIX C, Indian Standard, Methods for Sampling of Coal and Coke.

Proximate analysis is done as per IS: 1350 (Part I) – 1984, Indian Standard, Methods for Test for Coal and Coke, (Part I) Proximate Analysis. Ultimate analysis has been done as per IS: 1350 (Part IV / Sec 2) – 1974, Indian Standard, Methods for Test of Coal and Coke, Part IV (Ultimate Analysis), Section I.

Chemical studies

The chemical study deals with determination of moisture, ash, volatile matter and fixed carbon percentage^{5,6,7} (Table No.1& Graph No.1).



Graph No.1: Representation of Proximate Analysis data

Table no. 1

Depth (m)	Thickness (m)	Seam	Sample no.	PROX. (AT 60%RH & 40°C) (AD Basis)				GCV
				M%	A%	VM%	FC%	Kcal/kg
1	2	3	4	5	6	7	8	9
16.74	3.02	XI	A1	1.8	42.4	22.0	33.8	(8328)
36.64	1.29	XI	A2	1.5	36.8	24.6	37.1	(8369)
39.84	4.78	XB	A3	1.6	31.4	28.3	38.7	(8127)
84.78	1.52	IX	A4	1.3	30.9	24.7	43.1	(8433)
148.47	2.93	VIII	A5	1.8	45.3	10.0	42.9	(8327)
224.99	1.77	VI	A6	1.2	16.4	25.8	56.6	(8400)
270.80	12.20	V	A7	0.7	22.6	25.7	51.0	(8537)
299.40	3.75	IV	A8	0.7	26.6	23.0	49.7	(8777)
309.77	0.44	IIIB	A9	0.7	41.9	20.6	36.8	(8774)
320.00	4.80	III	A10	0.6	25.3	23.2	50.9	(8610)
363.55	1.25	II T	A11	0.6	27.6	22.8	49.0	(8752)
366.41	0.80	II B	A12	0.7	43.7	19.7	35.9	(8892)
407.70	2.30	I	A13	1.4	31.5	25.6	41.5	(8566)

On the basis of statistical data of proximate analysis, the bar graph as represented in Graph no.1 depicts that there is a large deflection of fixed carbon in sample no.A6 i.e Seam no VI encountered at a depth of 200 m approximately from the surface. Here the fixed carbon shows gradational higher values. This infers that the coal seam shows maturity at greater depth, which can be supported by Hilt's Law which states that the coal seams

gains maturity with increase in depth. This graph also shows a fall in VM % in sample no A5 in comparison to others seams which may be due to the result of faulting.

Classification of Coal

On the basis of statistical proximate data an attempt has been made to classify coal on the basis of Fraser's classification⁸.

Table No.2: Fuel Ratio: Fraser (1877) classified coal on the basis of fuel ratio i.e FR=FC/VM

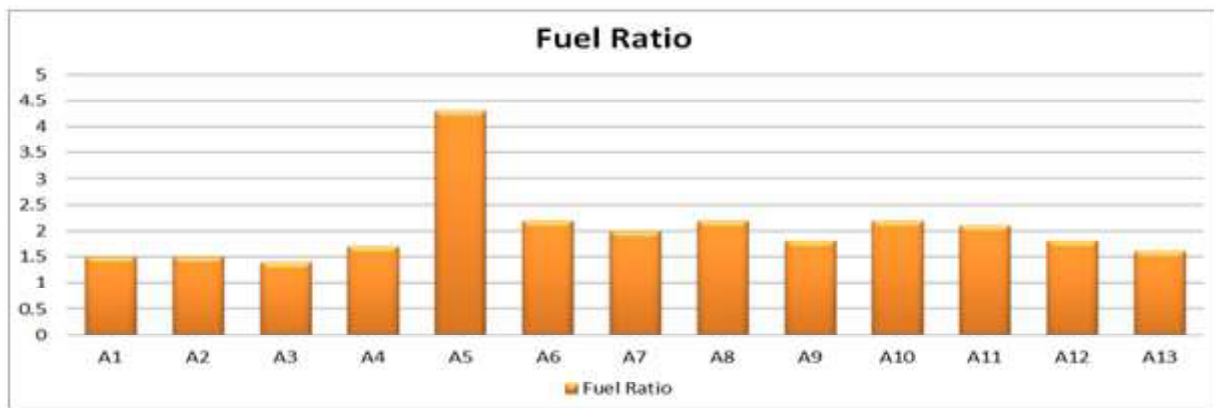
Type	Fuel Ratio = Fixed carbon/Volatile matter (unit coal basis)
Anthracite	100 – 12
Semi – Anthracite	12 – 8
Semi – Bituminous	8 – 5
Bituminous	5 – 0

Table No.3: Data Plots of Fuel Ratio on the basis of proximate analysis data

Depth(m)	Thickness(m)	Seam	Sampleno.	VM%	FC%	Fuel Ratio
1	2	3	4	5	6	7
16.74	3.02	XI	A1	22.0	33.8	1.5
36.64	1.29	XI	A2	24.6	37.1	1.5
39.84	4.78	XB	A3	28.3	38.7	1.4
84.78	1.52	IX	A4	24.7	43.1	1.7
148.47	2.93	VIII	A5	10.0	42.9	4.3
224.99	1.77	VI	A6	25.8	56.6	2.2
270.80	12.20	V	A7	25.7	51.0	2.0
299.40	3.75	IV	A8	23.0	49.7	2.2
309.77	0.44	IIIB	A9	20.6	36.8	1.8
320.00	4.80	III	A10	23.2	50.9	2.2
363.55	1.25	II T	A11	22.8	49.0	2.1
366.41	0.80	II B	A12	19.7	35.9	1.8
407.70	2.30	I	A13	25.6	41.5	1.6

Form Table no.3, the fuel ratio values incurred from the proximate analytical data when compared with the Fraser's Classification it revealed that the coal seams of Pundi Area

falls in the range of Bituminous type i.e.1.4 – 4.3 of the data range.



Graph No.2: Representation of fuel ratio from an analytical data

The graph no.2 shows a drastic increase in fuel ratio encountered at depth of 148.47m i.e sample no.A5, although predicted that at this position there was a probability of a fault and due to faulting there was an

increase in pressure and temperature that resulted in increase of fuel ratio. This could be the possible explanation in support to the plots of graph no.2.

CONCLUSION

The proximate data shows that moisture, ash, volatile matter and Fixed carbon percentage ranges from 0.6 – 1.8, 16.4 – 45.3, 10.0 – 28.3 and 33.8 – 56.6 respectively. The Fuel Ratio and Gross Calorific Value range from 1.4 – 4.3 and 8127 – 8892 respectively. The ranges of data shows that the coal seams have low moisture, moderate to high ash, medium to low volatile matter and good fixed carbon which holds good for coalification path of maturity^{9,10}. The fuel ratio and gross calorific value further determines that the coal seams are best suitable for Coke Purpose. Hence, the coal seams of Pundi area are high grade Bituminous – a rank coal.¹¹

ACKNOWLEDGEMENT

The author is grateful to Dr.P.K.Verma, Head of Department of Geology for his encouragements. Sincere thanks to CMPDIL- RI – III, Ranchi through the courtesy of CSIR- Ranchi Unit for providing samples and analytical facilities.

REFERENCES

1. **G.S.I. (1987)** Geological survey of India. Coal resources of Bihar India. Bulletin. Geol. Surv. India, Ser-A, No.45.
2. **Report Publication**, CMPDI- Central Mine Planning and Designing Institute Ltd. Kanke.
3. **IS: 436 (Part I) – 1976**, Indian Standard, Methods for Sampling of Coal and Coke, PART – I, Sampling of Coal.
4. **IS: 436 (Part I / Sec I) – 1964**, Indian Standard, Methods for Sampling of Coal and Coke, APPENDIX C (Clauses 10.1, 10.1.1, 10.2 and 10.3) Reduction of Gross Samples.
5. **IS: 436 (Part I/ c 10. 1. 1) – 1961**, Indian Standard, Methods for Sampling of Coal and Coke, PART – I, c 10.1.1 Laboratory Sample of Coal.
6. **IS: 1350 (Part II) – 1970**, Indian Standard, Methods for Test for Coal and Coke, (Part II) Determination of Calorific Value.
7. **IS: 1350 (Part I) – 1984**, Indian Standard, Methods for Test for Coal and Coke, (Part I) Proximate Analysis.
8. **Fraser, P. (1877)** Trans. Am. Inst. Mining Met. Engrs., No. 36, pp. 32
9. **Jha,B.R., Banra,M.L. and Sinha, A.K. (2014)** Physico-chemical characterization of coals of Chano-Rikba block, North Karanpura coalfield, District-Hazaribagh, Jharkhand (India), Min.Process.Tech.2014.,pp.182
10. **Jha, B.R., Banra, M.L. and Sinha. A.K. (2015)** Characterization of coals of Chano-Rikba Block North Karanpura coalfield, District-Hazaribagh, Jharkhand (India), Vist.In. Geol. Res, Vol.13, pp.183-193.
11. **Sanga, T., Jha, B.R., Sinha. A.K. and Lakra, Chanchal (2016)** Classification and Quality determination of Rohne – Rautpara coals of North Karanpura coalfield, Ranchi Univ. Jour. of Sci. and Tech.,Vol.04, pp.96 – 100, ISSN :2319 – 4227.



Clean coal technology in environmental amelioration: A case study from north karanpura coalfields, Jharkhand

Uday Kumar^{a*}, R.P Singh^b, Debashree P. Singh^c & Anubha Tigga^a

^aDepartment of Geology, Ranchi University, Ranchi, Jharkhand, India

^bDeputy Manager, CMPDIL, Ranchi, Jharkhand, India

^cSenior Geologist, Geological Survey of India, Ranchi, Jharkhand, India

**Corresponding author : Phone : 9431325230 , E-mail : kumaruday10@gmail.com*

Abstract: The modern industrial and agricultural activities depend largely on electric power for their growth and sustenance. More than 70% of India's Power generation comes from Thermal Power Plants (TPPs), out of which more than 90% are coal based. In India, out of the total coal production 78% coal is utilized for thermal power generation. Indian coal mining organizations has a target of more than 500 MT annual coal production by next three years and their subsequent utilization in TPPs would lead to severe stress on environment by production of 150 MT of fly ash as well as large amounts of suspended particulate matter (SPM). The Indian Gondwana coals are characterized by high percentage of inertinite and high mineral matter content, due to its allochthonous origin, but they can burn satisfactorily to give high heat value. Generally, the reactive macerals, vitrinite and liptinite as well as reactive inertinite participate in the burning activity. All these organic constituents are associated with the inorganic constituents or mineral matters. The trace elements in Gondwana coal are mostly associated with mineral matter like silicates, oxides, sulfides, sulfates, and carbonates, many of which are concentrated in coal more than their Clarke Value. The combustion of such coal leads to further enrichment of trace elements in various components of ash, many of which are potential health hazards. The trace elements namely Antimony, Arsenic, Beryllium, Cadmium, Chromium, Cobalt, Copper, Lead, Manganese, Mercury, Nickel, Selenium, Thorium, Uranium and Zinc falls under the category of Hazardous Atmospheric Pollutant (HAP). The high concentration of trace element affect our biological system by their cytotoxicity or genotoxicity. The trace elements associated with inorganic fraction of coal can be partially removed by conventional coal preparation techniques and as such can help in environmental amelioration.

Paper History:

Received

7th May 2017

Revised

2nd June 2017

Peer reviewed

20th June 2017

Accepted

1st July 2017

Key words:- Karanpura coalfields, SPM, HAP, TPPs, Health

INTRODUCTION

The modern industrial and agricultural activities depend largely on electric power for their growth and sustenance. More than 70% of India's Power generation comes from Thermal Power Plants (TPPs), out of which more than 90% are coal based. In India, out of the total coal production 78% coal is utilized for thermal power generation. Indian coal mining organizations has a target

of more than 500 MT annual coal production by next three years and their subsequent utilization in TPPs would lead to severe stress on environment by production of 150 MT of fly ash as well as large amounts of suspended particulate matter (SPM) in the atmosphere. The Indian Gondwana coals are characterized by high percentage of inertinite and high mineral matter content, due to its allochthonous origin (Stach et al., 1982)¹, but are capable

of producing thermal energy satisfactorily to give high heat values. Generally, the reactive macerals, vitrinite and liptinite and also reactive inertinite participate in the burning activity (Clove *et. al* 1994², Choudhury *et al.*, 2008³, Mandal and Kumar, 2009⁴). All these organic constituents are associated with the inorganic constituents or mineral matters which are in the form of carbonates, sulfates, sulphides and silicates. The trace elements in Gondwana coal are mostly associated with mineral matter such as silicates, oxides, sulfides, sulfates, and carbonates many of which are concentrated in coal more than their Clarke Value⁵. The combustion of such coal leads to further enrichment of trace elements in various components of ash, many of which are potential health hazards. As per the US EPA Clean Air Act Amendment 1990, Trace Elements namely Antimony, Arsenic, Beryllium, Cadmium, Chromium, Cobalt, Copper, Lead, Manganese, Mercury, Nickel, Selenium, Thorium, Uranium and Zinc falls under the category of Hazardous Atmospheric Pollutant (HAP)⁶. The high concentration of trace element affect our biological system by their cytotoxicity or genotoxicity.

The present paper is aimed at a brief petrographic study to know about the mineral-maceral association along with a detail study of trace elements present and its environmental impact.

The trace elements associated with inorganic fraction of coal can be partially removed by conventional coal preparation techniques.

STUDY AREA

North Karanpura Coalfield (NKCF), situated between latitudes 23° 38'N - 23° 56'N and longitudes 84° 46'E - 85° 23'E covering an area of 1230sq km, is a major depository of noncoking coals in the Gondwana Basin of India. The area is gradually becoming a major coal supplier to Thermal Power Plants of north India. The study area includes four adjoining blocks of NKCF, which are Ashok, K D Hesalong, Karkata and Piparwar (Fig.1). The area covers about 100 sq km. where the mining operation is active at present.

GEOLOGY

The study area falls in the South Central Sector of NKCF, which displays the geological succession of lower Gondwana rocks while the Pre-Cambrian rocks form the basement for the overlying stratigraphic sequence, which

is represented by Talcir, Karharbari, Barakar, Barren Measure and Raniganj Formations. The rolling basinal configuration has resulted the occurrence of Barakar Formation, which is a major coaliferous zone, under not very thick overburden in the study area. In the three blocks viz. Ashok, K D Hesalong and Piparwar, Seam I to Seam IV are present, while Seam V is present along with the other four in Karkata Block. All these seams, in this area are termed as Seam I = Dakra, Seam II = Bukbuka, Seam III = Bistrampur, Seam IV = Karkata and Seam V = Raniganj. No major igneous intrusions have been reported to affect the coal seams in the central part of the coalfield. Broadly, the strike is almost ENE-WSW with very low dip towards NNW. The strike gradually changes to Northwest-Southeast across the Damodar River with moderate dip towards southwest. Finally the NW-SW striking sequence abuts against the southern boundary fault.

METHODS

For petrographic study, the channel samples were taken from the mine faces of the Dakra, Bukbuka and Bistrampur seams in all the four blocks. In total 27 samples were studied taking 6 samples from each block. The analytical technique includes the study of maceral composition and vitrinite reflectance measurement. The study of maceral composition and the reflectance measurement were carried out with a Leica DMRX polarized light microscope following IS: 9127 (part I): 1992 and IS: 9127 (part III): 1992⁷. The reflectance measurement was done by MSP 200 software and the photomicrographs were taken using QWin Image analysis software. For petrochemical study, feed coal from each seam and washed coals were taken and all were powdered to 70 mesh size. The trace element study has been carried out by ICP-MS analysis using SRM 1633b as the reference material.

RESULTS & DISCUSSION

Petrographic Analysis

The petrographic analysis shows that vitrinite is the dominating maceral group in the coals of K D Hesalong and Piparwar blocks, while inertinite is dominating in Karkata Block of the study area. In the Ashok Block the volume percentage of these two maceral groups decreases and increases in the lower and upper seams respectively.

Kumar *et.al.*: Clean coal technology in environmental amelioration: a case study from north karanpura coalfields, Jharkhand

Among the macerals of Vitrinite group Collodetrinite is the most common maceral, followed by collotelinite and vitrodetrinite (Vitrinite Classification ICCP, 1994)⁸. In all the seams vitrinite content varies from 19.5% to 60.8%. In the Liptinite group of macerals, sporinite (microsporinite and megasporinite) and cutinite are observed in which sporinite is more common. The liptinite content varies from 5.2% to 17%. The proportion of inertinite in these coals is high. Inertodetrinite is the major component in all the samples followed by semifusinite and fusinite. Bogen structure is a common feature. The inertinite content varies from 22% to 49.5%.

During the combustion the extent of char fragmentation depends on the swelling behavior of the individual macerals. If the macerals swell extensively, the resulting char may fragment and minerals inside the char fragments will form fine ash particles (Yan *et al.*, 2002)⁹. The proportion of such char may be estimated from the vitrinite content of the coal. These can be known by the study of mineral maceral association.

In these coal samples mineral matter shows a varied association as observed in other Indian Gondwana coals (Stach *et al.*, 1982)¹. Silicate minerals (clay+quartz) are the most common minerals along with siderite and pyrite, which are present in a lesser proportion, as observed in the adjoining areas (Kumar *et al.*, 2005)¹⁰. Clay and quartz are present both as individual grains and also in the vitrinite as mineral inclusions. The Collotellinite embraces the mineral inclusions in coals of Upper Dakra Seam (Plate 1) and Upper Bukbuka Seam (Plate 2). Siderites are mainly present as spherulitic nodules embedded in inertinites (Plate 3) or as individual grains, while pyrite is present mainly as mineral inclusion in vitrinite and less commonly in inertinites and sometimes also as individual grains. The proportion of mineral matter and their association with vitrinites give an idea about the fate of these coals during the combustion.

The vitrinite reflectance values of these coals vary from 0.47% to 0.59%, which characterize the rank of these coals (Mandal 2010)¹¹. The vitrinite reflectance values characterize these coals as low rank sub bituminous coals.

Petrochemistry

Trace elements in coals may be associated organically or inorganically as different syngenetic, epigenetic and

clay minerals. In Godwana coals the trace elements are mostly associated with mineral matters such as silicates, sulfides, sulfates and carbonates many of which are concentrated in coal more than their Clark value. The combustion of such coal leads to further enrichment of trace elements in various components of ash, many of which are potential health hazards.

Statistical analyses have been widely used to quantify affinity behavior between trace elements in coals. Correlation coefficients have proven quite powerful in inferring trace element occurrence mode for coals. In the present paper the element studied are divided into four groups according to their correlation coefficients with ash content-

Pearson Correlation coefficients and element association:

Correlation coefficient	Association
Less than - 0.22	Organic
Between ± 0.22	May be associated with organic & inorganic.
Between + 0.22 and 1 (Kortenski and Sotirov 2002) ¹²	Inorganic

Group of elements according to correlation coefficients

Group 1: $r_{\text{ash}} = -0.51$ to -1.0 , Sr (-0.51), Ce (-0.52), Ba (-0.53), La (-0.54), Pr (-0.54), Nd (-0.54), Sm (-0.54), Gd (-0.54), Tb (-0.57), Dy (-0.57), Y (-0.59), Ho (-0.60), Yb (-0.60), Er (-0.61), Tm (-0.63), Lu (-0.63).

Group 2: $r_{\text{ash}} = -0.22$ to -0.5 , Rb (-0.30), Co (-0.35), Pb (-0.35), V (-0.38), Zn (-0.41), Eu (-0.50).

Group 3: $r_{\text{ash}} = -0.22$ to 0.22 , Ni (-0.21), U (-0.20), Th (-0.20), Cs (-0.18), Sc (0.084), Cr (0.13), Ta (0.15), Ga (0.21), Hf (0.22).

Group 4: $r_{\text{ash}} = +0.22$ to 1 , Cu (0.29), Zr (0.33), Nb (0.45).

The first group includes elements with negative correlation coefficient from -0.51 to -1.0 (Sr, Ce, Ba, La, Pr, Nd, Sm, Gd, Tb, Dy, Y, Ho, Yb, Er, Tm, Lu). This suggests that these elements have mainly organic affinity. They may associate also with the mineral matter but in relatively low amount (except REE). In the present study REE (LREE and HREE) comes under this group.

The second group of elements have negative correlation coefficient with the ash content, but their values vary between the minimum statistical significant values (-0.22 to -0.50). This group includes Rb, Co, Pb, V, Zn and Eu. It may be assumed that this group of elements has organic affinity too but some of these elements are found in mineral association (Pyrite and clay minerals).

The third group includes elements with correlation coefficients between the statistically significant value ($r_{\text{ash}} \pm 0.22$): Ni, U, Th, Cs, Sc, Cr, Ta, Ga, Hf. They probably have intermediate (organic and inorganic) affinity.

The fourth group includes elements with prevailing inorganic affinity i.e. they are second generation trace elements/lithophilic elements. They have positive correlation coefficients with the ash content which vary between +0.22 to 1. Cu, Zr, Nb comes under this group. These elements are concentrated in the mineral matter of coal.

Trace element studies in beneficiated coals

As the trace elements associated with coals are organophylic or lithophylic, the likelihood of elemental release to the environment and the effectiveness of coal washing as a means of mitigating this release, are controlled significantly by the mode of occurrence of an element, (Finkelman, 1995)¹³, size and textural relationship e.g. elements housed in large mineral grains in cleats or fracture would be relatively easy to remove by coal washing. Washing may produce even higher element levels in coals in some cases (Wang *et.al.* 2009).¹⁴

Piparwar coal washery in North Karanpura coalfields was the first non-coking coal washery exclusively for TPPs of Northern power grid of India. The trace element studies of beneficiated coals of piparwar coal washery confirmed their reduction up to 50% by conventional coal beneficiation techniques of jigging and cyclone. It was noticed that Ni (red% 66), Cu (red% 58), Zn (red% 55), Ba (red% 53%) and Nb (red% 53) concentration decreased significantly to 50% after washing. The concentration of REE (red% 25 – 35), Ta (red% 41), Cr (red% 37), Co (red% 27), Pb (red% 26) and Sr (red% 26) decreased between 25 to 41%. In case of element like Th (red% 20), Ga (red% 20), Hf (red% 18), V (red% 14), U (red% 13), Zr (red% 2.5), Zr (red% 2.5) the red% varied between 2.5% to 20%.

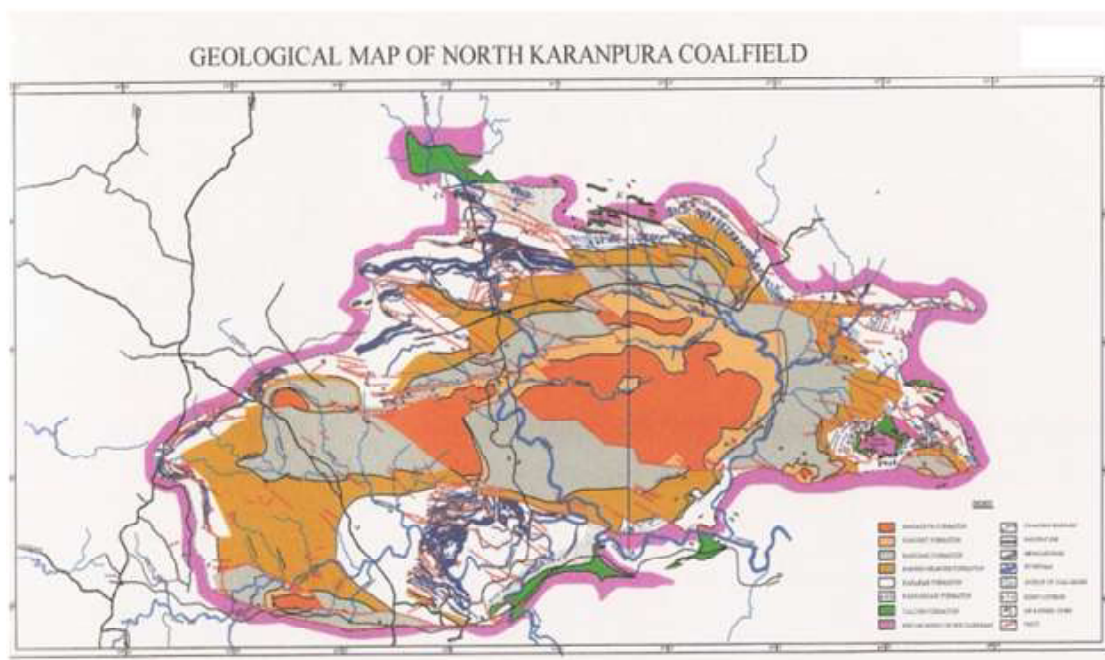


Fig :1 Geological Map of North Karanpura Coalfield



Collotelinite with Mineral Inclusion,
Upper Dakra, Piparwar Block $\times 50$
Plate No. 1



Collotelinite with Mineral Inclusion,
Upper Bukbuka Seam, Piparwar Block
 $\times 50$ Plate No. 2

PLATES



Semifusinite with Siderite nodule,
Upper Dakra Seam, Piparwar Block
 $\times 50$ Plate no. 3

It was observed that reduction in ash percentage (red %) ranges between 4 to 6% after washing of coal. In the case of trace element, the reduction percentage varied 0.32% to 66%. An opposite trend was noticed in the case of Rb, it showed an increase in concentration (6% increases) after washing of coal. Cs showed slight decreased in its concentration after washing (red% 0.32). Rb and Cs are inherently associated with clay fraction & organic fraction in coals which have difficult washing characteristics. This may be the probable cause of their slight decrease or increase, as trace elements in clays in porous pyrite, or in micron-sized sulfides enmeshed in organic matrix would be difficult to remove by washing (Ozbayoglu, 2013)¹⁵.

CONCLUSION

Health and environmental impacts from coal are primarily associated with inhalation of airborne particulates generated by coal mining or combustion and using ground or surface waters that comes in contact with coal or its combustion waste products (Finkelman *et.al.* 2002)¹⁶. The preliminary findings of reduction in concentration of trace element is very significant as Ni, Cr, Co, Pb, Th and U are HAP trace elements whereas Ba, Zn and Cu are drinking water pollutant and V is a threat to aquatic life. All these elements in the coals of the study area are either associated with the inorganic fraction of coal or have intermediate affinity i.e. associated with organic or inorganic fraction of coal as revealed by correlation coefficient of trace elements with ash content of coal.

These hazardous toxic elements showed marked decrease in their concentration after beneficiation of coal, which is a very positive indicator for curtailing environmental pollution due to coal combustion in TPP. Besides partial elimination of HAP Trace Elements, beneficiation also increases the Calorific Value of coal resulting in reduction of their consumption for power generation from 770 gm to 530 gm/Kwh and as such lesser amount of coal combustion means lesser loading of HAPs and GHGs in the atmosphere and thus lower will be global warming.

ACKNOWLEDGEMENT

The authors are thankful to the authorities of C.C.L. Ranchi, CMPDIL, Ranchi and NGRI, Hyderabad for their help in sample procurement and analyses. The fourth author, a UGC NFHE (ST) Fellow, extends thanks to the UGC for providing research fellowship.

REFERENCES

1. **Stach E, Mackowsky T, Teichmuller M, Taylor G. H, Chandra D, Teichmuller R(1982)** Stachs Text Book of Coal Petrology 535p.
2. **Cloke. M., Lester, E., 1994.** Charaterization of coals for combustion using petrographic analysis, a review, *Fuel*, 73, 315 – 320
3. **Choudhury, N., Boral, P., Mitra, Tandra, Adak, A.K., Choudhury, A., Sarkar, P., (2008),** Assessment of nature and distribution of inertinite in Indian coals for burning characteristics, *International Journal of Coal Geology*, V 72 , pp.141-152
4. **Mandal Debashree & Kumar Uday (2009)** Petrographic studies of NonCoking Coals for combustion characterization: a case study from Bukbuka Seam, South Central Sector, North Karanpura Coalfield, Jharkhand".*Journal Indian Association of Sedimentologists*, V 28 No.1pp.31-37.
5. **Fleischer M(1967)** Data on Geochemistry, USGS Geological Survey Professional Paper 440-D,23p
6. **US EPA (2003)**"National Emission Standards for Hazardous Air Pollutants for Industrial/CommercialInstitutional Boilers and Process Heaters";Proposed Rule,40 CFR Part 63, Federal Register 68,pp 1660-1763
7. **IS : 9127, Part I, II, III**
8. **The new vitrinite classification(ICCP System 1994)** *Fuel* Vol. 77, No. 5, pp. 349-358, 1998
9. **Yan L,Gupta R P and Wall T F (2002)**"A mathematical model of ash formation during pulverised coal combustion" *Fuel* Vol. 81,pp 337-344
10. **Kumar Uday (2005)**"Trace Element Geochemistry of Jharkhand Block Coal Seams,West Bokaro Coal Basin:a case study"Proc. 92thInd.Sc. Cong.pp.26-27
11. **Mandal Debashree(2010)**"Petrography of Coals of SouthCentral Sector of North Karanpura Coalfields(Jharkhand)R.U.Ph.D. Thesis (Unpublished)
12. **Kortenski J and Sotirov A(2002)**"Trace and Major Element content and Distribution in Neogene Coal from the Sofia Basin, Bulgaria" *International Journal of Coal Geology*, V 52 pp 63-82
13. **Finkelman, R.B. (1995)** "Mode of occurrence of environmentally sensitive trace element in coal", in Swaine D J ,Goodarzi F(Eds.) *Environmental aspects of Trace Elements in Coal*, Kluwer Academic Publ. , Dordrecht, pp 24-50
14. **Wang Wen-feng,Quin Yong,Wang Jun Yi, Li Jian (2009)** "Partitioning of hazardous trace elements during coal preparation" *Procedia Earth and Planetary Science*,Elsevier, V1,Issue 1, pp 838-844
15. **Ozbayoglu,G (2013)** Removal of Hazardous Air Pollutants based of commercial coal preparation plant data , *Physicochem. Probl. Miner. Process.* 49(2), , 621"629
16. **Finkelman, R.B., Orem, W., Castranova, V., Tatu, C.A., Belkin, H.E., Zheng, B., Lerch, H.E., Maharaj, S.V., Bates, A.L., 2002.** Health impacts of coal and coal use; possible solutions. *International Journal of Coal Geology* 50, 425 – 443.



Effects of rain water harvesting induced artificial recharge on the ground water in the areas of Palamu

Shweta Mishra^{a*}, P. K. Verma^b & Uday Kumar^b

^{a*}Department of Geology, Ranchi College, Ranchi, Jharkhand, India

^bDepartment of Geology, Ranchi University, Ranchi, Jharkhand, India

*Corresponding author : Phone : 9334892273, E-mail : shweta0502@gmail.com

Abstract : The increasing demand for water has increased awareness towards the use of Artificial Recharge to augment ground water supplies. It refers to the movement of water through man-made systems from the surface of the earth to underground water-bearing strata where it may be stored for future use. In the olden days, the recharge movement initiated by the local communities was aided and supported by those who valued water and practiced conservation. There are numerous examples and stone inscriptions from as early as 600 A.D. citing that ancient kings etc considered construction of small dug out ponds (ooranies), as one of their bounden duties to collect rain water and use it to recharge wells constructed within or outside ooranies to serve as drinking water source. This investigation was carried out in the areas of Patan and Daltonganj Blocks, Palamau Distt. The area has low groundwater potential due to poor recharge, surface runoff and evapotranspiration.

Paper History

Received

17th May 2017

Revised

22nd June 2017

Peer reviewed

29th June 2017

Accepted

5th July 2017

Keywords : Groundwater, scarcity of water, low cost structures, Watertable, cropping, sustainable growth

INTRODUCTION

Water on the earth is in motion through the hydrological cycle. The utilisation of water for most of the users i.e. human, animal or plant involves movement of water. Groundwater exploitation in India has increased with leaps and bounds and the number of shallow wells also has increased rapidly over the last fifty years. The growths of groundwater abstraction structures from 1950 to 1990 clearly depict the increasing use of groundwater utilization in domestic, industrial and agricultural sectors. As per the statistics, the number of dug wells increased from 38.6 lakhs (1951) to 94.9 lakhs (1990) and the shallow tube wells from 3000 (1951) to 47.5 lakhs (1990).

Artificial recharge of ground water is a process by which the ground water reservoir is augmented at a rate exceeding that obtaining under natural conditions of replenishment. Any man-made scheme or facility that adds water to an aquifer may be considered to be an artificial recharge system.

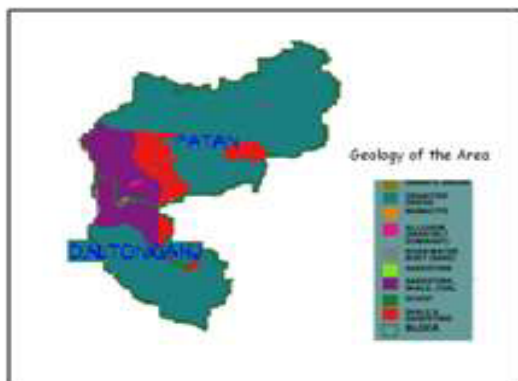
In the olden days, the recharge movement initiated by the local communities was aided and supported by those who valued water and practiced conservation. There are numerous examples and stone inscriptions from as early as 600 A.D. citing that ancient kings etc considered construction of small dug out ponds (ooranies), as one of their bounden duties to collect rain water and use it to recharge wells constructed within or outside ooranies to serve as drinking water source.

Roof water harvesting and storing that water in supply tanks or underground is a very common phenomenon in many states of India experiencing acute shortage of drinking water supplies. Ahar-Pyne is a traditional flood water harvesting system, indigenous to south Bihar, where an Ahar resembled a rectangular catchment basin with embankments on three sides. Pynes are channels constructed to divert the water flowing through hilly rivers into the Ahars. In south Bihar, rivers are generally dry for most of the year, but swell during the monsoon season.

Given the slope and the sandy soil prevalent in the region, the water is either carried away rapidly or it percolates through the sand. Hence, a system of Pynes was usually developed to lead off water from these rivers to agricultural fields. For eg. Tiwary ka Ahar, Ahars in Tandwa and Sakanpirhi in Palamu.



The Study Area



Geology of the area



Lineaments and drainage system of the area

The Artificial recharge structures in the Area

Initially the operational area was surveyed to know the perennial sources like River, Canal, Nallah, Checkdam, Ponds and type of land and adjoining topography. Different low cost techniques were used in the area depending upon the terrain.

Small tanks

The existing village tanks, which are often silted up or damaged, were modified to serve as recharge structures during rainfall by desilting its bed and providing a Cut off Trench on the upstream end of the bund.



Percolation Tanks

It is an artificially created surface water body, submerging in its reservoir a highly permeable land area so that the surface runoff is made to percolate and recharge the ground water storage. The tanks at 10' away from flowing source with 10' depth were having eternal, internal charging. The steps of 3' at each 1' by all sides drastically reduced the cost and water became available around the year due to such tanks.



Boulder Checks

At very low cost boulders were systematically arranged with patches of clay between layers to intervene flowing water. This was a valid intervention in cases where speed of flow was slow and this type of barrier cost for 30'*5" bund about Rs. 7,000 (Rs. 70*100 mandays).

Mishra *et.al.*: Effects of rain water harvesting induced artificial recharge on the ground water in the areas of Palamu



Tie ridges/Staggered Trenches

It was the most successful insitu soil moisture conservation technique used in SHRMS Plantation areas. Small Tie ridges of 5'x5' spacing formed by connecting corners of plants stored rainwater for a very long time and insitu percolation restricted the sudden flow of rainwater, charging the ground water of the area. About 4,000 Tie ridges at a cost of Rs.3.50/Tieridge were made per hectare which drastically improved the soil moisture of the area where slope was more than 8°. It cost about $\text{Rs.}4000 \times 3.50 = \text{Rs.}14,000/\text{hectare}$ (Rs.70*200 mandays).



Earthen Wells

In the area there are dug wells which have either gone dry or the water level has declined rapidly. Rainwater was diverted into the well to recharge the dried aquifer. The recharge water was guided through a pipe to the bottom of the well, below the water level to avoid scouring of bottom and entrapment of air bubbles in the aquifer. Some new Earthen wells of diameter 10' upto a depth of 20' were also dugout at a cost of below Rs. 15,000 with arrangement of lath-kuri in Rs. 2,500 and was good for irrigation of about ½ acre of land. This technique was commonly used for vegetable cultivation.



Ring-Ridge technique

In this technique big round and ring shaped ridges were made to surround fruit plants. This kept the soil moisture for longer duration. 250 plants per hectare were planted at a distance of 20'x20'. The cost of the plant ranged from Rs. 25 to 30 and plantation cost about Rs. Rs. 15/ plant. Thus total cost varied from Rs. 8,000 to 10,000/ hectare. These plants needed maintenance at a cost of Rs. 5,000/hectare for 2 more years. Thus the total cost of orchard development became around Rs. 20,000 per hectare. These plants were given social fencing so cost on fencing was saved.



Ridge-Ditch technique

If gradient or slope of land is high, then one another technique is helpful. In it 20'x2' ridges with 20'x1' ditch was dugout. Fast growing species or sabai or khus grass was planted at ridges which caused storage of rain water in ditches. This type of intervention broke the speed of flow of rain water and stored water for longer duration in ditches. The total cost came out to Rs. 9,000/hectare. (180 mandays/hect.).

Recharge pits

Recharge pits were constructed for recharging the shallow aquifers. These were constructed 1 to 2m wide and 2 to 3m deep which were backfilled with boulders, gravels and coarse sand. Average cost of construction of a recharge pit was around Rs. 5000 to Rs. 7500.



RESULTS

The open well, pond and hand pump data were collected from available sources for a span of three years and the data were analysed. From the data it is apparent that in all cases the water table had increased ranging from 0.3 meter in case of ponds to 6-7 meter in case of hand pumps. These ground data's not only shows a theoretical improvement due to vegetative cover but simultaneously it has improved the overall production of crops in the village. The overall water percolation has improved the soil and reduced the average temperature which is apparently felt on entering the plantation and comparing with outside plantation temperature.

From the analysis of survey data we concluded that Localized rainwater harvesting systems were an effective solution to the water crisis. This offered a decentralized system for decreasing the impact of drought and allowed the people's involvement in critical water management tasks with simple, local skill-based, cost-effective and environment-friendly technologies. The Conservation and harvesting of surplus monsoon runoff was taking place in ground water reservoir which otherwise was going unutilised outside the watershed/ basin. Before Artificial Groundwater Recharge impact, the groundwater flow direction was from North to Southeast, but after Artificial Groundwater Recharge impact the flow direction spreads to all surrounding areas.

Some bore wells that were dry previously were functioning for the irrigation uses. After the influence of Artificial Groundwater Recharge structures, all the defunct wells are functioning. Some parameters like fluoride are diluted due to Artificial Groundwater Recharge impact. Part of the seepage from recharge structures reaches the local groundwater system as artificial recharge. There is no ground water quality deterioration after Artificial Groundwater Recharge structures influence. In the period of heavy rainy season, two tanks over flowed 4 months in non- Artificial Groundwater Recharge executed area, but in Artificial Groundwater Recharge executed area two tanks over flowed for 3 months only. The remaining tanks located in Artificial Groundwater Recharge executed areas with injection well, never overflowed during this heavy rainy season indicating that the rainwater immediately percolated into the aquifer system through the injection well.

CONCLUSION

Artificial recharge of ground water is expected to increase worldwide, particularly in water scarcity areas, including several parts of India. Artificial recharge of ground- water can be used to preserve the water resources and restore the water table aquifer which has been threatened due to overexploitation and a fall in piezometric level.

Several artificial recharge methods like percolation ponding, recharge pitting induced recharging and construction of battery of wells are being practiced successfully all over the world. Various other soil and water conservation methods, which are also commonly adopted, include contour trenching, terracing, nala bunding etc.

It is very important to make water everybody's business. It means a role for everybody with respect to water. Every household and community has to become involved in the provision of water and in the protection of water resources. Make water the subject of a people's movement. It means the empowerment of our Urban and Rural community, i.e., to manage their own affairs with the state playing a critical supportive role. Further involving people will give the people greater ownership over the water project including watershed development, soil and water conservation and water harvesting will go a long way towards reducing misuse of government funds. It will also develop the ownership (own water supply systems), they

Mishra *et.al.*: Effects of rain water harvesting induced artificial recharge on the ground water in the areas of Palamu

will also take good care of them. In this way it is possible to solve water problems facing the county in the 21st century.

DISCUSSION

Water is a very valuable resource. There are no serious efforts to gain water by practices like rainwater harvesting, watersheds and mini-ponds. Rainwater harvesting should be made mandatory. Sequential water use (reuse, recovery and recycling of waste waters) should be planned wherever possible so that the load on fresh water can be reduced. Water's presence in agro-ecosystems should be treated on a holistic approach, and by employing scientific management tools it should be judiciously used. For agriculture, an integrated water management practice consisting of three main components –rain water harvesting, water-saving micro-irrigation, and highly efficient crop production—should be adopted. Conservation of water should be taken as a way of life and widely adopted.

ACKNOWLEDGEMENT

The author is grateful to Dr. P. K.Verma, Head of Department of Geology for his encouragements and support.

REFERENCES

1. **Muralidharan D and Athavale R.N, (1998)**, The Ground Water Recharge Movement in India by Ramaswamy Sakthivadivel, Pg 195
2. Rain water harvesting and artificial recharge to ground water: A guide to follow
3. **Pekka Nojd, Antti-Jussi Lindroos, Aino Smolander, John Derome, Llari Lumme, Helja-Sisko Helmisaari 2009** “Artificial Recharge of Groundwater through Sprinkling Infiltration: Impacts on Forest Soil and the Nutrients Status and Growth of Scots Pine,” Science of the Total Environment, Vol. 407, No. 10, , pp. 3365-3371
4. **Troch F R, Hoopa J A and Donahue R L, (1980)**, Soil and water conservation for productivity and environmental protection (Prentice-Hall, New Jersey), p. 718.



Evaluation of fluoride contamination in ground water in hard rocks terrains in and around Chukru–Chianki areas, Palamau, Jharkhand, India

Vijay Pandey^{a*}, P.K.Verma^b & Uday Kumar^b

^{a*}Department of Geology, N.P. University, Medininagar, Jharkhand, India

^bDepartment of Geology, Ranchi University, Ranchi, Jharkhand, India

*Corresponding author : Phone : 9470174036 , E-mail : vijaypandey1961@gmail.com

Abstract : Water is increasingly debated and contested. Very few studies on source and genesis of fluoride in water have been documented in and around village Chukru which is reported to be endemic for fluorosis. The authors had undertaken a study in and around Chukru village, Medininagar block of Palamau district of Jharkhand state to know the source and genesis of fluoride in groundwater. The major sources of drinking water in these villages are groundwater. The present paper deals with the evaluation of fluoride contamination in ground water in hard rocks terrains.

Paper History

Received

27th May 2017

Revised

12th June 2017

Peer reviewed

29th June 2017

Accepted

8th July 2017

Keywords : Fluoride, Rocks, Groundwater,

INTRODUCTION

Ground water is a major source of human intake of fluoride even through food items like tea sometimes contribute substantially (CaO *et al.*, 2000). High fluoride groundwater causing fluorosis, is a considerable health problem in several countries of the world. Endemic fluorosis has been identified in 20 states of India where about 62 million people, including 6 million children are at risk suffering from dental, skeletal and non-skeletal fluorosis. Excess fluoride concentration in drinking water is a major cause of fluorosis and the safe limit of fluoride in ground water is 1-1.5mg/L prescribed by WHO in 1984.

Water is increasingly debated and contested. Very few studies on source and genesis of fluoride in water have been documented in and around village Chukru which is reported to be endemic for fluorosis. The authors had undertaken a study in and around Chukru village, Medininagar block of Palamau district of Jharkhand state

to know the source and genesis of fluoride in groundwater. The major sources of drinking water in these villages are groundwater.

Source of fluoride:

The major sources of fluoride in groundwater are fluoride bearing minerals such as Fluor-apatite, Cryolite, Biotite, and Fluorite are the sources of fluoride in nature and are not found in free state. Fluorite occurs as accessory mineral in Granite, Gneisses and Pegmatite and it releases fluoride to groundwater through weathering of primary silicates and other accessory minerals.

Insecticides, Phosphate, Fertilizers, Herbicides used in agricultural practices are the anthropogenic contamination in groundwater (Verma *et al.*, 2003).

The fluoride content in groundwater is a function of many factors such as availability and solubility of fluoride minerals, probability and velocity of flowing, temperature

,PH, concentration of calcium, sodium and bicarbonate ions in water, etc(Santha kumari *et al.*,2007).

Location of the study area:

Study area is in and around Chukru village, Medininagar block of Palamau District, Jharkhand, India. It is situated about 12Kms South-East of Medininagar. It lies between Latitude 23°56'44" to 24°01'22"N and Longitude 84°05'53"E to 84°11'29"E (fig.1).

Climate:

It slopes from East to West. Generally the region has a hot climate with a short spell of rainy season and winter. Temperature is low during the month of December and January 4.5°C and hottest month is May 2009 48.5 C. The study area received intermittent rainfall.

Methodology:

In order to understand the probable source and genesis of fluoride in ground water care is taken to collect

fresh samples of schistose rocks as far as possible. Chip sampling method was used to collect calc-magnesian silicate rocks and amphibolites at random intervals. The size of the rock samples normally varied to 6"*4"*1"to5"*3"*1" and about 120 rock samples were collected during course of study. Chips were also collected with an idea for chemical analysis requirement. The samples were broken up into two parts-one part was kept for the petro graphical studies while the other half was used for chemical analysis. The rocks were analysed by X-ray Fluorescence Spectrometer (XRF) in RDCIS, SAIL, RANCHI and by ICP spectrophotometer. Water samples collected from dug wells and bore wells were analysed for fluoride concentration on site using colorimetric method using zirconium alizarin reagent. PH, bicarbonate, calcium, sodium and fluoride in ground water samples is analysed in the State Geological laboratory, Hazaribagh.

Table-2: Chemical analyses and trace elements of Granite rocks around Chukru village.

Major Oxides ↓	Pink Granite		Grey Granite	
Sample nos. →	Ch/33	Ch/38	Chuk42	Chuk44
SiO ₂	71.35	71.32	71.46	71.40
Al ₂ O ₃	16.55	16.60	17.05	17.10
Fe ₂ O ₃	0.62	0.63	0.56	0.58
Feo	1.19	1.18	1.23	1.22
Mno	0.05	0.06	0.04	0.05
Mgo	0.48	0.47	0.06	0.61
Na ₂ O	2.15	2.10	2.36	2.35
K ₂ O	6.71	6.72	5.33	5.34
CaO	0.80	0.82	1.02	1.05
TiO ₂	0.15	0.18	0.31	0.32
P ₂ O ₅	0.05	0.07	0.06	0.07
[o]	0.31	0.34	0.46	0.40
Total	100.41	100.49	100.48	100.49

Location:

Ch/33- ½ km south of yatrished Chianki Ranchi Road. Ch/38-1/2 km south of government middle school Chianki. Chuk/42-3/4 km west of yatrished Chukru Main road. Chuk/44-1 km south of Chukru Village.

Trace Element (ppm).

Ni	6	4	12	11
Co	4	5	12	14
Cr	8	9	14	15
Y	1.5	1.6	2.8	3.0
Zr	51	53	62	65
V	27	30	60	62
Nb	12	13	19	18

Table-3: Chemical analysis and Trace Elements of Amphibolites around village Chukru

Minerals	Massive amphibolites				Schistose amphibolites			
Sample nos→	Chuk33	Chuk35	Bh/23	Bh/27	Ch/21	Ch/28	Ba15	Ba20
<i>Sio₂</i>	47.24	47.62	50.61	50.64	48.50	48.51	48.49	48.46
<i>Al₂O₃</i>	15.43	15.55	14.80	14.45	13.90	13.95	13.92	13.91
<i>Fe₂O₃</i>	1.85	1.83	1.48	1.66	2.60	2.64	2.61	2.59
<i>Feo</i>	11.25	10.40	10.85	09.55	10.78	10.75	10.71	10.72
<i>Mno</i>	0.28	0.27	0.30	0.31	0.22	0.21	0.23	0.24
<i>Mgo</i>	7.12	6.60	8.65	7.18	6.95	6.91	6.88	6.93
<i>Na₂O</i>	2.22	2.15	2.25	2.45	2.15	2.14	2.11	2.13
<i>K₂O</i>	1.35	1.42	1.45	0.95	1.80	1.81	1.82	1.82
<i>Cao</i>	11.14	11.60	7.80	10.50	10.61	10.62	10.60	10.63
<i>Tio₂</i>	1.62	1.43	0.98	1.36	1.55	1.63	1.62	1.64
<i>P₂O₅</i>	0.20	0.21	0.18	0.20	0.21	0.23	0.23	0.25
<i>H₂O⁺</i>	1.20	1.42	1.21	1.38	1.34	1.30	1.40	1.41
Total	100.73	100.50	100.56	100.53	100.61	100.70	100.62	100.73

Trace Element

Ni	110	124	145	157	163	187	185	186
Cr	115	130	163	195	211	194	195	196
Co	36	45	49	51	41	43	45	44
Zr	531	488	545	511	509	496	510	507
Nb	26	25	27	24	25	26	25	23

Location:

Chuk/33- 1.5 km west of yatrished Chukru, main road. Ba/15-1/2km west of Govt primary middleschool, Bakhari. Chuk/35- ½ km south of new primary school (Nawatikar tola), Chukru. Bh/23- ¾ km west of yatrished, Bhusaria. Ba/20-1/4km east of Bakhari pahar Bh/27- ¼ km south of yatrished, Bhusaria. Ch/21- ¼ km west of yatrished, Chianki, near Govt. Middle school. Ch/28- 1 km south of Chianki yatrished, south of Chianki hill.

Table-4: Chemical analysis and Trace Elements of Gneissic rocks around village Chukru (Palamau)

Major Oxides↓	Pink Gneisses		Grey Gneisses		Migmatites	
Sample nos→	Chuk/8	Chuk/15	Bh/25	Bh/38	Bh/24	Ch/27
SiO_2	72.06	72.20	72.45	72.15	71.80	71.75
Al_2O_3	14.50	14.45	14.50	14.54	14.46	14.60
Fe_2O_3	0.71	0.65	0.55	0.64	0.66	0.64
Feo	1.90	1.80	1.85	1.88	1.90	1.87
Mno	0.06	0.04	0.05	0.03	0.05	0.04
Mgo	0.87	0.85	0.82	0.84	0.62	0.64
Na_2O	3.20	3.14	3.15	3.20	3.22	3.21
K_2O	4.77	4.82	4.81	4.81	4.83	4.82
Cao	1.09	1.08	1.11	1.10	1.08	1.09
TiO_2	0.25	0.23	0.25	0.24	0.66	0.67
P_2O_5	0.07	0.08	0.07	0.06	0.12	0.13
[o]	0.35	0.38	0.38	0.36	0.37	0.36

Trace Element (ppm).

Ni	12	07	08	16	15	14
Co	12	07	11	17	13	15
Cr	17	16	15	18	22	24
Y	6.20	4.20	6.00	9.20	8.25	9.00
Zr	65	67	66	68	81	83
V	26	31	41	44	42	51

Location

Chuk/8- 3/4 km of yatrished, Chukru main road. Chuk/15- ¼ km east of yatrished, Chukru. Bh/25- ½ km north of yatrished, Bhusaria. Bh/38- 1/4 km east of yatrished, Bhusaria. Ba/24-1/2 km west of Govt. middle school, Bakhari near Mangru Ram's house. Ch/27- ½ km s-w of yatrished, Chianki.

Table 5: Major Element Analysis (WT %) of Calc-Magnesian Silicate rocks of the present area.

Minerals	Tremolite-Actinolite Schist		Talc-Tremolite Schist		
Sample nos	Chuk/32	Bh/56	Ka/36	Ch/19	Ch/34
SiO_2	58.95	59.00	59.20	59.10	58.98
Al_2O_3	0.02	0.03	0.03	0.03	0.02
Fe_2O_3	0.74	0.75	0.76	0.75	0.76
Feo	2.20	2.22	2.22	2.23	2.21
Mno	0.39	0.38	0.40	0.42	0.41
Mgo	24.62	24.66	24.66	24.70	24.71
Na_2O	1.48	1.50	1.51	1.48	1.50
K_2O	0.31	0.32	0.34	0.36	0.35
Cao	9.60	9.65	10.00	10.05	10.04
TiO_2	0.62	0.63	0.62	0.63	0.64
P_2O_5	0.14	0.16	0.10	0.10	0.11

Pandey *et al.*: Evaluation of fluoride contamination in ground water in hard rocks terrains in and around Chukru – Chianki areas, Palamau, Jharkhand, India

Trace Element

Zn	29	19	20	19	21
Cu	36	35	36	32	38
Pb	20	18	18	20	22
Ni	10	09	11	12	14
Cr	09	08	07	08	09
V	10	09	11	12	10
Ba	24	26	28	27	25

Location

Ch/19 -1/2 km southwest of aerodrome Daltonganj-Ranchi road. Ch/34 -1/2 km west of yatrished Chianki near Govt. School. Kau/36 -1/2 km east of Chianki Railway Station. Chuk/32 - 1.5 km west of Chukru (Nawatikar). Bh/56- 1/4 km east of D.A.V Engineering College Bhusaria.

Table 6: Chemical analysis data of pelitic schist of the area and its comparison with average medium grade metapelite (after Shaw, 1954; 1956)

Chemical constituent	Pelitic schist				Average medium grade metapelite Shaw, 1954;1956
Sample nos	PO/11	PO/21	Chuk20	Chuk25	
SiO_2	64.81	64.85	65.10	65.15	61.54
Al_2O_3	16.40	16.56	15.66	15.70	16.95
Fe_2O_3	4.05	4.02	4.12	4.05	1.13
Feo	2.50	2.56	2.62	2.57	6.02
Mno	0.12	0.11	0.12	0.13	0.09
Mgo	2.62	2.65	2.68	2.75	2.52
Na_2O	1.81	1.82	1.84	1.83	1.84
K_2O	4.94	4.92	4.70	4.67	3.45
Cao	1.11	1.15	1.14	1.16	1.76
TiO_2	0.68	0.72	0.80	0.78	0.82
P_2O_5	0.06	0.05	0.05	0.06	0.14

Trace Element

Cr	362	364	366	365	113
Ni	117	120	124	128	73
Co	40	38	35	36	19
Cu	25	24	26	25	23
Y	220	241	222	244	379
V	127	125	130	128	125
Zr	16.5	16.0	16.10	16.20	21.30

Location

Near confluence of Ranchi road and Barwadih road (Dubiakhar more) east and west of Chukuru.(Po11-1/4km south of Dubiakhar more ,Po21-1/2km southwest of Dubiakhar more ,Chuk20-1/4km east of yatrished ,Chukru main road ,Chuk25-1/4km west of yatrished ,Chukru main road).

Table7: Chemical analysis of Granite rocks (Weight percent oxides)

Chemical constituent↓	Biotite granite gneiss		Pegmatite	
Sample nos →	Chuk/26	Chuk/50	chuk/39	chuk/45
SiO_2	71.25	71.30	71.36	71.24
Al_2O_3	14.95	15.00	14.90	15.03
Fe_2O_3	0.70	0.65	0.68	0.71
Feo	1.90	1.88	1.91	1.90
Mno	0.04	0.05	0.07	0.08
Mgo	0.62	0.66	0.61	0.62
Na_2O	3.11	3.14	3.12	3.10
K_2O	4.70	4.71	4.68	4.65
Cao	1.08	1.07	1.09	1.10
TiO_2	0.24	0.30	0.32	0.33
P_2O_5	0.06	0.07	0.11	0.10

Trace Element

Ni	09	07	13	15
Co	08	06	13	16
Cr	12	13	15	17
V	26	31	41	50
Zr	69	82	38	40

Location

Chuk/26-1.5 km S-W of yatrished, Chukru main road near Babulal's house (Nawatikar tola). Chuk/39- ¼ km N-E of yatrished, Chukru. Chuk/45- 1*1/2km west of Chukru yatrished, Nawatikar tola. Chuk/50- Near new Govt. primary school, Nawatikar tola , Chukru.

Table 8: Geochemical analysis of groundwater in and around Village-Chukru, Medininagar block, Dist- Palamau (Jharkhand) during May 2008

Sl. no.	Location	Source	Temp,(C)	PH	Ca ⁺² , mg/L	Na ⁺ , mg/L	HCO ₃ ⁻ mg/L	F ⁻ ,mg/L
1	Yatrished, Chukru main road	Bore well	27.2	8.6	9.0	160	995	9.90
2	Doman Singh	Dug well	27.0	7.2	27.0	110	195	2.00
3	Govt. middle school, Chukru	Bore well	27.4	8.2	14.0	100	720	6.10
4	Govt. New Primary School(Nawatikar Tola)	Bore well	27.0	8.0	21.0	66	375	3.75
5	Saatnarayan Oroan,(Nawatikar), Chukru	Dug well	27.0	7.5	25.0	75	256	3.20
6	Chakriya vikas Office near Bajrangi Singh's house (Nawatiker tola), Chukru	Dug well	26.8	7.7	20.0	64	390	3.95
7	Shiv kumar Bhuiya (Nawatiker tola)	Bore well	27.2	8.3	11.0	150	900	9.10
8	Jagnath pal (Nawatikar tola), Chianki	Bore well	27.3	8.4	10.0	156	910	9.30
9	Govt. middle school, Chianki	Bore well	27.8	6.6	27.0	118	210	2.00
10	Krshna Paswan, Chianki	Dug well	26.0	7.3	28.0	120	100	2.90
11	M.K.DAV Public School Chianki Main Road	Bore well	27.0	7.2	32.0	98	210	2.00
12	Homeguard training center, Chianki	Bore well	27.0	7.1	33.0	95	199	1.99
13	Yatrished, Chianki	Bore well	27.2	7.0	35.0	90	193	1.90
14	Yatrished, Jorkat	Bore well	27.0	6.9	38.0	120	178	1.85
15	Bablu Oroan Near NH-75 pole, jorkat	Dug well	26.0	7.2z	32.0	98	200	1.98
16	Yatrished, Bhusaria	Bore well	26.0	6.8	39.0	85	160	1.66
17	Ram swarup Singh Azad ghat, Bhusaria	Dug well	27.0	7.0	35.0	51	192	1.90
18	Govt. school, Bakhari	Bore well	28.6	8.8	9.0	160	1050	10.00
19	Late Mangru Ram near Kaushalya's devi house, Bakhri	Dug well	27.4	8.8	8.0	166	1080	11.00
20	Kardhani vishwakarma, Sua-kauria	Dug well	26.8	7.1	29.0	185	192	1.95
21	Govt. middle school, Kauria	Bore well	27.0	7.5	27.0	120	310	3.00
22	Ramanuj Tiwari, sarja	Dug well	26.0	6.6	40.0	90	165	1.61
23	Basic school Polpol	Bore well	26.0	6.6	40.0	90	160	1.60

Table 9: Geochemical analysis of groundwater in and around Village-Chukru, Medininagar block, Dist- Palamau (Jharkhand) during December 2008

Sl. No	Location	Source	Temp,(C)	PH	Ca ⁺² , mg/L	Na ⁺ , mg/L	HCO ₃ ⁻ mg/L	F ⁻ ,mg/L
1	Yatrished, Chukru main road	Bore well	20.5	8.5	15	81	605	6.01
2	Doman Singh	Dug well	20.0	7.5	35	50	186	1.80
3	Govt. middle school, Chukru	Bore well	20.2	8.0	20	135.5	430	4.21
4	Govt. New Primary School(Nawatikar Tola)	Bore well	20.1	7.8	31	8.0	265	2.50
5	Saatnarayan Oroan,(Nawatikar),Chukru	Dug well	20.0	7.5	27	1.16	200	1.99
6	Chakriya vikas Office near Bajrangi Singh's house (Nawatiker tola), Chukru	Dug well	20.0	7.7	28	1.25	285	2.80
7	Shiv kumar Bhuiya (Nawatiker tola)	Bore well	20.7	8.2	16	2.54	500	5.00
8	Jagnath pal (Nawatikar tola) ,Chianki	Bore well	20.7	8.2	16	2.54	550	5.21
9	Govt. middle school, Chianki	Bore well	20.0	7.4	30	6.68	120	1.20
10	Krshna Paswan,Chianki	Dug well	20.1	7.5	32	96.5	140	1.31
11	M.K.DAV Public School Chianki Main Road	Bore well	20.0	7.1	34	45.6	100	1.00
12	Homeguard training center,Chianki	Bore well	20.0	7.1	42	72.6	120	1.20
13	Yatrished,Chianki	Bore well	20.1	7.6	39	76	252	1.26
14	Yatrished,Jorkat	Bore well	20.0	7.1	34	45.6	100	1.00
15	Bablu Oroan Near NH-75 pole,jorkat	Dug well	20.0	7.1	44	27.5	180	0.60
16	Yatrished,Bhusaria	Bore well	20.0	7.1	44	27.5	180	0.60
17	Ram swarup Singh Azad ghat, Bhusaria	Dug well	20.3	7.5	39	75.5	100	1.00
18	Govt. school, Bakhari	Bore well	20.8	8.5	17	80	399	4.00
19	Late Mangru Ram near Kaushalya's devi house, Bakhri	Dug well	20.8	8.5	17	80	399	4.00
20	Kardhani vishwakarma, Sua-kauria	Dug well	20.2	7.2	44	27.5	180	0.60
21	Govt. middle school, Kauria	Bore well	20.1	7.2	45	55	100	1.00
22	Ramanuj Tiwari,sarja	Dug well	20.2	7.2	45	55	100	1.00
23	Basic school Polpol	Bore well	20.2	7.2	44	27.5	180	0.06
24	Yatrished, Dubiakhar,main road	Bore well	20.1	7.2	45	55	100	1.00

Pandey *et. al.*: Evaluation of fluoride contamination in ground water in hard rocks terrains in and around Chukru – Chianki areas, Palamau, Jharkhand, India

Table10: Geochemical analysis of groundwater in and around Village-Chukru, Medininagar block, Dist- Palamau (Jharkhand) during May 2009.

Sl. no	Location	Source	Temp,(C)	PH	Ca ⁺² , mg/L	Na ⁺ ,mg/L	HCO ₃ ⁻ 'mg/L	F ⁻ ,mg/L
1	Yatrished, Chukru main road	Bore well	27.4	9.8	10	151.5	1080	10.50
2	Doman Singh	Dug well	27.8	8.0	28	120	325	3.00
3	Govt. middle school, Chukru	Bore well	27.5	9.0	12	164	930	9.25
4	Govt. New Primary School(Nawatikar Tola)	Bore well	27.6	8.6	14	81	700	6.51
5	Saatnarayan Oroan,(Nawatikar),Chukru	Dug well	27.8	8.1	28	120	345	3.50
6	Chakriya vikas Office near Bajrangi Singh's house (Nawatiker tola), Chukru	Dug well	27.7	8.5	21	66	410	4.01
7	Shiv kumar Bhuiya (Nawatiker tola)	Bore well	27.1	9.5	10	151.5	1100	10.00
8	Jagnath pal (Nawatikar tola) ,Chianki	Bore well	27.1	9.5	10	151.5	1080	10.55
9	Govt. middle school, Chianki	Bore well	27.9	7.7	25	70	215	2.05
10	Krshna Paswan,Chianki	Dug well	27.8	8.0	28	120	325	3.00
11	M.K.DAV Public School Chianki Main Road	Bore well	27.9	7.6	30	76	220	2.16
12	Homeguard training center,Chianki	Bore well	27.9	7.5	31	80	265	2.50
13	Yatrished,Chianki	Bore well	27.9	7.5	30	75	220	2.01
14	Yatrished,Jorkat	Bore well	27.9	7.5	32	97	196	1.98
15	Bablu Oroan Near NH-75 pole,jorkat	Dug well	27.9	7.6	27	115	200	2.00
16	Yatrished,Bhusaria	Bore well	28.0	7.2	35	80	160	1.50
17	Ram swarup Singh Azad ghat, Bhusaria	Dug well	27.8	8.0	16	95	215	2.15
18	Govt. school, Bakhari	Bore well	27.2	9.2	11	173	1170	11.65
19	Late Mangru Ram near Kaushalya's devi house, Bakhri	Dug well	27.1	9.8	09	151	1280	12.80
20	Kardhani vishwakarma, Sua-kauria	Dug well	27.8	7.8	17	78	210	2.00
21	Govt. middle school, Kauria	Bore well	27.8	7.8	23	80	355	3.60
22	Ramanuj Tiwari,sarja	Dug well	28.0	7.7	30	90	170	1.77
23	Basic school Polpol	Bore well	28.0	7.5	20	63.3	220	1.20
24	Yatrished, Dubiakhar,main road	Bore well	27.9	7.5	27	118	252	2.52

Table 11: Geochemical analysis of groundwater in and around Village-Chukru, Medininagar block, Dist-Palamau (Jharkhand) during December 2008 and November 2009.

Sl. no	Location	Source	Previous Fluoride content in mg/l during Dec. 2008 (a)	Fluoride content in mg/l water samples +rock samples during Nov. 2009 (b)	b - a	Rock Samples
1	Yatrished, Chukru main road	Bore well	3.61	4.22	0.61	Pegmatite
2	Doman Singh	Dug well	2.50	3.35	0.85	Biotite
3	Govt. middle school, Chukru	Bore well	3.00	3.70	0.70	Biotite Schist
4	Chakriya vikas Office near Bajrangi Singh's house (Nawatiker tola), Chukru	Dug well	4.01	5.06	1.05	Quartz + Biotite
5	Shiv kumar Bhuiya (Nawatiker tola)	Bore well	4.00	4.66	0.66	Pegmatite
6	Jagnath pal	Bore well	4.00	4.60	0.60	Pegmatite
7	Govt. middle school, Chianki	Bore well	1.20	2.21	1.01	Biotite Granite gneiss
8	Krishna Paswan, Chianki	Dug well	1.90	2.65	0.75	Pink Granite Gneiss
9	Homegaurd training centre, Chianki	Bore well	2.05	2.25	0.20	Hornblende
10	Raj kumar Bhuiya, Jorkat	Dug well	1.00	2.02	1.02	Biotite Granite gneiss
11	Yatrished, Jorkat	Bore well	1.50	1.85	0.35	Amphibolite
12	Yatrished, Dubiakhar more	Bore well	2.06	3.02	0.96	Quartz + Biotite
13	Ram swarup Singh Azad ghat, Bhusaria	Dug well	1.99	2.30	0.66	Grey Granite gneiss
14	Yatrished, Bhusaria	Bore well	0.99	1.86	0.87	Biotite
15	Govt. School, Bakhari	Bore well	1.50	2.15	0.65	Pegmatite
16	Late Mangru Ram near Kaushalya's devi house, Bakhri	Dug well	3.60	4.22	0.62	Pegmatite
17	Kardhani vishwakarma, Sua-kauria	Dug well	1.90	2.82	0.92	Quartz + Biotite
18	Govt. middle school, Kauria	Bore well	3.30	3.68	0.38	Amphibolite
19	Helth centre, Sarja	Bore well	1.92	2.83	0.91	Muscovite + Biotite
20	Govt. basic school, Polpol	Bore well	2.01	2.20	0.29	Muscovite

RESULTS & DISCUSSION

Chemical analysis data of rock samples (table 1 to 7) show higher silica % and others are less. Chemically pink gneisses, grey gneisses and migmatites are characterised by high silica and potash but other oxides of Fe, Mg, Ca, Mn, Na etc. are less. The $\text{Na}_2\text{O}/\text{K}_2\text{O}$ ratio is less in gneissic rocks. Similarly grey gneisses are characterised by the higher % of SiO_2 and Al_2O_3 . The composition of different varieties of granite varies widely. The pink granites are rich in alkalis but have poor % of FeO in comparison to grey granites. The characteristic feature of pink granites is the high content of normative orthoclase and quartz with absence of hypersthene molecule. The oxide ratio of pink granites viz. FeO/MgO , $\text{Fe}_2\text{O}_3/\text{FeO}$, and $\text{CaO}/\text{Na}_2\text{O}+\text{K}_2\text{O}$ are higher than grey granites. The ratio $\text{K}_2\text{O}/\text{Na}_2\text{O}$ is relatively higher in pink granite in comparison to grey granites. C.I.P.W norms also show the quartz is also less than orthoclase and apatite and biotite minerals present in trace amount, (Verma 2006).

Thus it has been concluded that granites are formed at high temperature and pressure and in gneisses, the iron rich biotite had effectively lowered the melting temperature and enriched K-component to the melt. More potash feldspar, low abundance of mafic minerals and low $\text{Na}_2\text{O}/\text{K}_2\text{O}$ ratio are the characteristics of Chhotanagpur granite. The diorite associated with migmatite appears to be an anatectic that residue.

The amphibolites are hard, compact and massive dark, coloured rock and composed mainly of hornblends, plagioclase with little sphene and magnetite. The amphibolites which occur in vicinity of migmatites are rich in biotite. Schistose amphibolites are fine to medium grained, hard and compact. It is recrystallised granoblastic plagioclase, minor quartz, biotite, garnet, and sphene. Massive amphibolite is fine grained, hard and dark coloured rock. They have been affected by pegmatites and quartzo feldspathic veins.

In the present area joints are the most commonly found structure in almost all types particularly in the granitic rocks. Joints are also excellently displayed in amphibolites and quartzites.

On the basis of above discussion and study authors may conclude that the amphibolites do not seem to have undergone any contamination through assimilation or

mixing. Partial melting of depleted mantle, previously altered followed by fractional crystallisation of the magma thus generated seem to have yielded the precursors to the amphibolites that find today.

The results of geochemical analysis of ground water samples collected from dug wells and bore wells are presented in Table 8, 9, 10 and 11. The PH value varies from 6.62 to 8.8 during May 2008, 7.1 to 8.5 during December 2008 and 7.5 to 9.8 during May 2009 as shown in Table 8, 9, 10 respectively. Indicating an alkaline condition which favours the solubility of fluorine-bearing minerals. In acidic condition fluoride is adsorbed in clay; however, in alkaline condition it is desorbed, and thus alkaline PH is more favourable from fluoride dissolution activity ⁶.

The bicarbonate content varies from 160 to 1080 mg/L during May 2008, 100 to 605 mg/L during December 2008, and 160 to 1170 mg/L during May 2009 in Table 8, 9, 10 respectively. The calcium content in the study area varies from 9.0 to 4.0 mg/L, 15 to 45 mg/L and 0.9 to 35 mg/L during May 2008, December 2008 and May 2009 respectively. Sodium content varies from 64 to 185 mg/L during May 2008, 27.5 to 254 mg/L during December 2008 and 63.3 to 173 mg/L during May 2009. Due to common ion effect, the dissolution of fluoride is suppressed, when the concentration is above the limit of fluoride solubility. The calcium concentrations were lower than the sodium concentration which indicates that higher fluoride content in the ground water of the present area. A strong negative correlation between calcium and fluoride in the ground water that contain calcium in excess of that required for the solubility of fluoride-bearing minerals have been observed by many researchers. Generally, high concentrations of Sodium will increase the solubility of the fluoride-bearing minerals in the waters. This is the main cause for the higher levels of fluoride in the ground water of the study area. Under the prevailing semi-arid hot climate conditions during weathering of granite and gneissic rocks, fluorine is released from apatite, hornblende and biotite to the circulating alkaline

Ground water⁶ Geogenic contamination of ground water is mainly a natural process, that is leaching of fluoride-bearing minerals, since no man-made pollution have been noticed.

The fluoride concentration varies from 160 to 9.90 mg/L during May 2008, 0.60 to 6.01 mg/L during

December 2008 and 1.20 to 12.80 mg/L during May 2009. The authors carried out investigations on the genesis and content of fluoride in ground water of the villages affected with dental, skeletal and non-skeletal fluorosis and also the probable sources from which the fluoride is leaching out to the ground water and causing high concentration of fluoride in the area. In the fluoride affected villages, villagers both children and adults suffer from health-disorders like mottling of teeth, deformation of ligaments, bending of spinal column and ageing problem. High fluoride (>1.5 mg/L) concentration distribution was found mainly in the villages of Chianki, Jorkat, Dubiakhar, Azad ghat, Pokhrah, Bhusaria, Bakhari, Taliabandh, Sarja, Polpol and Sua-kauria.

Remedial Options for Fluoride Reduction in Ground water:

The widespread incidence of fluorosis in India bearing both health and social problem has now become a great-concern now a day. Malnutrition because of poverty and diets deficient in calcium, vitamin seems to aggravate symptoms of fluorosis. Habitual consumption of excess amounts of tea and tobacco-based items were observed in all age groups. We are working with the problem of in groundwater agrees to overcome the problem and need of fluoride free drinking water. As an immediate solution, to alleviate the human sufferings defluoridation of ground water and supply of safe drinking water is the only option, although many attempts have been made still it remains a problem. Excessive fluoride ingestion by human beings can be prevented by using the following methods:-

- I. Defluoridation: The available defluoridation processes have their own limitations in terms of either the cost or techno feasibility. The acceptable methods are:
 - a. Nalgonda technique.
 - b. Ion exchange method.
 - c. Alumina based filters are suggested by the society to the people.
 - d. Venkatraman et al developed technique using paddy husk carbon impregnated with alum.
 - e. Distillation of water can effectively remove salts and hence fluoride from water.

II. Alternate water sources: Using alternate water sources in the surface water, rain water and low fluoride ground water.

III. Changing the dietary habits of the people without disturbing the available resources of food and the customs of the people. This can be done by minor changes in the diet (use of diet rich in calcium and vitamin C) and dietary habits (e.g. cooking practices which destroy vitamin C during cooking) of the people within their social system and available resources.

Considering the limitations and difficulties of the methods, the authors develop a simple, low cost and technofeasible method to know source and leaching of fluoride in ground water from fluoride bearing minerals. The locally available natural fluoride bearing minerals are used as adsorbents. Purchased 20 plastic jar and collected ground water from dug well and bore wells were analysed within 24 hrs. For fluoride concentration during December 2008. The fluoride content varies from 0.60 to 6.01 mg/L. The known volume of analysed water samples were kept in plastic jar with known weight of rocks samples for about 11 months. After 11 months analysed water samples were reanalysed during November 2009. On the basis of results and study we concluded that fluoride concentration was increased. It is clear that fluoride is leaching from fluoride bearing minerals (table 11). The case study indicates the sources and genesis from which fluoride is leaching out from fluoride bearing minerals to the ground water and causing high concentration of fluoride in ground water of the study area.

On the basis of above results and discussion we may conclude that the highest fluoride content was found to corroborate with low calcium values and high sodium content in ground waters. Weathering and leaching of fluorine bearing minerals in the rock formations under alkaline environment lead to the enrichment of fluoride in ground water. Comparatively low rainfall, intensive irrigation and heavy use of fertilizers, alkaline environment, longer residence time of water in the weathered aquifers zone and low rate of dilution are favourable factors for the dissolution of fluorine bearing minerals and thereby increase of fluoride concentration in ground water. According to Handa (1975) an inverse relationship is found

Pandey *et. al.*: Evaluation of fluoride contamination in ground water in hard rocks terrains in and around Chukru – Chianki areas, Palamau, Jharkhand, India

between fluoride and calcium in investigations. Decreasing calcium concentrations are found under alkaline conditions, when sodium content is increasing. On the other hand, Apambire et al, 1997. Pointed out that sodium may exhibit a positive correlation with fluoride. High concentration of sodium will increase the solubility of fluorite in water.

SUGGESTION

- I. Environmental awareness programme for the health implications of fluoride should be emphasized through education of the public community participation.
- II. Nutritional diet such as calcium and vitamin rich food should be recommended to those affected with fluorosis, as it decreases rate of accumulation of fluoride in the human body.
- III. Rain water harvesting technique through watershed management should be implemented at earliest for safety of local population

REFERENCES

1. Venkatramanan, K., Krishnaswamy, N., Ramkrishnan, I., 1951. Ind.J.Med.Res, 39, 211.
2. Handa, B.K., 1975. Geochemistry and genesis of fluoride containing ground waters in India, Ground water 13, 275-281.
3. WHO, 1984. Fluorine and Fluorides, Environmental health criteria 36, World Health Organisation, Geneva.
4. APHA, 1995 Standard methods for the examination of water and wastewater. American Public Health Association, Washington, DC.
5. Apambire, W.B., Boyke, D.R., and MicaL, f.a., 1997. Geochemistry, genesis and health implications of fluoriferous ground waters in the upper regions of Ghana. Environmental Geology, 33(1), 13-24.
6. Cao.J., Zhao, Y., Xirao, R.D., Danzeng, S.B., 2000. Environmental fluoride in Tibet, Environ, res, 83, 333-337.
7. Verma, P.K., Kumar, U., Sinha, S.P., 2002. Paper presented on genesis of fluoride in ground water of village Chukru, District-palamau, Jharkhand state.
8. Susheela, A.K., 2003. A treatise on fluorosis-revised 2nd edition, fluoride 36(3).
9. Verma, P.K., 2006. Petrochemistry of the amphibolites and the associated rocks around Betla, District-Palamau, Jharkhand.
10. Shantha Kumari, D., SRinivasalu, S., Subramanian, S., 2007. Fluoride contaminated water and its implications on human health in Vellore District, Tamil Nadu, India.
11. Janardhan Raju, N., Dey, S., and Das, K., 2009. Fluoride contamination in ground water of Sonbhadra District, Uttar Pradesh, India, Curr, Sci, Vol.96, No7, 979-985 pp



Comparative study of change in soil composition due to the biomass generation through Chakriya Vikas Pranali Project - A case study of Tandwa, district Palamu.

Shyam Lal Singh*, P. K. Verma & Shweta Mishra

University Department of Geology, Ranchi University, Ranchi, Jharkhand, India.

*Corresponding author : Phone : 8757169443 , E-mail : ssgeology11@gmail.com

Abstract : Soil composition reflects dynamic properties and is subject to various types of changes due to several factors. One of the factors is biomass generation which has been reported in this paper through a case study on comparative scale of the soil composition of various pockets of Tandwa district of Palamu. A specific project- C.V.P (Chakriya Vikas Pranali) has been taken up as the research methodology which involved multitier cropping system in a single piece of land.

Paper History

Received

17th May 2017

Revised

22nd June 2017

Peer reviewed

29th June 2017

Accepted

5th July 2017

Keywords : Soil composition, Biomass regenerations, C.V. P, Tandwa, district Palamu.

INTRODUCTION

The biomass is generated due to decomposition of leaf litters of different kinds of plants. Due to generation of biomass and mixing up with it, the soil composition also changes. Different kinds of plants contain different kinds of elements and thus the biomasses generated have also of different compositions and as such the enriched soil composition contains the certain kinds of elements along with varying water contents^{1,2,3}. Organic matter reduces surface runoff and erosion as a result there is more available water for plant growth. Organic matter serves as reservoir of chemical elements that are essential for plant growth⁴.

Location

The Palamu division falls within the latitudes 23°30'N to 24°30'N and longitudes 83°15'E to 85°0'E. The project village Tandwa is located in Patan block of Palamu district. The area is covered in Toposheet No. G45S4 of Survey of India in the scale of 1:50000.

General Geology of the area –

The study area forms a part of Chotanagpur Gneiss Granulite Complex. It is a composite mass which consist mainly of gneisses and migmatites with metasedimentary enclave (pelitic, calcareous and psammatic) rocks intrusive granite of different ages. Important metabasic rocks like amphibolites, metadolerites and metagabbro are generally aligned parallel to the regional foliation and have intruded into metasedimentary and gneisses.

Geological structures like foliation, schistosity, and lineation are present in various rock formations⁵.

The tentative Geological sequence is as below-

Pegmatite and Quartz veins

Metadolerites, Metagabbro

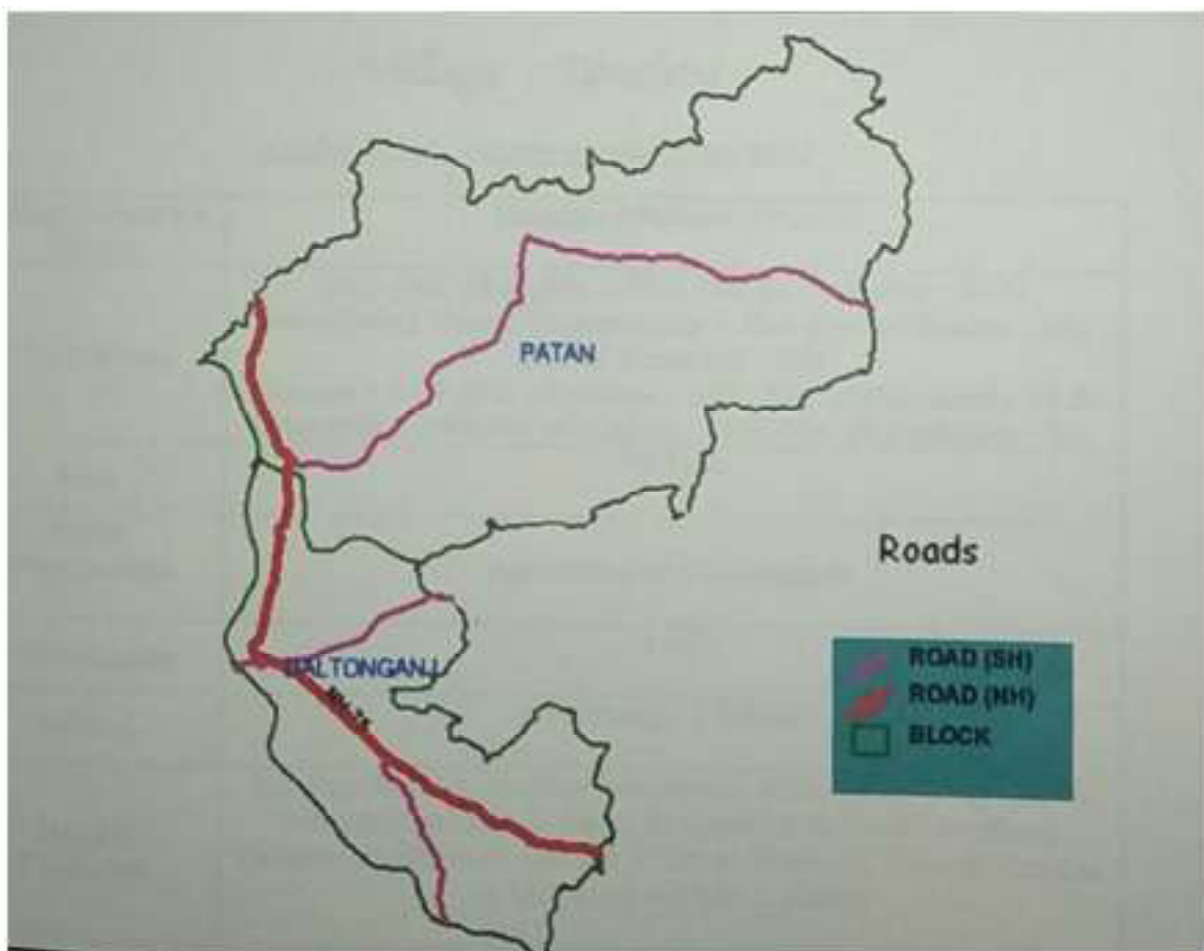
Granite

Biotite bearing Porphyritic granite

Massive amphibolites

Metasedimentary, Quartzite, Schistose rocks,

Schistose amphibolites etc.



Geomorphology

Palamu district has an undulating terrain and contains a series of interlinked rivers.

The slope of the land along the river side varies between 4° to 24° which facilitates the flow of rain water to the river and prevents percolation causing less recharge of groundwater.

Due to lateral force the vegetative growth is well developed in certain pockets but the study area contain plantation between Tandwa and Sankapirhi villages. Canals are present for irrigation purpose. Seasonal crops are taken round the year.

Chakriya Vikas Pranali Pattern

Chakriya Vikas Pranali Project has taken up multitier cropping system in a single piece of land which includes root crops, seasonal vegetables, fruit species and forest

species. The leaf litters fall and mixes as the biomass with the top cover of soil during rainy season and bring about change in the soil composition and thus changes and increases the soil fertility⁶.

Soil sample analysis

As a sample case 5 samples of Non treated 5 samples of Treated zones were collected and analysed at Analytical and Environmental Engineering Laboratory of Yugantar Bharti. The parameters which were taken into consideration are pH, Ca, T-N, P and K.

For pH calculation- IS 2720 (P -26) method, for Ca IS 2720 (P- 23), for T-N Kjeldahl method and for K and P Colourimetry methods were adopted for analysis process.

Required precautions were taken and process was followed for obtaining accurate data.

Singh et. al. - Comparative study of change in soil composition due to the biomass generation through Chakriya Vikas Pranali Project - A case study of Tandwa, district Palamu.

Chart below given the analysis data of Treated and Non- treated zones



YUGANTAR BHARATI

ANALYTICAL & ENVIRONMENTAL ENGINEERING LABORATORY

LAB ACCREDITED BY: **National Accreditation Board for Testing & Calibration Laboratory (NABL), New Delhi**
Jharkhand State Pollution Control Board (JSPCB)

(T 2982, T-2918)
(B-1874)

Test Report

Issued to	Mr. Shyam Lal Singh Ranchi University, Ranchi Jharkhand	Sample Code	170906-Soil-A01, 170906-Soil-A02, 170906-Soil-A03, 170906-Soil-A04, 170906-Soil-A05,
		Report ID	YBAEEL/RNC/17-09-06/Soil/01
		Date of Issue	17 th October 2017

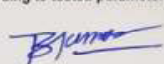
Sample Particulars		Details of Sampling	
Sample Name/Description	Soil sample	Date of sampling	Unknown
Sample Quantity	1 kg approx	Sample Received Date	6 th September 2017
Sample pkg. Condition	Sealed in Plastic bag	Sample collected by	Customer
Test started on	7 th September 2017	Sampling Location	TPST -1, TPST -2, TPST -3, TPST -4, TPST -5,
Test completed on	5 th October 2017		

Test Results

Sl. No.	PARAMETERS	UNIT	METHOD	TPTS -1	TPTS -2	TPTS -3	TPTS -4	TPTS -5
1	pH		IS 2720 (p-26)	6.48	6.41	5.41	6.27	6.5
2	CALCIUM	%	IS 2720 (p-23)	1.4	1.6	1.4	1.8	1.4
3	T. NITROGEN	%	Kjeldahl Method	19.6	12.6	11.6	11.48	10.36
4	POTASSIUM	Kg/Acre	Colourimetric Method	81-120	50-80	50-80	81-120	81-120
5	PHOSPHOROUS	Kg/Acre	Colourimetric Method	2	5	2	<15	2

*****End of Test*****

Remarks:-According to tested parameter, the results found as above results.


(Bajrang Kumar)
 Tested by
 Analyst


(Sunil Singh)
 Checked by
 Authorized signatory


(Umesh Das)
 Issued by
Technical Manager
 Yugantar Bharati Analytical &
 Environmental Engineering Laboratory






An ISO 9001: 2008 & OHSAS 18001:2007 Certified Laboratory

Post Box no. 32 | Namkom Post Office | Sidroul | Ranchi - 834010 (Jharkhand)

Ph. 0651-6003372, 098351-97960 | Tele Fax : 0651-2260787 | E-mail : ybaeel@gmail.com





YUGANTAR BHARATI

ANALYTICAL & ENVIRONMENTAL ENGINEERING LABORATORY

LAB ACCREDITED BY: National Accreditation Board for Testing & Calibration Laboratory (NABL), New Delhi
Jharkhand State Pollution Control Board (JSPCB)

(T 2532, T-2918)
(B-1874)

Test Report

Issued to	Mr. Shyam Lal Singh Ranchi University, Ranchi Jharkhand	Sample Code	170906-Soil-A06, 170906-Soil-A07, 170906-Soil-A08, 170906-Soil-A09, 170906-Soil-A10,
		Report ID	YBAEEL/RNC/17-09-06/Soil/02
		Date of Issue	17 th October 2017

Sample Particulars		Details of Sampling	
Sample Name/Description	Soil sample	Date of sampling	Unknown
Sample Quantity	1 kg approx	Sample Received Date	6 th September 2017
Sample pkg. Condition	Sealed in Plastic bag	Sample collected by	Customer
Test started on	7 th September 2017	Sampling Location	NPST -1, NPST -2, NPST -3, NPST -4, NPST -5,
Test completed on	5 th October 2017		

Test Results

Sl. No.	PARAMETERS	UNIT	METHOD	NPTS -1	NPTS -2	NPTS -3	NPTS -4	NPTS -5
1	pH		IS 2720 (p-26)	5.9	5.76	4.92	5.72	5.76
2	CALCIUM	%	IS 2720 (p-23)	1.6	1.4	1.6	1.6	2
3	T. NITROGEN	%	Kjeldahl Method	12.04	10.08	13.4	15.12	12.04
4	POTASSIUM	Kg/Acre	Colourimetric Method	50-80	50-80	50-80	50-80	121-150
5	PHOSPHOROUS	Kg/Acre	Colourimetric Method	8	<1	<1	8	8

*****End of Test*****

Remarks:-According to tested parameter, the results found as above results.

B Kumar
(Bajrang Kumar)
Tested by
Analyst



Sunil Singh
(Sunil Singh)
Checked by
Authorized signatory

Umesh Das
(Umesh Das)
Issued by
Technical Manager
Yugantar Bharati Analytical &
Environmental Engineering Laboratory



An ISO 9001: 2008 & OHSAS 18001:2007 Certified Laboratory

Post Box no. 32 | Namkom Post Office | Sidroul | Ranchi - 834010 (Jharkhand)
Ph. 0651-6003372, 098351-97960 | Tele Fax : 0651-2260787 | E-mail : ybaeel@gmail.com



Singh et. al. - Comparative study of change in soil composition due to the biomass generation through Chakriya Vikas Pranali Project - A case study of Tandwa, district Palamu.

DISCUSSION

The pH value in all the 5 samples is found to be little higher in Treated zone in comparison to Non treated zone.

For Ca content in the soil there were no marked changes in percentage. The site having Eucalyptus tree (TPTS-5) has decreased the Ca% by 0.6%. Initially the percentage was 2 at NPTS-5. This indicates change in Ca content due to biomass generation.

For N content there is a marked improvement in Treated zone in comparison to Non-treated zone, particularly in TPTS-1 and TPTS-2, however at TPTS-3, TPTS-4 and TPTS-5 there is reduction of N%.

This indicates orchard having mango, few guava and few su-babool shows the increase of N-content. It may be concluded that due to these trees there is increase in the N- content in the soil.

K-content has drastically increased at TPTS-1, TPTS-4 and TPTS-5 whereas at TPTS-2 and TPTS-3 the percentage remains the same.

The entire process changes the P content of the soil. At places the weight percentage in per acre has either increased or decreased which is clearly evident from the data above in chart 1 & 2.

CONCLUSION

The comparative study of Treated and Non-treated zones clearly indicates that there is change in soil composition due to biomass generation. This also affects the fertility of soil and we will be agriculturist to adopt change in cultivation for a better socio- economic return.

In further steps soil scientists of BAU will be approached for their suggestions and guidance in crop pattern suitable to the changed soil of Treated zone due to biomass generation.

A sample case was studied a year back in which Onion cultivation replaced the Sugarcane cultivation which led to the bumper crop and facilitated good economic return to the agriculturist.

The relevance of this scientific study is to promote and bring out socio-economic growth in the project villages with the new techniques.

REFERENCES

1. **M. Hazra, K. Avisher, P. Gopal, M.S. Nathawal (2010)** - Water stress assessment in Jharkhand state using Soil Data and GIS journal of Applied sciences and Environmental management Vol- **15**, No.-1.
2. **Central Ground water Board (2006)** Activities and achievement of Central Ground Water Board on rain water harvesting and artificial recharge, Ministry of Water Resources, New Delhi, India.
3. **Mishra Shweta, Verma P.K. (2010)**- Abstract Vol. of Regional workshop of all exploration, development & management of ground water in hard rock by C.G.W.B. **A-16**, pp 23-24
4. **R.V. Tamhane, D.P. Motiramani & Y.P. Bali (1964)**- Soil organic matter; *Soil their chemistry and fertility in Tropical Asia*, pp- 216
5. **Ghose , N. C., (1992)**- Chhotanagpur Gneiss Granulitic complex, Eastern India present status and future prospects in India. *Jour. Geol*; V. 64, No.- **1**, pp 100-121.
6. **Verma P.K., Sinha S.P., (2000)** Artificial recharge of Ground water in hard Rock terrain through Chakriya Vikas Pranali - A case study of Palamu district in Bihar.



Evaluation of portfolio performance

Mrinalini Smita** & Anita Mehta^b

^bDepartment of Mathematics, Ranchi College, Ranchi, Jharkhand, India

*Corresponding author : Phone : 7766904575 ; E-mail : nikismita@gmail.com

Abstract: Stock market is a game of risk and return factors. Risk is ginger and return is jam in stock market. Hence portfolios need to be evaluated regularly in order to ensure that their performance is in accordance with the expectations of the investors. Since both risk and return are important in the evaluation of a portfolio, we are confronted with the problem of how to combine these two factors into an index for the evaluation of a portfolio. Initially investors evaluated portfolios almost entirely on the basis the rate of return as they did not know how to quantify risk, so they could not consider it explicitly. Sharpe, Treynor, Jensen and others have developed models for portfolio performance evaluation and that considers both risk and returns and allows a set of portfolios to be ranked and compared to a naive market standard. The present paper deals with the various mathematical models to evaluate the portfolio performance in different fields of IT sector revolution.

Paper History:

Received

11th May 2017

Revised

2nd June 2017

Peer reviewed

13th June 2017

Accepted

21st July 2017

Keywords: Mathematical Models, IT Sector Revolution, CAPM.

INTRODUCTION

Stock price prediction is an important topic in finance and economics which has captured the interest of researchers over the years to develop predictive models. Now-a-days any small incident of corporate sector is known by stock market within the fraction of minutes. The IT revolution has changed the affairs of stock market operations. Stock market is a game of risk and return factors. *Risk is ginger and return is jam in stock market.* Hence portfolios need to be evaluated regularly in order to ensure that their performance is in accordance with the expectations of the investors. Since both risk and return are important in the evaluation of a portfolio, we are confronted with the problem of how to combine these two factors into an index for the evaluation of a portfolio. Initially investors evaluated portfolios almost entirely on the basis the rate of return as they did not know how to quantify risk, so they could not consider it explicitly.

Sharpe, Treynor, Jensen and others have developed models for portfolio performance evaluation and that considers both risk and returns and allows a set of portfolios to be ranked and compared to a naive market standard. These models develop one number that reflects both risks and return, in order to measure the performance of each portfolio and are based on the CAPM.

OBJECTIVE OF THE STUDY

- To help individual to select securities
- To provide an excellent feedback about the portfolio performance to the portfolio managers to evolve better management strategy.
- To ensure that evaluation of portfolio performance is in accordance with the expectation of the investors
- To enable public to invest wisely in stock market.

METHODOLOGY

The most of the data are secondary data collected from publication of research institutes, research journals, regarding text books, websites and Google searches.

SIGNIFICANCE OF THE STUDY

- This study will educate laymen for proper investment without any risk in stock market.
- It will provide an excellent feedback about the portfolio performance to the portfolio managers to evolve better management strategies.
- This study will definitely enable public to invest wisely in stock market.

Portfolio means a blend of mix of different kinds of financial assets. Minimizing risk and maximizing the return is aim of portfolio. Portfolios need to be evaluated regularly in order to ensure that the performance is in accordance with the expectations of the investors. The portfolio performance is based on the quality of assets introduced in it. The evaluation of portfolio performance by portfolio manager provides an excellent feedback about the performance to evolve better management strategy. Portfolio performance evaluation involves determining periodically how the portfolio performed in terms of not only returns earned but also the risk experienced by the investor. The evaluation of portfolio performance requires appropriate measure of returns and risk as well as the standards on which the portfolio is supposed to perform. Risk Adjusted Return (RAR) helps to understand the return generated with respect to the risk taken. This is the most ideal way to decide on any investment some of the commonly used measures for evaluating the performance of portfolio are as follows:

- Sharpe ratio
- Treynor ratio
- Jensen ratio

SHARPE RATIO

Sharpe ratio is used to determine which fund has provided superior returns verses the risk it took. It is calculated by using standard deviation (the deviation from the mean or expected returns which ideally helps to find the range of return of the asset) and excess return to

reward per unit risk. While a high and positive Sharpe ratio shows a superior risk adjusted performance of a fund, a low and negative Sharpe ratio is an indication of unfavourable performance.

FORMULA

Sharpe ratio = excess portfolio return/ portfolio standard deviation

$$= (R_p - R_f) / \text{standard deviation(S.D.)}$$

Where R_p = Average of return on the portfolio

R_f = Risk free return

TREYNOR RATIO

Treynor Ratio is associated with comparison of two funds or portfolios, the performance of portfolio is based on the concept of characteristic line which is the relationship between market return and funds/portfolios return. Treynor Ratio is used to determine which fund has provide superior returns verses the risk it took keeping in mind the market risk also.

FORMULA

Treynor ratio = Excess portfolio return/ portfolio beta

$$=(R_p - R_f) / \beta$$

Where R_p = Average rate of return on the portfolio

R_f = Risk free return

β = beta of the portfolio (Systematic Risk)

JENSEN RATIO

Jensen ratio gives a measure of absolute performance of the portfolio on a risk adjusted basis. This measures the premium earned by the portfolio over the target return, for a given level of beta. Thus it shows the relationship between beta and portfolio return. It involves two steps:

1. The expected return
2. Compare with actual return, afterwards the performance will be assigned with rank.

FORMULA

$$\text{Jensen Ratio} = [R_f + (R_m - R_f) \beta]$$

Where,

R_f = Average rate of return on the portfolio

R_f = Risk free return

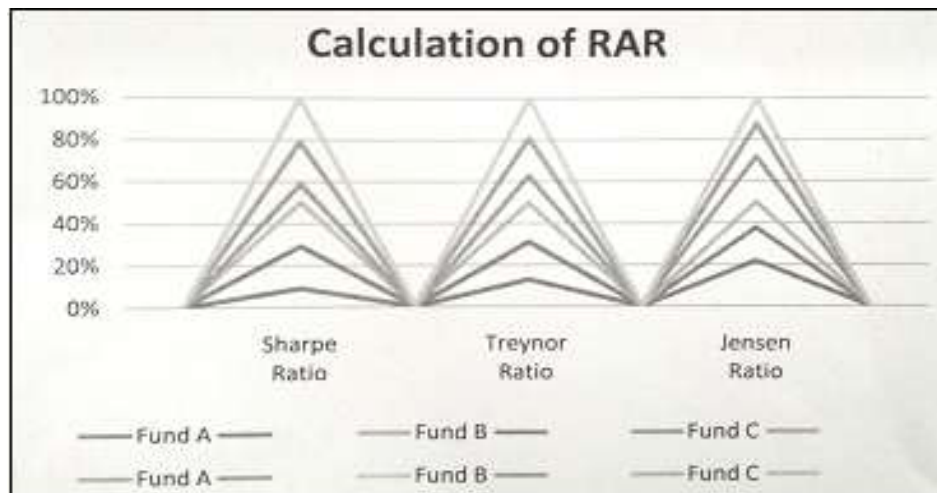
β = beta of the portfolio

R_m = Average market return

ILLUSTRATION

	FUND A	FUND B	FUND C
R_p	10%	12%	11%
β	1.1	1.3	1
R_m	11%	11%	11%
R_f	7%	7%	7%
S.D	3	2.2	1.7

	Fund A	Fund B	Fund C
Sharpe Ratio	1	2.27	2.35
Treynor Ratio	2.72	3.85	4
Jensen Ratio	3	2.2	1.7



CONCLUSION

The portfolio performance is based on abilities. The abilities are the reflection of capabilities. Capabilities are acquired by knowledge, experience, observation and talent. An expert portfolio manager will evaluate the performance to evolve better management strategy by identifying the advantages and disadvantages. The selection of the best fund/ portfolio is based on higher ranks. The three measures of portfolio performance discussed above provide

guidance to the investors for selection of best fund in the stock market. All the three measures suffer from potential problems. It can be seen that Sharpe ratio takes the total risk into account by considering the standard deviation (S.D), as against the Treynor Ratio which considered only the systematic risk (beta). If in estimating the measures the analyst assumes the wrong form of the CAPM holds in the market place, he will get biased measures of performance, usually in favour of low-risk portfolios. This

problem is easily corrected in case of the Jensen and Treynor measures, but the problem is not easily handled in case of Sharpe. The Jensen and Treynor measures also suffer the problem of misspecification of the market portfolio. In constructing the measures, the analyst should use the broadest market indices which most closely approximate the market portfolio.

REFERENCES

1. **Babu, G.R.** , “portfolio management including security analysis” pp 579-591
2. **Maheswari, Yogesh**, “Investment Management” pp 248-251
3. **Bhalla, V.K.** ,”Fundamentals of Investment Management” pp 836-847
4. **Shah, Kirtan**, “ Train the trainer program on portfolio analysis and management” pp 18-21
5. **Google searches on** “ evaluation of portfolio performance” on 25th jan 2017, 10.05 pm
6. **Investopedia.com**



New approach for dual simplex method to solve linear programming models

Rahidas Kumar^{a*} & Sahdeo Mahto^b

^aDepartment of Mathematics, Ranchi University, Ranchi, Jharkhand, India

*Corresponding author : Phone : 8709976350 ; E-mail : kumarahidas@gmail.com

Abstract: The dual simplex algorithm is an attractive alternative solution for linear programming problems. This algorithm over the other method is that there does not require any artificial variables. Hence a great deal of work or lot of labour is saved. Dual simplex method is applicable to those linear programming problems (LPP) which start with infeasible but optimal solution. Whenever linear programming problems start with feasible solution but not optimal condition that time we can't use regular dual simplex method. So this method continue to solve this types of LPP we introduce a new approach an artificial constraint method for dual simplex method. This artificial constraint method for dual simplex method is easy to solve LPP which start with feasible and not optimal solution.

Paper History:

Received

17th April 2017

Revised

12th May 2017

Peer reviewed

9th June 2017

Accepted

25th June 2017

Keywords: Linear programming problem, Primal condition, Dual condition, Canonical form, Dual simplex method, Artificial constraint method.

INTRODUCTION

The dual simplex method based on duality theory, it was discovered by C.E. Lemke.¹ This method can be thought the mirror image of the simplex method. The simplex method deals directly with basic solution in the primal problem that are primal feasible but not dual feasible. Also the regular simplex method starts with a basic feasible but non optimal solution and proceeds towards the optimality, dual simplex method starts with a basic infeasible but optimal solution and proceeds towards the feasibility.^{1,2,3}

Not long after the publication of Danzig's primal simplex algorithm⁴ (in 1951) its dual version, developed by Lemke⁵, also appeared (in 1954). It has long been known that the dual simplex algorithm (DSA) is a better alternative to the primal simplex for solving certain types of linear programming (LP) problems. Its importance has been recognized in many areas, in particular in the case of the

Branch and Bound (BB) type methods for Mixed Integer Linear Programming (MILP). BB requires the repeated solution of closely related continuous LP problems (c.f. Nemhauser and Wolsey)⁶. At each branching node two new sub problems (child problems) are created that differ from the parent problem in the individual bound of the branching variable. Usually the right-hand-sides of the child problems also change. The result is that the basis of the parent problem becomes primal infeasible for the derived problems but it remains (or can easily be made) dual feasible. This makes the dual simplex method an obvious choice for the required 'reoptimization'.^{7,8}

Dual simplex method also can be useful in solving huge linear programming problems from scratch because it is such an efficient algorithm¹. Computational experience with the most powerful versions of CPLEX indicates that dual simplex often is more efficient than the simplex

method for solving particularly massive problems encountered in practice.^{9,10}

In real world LP problems all sorts of variables and constraints can be present. The standard dual algorithm has been worked out for the case where all variables are nonnegative and a dual feasible basis is available. The LP relaxation of a MILP problem can contain many bounded variables. Free and fixed variables may also be present. The increasing need for solving various types of LP problems with the dual simplex method necessitates the design and implementation of a version of the DSA where variables of arbitrary type are allowed and they all, especially the bounded primal variables, are treated efficiently⁷. The main purpose of this paper is to present such an algorithm. This is achieved by discussing increasingly more capable dual algorithms that evolve into one that has the potential of this efficiency.¹¹

Introduce some primal dual related expression.

Primal Problem: Find a column vector x , which

$$\text{Max } Z_p = c \cdot x$$

s.t. $Ax \leq b$ and $x \geq 0$ where $x = [x_1, x_2, \dots, x_n]$

Dual Problem: Find the column vector w , which

$$\text{Min } Z_D = b' \cdot w$$

s.t. $A'w \geq c'$ and $w \geq 0$ where $[w_1, w_2, \dots, w_m]$

and A' , b' , c' are the transpose of A , b and c respectively.

Canonical Form: Canonical form is a Mathematical model which contains maximization type's objective function and set of constraints \leq types.

Working procedure for the Dual Simplex Algorithm

- I. The given LPP convert into canonical form
If the problem is of minimization, convert into maximization problem. Write all the constraints into \leq type. Doing this process some b_i 's may be negative.
- II. Find the initial basic solution.
Introducing the slack variables in the constraint to convert into equalities. All the given variables put is equal to zero we get the values of slack variables. This is the initial basic solution, which may not be feasible. Let $X_B = (x_{B1}, x_{B2}, \dots, x_{Bm})$ be the initial basic feasible solution corresponding to the basis matrix $B = (\beta_1, \beta_2, \dots, \beta_m)$.
- III. Create the initial table as usual as simplex method.

IV. Test the initial solution for optimality; compute $Z_j - c_j$ for each column.

- (i) If all $Z_j - c_j \geq 0$ and each X_{Bi} are non-negative, then we get optimum basic feasible solution.
- (ii) If $Z_j - c_j \geq 0$ all and at least one is negative, then proceed to number V.
- (iii) If any $Z_j - c_j < 0$ then this method does not applicable.

V. To find the vector which is entering and departing the basis? Here determined the departing vector.

- (i) To determine the departing vector: Here β_r i.e., the r -th column in the basis i.e., the corresponding vector x_r in the basis is the departing vector, if

$$X_{Br} = \text{Min. } \{x_{Bi}, x_{Bi} < 0\}$$

- (ii) To determine the incoming vector (α_k): If β_r is the outgoing vector, then α_k is taken as the entering vector for the value of k , for which

$$\frac{Z_j - c_j}{y_{rk}} = \text{Min } \left[\frac{Z_j - c_j}{y_{rj}}, y_{rj} < 0 \right]$$

If all $y_{rj} \geq 0$, then the problem has no feasible solution.

VI. Test the optimality condition

If entering the vector α_k in place of β_r in the basis all basic variables reduces to non negative values, then the solution is optimal solution feasible solution. But at least one basic variable is negative, and then solution is not feasible solution. In this case repeat serial number IV. and V, iteratively till an optimal feasible solution is obtained.

New approach an Artificial Constraint Method for Dual Simplex Method:(For initial basic feasible solution)

Generally if $Z_j - c_j \geq 0$, we use dual simplex method but when $Z_j - c_j < 0$ we cannot use dual simplex method. But this artificial constraint method it converted into equivalent problem such that optimality condition $Z_j - c_j \geq 0$ will be satisfied for all j .

If at least one $Z_j - c_j < 0$, we introduce one new constraint

$\sum_j x_j \leq M$; Where $M > 0$ is sufficiently large, known as Artificial Constraint. Now introducing slack variable x_M convert the inequality into equality. That is

Kumar & Mahto: New approach for dual simplex method to solve linear programming models

$\sum_j x_j + x_M = M$ where $x_j, x_M \geq 0$ for all j . Now if for $j=p$ then $|Z_p - c_p|$ has maximum value in this case we write $x_p = M - (x_M + \sum_{j \neq p} x_j)$

This value of x_p is substituted in the original objective function as well as in the constraints. So we get modified problem where objective function as well as constraints are modified. And this particular problem we insure that optimality condition must be satisfied.

SOLVED PROBLEMS

Problem:

Use Dual simplex method to solve the following linear programming problem :

$$\text{Max } Z = 3x_1 + 2x_2$$

Subject to constraints:

$$2x_1 + x_2 \leq 5$$

$$x_1 + x_2 \leq 3, x_1, x_2 \geq 0.$$

Solution: Now write the given problem in canonical form. Introducing slack variables x_3 and x_4 , convert the inequality into the equality.

$$\text{Max } Z = 3x_1 + 2x_2 + 0x_3 + 0x_4$$

Subject to constraints:

$$2x_1 + x_2 + x_3 + 0x_4 = 5$$

$$x_1 + x_2 + 0x_3 + x_4 = 3 \text{ and } x_i \text{ where } i = 1, 2, 3, 4$$

$$\text{Initial basic feasible solution, } \begin{bmatrix} x_3 \\ x_4 \end{bmatrix} = \begin{bmatrix} 5 \\ 3 \end{bmatrix}$$

Here we cannot apply dual simplex method, because all $Z_j - c_j$ not greater than or equal zero. So this method continue we introduce artificial constraint which is $x_1 + x_2 \leq M$ where $M > 0$ and sufficiently large.

Now introduce slack variable x_M convert this inequality constraint into equality constraint.

Initial table

		c_j	3	2	0	0
B	C_B	X_B	X_1	X_2	X_3	X_4
X_3	0	5	2	1	1	0
X_4	0	3	1	1	0	1
		$Z_j - c_j$	-3	-2	0	0

$$x_1 + x_2 + x_M = M$$

Now $M = \max\{|Z_1 - c_1|, |Z_2 - c_2|\} = \{3, 2\} = 3$, corresponding of x_1 .

Hence $x_1 = (M - x_2 - x_M)$. Therefore the modified problem written as

$$\text{Max } Z = 3M - x_2 - 3x_M$$

Subject to constraint:

$$-x_2 + x_3 - 2x_M = 5 - 2M$$

$$x_4 - x_M = 3 - M$$

$$x_1 + x_2 + x_M = M \text{ and } x_i, x_M \geq 0 \text{ where } i = 1, 2, 3, 4.$$

Now the above problem can be write in standard form

$$\text{Max } Z = -3x_M + 0x_1 - x_2 + 0x_3 + 0x_4 + 3M$$

Subject to constraint:

$$-2x_M + 0x_1 - x_2 + x_3 + 0x_4 = 5 - 2M$$

$$-x_M + 0x_1 + 0x_2 + 0x_3 + x_4 = 3 - M$$

$$x_M + x_1 + x_2 + 0x_3 + 0x_4 = M \text{ and } x_i, x_M \geq 0 \text{ where } i = 1, 2, 3, 4.$$

Here the modified problem, initial basic feasible solution

$$\begin{bmatrix} x_3 \\ x_4 \\ x_1 \end{bmatrix} = \begin{bmatrix} 5 - 2M \\ 3 - M \\ M \end{bmatrix}, \text{ also these are forming the basis.}$$

Now the modified problem solved by DUAL SIMPLEX METHOD

INITIAL TABLE

		c_j	-3	0	-1	0	0	
B	C_B	X_B	x_M	x_1	x_2	x_3	x_4	
x_3	0	$5 - 2M$	-2	0	-1	1	0	→
x_4	0	$3 - M$	-1	0	0	0	1	
x_1	0	M	1	1	1	0	0	
		$Z_j - c_j$	3	0	1	0	0	
					↑			

Here all $Z_j - c_j \geq 0$ and present infeasible condition, then we applying dual simplex method. Therefore the departing vector (mini $\{5-2M, 3-M\} = 5-2M$) X_3 and

$\max \left\{ \frac{3}{-2}, \frac{1}{-1} \right\} = -1$ corresponding to X_2 is the entering vector. Now same work has done as dual simplex method.

2nd SIMPLEX TABLE

		C_j	-3	0	-1	0	0	
B	C_B	X_B	X_M	X_1	X_2	X_3	X_4	
X_2	-1	$2M-5$	2	0	1	-1	0	
X_4	0	$3-M$	-1	0	0	0	1	\rightarrow
X_1	0	$5-M$	-1	-1	0	1	0	
		$Z_j - c_j$	1	0	0	1	0	
			\uparrow					

Similar process we construct the next simplex table. So

3rd SIMPLEX TABLE

		C_j	-3	0	-1	0	0	
B	C_B	X_B	X_M	X_1	X_2	X_3	X_4	
X_2	-1	1	0	0	1	-1	2	
X_4	0	$M-3$	1	0	0	0	-1	
X_1	0	2	0	1	0	1	-1	
		$Z_j - c_j$	0	0	0	1	1	

Here all X_B are non negative because M is sufficiently large, so $(M-3)$ is positive and all $Z_j - c_j$ non negative. Hence the optimal basic feasible solution, $x_1 = 2$ and $x_2 = 1$ and Max $Z = 8$

3.2 Problem 2:

Use Dual simplex method to solve the following linear programming problem:

$$\text{Max } Z = 3x_1 + 5x_2 + 4x_3$$

Subject to constraints:

$$2x_1 + 3x_2 \leq 8$$

$$2x_1 + 5x_3 \leq 10$$

$$2x_2 + 4x_3 \leq 15 \text{ and, } x_1, x_2, x_3 \geq 0$$

Solution: Now write the given problem in canonical form. Introducing slack variables x_4, x_5 and x_6 convert the inequality into the equality.

$$\text{Max } Z = 3x_1 + 5x_2 + 4x_3 + 0x_4 + 0x_5 + 0x_6$$

Subject to constrains:

$$2x_1 + 3x_2 + 0x_3 + x_4 + 0x_5 + 0x_6 = 8$$

$$2x_1 + 0x_2 + 5x_3 + 0x_4 + x_5 + 0x_6 = 10$$

$$0x_1 + 2x_2 + 4x_3 + 0x_4 + 0x_5 + x_6 = 15 \text{ and, } x_i \geq 0 \text{ for all } i \text{ and } i=1,2,\dots,6$$

Initial basic feasible solution, $\begin{bmatrix} x_4 \\ x_5 \\ x_6 \end{bmatrix} = \begin{bmatrix} 8 \\ 10 \\ 15 \end{bmatrix}$

INITIAL TABLE

		C_j	3	5	4	0	0	0
B	C_B	X_B	X_1	X_2	X_3	X_4	X_5	X_6
X_4	0	8	2	3	0	1	0	0
X_5	0	10	2	0	5	0	1	0
X_6	0	15	0	2	4	0	0	1
		$Z_j - c_j$	-3	-5	-4	0	0	0

Kumar & Mahto: New approach for dual simplex method to solve linear programming models

Here we cannot apply dual simplex method, because all $Z_j - c_j$ not greater than or equal zero. So this method continue we introduce artificial constraint which is

$x_1 + x_2 + x_3 \leq M$ where $M > 0$ and sufficiently large.

Now introduce slack variable x_M convert this inequality constraint into equality constraint.

$$x_1 + x_2 + x_3 + x_M = M$$

Now $\max x = \{|Z_1 - c_1|, |Z_2 - c_2|, |Z_3 - c_3|\} = \{3, 5, 4\} = 5$, corresponding of x_2 .

Hence $x_2 = (M - x_1 - x_3 - x_M)$. Therefore the modified problem written as in standard form

$$\max Z = -5x_M - 2x_1 - 0x_2 - x_3 + 0x_4 + 0x_5 + 0x_6 + 5M$$

Subject to constraint:

$$-3x_M - x_1 + 0x_2 - 3x_3 + x_4 + 0x_5 + 0x_6 = 8 - 3M$$

$$0x_M + 2x_1 + 0x_2 + 5x_3 + 0x_4 + x_5 + 0x_6 = 10$$

$$-2x_M - 2x_1 + 0x_2 + 2x_3 + 0x_4 + 0x_5 + x_6 = 16 - 2M$$

$$x_M + x_1 + x_2 + x_3 + 0x_4 + 0x_5 + 0x_6 = M \text{ and } x_i, x_M \geq 0$$

where $i = 1, 2, 3, 4, 5, 6$

Here the modified problem, initial basic feasible solution

$$\begin{bmatrix} x_4 \\ x_5 \\ x_6 \\ x_2 \end{bmatrix} = \begin{bmatrix} 8 - 3M \\ 10 \\ 16 - 2M \\ M \end{bmatrix},$$

also these are forming the basis.

Now the modified problem solved by DUAL SIMPLEX METHOD.

INITIAL TABLE

		c_j	-5	-2	0	-1	0	0	0	
B	C_B	X_B	X_M	X_1	X_2	X_3	X_4	X_5	X_6	
X_4	0	$8-3M$	-3	-1	0	-3	1	0	0	\rightarrow
X_5	0	10	0	2	0	5	0	1	0	
X_6	0	$16-2M$	-2	-2	0	2	0	0	1	
X_2	0	M	1	1	1	1	0	0	0	
		$Z_j - c_j$	5	2	0	1	0	0	0	
						\uparrow				

Here all $Z_j - c_j \geq 0$ and present infeasible condition, then we applying dual simplex method. Therefore the departing vector (mini $\{8-3M, 16-2M\} = 8-3M$) X_4 and max

$\left\{ \frac{5}{-3}, \frac{2}{-1}, \frac{1}{-3} \right\} = \frac{1}{-3}$ corresponding to X_3 is the entering vector. Now same work has done as dual simplex method.

2nd SIMPLEX TABLE

		C_j	-5	-2	0	-1	0	0	0	
B	C_B	X_B	X_M	X_1	X_2	X_3	X_4	X_5	X_6	
X_3	-1	$M - \frac{8}{3}$	1	$\frac{1}{3}$	0	1	$-\frac{1}{3}$	0	0	
X_5	0	$\frac{70}{3} - 5M$	-5	$\frac{1}{3}$	0	0	$\frac{5}{3}$	1	0	\rightarrow
X_6	0	$\frac{64}{3} - 4M$	-4	$-\frac{8}{3}$	0	0	$\frac{2}{3}$	0	1	
X_2	0	$\frac{8}{3}$	0	$\frac{2}{3}$	1	0	$\frac{1}{3}$	0	0	
		$Z_j - c_j$	4	$\frac{5}{3}$	0	0	$\frac{1}{3}$	0	0	
			\uparrow							

3rd SIMPLEX TABLE

		C_j	-5	-2	0	-1	0	0	0
B	C_B	X_B	X_M	X_1	X_2	X_3	X_4	X_5	X_6
X_3	-1	2	0	$\frac{6}{15}$	0	1	0	$\frac{1}{5}$	0
X_M	-5	$M - \frac{14}{3}$	1	$-\frac{1}{15}$	0	0	$-\frac{1}{3}$	$-\frac{1}{5}$	0
X_6	0	$\frac{8}{3}$	0	$-\frac{44}{15}$	0	0	$-\frac{2}{3}$	$-\frac{4}{5}$	1
X_2	0	$\frac{8}{3}$	0	$\frac{2}{3}$	1	0	$\frac{1}{3}$	0	0
		$Z_j - C_j$	0	$\frac{29}{15}$	0	0	$\frac{5}{3}$	$\frac{4}{5}$	0

Here all X_B are non negative because M is sufficiently large, so $(M - \frac{14}{3})$ is positive and all $Z_j - C_j$ non negative. Hence the optimal basic feasible solution, $x_1 = 0$, $x_2 = \frac{8}{3}$ and $x_3 = 2$ and Max $Z = 21.33$

CONCLUSION

This article we presented the mathematical algorithms, computational techniques and implementation details of our dual simplex method, which performs the best existing open source, research and is competitive to the leading commercial LPP. An artificial constraint method for dual simplex method is powerful optimization tool in linear optimization problems. Dual simplex method efficiently used in day by day life for solving on numerical problems. This technique cannot use more decision so lot of work or labour is saved.

REFERENCES

- Hiller, F. S., Lieberman, G. J, Introduction to Operations Research, Tata McGraw- Hill Publishing Company Limited, 2006.
- Gupta, R. K., Operations Research, Krishna Prakashan Media (P) Ltd.2013.
- R. Fourer. Notes on the dual simplex method. Technical report, Draft Report, NorthwesternUniversity, 1994.
- Dantzig, G.B., Linear Programming and Extensions, Princeton University Press, Princeton, N.J., 1963.
- Lemke, C.E., "The Dual Method of Solving the Linear Programming Problem", Naval Research Logistics Quarterly, 1, 1954, p. 36–47.
- Nemhauser, G.L., Wolsey, L.A., Integer and Combinatorial Optimization, John Wiley, 1988.
- Wagner, H.M., "The dual simplex algorithm for bounded variables" Naval Research Logistics Quarterly, Vol. 5, 1958, p. 257–261.
- H. M. Wagner. The dual simplex algorithm for bounded variables. Naval Research Logistics Quarterly, 5:257–261, 1958.
- R. E. Bixby and A. Martin. Parallelizing the dual simplex method. INFORMS Journal on Computing, 12(1):45–56, 2000.
- I. Maros. A generalized dual phase-2 simplex algorithm. European Journal of Operational Research, 149(1):1–16, 2003.
- Achim Koberstein. Progress in the dual simplex algorithm for solving large scale LP problems.



Grain-size and dielectric properties of perovskite structure lead-free potassium-sodium-niobate ($\text{K}_{0.5}\text{Na}_{0.5}\text{NbO}_3$) ceramics

Anurag Mishra* & J. P. Sharma

Department of Physics, Ranchi College, Ranchi, Jharkhand, India

*Corresponding author : Phone : 9931864529, E-mail : anuragmishrabokaro@gmail.com

Abstract : Perovskite structure lead-based ceramics specially PZT and PZT-based are showing superior electrical properties due to presence of Pb. But Pb is toxic and hazardous for human health and environment, so use of lead based ceramics is strictly prohibited. Lead-free perovskite structure ceramics with nominal composition ($\text{K}_{0.5}\text{Na}_{0.5}\text{NbO}_3$) in short KNN is considered as a promising candidate showing comparatively higher electrical properties. KNN is prepared by solid state reaction method and then the powder is calcined at 850°C for 3 hours. The phase structure of KNN ceramics is determined by X-ray diffraction technique which gives the phase is orthorhombic(O) at room temperature, rhombohedral (R) at low temperature(<123°C), tetragonal(T) at temperature(200-400°C) and cubic(C) at temperature(>400°C). The pellet of KNN is sintered at 900°C and LS modified KNN at 1050°C. The SEM characterization revealed the grain size of sintered KNN in order of 200-500nm. The temperature dependence dielectric constant is calculated to observe the transition temperature of pure KNN ceramics with varying temperature in order of 30°C-600°C. Doped KNN with LiSbO_3 reveals the good temperature stability and exhibits superior electrical properties. The detailed study suggests that it is a useful lead-free composition.

Paper History:

Received

15th May 2017

Revised

22nd May 2017

Peer reviewed

15th June 2017

Accepted

21st June 2017

Keywords: lead- free, KNN, perovskite, PZT, XRD, SEM, KNN-LS

INTRODUCTION

In 1880's, two brothers Pierre and Jacques Curie discovered that some crystalline materials when compressed, produces a voltage proportional to applied pressure. This property is named as piezoelectricity. They developed an idea that some materials like tourmaline, quartz, cane sugar, topaz and rochellet salt etc. shows superior piezoelectric properties¹⁻⁶. During world war II, research group in US, Russia and Japan discovered a new class of man made material called ferroelectrics which exhibited piezoelectric constant many times higher than natural piezoelectric materials^{5,6}. Although, quartz crystal was the first commercially exploited material and still used in various applications. Scientists kept searching for higher performance materials. Piezoelectric ceramics, which play an important role as functional electronic materials, have

been widely used in various applications such as sensors, actuators, transducers and so on¹⁻⁶.

Piezoelectric ceramics are widely used for sensors, actuators, transducers, buzzers and other electronic devices^{1,2}. However, these piezoelectric ceramics are mostly $\text{Pb}(\text{Zr}, \text{Ti})\text{O}_3$ (PZT) based ceramics, which contain more than 60 wt% lead³⁻⁵. Lead is a very toxic substance, which can cause damage to the kidney, brain and nervous system, especially the intelligence of children⁶⁻⁹. In recent years, some countries have made it mandatory for all new electronic products to be lead-free for environmental protection and human health^{10,11}. Therefore, it is urgent to develop lead-free piezoelectric ceramics for replacing PZT-based ceramics. Currently, extensive studies on perovskite lead-free piezoelectric ceramics are focused on $(\text{Bi}_{0.5}\text{Na}_{0.5})\text{TiO}_3$ (BNT) and $(\text{K}_{0.5}\text{Na}_{0.5})\text{NbO}_3$ (KNN) because

of their relatively high piezoelectric and ferroelectric properties¹²⁻¹⁴.

BNT is considered to be one of the good candidates for lead-free piezoelectric ceramics because of its strong ferroelectricity at room temperature. However, pure BNT ceramics have two disadvantages: higher coercive field and lower phase transition temperature, which can be called the depolarization temperature (from the ferroelectric to the anti ferroelectric phase)⁸. In order to improve the piezoelectric properties of BNT ceramics, $(\text{Bi}_{0.5}\text{K}_{0.5})\text{TiO}_3$, BaTiO_3 , and BiFeO_3 are added to form new solid solutions²²⁻²⁵. Although, these BNT-based ceramics show relatively high piezoelectric properties.

Recently, considerable attention given to lead-free piezoelectric ceramics has focused on KNN-based piezoelectric ceramics because of their relatively high piezoelectric properties and high Curie temperature (420 °C)¹¹⁻¹⁹. Nevertheless, pure KNN ceramics are known to be difficult to densify by the ordinary sintering method. To improve densification and piezoelectric properties of KNN ceramics, different additions are added into KNN to form new KNN-based ceramics, such as $\text{KNN}-\text{BaTiO}_3$ ¹⁵, $\text{KNN}-\text{SrTiO}_3$ ¹⁶, $\text{KNN}-\text{LiNbO}_3$ ¹⁷, $\text{KNN}-\text{LiSbO}_3$ ¹⁸, $\text{KNN}-\text{LiTaO}_3$ ¹⁹ and $\text{KNN}-\text{LiNbO}_3-\text{AgTaO}_3$ ²⁰. These KNN-based ceramics show relatively high piezoelectric properties owing to the presence of a polymorphic phase transition (from the orthorhombic to the tetragonal phase) (PPT) at room temperature¹⁵⁻¹⁶. Unfortunately, piezoelectric properties of these KNN-based ceramics are still not as good as those of $\text{Pb}(\text{Zr},\text{Ti})\text{O}_3$ (PZT) based, so they cannot replace lead-based piezoelectric materials. Therefore, it is necessary to look for new compositions with high piezoelectric properties²¹⁻³⁹.

MATERIALS AND METHODS

Powder Preparation

Sodium carbonate (Na_2CO_3 , 99.9% purity), potassium carbonate (K_2CO_3 , 99.9% purity), niobium penta-oxide (Nb_2O_5 , 99.9% purity), lithium carbonate (Li_2CO_3 , 99.9% purity) and antimony penta-oxide (Sb_2O_5 , 9.9% purity) were used as starting materials. Stoichiometric weights of all the powders were mixed with acetone in agate mortar for 8 hours. Grinded material was dried with Infra-Red lamp and then mixed powders were collected by spatula. The calcination of the powders

was carried out at 850°C temperature for 3 hours and single perovskite phase formation was confirmed by X-ray diffraction (XRD) technique.

Pellet formation

The calcined powders were mixed thoroughly with 2 wt% polyvinyl alcohol (PVA) binders solution and then pressed into disks of diameter of 10 mm and thickness of 1.5 mm under 100 MPa pressure. The sintering of the pure KNN ceramic was carried out at 900 °C for 4 hours. Silver paste was applied on both sides of the ceramics and fired at 500 °C for 30 min for good adhesion. Whereas, LS modified KNN ceramics were sintered at 1050 °C for 4 hours in air with a heating rate of 5 °C/min.

Phase analysis

In order to examine the phases present in the system, XRD analysis of the sintered KNN ceramics were performed by diffractometer using $\text{Cu}\alpha$ radiation. The sintered microstructures were observed using a scanning electron microscope (SEM). The experimental densities of the samples were measured by the Archimedes method. Dielectric constant (ϵ_r) and dielectric loss ($\tan\delta$) were measured as a function of temperature using a computer interfaced HIOKI LCR-metre.

RESULTS AND DISCUSSION

Structure of the composition

Pure KNN composition in the form $(\text{K}_{0.5}\text{Na}_{0.5}\text{NbO}_3)$ showing the Perovskite structure like ABO_3 where the Sodium ions are taken as large cations(A) and Potassium-niobium ions are taken as small cations (B). Hence the structure will be like as given in figure 1(i) and (ii).

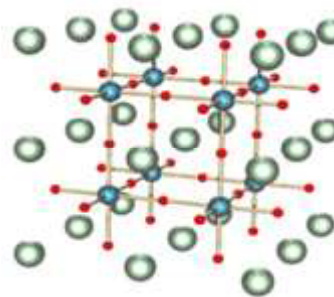


Fig (i)

Green- A(Na), Blue- B(KNb), Red-O(Oxygen)

Mishra & Sharma: Grain-size and dielectric properties of perovskite structure lead-free potassium-sodium-niobate ($K_{0.5}Na_{0.5}NbO_3$) ceramics

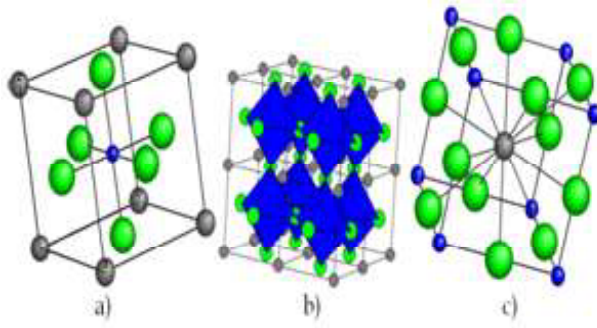


Fig (ii)

Figure1 :- (i) Showing perovskite structure ABO_3 .
(ii) Perovskite structure in 3-D form.

XRD at room temperature

The peak of the graph taken by XRD shows that pure KNN compositions were in orthorhombic phase at room temperature. First graph in figure 2(a) is showing first peak between 20 to 30 degree and the second peak is between 30 to 40 degree. In figure 2(b), graph is showing peak at (001)/(100) between 20 to 30 degree, at (101) between 30 to 35 degree, next at (002)/(200), (201)/(210) and (112)/(211) between 45 to 50, 50 to 55 and 55 to 60 respectively.

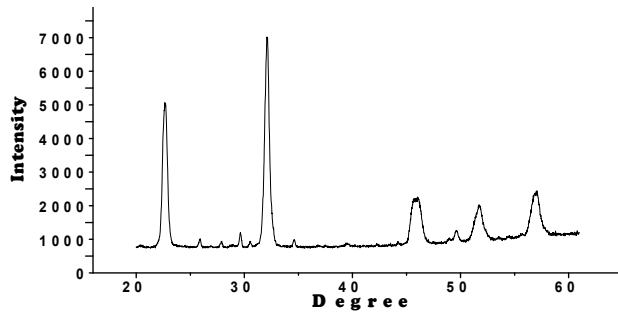


Figure 2 : (a)

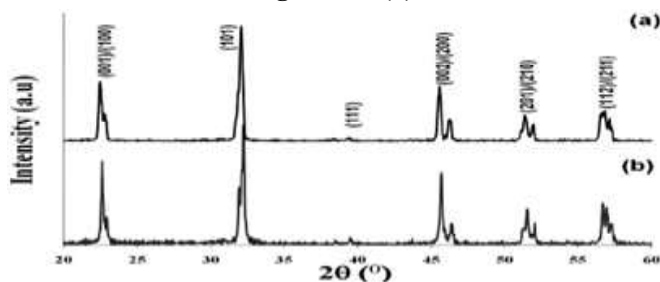


Figure 2 (b)

Figure 3, shows the XRD patterns of the sintered $(1-x)KNN-xLiSbO_3$ (KNN-LS) ($x=0, 0.04, 0.05, 0.06$) ceramics. This suggests that LiO_2 and Sb_2O_5 ions have completely diffused into the KNN lattice to form a homogeneous solid solution. It can be seen that pure KNN ceramics with $x=0$, possess orthorhombic structure at room temperature and is confirmed by matching the XRD patterns from figure. The orthorhombic phase is characterized by (002)/(200) peak splitting from figure (a) for $x=0$. Whereas, the tetragonal phase is characterized by (002)/(200) peak splitting from figure (d) for $x=0.06$. It is clear that pure KNN changes its phase from orthorhombic to tetragonal with the LS contents. Therefore, it can be concluded that the orthorhombic and tetragonal phase coexist in KNN-LS ceramics for 0.04 to 0.06. In order to quantitatively investigate the effect of LS content on the crystalline phases in KNN-LS ceramics, peak de-convolution has been performed on the XRD patterns in the 2θ range of (44.5–46.5) degrees for all the compositions. Figure shows the XRD patterns of KNN-LS ceramics in the 2θ range of (44.5–46.5) degrees.

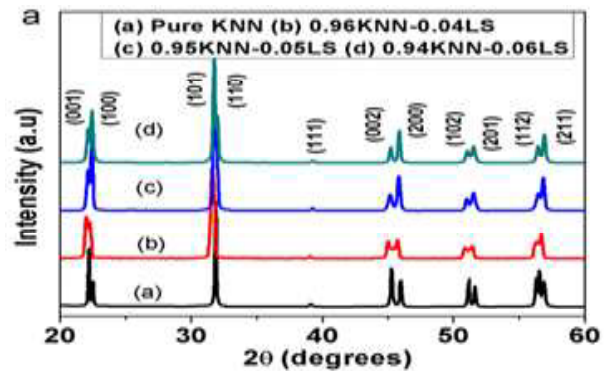


Fig 3:- XRD patterns of sintered $(1-x)KNN-xLS$ compositions with ($x=0, 0.04, 0.05$ and 0.06)

Microstructure of Li and Sb modified ceramics is taken for the composition $(1-x)KNN-xLS$ for different values of x ($= 0, 0.04, 0.05$ and 0.06). Figures 4 (i) and (ii) (a), (b) And (c) shows SEM images of $(1-x)KNN-xLS$ ceramics with $x = 0.04, 0.05$, and 0.06 , respectively. It can be seen that, when $x = 0.04$, the morphology of the grains clearly confirms an orthorhombic structure for the material, similar to pure KNN, while in the case of $x = 0.06$ a relatively homogeneous pseudo-cubic morphology

of the grains can be found, which thus should correspond to the tetragonal phase. Slight shrinkage in the unit cell volume in KNN ceramic has been found due to transformation of the crystal structure from an orthorhombic to a pseudo-cubic structure²⁷. Coexistence of the tetragonal and orthorhombic phases is found for $x=0.05$, with a reduction in grain sizes. It can finally be concluded that the tetragonality of the ceramic increases with increasing x .

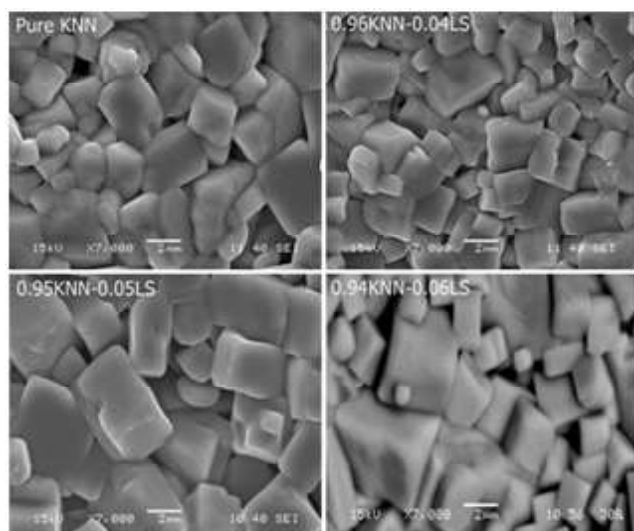


Figure 4 (i)

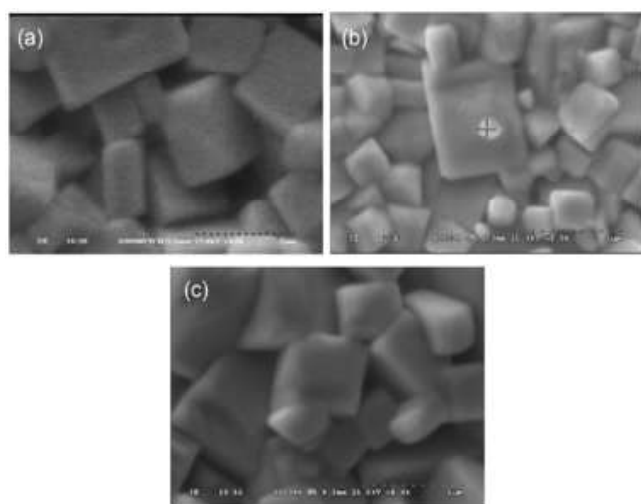


Figure 4(ii)

Figure 4 (i) and (ii) :- SEM characterization of (1-x)KNN-xLS with ($x = 0, 0.04, 0.05$ and 0.06)

CONCLUSION

The above results show that pure KNN in the composition ($K_{0.5}Na_{0.5}NbO_3$) have orthorhombic phase at room temperature and it will change its phase into tetragonal by adding impurities $LiSbO_3$. Structural and electric properties of pure KNN and (Li, Sb) modified compositions in this form (1-x)KNN-xLS for ($x=0, 0.04, 0.05$ and 0.06) ceramics have been investigated in detail. XRD patterns of the sintered KNN show that the phase is orthogonal and the composition in the form of (1-x)KNN-xLS ceramics indicate the transformation of orthorhombic to tetragonal structure with the increase in LS content. Dielectric study revealed the shifting of T_{O-T} and T_c towards room temperature with the increase in LS content in (1-x)KNN-xLS ceramics.

ACKNOWLEDGEMENT

This work was supported by Department of Physics project lab, Ranchi College Ranchi, PG Department of Physics Lab of Ranchi university and BIT Mesra CIF lab, Ranchi.

REFERENCES

1. Uchino K 2000; Ferroelectric Devices (New York) p 158
2. Jaffe B, Cook W R and Jaffe H 1971; Piezoelectric Ceramics (London: Academic) p 271
3. G. H. Haertling, J. Am. Ceram. Soc. **82** (1999) 797.
4. S.E. Park, T.R. Shrout, J. Appl. Phys. **82** (1997) 1804.
5. Cross L E 2004 *Nature* **432** 24–5
6. B. Jaffe, W.R. Cook, H. Jaffe, Piezoelectric Ceramics (Academic press, New York, 1971), pp. 140–148
7. T. Takenaka, H. Nagata, Y. Hiruma, Jpn. J. Appl. Phys. **47**(5) (2008) 3787–3800
8. Y. Ming Li J. Electroceram, **31**(2013) 42–47
9. P. Kumar, Ceramics International, **39** (2013) 65–69
10. Waste Electrical and Electronic Equipment (WEEE), Off. J. Eur. Union. **46** (2003) 24–38

Mishra & Sharma: Grain-size and dielectric properties of perovskite structure lead-free potassium-sodium-niobate ($\text{K}_{0.5}\text{Na}_{0.5}\text{NbO}_3$) ceramics

11. Restriction of the Use of Certain Hazardous Substances in Electrical and Electronic Equipment (RoHS), Off. J. Eur. Union. **46** (2003)19-23
12. Y. Saito , Nature **432**, (2004) 84–87
13. Li Y, Moon K and Wong C P 2005; Science **308** 1419
14. Wang X X, Tang X G and Chan H L W 2004; Appl. Phys. Lett. **85** 91
15. Sasaki A, Chiba T, Mamiya Y and Otsuki E 1999; Japan. J. Appl. Phys. **38** 5564
16. Wang X X, Chan W H L and Choy C L 2003; J. Am. Ceram. Soc. **86** 1809
17. Nagata H and Takenaka T 1999; Key Eng. Mater. **37** 169
18. Z. Zhang; Journal of Alloys and Compounds **624** (2015)158–164.
19. Guo Y, Kakimono K and Ohsata H 2004; Mater. Lett. **59** 241
20. Wang Y Y, Wu J G, Xiao D Q, Zhu J M, Jin Y, Zhu J G, Yu P, Wu L and Li X 2007; J. Appl. Phys. **102** 054101
21. Takenaka T, Maruyama K and Sakata K 1991; Japan. J. Appl. Phys. **30** 2236
22. Park H Y, Ahn C W, Song H C, Lee J H, Nahm S, Uchino K and Lee H J 2006; Appl. Phys. Lett. **89** 062906
23. Bobnar V, Bernard J and Kosec M 2004; Appl. Phys. Lett. **85** 994
24. Guo Y, Kakimono K and Ohsata H 2004; Appl. Phys. Lett. **85** 4121
25. Zang G Z, Wang J F, et al. 2006; Appl. Phys. Lett. **88** 212908
26. Z. Zhang; Ceramics International, **41**(2015) S9–S14
27. Y. Liu; Journal of Alloys and Compounds, **603** (2014) 95–99
28. R. Gaur; Ceramics International **41**(2015)1413–1420.
29. J. Wu ; Journal of Alloys and Compounds **651**(2015) 302-307.
30. E. Akca, H.Yılmaz, Ceramics International **41**(2015)3659–3667.
31. J. Du; Ceramics International **42** (2016)1943–1949.
32. X. Yan; Journal of Alloys and Compounds **653** (2015) 523-527.
33. H. Yang; J Mater Sci **48**(2013) 2997–3002.
34. Q. Yin; Journal of Alloys and Compounds **622** (2015) 132–136.
35. Yue-Ming Li; J Mater Sci: Mater Electron, **25** (2014) 1028–1032
36. Hua Wang; J Mater Sci: Mater Electron, **24**(2013) 2469–2472.
37. Zhiming Geng; J Mater Sci: Mater Electron, **26**(2015)6769–6775.
38. Hua Wang ; J Electroceram, **30** (2013) 217–220.
39. Jigong Hao; J Mater Sci, **50**(2015) 5328–5336.



Diffractionless propagation of elliptic gaussian laser beams in disordered ferroelectrics

Binay Prakash Akhouri^{a*}, Sumit Kaur^b, Rajesh Kumar^c & Pradeep Kumar Gupta^d

^aDepartment of Physics, Birsa College, Khunti, Jharkhand, India.

^bDepartment of Physics, Nirmala College, Ranchi, Jharkhand, India

^cDepartment of Physics, Ranchi College, Ranchi, Jharkhand, India.

^dDepartment of Applied Sciences and Humanities SVKMS' NMIMS Deemed University, Shirpur, Maharashtra, India.

*Corresponding author : Phone : 9798306630 ; E-mail : binayakhouri@yahoo.in

Abstract: When disordered and impurity doped photorefractive relaxor ferroelectrics such as Pottasium Lanthanium Tantaneium Niobate (KLTN) are rapidly cooled below Burns temperature they exhibit polar nano-region (PNR). These highly polarizable randomly distributed ferroelectric-like regions provide enormous advancement of the photorefractive optical nonlinearity. In this paper, we have investigated the self-trapped propagation of elliptic Gaussian laser beams in such media. Using WKB and paraxial ray approximation, we have developed nonlinear dynamical equations that describe the propagation of the beam. We have shown that unlike other conventional nonlinear media, self trapped propagation does not require a threshold power of the laser beam.

Paper History:

Received

7th May 2017

Revised

12th May 2017

Peer reviewed

12th June 2017

Accepted

18th June 2017

Keywords: K, L, T, N, WKB approximate, Burn Temperature, Self trapped propagation, Scalefree optics.

INTRODUCTION

In recent years, there has been significant interest in the scale free propagation of optical beams¹⁻¹⁵. The basic mechanism underlying scale free optics is the existence of a nonlocal intensity independent nonlinearity. In principle, light matter interactions can give rise to such nonlinearity. When disordered and impurity doped photorefractive relaxor ferroelectrics such as Potassium Lanthanium Tantenium Niobate (KLTN) crystals are rapidly cooled below burn temperature, they exhibit Polar nano-regions (PNR). These ferroelectric like regions provide enormous enhancement of the photorefractive optical nonlinearity. The effective susceptibility of the crystal can be identified easily, we omit details which can be found elsewhere, and write the change in refractive index Δn due to nonlinearity as follows¹:

$$\Delta n = \Delta n_{PNR} = -g \frac{n^3}{2} \epsilon_0^2 \chi_{PNR}^2 \left(\frac{K_B T}{q} \right)^2 \times \frac{(\partial_x I)^2 + (\partial_y I)^2}{I^2} \quad (1)$$

where χ_{PNR} is the contribution of the PNR to the susceptibility and χ_p is the equilibrium para-electric susceptibility ($\chi_p \ll \chi_{PNR}$), I is the intensity of the optical field.

Model

The nonlinear Schrödinger equation for a linearly polarized light beam which is propagating in a disordered and impurity doped photorefractive relaxor ferroelectrics such as KLTN, can be written in the following form^{1, 15, 20}:

$$2ik\partial_z A + \nabla_{\perp}^2 A + \frac{2k^2}{n} \Delta n A = 0 \quad (2)$$

where, $k = (\omega/c)n$ is the wave number, ω is the optical angular frequency, z is the direction of propagation. By virtue of eqn.(1), equation (2) can be recasted in the following form

$$i \frac{\partial A}{\partial Z} + \frac{1}{2k} \nabla_{\perp}^2 A - K \frac{\left(\frac{\partial |A|^2}{\partial x} \right)^2 + \left(\frac{\partial |A|^2}{\partial y} \right)^2}{|A|^4} A = 0, \quad (3)$$

$$\text{where } \nabla_{\perp}^2 = \frac{\partial^2}{\partial x^2} + \frac{\partial^2}{\partial y^2} \text{ and } K = kg \left(\frac{n \epsilon_0 \chi_{PNR} K_B T}{\sqrt{2} q} \right)^2$$

In order to find out the solution of the propagating elliptic Gaussian beam¹⁶⁻²³, we introduce the following ansatz $A(x, y, z) = A_0(x, y, z)e^{-i\Omega(x, y, z)}$ in equ. (3) to get,

$$\begin{aligned} & \left(i \frac{\partial A_0}{\partial Z} + A_0 \frac{\partial \Omega}{\partial Z} \right) \\ & + \frac{1}{2k} \left\{ \left(\frac{\partial^2 A_0}{\partial x^2} + \frac{\partial^2 A_0}{\partial y^2} \right) - 2 \left(\frac{\partial A_0}{\partial x} \frac{\partial \Omega}{\partial x} + \frac{\partial A_0}{\partial y} \frac{\partial \Omega}{\partial y} \right) - i \left(A_0 \frac{\partial^2 \Omega}{\partial x^2} + A_0 \frac{\partial^2 \Omega}{\partial y^2} \right) - \left(A_0 \left(\frac{\partial \Omega}{\partial x} \right)^2 + A_0 \left(\frac{\partial \Omega}{\partial y} \right)^2 \right) \right\} \\ & - K \frac{\left(\frac{\partial |A_0|^2}{\partial x} \right)^2 + \left(\frac{\partial |A_0|^2}{\partial y} \right)^2}{|A_0|^4} A_0 = 0 \end{aligned} \quad (4)$$

Equating real and imaginary parts of the above equation separately, we get following two equations:

$$A_0 \frac{\partial \Omega}{\partial Z} + \frac{1}{2k} \left\{ \left(\frac{\partial^2 A_0}{\partial x^2} + \frac{\partial^2 A_0}{\partial y^2} \right) - \left(A_0 \left(\frac{\partial \Omega}{\partial x} \right)^2 + A_0 \left(\frac{\partial \Omega}{\partial y} \right)^2 \right) \right\} - K \frac{\left(\frac{\partial |A_0|^2}{\partial x} \right)^2 + \left(\frac{\partial |A_0|^2}{\partial y} \right)^2}{|A_0|^4} A_0 = 0 \quad (5)$$

and,

$$\frac{\partial A_0}{\partial Z} - \frac{1}{k} \left(\frac{\partial A_0}{\partial x} \frac{\partial \Omega}{\partial x} + \frac{\partial A_0}{\partial y} \frac{\partial \Omega}{\partial y} \right) - \frac{1}{2k} \left(A_0 \frac{\partial^2 \Omega}{\partial x^2} + A_0 \frac{\partial^2 \Omega}{\partial y^2} \right) = 0 \quad (6)$$

At this stage since we are dealing with elliptic Gaussian beam, we assume that the intensity distribution of the optical beam across its cross section is elliptic. Therefore we look for solutions of the form:

$$A_0(x, y, z) = \frac{A_{00}}{\sqrt{f_1(z)} \sqrt{f_2(z)}} e^{-\frac{x^2}{2r_0^2 f_1^2(z)}} e^{-\frac{y^2}{2r_0^2 f_2^2(z)}} \quad (7)$$

$$\text{and } \Omega = \frac{x^2}{2} \beta_1(z) + \frac{y^2}{2} \beta_2(z), \quad (8)$$

$$\text{where, } \beta_1(z) = -\frac{k}{f_1} \frac{\partial f_1}{\partial Z} \text{ and } \beta_2(z) = -\frac{k}{f_2} \frac{\partial f_2}{\partial Z}$$

and $r_0 f_1$ and $r_0 f_2$ are the beam width parameters in the x and y directions respectively; f_1 and f_2 are functions of z . The parameter k is a constant and as the beam propagates in the nonlinear media the value of k will vary with propagation distance. Consequently the width of the beam in x and y directions will vary. Constant k and r_0 signify stationary propagation of the beam¹⁸⁻²⁹. Putting (7) and (8) in equ.(5) we get

$$\frac{kx^2}{2f_1} \frac{\partial^2 f_1}{\partial Z^2} + \frac{ky^2}{2f_2} \frac{\partial^2 f_2}{\partial Z^2} + K \frac{4x^2}{f_1^4 r_0^4} + K \frac{4y^2}{f_2^4 r_0^4} - \frac{x^2}{2kf_1^4 r_0^4} - \frac{y^2}{2kf_2^4 r_0^4} + \frac{1}{2kf_1^2 r_0^2} + \frac{1}{2kf_2^2 r_0^2} = 0 \quad (9)$$

Equating the coefficients of x^2 and y^2 of the eqn. (10) to zero, we can easily derive the following pair of coupled nonlinear differential equations:

$$\frac{\partial^2 f_1}{\partial Z^2} = \left(\frac{1}{k^2} \right) \frac{1}{f_1^3 r_0^4} - \left(\frac{8K}{k} \right) \frac{1}{f_1^3 r_0^4} \quad 10(a)$$

$$\frac{\partial^2 f_2}{\partial Z^2} = \left(\frac{1}{k^2} \right) \frac{1}{f_2^3 r_0^4} - \left(\frac{8K}{k} \right) \frac{1}{f_2^3 r_0^4} \quad 10(b)$$

Since we are looking for stationary propagation of elliptic Gaussian laser beams, we set right hand side of both equations of 10(a) and (b) equal to zero. We immediately get $\frac{\partial^2 f_1}{\partial Z^2} = 0$ and $\frac{\partial^2 f_2}{\partial Z^2} = 0$. Thus, stationary propagation of elliptic Gaussian beam is independent of the strength of optical nonlinearity. This behavior is completely different from what one would expect in other nonlinear media such as Kerr or stationary nonlinear media.

CONCLUSION

We have shown that to self-trapped an elliptic Gaussian laser beam in a disordered ferroelectrics one does not require a threshold power of the beam. This behavior is entirely different from what one would normally encounter in the Kerr and stationary nonlinear media.

ACKNOWLEDGEMENT

The authors are thankful to Prof. Akhoury, Head, University Dept. of Physics, Ranchi University for encouragement & academic support.

REFERENCES

1. E.DelRe, E.Spinozzi, A .J.Agranant and C. Conti; Nature Photonics, Scale-free optics and diffractionless waves in nano-disordered ferroelectrics, **2010**, 5, 39-42.
2. Mishra, M. Konar, S.; *Prog. Electromag. Res.* **2008**, 78, 301-320.
3. Konar, S. Mishra, M. Jana, S.; *Phys. Letts.A* **2007**, 362, 505-510.
4. Sodha, M.S., Konar, S. , Maheshwari, K.P.; *J. Plasma Phys.* **1992**, 48, 107-118.
5. Medhekar, S., Konar, S., Sodha, M.S.; *Optics Letters* **20**, **1995**, 2192-2194.
6. Segev, M.; Crosignani, B.; Yariv, A.; Fischer, B. *Phys. Rev. Lett.* **1992**, 68, 923-926.
7. Konar, S.; Jana, S.; Mishra, M. *Optics Commun.* **2005**, 255, 114-129.
8. Christodoulides, D.N.; Carvalho, M.I. *J. Opt. Soc. Am, B* **1995**, 12, 1628-1633.
9. Gunter, P.; Huignard, J.P. *Topics in Applied Physics in Photorefractive Materials and their Application I and II*, Springer, Berlin, **1998**.
10. Valley, G.C.; Segev, M.; Crosignani, B.; Yariv, A.; Fejer, M.M.; Bashaw, M.C. *Phys. Rev. A*, **1994**, 50, R 4457-R4460.
11. Asif, N.; Shwetanshumala, S.; Konar, S. *Phys. Lett. A*, **2008**, 372, 735-740.
12. Zhang, G.; Liu, J. *J. Opt. Soc. Am. B*, **2009**, 26, 113-120.
13. Konar, S.; Shekhar, S.; Hong, W.P. *Opt. Laser Tech.*, **2010** , 42 ,1294-1300.
14. Konar, S.; Jana, S.; Shwetanshumala, S. *Opt. Com.* **2007**, 273, 324-333.
15. Del Re, E.; Crosignani, B.; Tamburrini, M.; Segev, M.; Mitchell, M.; Refaeli, E.; Agranat, A.J. *Opt. Lett.*, **1998**, 23, 421-423.
16. Konar, S.; Biswas, A. *Optical Maerials*, **2013**, 35, 2581-2603.
17. Akhmanov, S.A.; Sukhorukov, A.P.; Khokhlov, R.V. *Sov. Phys. USP* **1968**, 10, 609-636.
18. Vlasov, S.N.; Petrishev, V.A.; Talanov, V.I. *Sov.Radio Phys.*,**1971**, 14, 1062-1070.
19. G. Samara, J.; *Phys. Condens.Matter*, **2003**, 15, R367
20. E. DelRe, M. Segev, D.N. Christodoulides, B. Crosignani, and G. Salamo in P. Gunter and J.P. Huignard (Eds.) (Springer-Verlag, Berlin Heidelberg, **2006**)
21. S.R. Singh, D.N. Christodoulides, *Opt.Comm.*, **1995**, 118, 569-576.
22. Z. Chen, M. Mitchell, M.F. Shih, *Opt. Lett.* **1996**, 21, 629-631.
23. S.Konar, S. Jana, and S. Shwetanshumala, *Optics Communications*, **2007**, 273, 324-333.
24. S. Konar, M. Mishra, and Soumendu Jana, *Physics Letters A* , **2007**, 362 , 505-510.
25. Soumendu Jana , S. Konar;;*Optics Communications*, **2008**, 281 , 1197-1202.
26. S. Konar, A. Sengupta, *J. Opt.Soc. Am B*, **1994**, 11, 1644-1653.
27. M.Mishra, S.Konar ,*Progress In Electromagnetics Research*, PIER, **2008**, 78, 301–320.
28. S. Konar , S. Jana, *Optics Communication* **2004**, 236, 7-20.
29. S. Shwetanshumala, S. Jana, and S. Konar, *Journal of Electromagnetic Waves and Applications*, **2006**, 20, 1, 65-77.



Study of high energy radiotherapy beams and analysis of its characteristics in water

Sudha Singh^{a*} & Payal Raina^b

^aUniversity Department of Physics, Ranchi University, Ranchi, Jharkhand, India

^bRIMS, Radiotherapy Department & University Department of Physics, Ranchi University, Ranchi, Jharkhand, India

*Corresponding author : Phone : 9162066448, E-mail : ssingh8@gmail.com

Abstract: Radiation therapy uses high energy particles or waves, such as X rays, gamma rays, electron beams or protons, to destroy cancer cells. Various physical quantities are used in a dose calculation system devised to predict dose distribution in an actual patient. The present study measures the physical quantities and compares the beam characteristics. All the physical quantities are measured with ion chamber in Radiation field analyzer (RFA). Measured values are within the tolerance limit. All these data were utilized as input to the treatment planning system for clinical use.

Paper History:

Received

17th May 2017

Revised

25th May 2017

Peer reviewed

12th June 2017

Accepted

24th June 2017

Keywords: Photon, Electron, PDD, Beam Quality, Flatness, Symmetry

INTRODUCTION

Radiation therapy would not exist without physics. It begins with the discovery of X-rays. This therapy use ionizing radiation which is delivered by a linear accelerator. Linear accelerator is a device that uses high-frequency electromagnetic waves to accelerate charged particles such as electrons to high energies through a linear tube¹. The high-energy electron beam itself can be used for treating superficial target, or it can be made to strike a target to produce x-rays for treating deep-seated target. Radiation therapy works by damaging the DNA of cancerous cells. Photon cause indirect ionization happens as a result of the ionization of water, forming free radicals, which then damage. Charged particles such as electron, protons, boron, carbon, and neon ions can cause direct damage to target through high-LET (linear energy transfer)². The main focus of physics in radiation therapy is to increase the level of precision and accuracy of dose delivery to the

target volume. A major cornerstone of the success is the definition of the physical quantity of absorbed radiation dose, *i.e.* the energy imparted per unit mass. It is difficult to measure dose distribution directly in patients. Data on dose distribution are derived from measurements in tissue-equivalent materials (Phantom). Various physical quantities such as Percentage Depth Dose (PDD), Tissue Maximum Ratio (TMR), Beam Quality ($TPR_{20/10}$), Wedge factor etc are used in a dose calculation system devised to predict dose distribution in an actual patient³. Single photon beams are of limited use in the treatment of deep seated target, since they give a higher dose near the entrance at the depth of dose maximum than at depth. For deeper lesions, a combination of two or more photon beams is usually required to concentrate the dose in the target volume and spare the tissues surrounding the target as much as possible. In order to represent volumetric variation in absorbed dose distributions are depicted by means of isodose curves. It

is usually drawn at equal increments of percent depth dose, representing the variation in dose as a function of depth. Special filters or absorbing blocks are also placed in the path of a beam to modify isodose distribution. This is a wedge-shaped absorber that causes a progressive decrease in the intensity across the beam, resulting in a tilt of the isodose curves from their normal positions. The wedge is made of a dense material and is mounted on a transparent plastic tray, which is inserted in the beam at a specified distance from the source. The presence of a wedge filter decreases the output of the machine, which is taken into account in treatment calculations.

MATERIALS & METHODS

All measurements were performed at the Radiotherapy Center RIMS using a linear accelerator SYNERGY. This type of accelerator generates high-energy photons of 6 MV & 15 MV and high-energy electrons of 4,6,8,9,10,12,15 and 18 MeV. Relative and absolute measurements were performed using water phantom, ionization chambers with sensitive volumes of 0.125cc & 0.6cc, RFA and electrometer. The experimental data collected are then analyzed using adequate software. In this study different physical quantities PDD, TMR, Beam Profile, TPR 20/10, wedge factor were measured which is required for the treatment planning system. PDD was analyzed with 0.125cc ion chamber in RFA. It is the quotient of the absorbed dose at any depth d to the absorbed dose at a fixed reference depth d_0 , along the central axis of the beam. These measurements were performed at Source to Surface Distance (SSD) 100 cm with scan depth 30cm in RFA⁴. Setup arrangement is shown in Fig1

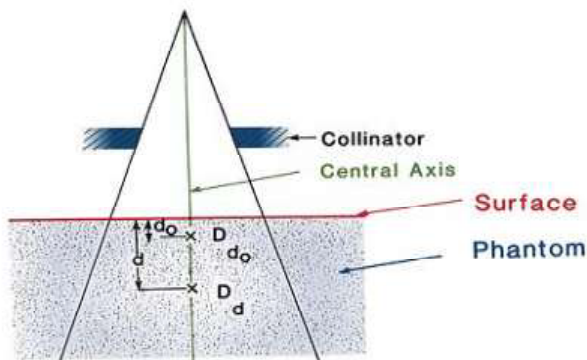


Fig1. Setup for PDD

In rotation therapy, the radiation source moves in a circle around the axis of rotation. Although the source to surface distance (SSD) may vary depending on the shape of the surface contour, the source-axis distance (SAD) remains constant. Since the percent depth dose depends on the SSD, correction to the PDD will have to be applied to correct for the varying SSD. A simpler quantity TMR has been defined to remove the SSD dependence. TMR was generated from PDD. It is the ratio of the dose at a given point in phantom to the dose at the same point at the reference depth of maximum dose. For high-energy photons, beam quality Q is specified by the tissue-phantom ratio, $TPR_{20,10}$. It is calculated by taking the ratio of the absorbed doses at depths of 20 cm and 10 cm in a water phantom, measured with a constant source-chamber distance of 100 cm and a field size of 10 cm x 10 cm at the plane of the chamber⁴. For electron beams the beam quality index is the half-value depth in water R_{50} . This is the depth in water (in g/cm²) at which the absorbed dose is 50% of its value at the absorbed dose maximum. The beam profiles represent dose variation across the field at a specified depth. It consists of three distinct regions: central, penumbra and umbra. Beam profile was taken for different field size at 10cm depth. Beam uniformity is quantified by two parameters beam flatness and beam symmetry. The beam flatness F was assessed by finding the maximum D_{max} and minimum D_{min} dose point values on the beam profile within the central 80% of the beam width and then using the relationship.

$$F = 100 \times \frac{D_{max} - D_{min}}{D_{max} + D_{min}}$$

The beam symmetry was assessed by ratio between measured values for each pair of symmetrical points for a range of field sizes must lie between 0.98 and 1.02 within the central 80%^{4,5}

RESULT & DISCUSSION

For Photon

The dose is described usually as PDD which depends on the depth, field size, energy and SSD. PDD values measured at 10 cm depth for 10 x 10 cm² field size for photon beams are presented in the Table-1 and it can be seen that it increases with the beam energy.

Table1: Measured and tabulated values for PDD (at 10cm) for photon energies

Energy in MV	PDD(Measured)	PDD(Tabulated)
6 MV	67.9%	67.1%±1.5%
15 MV	76.3%	77.3%±2.0%

When radiation beam enters in medium attenuation takes place and percentage depth dose varies with depth due to the attenuation. Depth dose curves for 6MV photon beam is shown in Fig.2 and for 15MV is shown in Fig.3. It shows that the maximum dose is not at the surface but at some Depths. This is because of electrons deposit their

energy at significant distance away from their site of origin. The absorbed dose increase with depth and reach to maximum. Beyond a certain depth the dose eventually begins to decrease due to decrease in photon energy fluence⁶ ..

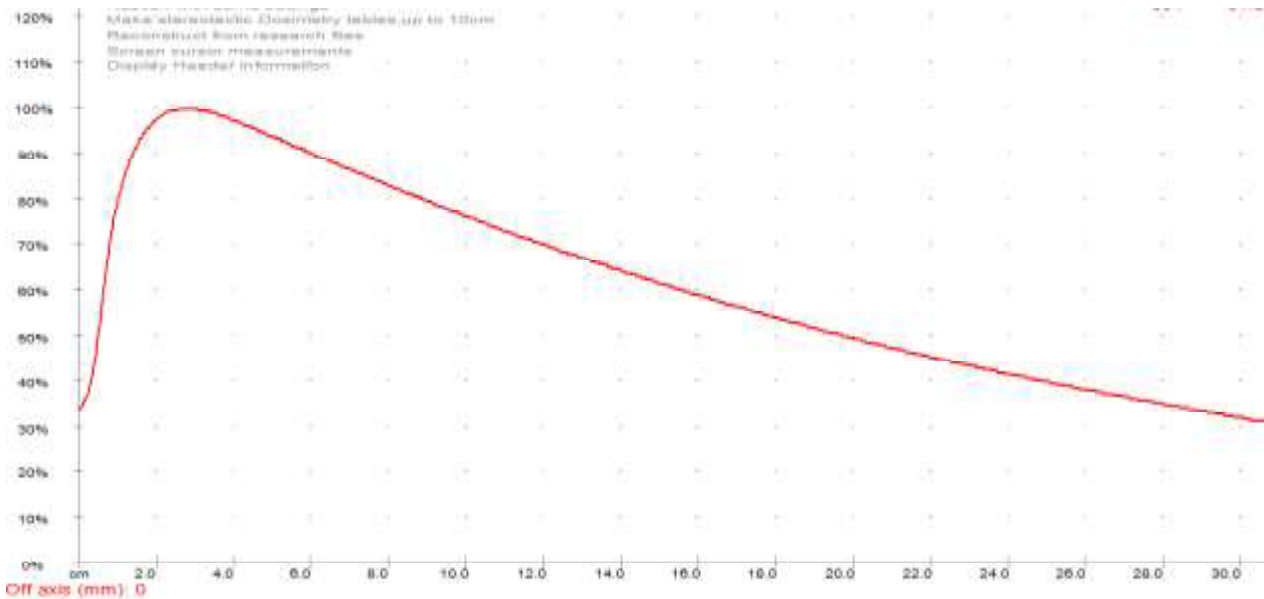


Fig 2. PDD curve for 15 MV photon beam

It is observed from Fig2 and Fig3, that the maximum dose is delivered at 16mm depth for 6MV and 27mm depth for 15MV photon beams respectively. It shows that the higher the energy of the beams the greater is their penetrating power and can thus deliver a high percentage

depth dose. TMR values are generated from PDD. Calculated values at 10 cm for 10 x 10 cm² field size for photon beams are presented in the Table-2. Beam quality index $TPR_{20,10}$ for 6MV and 15 MV are presented in Table3.

Energy	TMR for10 x 10cm ²
6 MV	0.803
15 MV	0.795

Table2. TMR (at 10cm) for photon energies

Energy	Beam Quality($TPR_{20,10}$) measured	Beam Quality($TPR_{20,10}$) tabulated
6 MV	0.680	0.676±0.009
15 MV	0.755	0.75±0.005

Table3. Beam Quality Index

Beam profile for 6MV photon beam for 10 x 10 cm² field size at 10cm depth is shown in the Fig.4. Beam flatness, symmetry and Penumbra are represented in Table4. Tolerance limit for flatness and symmetry for photon beams is $\pm 3\%$. Result shows that flatness and

symmetry for photon beams are with the tolerance limit point in phantom along the central axis of the beam. Fig5 and 6 represents isodose curve without wedge and with wedge respectively. Wedge factor for 6MV for 10x10cm² field size is 0.201 and for 15 MV is 0.2707.

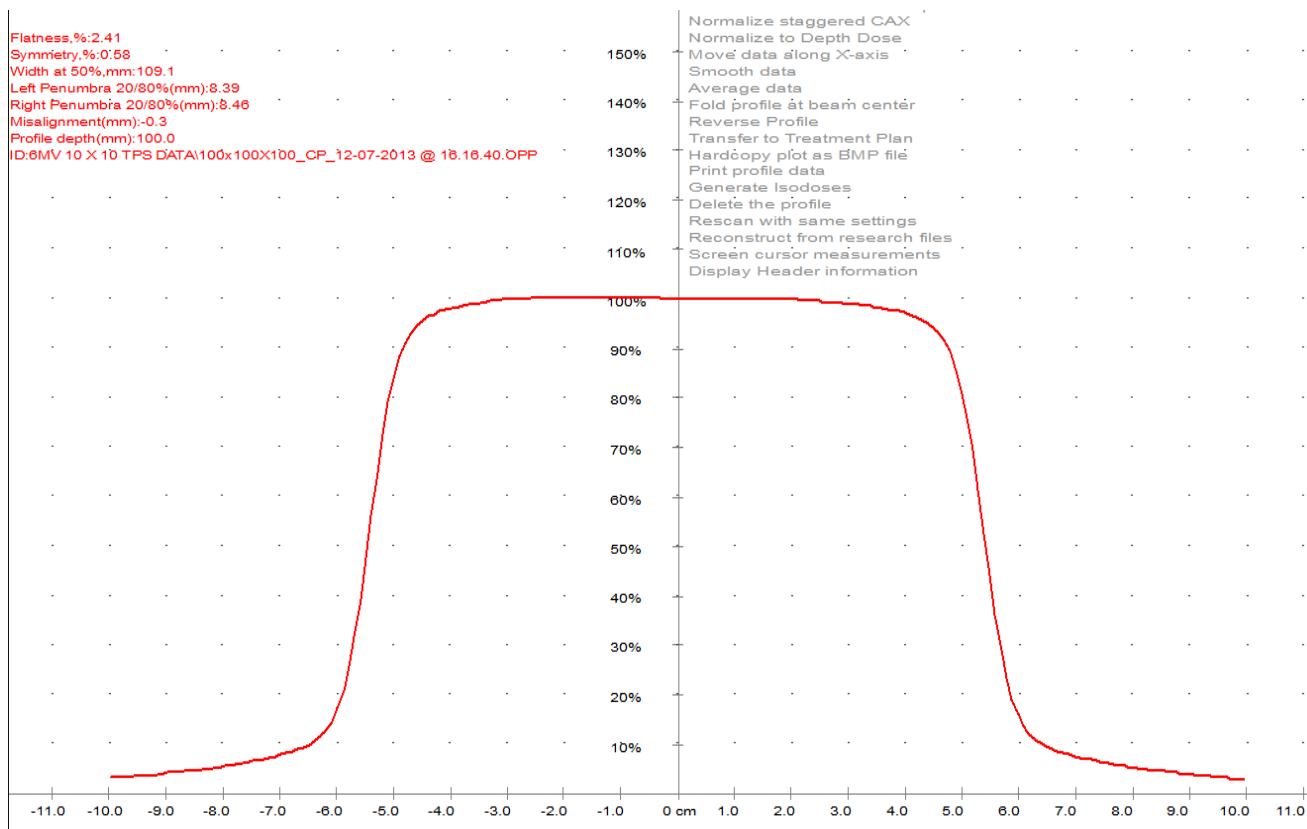


Fig4. Beam profile for 6 MV photon beam for 10 x10 cm² field size

Table4: Beam Parameter

Energy	Flatness	Symmetry	Right Penumbra	Left Penumbra
6MV	2.41%	0.58%	8.48%	8.38%
15MV	1.91%	0.06%	8.59%	8.55%

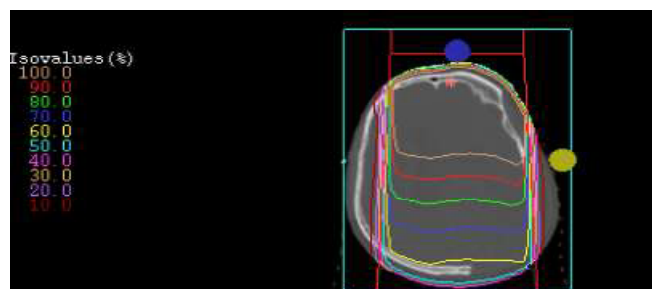


Fig 5. Isodose curve

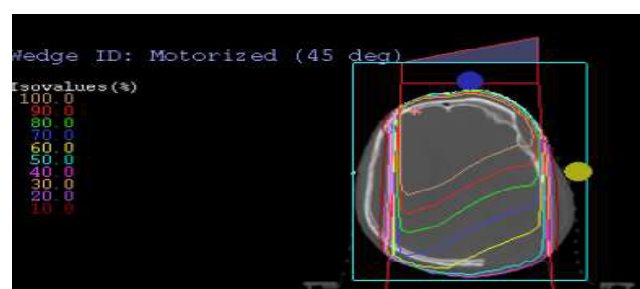


Fig.6 .Isodose curves for 45 deg wedge filter

For Electron

The shape of the central axis depth dose curves for electron beams differ from that of photon beams. This is shown in the Fig.7. For all electron energy PDD was measured at 100cm SSD for a 10 x10 cm² applicator in

RFA with parallel plate chamber. It was observed that the surface dose of electron beams is much higher than that for photon beams because electrons rapidly drop-off their energy due to collision and radiative processes. Typical dose parameters of electron beams are presented in Table5.

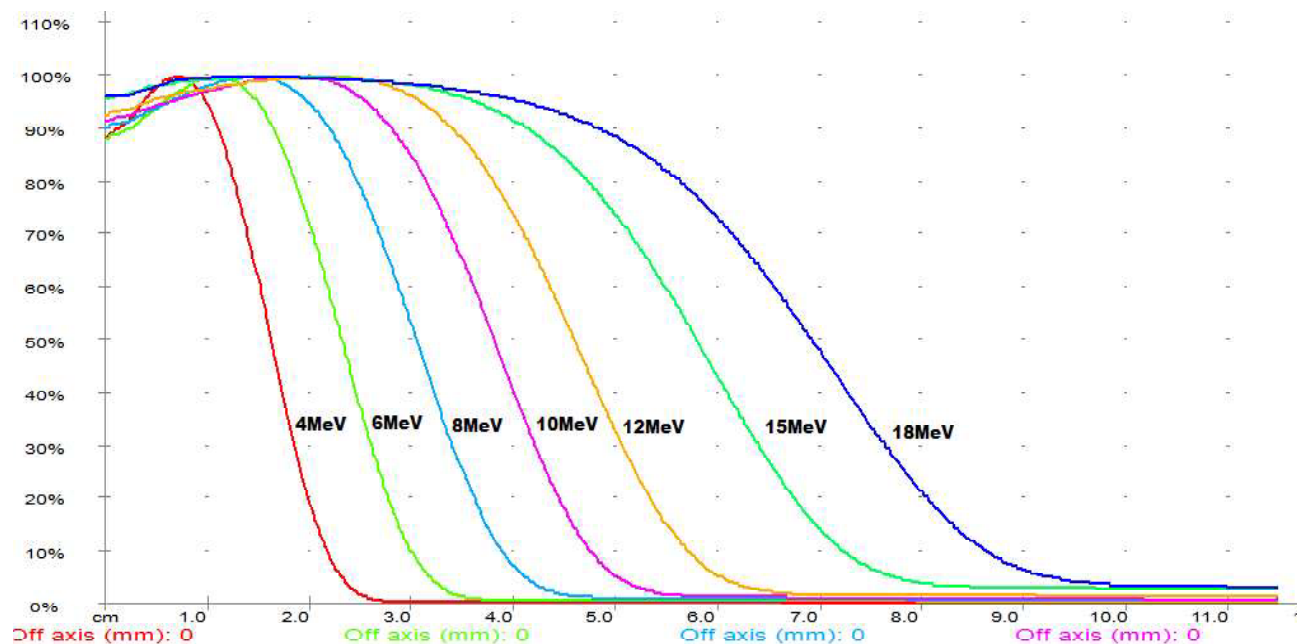


Fig 7. PDD curve for electron beams

The Table below shows the beam quality for electron beams.

Table 5. Typical Dose Parameters of Electron Beams

Energy	R ₁₀₀	R ₅₀	R ₈₀	R ₉₀
4MeV	9mm	18.1mm	14.6mm	13.0mm
6MeV	12.7mm	25.1mm	20.5mm	18.3mm
8MeV	15.7mm	32.2mm	26.4mm	23.7mm
10MeV	19.7mm	39.7mm	33.0mm	29.8mm
15MeV	15.7mm	57.2mm	46.9mm	41.3mm
18MeV	14.0mm	69.5mm	56.6mm	48.8mm

CONCLUSION

Study of the characteristics and analysis of depth dose of electrons and photons are helpful in achieving high degree of accuracy in radiotherapy. The clinically useful energy range for electron beams is 4 to 18 MeV. At these energies, the electron beam can be used for treating superficial tumor less than 5 cm deep with a

characteristically sharp drop off in dose. It was observed that energy of photon beam is the major element of uniqueness of absorbed dose at certain depth. Relative attenuation between two depths describes the way in which dose decreases or increases for certain energy⁷. Combination of two or more photon beams is used to treat deeper lesions. This study shows that all the measured

values are within the tolerance limit and match with the values given in the theory. Thus Linear accelerator can be used for clinical purpose. The outcome of the present analysis will be helpful to choose the appropriate beam for cancer treatment where a variety of beam energies are available.

ACKNOWLEDGEMENT

The authors are thankful to Prof. Akhoury, Head, University Dept. of Physics, Ranchi University & technicians of Radiotherapy Department of RIMS, for encouragement & academic support.

REFERENCES

1. **F. M. Khan. 2003.** *The Physics of Radiation Therapy*, Lippincott Williams & Wilkins. 3rd edition.
2. **Halperin EC, Perez CA, Brady LW. 2008.** *Principles and Practice of Radiation Oncology, Fifth Ed.* Philadelphia, Pa: Lippincott Williams & Wilkins.
3. **E. B. Podgorsak.2005.** *Basic Radiation Physics*, IAEA publication.
4. Absorbed Dose Determination in External Beam Radiotherapy: *An International Code of Practice for Dosimetry Based on Standards of Absorbed Dose to Water*, TRS 398, IAEA Protocol. PP-70-88-139.
5. **J. V. Dyk, R. B. Barnett, J. E. Cygler, and P. C. Shragge. 1993.** *Commissioning and quality assurance of treatment planning computer*, Int. J. Radiat. Oncol., Biol., phys. PP-261-273.
6. **Besim Xhafa, Tatjana Mulaj, Gezim Hodolli and Gazmend Nafezi. 2014.** *Dose distribution of photon beam by Siemens linear accelerator*, International Journal of Medical Physics, Clinical Engineering and Radiation Oncology.23. PP- 67-70.
7. **Turner JE.2005.** *Interaction of ionizing radiation with matter*. Health Phys.PP-520-44.



Exact dynamics for a two-level atom interacting with intensity dependent single-mode quantized cavity field in a Kerr medium

Sudha Singh* & Arun Kumar

University Department of Physics, Ranchi University, Ranchi, Jharkhand, India

*Corresponding author : Phone : 9162066448 , E-mail : ssingh8@gmail.com

Abstract: The present paper describes the dynamics of a single two-level atom interacting with intensity dependent quantized single mode field in an ideal cavity filled with a non-linear Kerr-like medium. The cavity mode interacts both with the atom as well as the Kerr-like medium. The unitary transformation method presented here for the special case of exact resonance, not only solves the time-dependent problem but also provides the eigen solutions of the interacting Hamiltonian at the same time. We have studied the photon statistics and the effect of Kerr like medium and the detuning parameter on the evolution of atomic inversion for the initial coherent as well as thermal field.

Paper History:

Received

27th May 2017

Revised

2nd June 2017

Peer reviewed

20th June 2017

Accepted

28th June 2017

Keywords: Jaynes-Cummings Model, Intensity Dependent Coupling, Kerr Non-linearity, Atomic Dynamics, Photon Statistics.

INTRODUCTION

One of the simplest and most non-trivial systems in quantum optics is the Jaynes Cummings model (JCM)¹ that describes the interaction of a two level atom with a single mode quantized electromagnetic field under the rotating wave approximations. It has been observed that the temporal behaviour of the model is very sensitive to the statistical properties of the radiation field in the initial state displaying a number of unexpected pure quantum features that have no classical counterpart²⁻⁴. For example, when the initial field is in a coherent state the mean atomic excitation energy and the mean photon number exhibit periodic collapses and revivals. The dynamics predicted by the model has been verified experimentally with Rydberg atoms in micro-wave cavities with high Q values⁵⁻⁷

Encouraged by the success of the Jaynes-Cummings Model, special attention is being paid to extend and

generalize the model in order to explore new quantum effects. There have been several generalizations of the Jaynes-Cummings Hamiltonian in which the interaction between the radiation and atom is no longer linear in the field variables. These are the JCM with intensity dependent coupling and its multi photon generalization⁸⁻¹². Intensity dependent Jaynes-Cummings Model proposed by Buck and Sukumar⁸⁻⁹ takes the coupling between matter and radiation to depend on the intensity of the electromagnetic field.

In this paper we consider an intensity dependent Jaynes-Cummings Hamiltonian in the rotating wave approximation incorporating an additional term for introducing Kerr-non-linearity. A Kerr-medium is non-linear in the sense that its refractive index has a component which varies with the intensity of the propagation field. All materials show a Kerr effect, but certain liquids display

it more strongly than others. Silica fibres are good example of Kerr-media. We study the quantum dynamics of the intensity dependent single mode Jaynes-Cummings model in the presence of a Kerr medium and analyse the atomic dynamics as well as photon statistics. To obtain the eigen values and eigen functions of the Hamiltonian of the interacting system method of Unitary transformation in quantum mechanics by Sudha Singh¹³ has been used.

Intensity Dependent Jaynes Cummings Model with Kerr non-linearity and its Solution

We consider an ideal cavity ($Q = \infty$) filled with a non-linear Kerr like medium containing single mode radiation field that interacts with a two-level atom via single mode intensity dependent process.. The cavity mode interacts with the atom as well as the Kerr-like medium. The atomic higher and lower level $|a\rangle$ and $|b\rangle$ have opposite parities. The effective Hamiltonian describing the above process can be written as

$$\hat{H} = \frac{\hbar\omega_0\hat{\sigma}_z}{2} + (\hbar\omega\hat{a}^\dagger\hat{a} + \chi\hat{a}^{\dagger 2}\hat{a}^2) + \hbar g(\hat{\sigma}_+ \hat{a} \sqrt{\hat{a}^\dagger\hat{a}} + \hat{\sigma}_- \sqrt{\hat{a}^\dagger\hat{a}} \hat{a}) \quad (1)$$

Here ω_0 is the transition frequency between the excited and ground state of the atom. $\hat{a}^\dagger(\hat{a})$ are the creation (annihilation) operators for the cavity field mode and g is the effective coupling constant. $\hat{\sigma}_z$ and $\hat{\sigma}_\pm$ are the atomic pseudo spin operators. The symbol χ describes the strength of the quadratic non-linearity modelling the Kerr medium for the field mode ω .

Denoting by $|a\rangle$ and $|b\rangle$ respectively the higher and lower eigenkets of the isolated atom and by $|n\rangle$ the eigenstate of the free field with frequency ω , the basis eigenkets of the interacting system can be designated by $|a, n\rangle$ and $|b, n\rangle$ and the state vector for the system at any time t is then

$$|\psi(t)\rangle = \sum_n a_n(t) |a, n\rangle + \sum_n b_n(t) |b, n\rangle \quad (2)$$

The state vector $|\psi(t)\rangle$ develops from the state vector $|\psi(0)\rangle$ at $t = 0$ according to

$$|\psi(t)\rangle = \hat{T}(t) |\psi(0)\rangle \quad (3)$$

where the unitary operator $\hat{T}(t)$ satisfies

$$i\hbar \frac{d\hat{T}(t)}{dt} = \hat{H} \hat{T}(t) \quad (4)$$

In the Heisenberg representation, at resonance, $\omega \approx \omega_0$, the time dependence of \hat{H} given by Eq. (1) drops out. A direct integration of Eq. (4) with \hat{H} given by Eq. (1) then yields

$$\hat{T} = \exp[-it\{\frac{\omega_0}{2}\hat{\sigma}_z + \omega\hat{a}^\dagger\hat{a} + \chi(\hat{a}^\dagger)^2(\hat{a})^2 + g(\hat{F}_+ + \hat{F}_-)\}] \quad (5)$$

where

$$\hat{F}_+ = \hat{\sigma}_+ \hat{a} \sqrt{\hat{a}^\dagger\hat{a}}, \quad \hat{F}_- = \hat{\sigma}_- \sqrt{\hat{a}^\dagger\hat{a}} \hat{a}^\dagger \quad (6)$$

Considering the initial state of the system as $|a, n\rangle$, we get from Eq. (3)

$$|\psi(t)\rangle = \hat{T}(t) |a, n\rangle \quad (7)$$

Expanding $\hat{T}(t)$ given by Eq. (5) and then operating each term of the expansion on the initial state $|a, n\rangle$, we get

$$\begin{aligned} \psi(t) = & [1 - it\{\frac{\omega_0}{2} + \omega n + \chi n(n-1)\} \\ & - \frac{t^2}{2!}\{\frac{\omega_0}{2} + \omega n\}^2 + g^2(n+1) + \chi n^2(n-1)^2 + \omega\chi n(n-1) + 2\omega\chi n^2(n-1)\} + \\ & + \frac{it^3}{3!}\{\frac{\omega_0}{2} + \omega n\}^3 + \chi^3 n^3(n-1)^3 + g^2\chi n(n+1)\{2(n^2-1) + (n+1)^2\} \\ & - \frac{\omega_0 g^2}{2}(n+1) + \frac{3}{2}\omega_0\chi^2 n^2(n-1)^2 + \frac{3}{2}\omega_0^2\chi n(n-1) + \omega g^2\{(n+1)^2 + 2n(n+1)\} \\ & + 3\omega\chi^2 n^3(n-1)^2 + 3\omega^2\chi n^3(n-1) + 3\omega_0\omega\chi n^2(n-1)\}] |a, n\rangle \\ & + [-it\{g(n+1)\} - \frac{t^2}{2!}\{g(n+1)\} \times \{2\chi n^2 + \omega(2n+1)\} \\ & + \frac{it^3}{3!}\{g(n+1)\} \times \{g^2(n+1)^2 + \chi^2 n^2(3n^2+1) + \omega_0^2 + 4\omega^2(3n^2+3n+1) + 2\omega_0\omega \\ & - \omega_0\chi n + 4\chi\omega n(6n^2+3n+1)\}] |b, n+1\rangle \end{aligned} \quad (8)$$

At resonance in which case $\omega \approx \omega_0$, the operators \hat{F}_+ and \hat{F}_- become time independent in the Heisenberg picture and the following properties that have been used in obtaining the above follow from the definitions of the operators

$$\begin{aligned} \hat{F}_+ |a, n\rangle &= 0; \quad \hat{F}_- |b, n\rangle = 0 \\ \hat{a}^{\dagger 2} \hat{a}^2 |n\rangle &= n(n-1) |n\rangle; \quad \hat{F}_+ \hat{F}_- |a, n\rangle = (n+1)^2 |a, n\rangle \\ \hat{F}_- |a, n\rangle &= (n+1) |b, n+1\rangle; \quad \hat{F}_+ |b, n\rangle = n |a, n-1\rangle \quad \text{etc.} \end{aligned} \quad (9)$$

In the light of Eqs.(3) and (7) it is seen that the coefficient of $|a, n\rangle$ and $|b, n+1\rangle$ on the right hand side of Eq.(8) gives the probability amplitude $a_n(t)$ and $b_{n+1}(t)$. Collecting the coefficient of $|b, n+1\rangle$ on the right hand side of Eq. (8) and making algebraic simplifications we obtain the transition probability for transition of the atom from the higher to the lower state as

Singh & Kumar: Exact dynamics for a two-level atom interacting with intensity dependent single-mode quantized cavity field in a Kerr medium

$$|b_{n+1}|^2 = \frac{4g^2(n+1)^2}{4g^2(n+1)^2 + \{2\chi n + \Delta\}^2} \sin^2\left(\frac{t}{2} \sqrt{4g^2(n+1)^2 + \{2\chi n + \Delta\}^2}\right) \quad (10)$$

Here the detuning Δ and the generalized Rabi frequency $\Omega(n)$ is defined as

$$\Delta = \{\omega_0 - \omega\} \quad (11)$$

$$\Omega(n) = 2\sqrt{g^2(n+1)^2 + \{\chi n + \frac{\Delta}{2}\}^2} \quad (12)$$

The level occupation probabilities of the system oscillate at the Rabi frequency $\Omega(n)$, the frequency at which the two-level atom and the field mode exchange a single photon. Eq. (12) reveals that different photon number states have different quantum Rabi flopping frequencies. It is clear that for $\chi = 0$, Eqs. (10) and (12) give the transition probability and Rabi frequency for the intensity dependent Jaynes Cummings model¹³ as expected.

Time evolution of atomic population inversions

We analyze the time evolution of atomic inversion which is defined as the difference between the probabilities to find the atom in the excited state and ground state and is given by the relation

$$W(t) = |\alpha, n|^2 - |b, n+1|^2 \quad (13)$$

For an initially excited atom the atomic inversion is given by

$$W(t) = \sum_{n_1, n_2=0}^{\infty} P_n(\bar{n}) \left(\frac{4g^2(n+1)^2}{\Omega^2} \cos \Omega t + \frac{4\left(\chi n + \frac{\Delta}{2}\right)^2}{\Omega^2} \right) \quad (14)$$

For $\chi = 0$ the above expression for the atomic inversion reduces to that of the atomic inversion in the intensity dependent Jaynes Cummings Model¹³.

The collapse revival phenomenon

For the cavity field modes initially prepared in the coherent state $|\alpha\rangle$ with probability distribution function P_n given by

$$P_n(\bar{n}) = |\langle n | \alpha \rangle|^2 = |C_n(\alpha)|^2 = \exp(-\bar{n}) \frac{\bar{n}^n}{n!} \quad (15)$$

There are collapses and revivals of Rabi oscillations in the atomic inversion due to the quantum nature of the cavity field. The collapse is due to the interference of Rabi flopping at different frequencies. Collapses occur¹⁴ a result of the spread of the probabilities $|P_n|^2$ about \bar{n} for photon numbers in the range $\bar{n} \pm \Delta n$, i.e. the frequencies in the range $\Omega(\bar{n} - \Delta n)$ to $\Omega(\bar{n} + \Delta n)$.

In weak nonlinear coupling $\chi \ll g$, under resonance condition ($\omega_0 = \omega$) we write the Rabi frequency

$$\Omega(n) = 2\sqrt{g^2(n+1)^2 + \{\chi n + \frac{\Delta}{2}\}^2} \text{ as } \Omega(\bar{n}) = 2g\bar{n}\left(1 + \frac{\chi^2}{2g^2}\right), \quad \bar{n} \gg 1.$$

The collapse time t_c can be evaluated from the time-frequency uncertainty relation $t_c [\Omega(\bar{n} + \Delta n) - \Omega(\bar{n} - \Delta n)] \approx 1$. For the initial coherent field, the root-mean-square deviation in the photon number $\Delta n = \sqrt{\bar{n}}$ so that for collapse time we must have

$$t_c [\Omega(\bar{n} + \bar{n}^{1/2}) - \Omega(\bar{n} - \bar{n}^{1/2})] \approx 1 \quad \text{or}$$

$$t_c \{2g(\bar{n} + \bar{n}^{1/2}) - 2g(\bar{n} - \bar{n}^{1/2})\} \left(1 + \frac{\chi^2}{2g^2}\right) \approx 1$$

So that for the collapse time, we obtain

$$t_c = \frac{1}{4g\bar{n}^{1/2}} \left(1 - \frac{\chi^2}{2g^2}\right) \quad (16)$$

For $\chi = 0$ we obtain $t_c = \frac{1}{4g\bar{n}^{1/2}}$ as obtained in Intensity dependent Jaynes Cummings Model¹³

In strong nonlinear coupling $\chi \gg g$, we write the Rabi frequency as

$$\Omega(\bar{n}) = 2\chi\bar{n} \left(1 + \frac{g^2}{2\chi^2}\right)$$

and proceeding as above we obtain

$$t_c = \frac{1}{4\chi\bar{n}^{1/2}} \left(1 - \frac{g^2}{2\chi^2}\right) \quad (17)$$

The revival phenomenon

W(t) in the Eq(14) consists of a sum of oscillating terms, each term oscillating at a particular Rabi frequency $\Omega(n)$. Since the photon numbers are discrete in the sum (14). The oscillations rephase in revival time. Revival property is a signature of quantum electrodynamics than the

collapse. Any spread in field strength will dipphase Rabi oscillations but revivals are entirely due to the quantum nature of the field so that the atomic evolution is determined by individual field quanta¹⁵.

We expect constructive (destructive) interference according as the two neighbouring terms differ in phase by 2π (π). Since only the frequencies around \bar{n} will contribute, revivals should occur for times $t = t_R$ such that

$$[\Omega(\bar{n} + \Delta n) - \Omega(\bar{n})]t_R = 2\pi k, \quad k = 0, 1, 2, \dots \quad (18)$$

In weak non-linear coupling $\chi \ll g$ writing the Rabi frequency as $\Omega(\bar{n}) = 2g\bar{n}(1 + \frac{\chi^2}{2g^2})$ for $\bar{n} \gg 1$, the period of revival is obtained as

$$t_R = \frac{\pi m}{g} \left(1 - \frac{\chi^2}{2g^2} \right), \quad m = 1, 2, 3, \dots \quad (19)$$

It is interesting to observe that revival time is independent of \bar{n} .

For $\chi = 0$, $t_R = \frac{\pi m}{g}$ as obtained in intensity dependent

Jaynes-Cummings models.

In Fig. 1 we plot the time evolution of atomic inversion for $\bar{n} = 6$. The left hand side panel shows the dynamics for different value of detuning $\Delta = 0, 10g$ whereas the right hand side panel shows the plots for different values of the parameter $\chi = 0.2g, 0.8g$, keeping $\Delta = 0$. We observe that the energy spectrum is linear. This is due to the linear dependence of the Rabi frequency on the quantum number n .

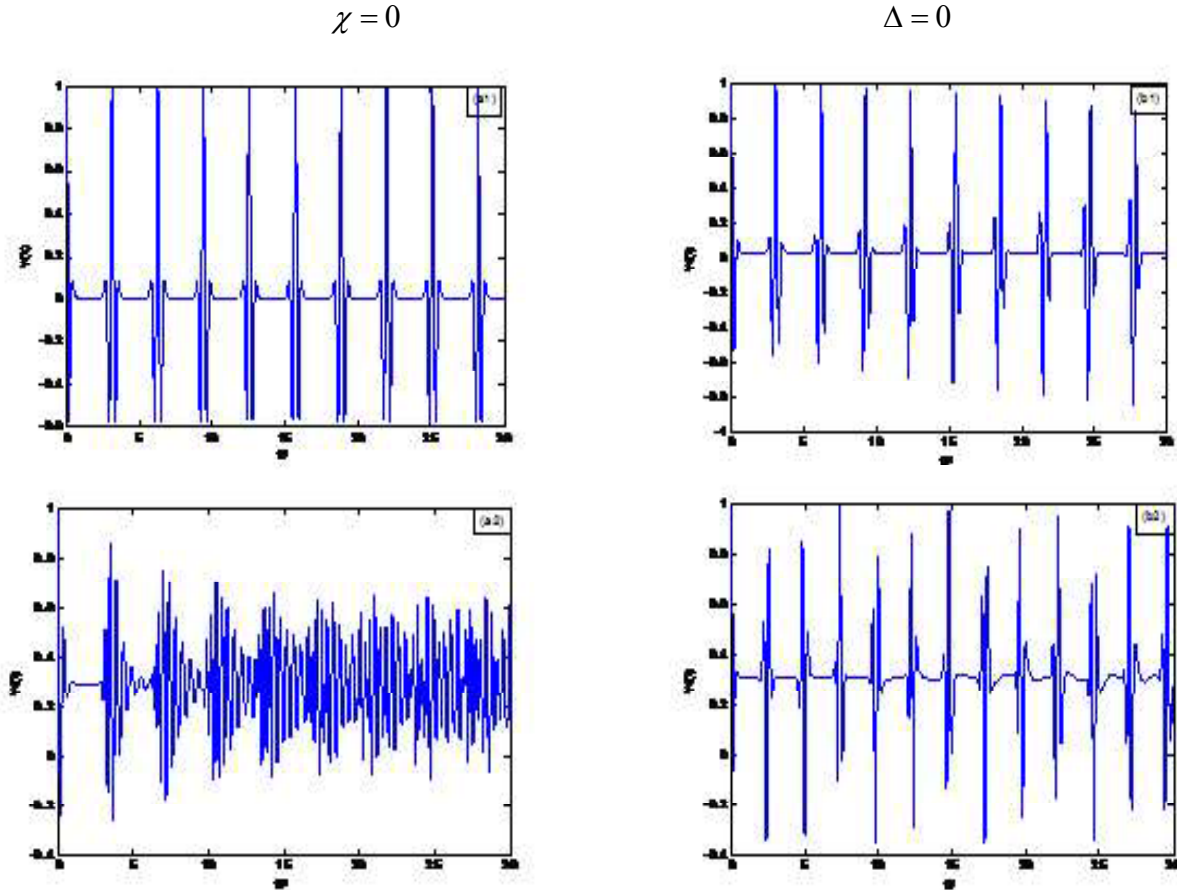


Fig. 1. Time evolutions of atomic inversion keeping $\bar{n} = 6$ for (a₁) $\Delta = 0, \chi = 0$ (a₂) $\Delta = 8g, \chi = 0$ (b₁) $\chi = 0.2g, \Delta = 0$ (b₂) $\chi = 0.8g, \Delta = 0$

Singh & Kumar: Exact dynamics for a two-level atom interacting with intensity dependent single-mode quantized cavity field in a Kerr medium

For $\bar{n} = 6, \chi = 0$ we obtain the revival times to be

$$t_R = \frac{\pi m}{g} \text{ giving}$$

$gt_R = 3.14, 6.28, 9.42, 12.56, 15.70 \text{ etc}$ as shown in Fig 1.(a₁). For $\chi = 0.2g$ Eq.(19) predicts the revivals at $gt_R = 3.078, 6.16, 9.24, 12.32, 15.4, 18.48, 21.56, 24.64..$ as also observed in Fig.1(b₂).

Strong nonlinear coupling can be defined as $\chi \gg g$, with $\bar{n} \gg 1$. In this case the expression for Rabi frequency can be written as

$$\Omega(\bar{n}) \approx 2\chi\bar{n} \left(1 + \frac{g^2}{2\chi^2} \right) \quad (20)$$

and the revivals are predicted to occur at

$$t_R = \frac{\left(\frac{\pi m}{\chi} \right)}{\left(1 + \frac{g^2}{2\chi^2} \right)} \quad (21)$$

For $\chi = 0.8g$, Eq.(21) predicts the revivals to occur at 2.20, 4.40, 6.61, 8.82 etc. This is also verified in Fig.1(b₂). From Fig.1 It is evident that detuning parameters affect the maximum values of inversion by bringing them down and elongate the revival time. In Fig.2 (a) and 2.(b) we plot the atomic inversion for the initial thermal field keeping $\chi = 0$ and $\chi = 0.2g$ respectively. For the thermal field the distribution function P_n is given

$$P_n = \frac{\langle n \rangle^n}{(1 + \langle n \rangle)^{n+1}}$$

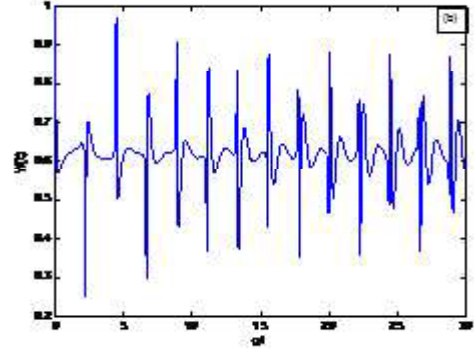
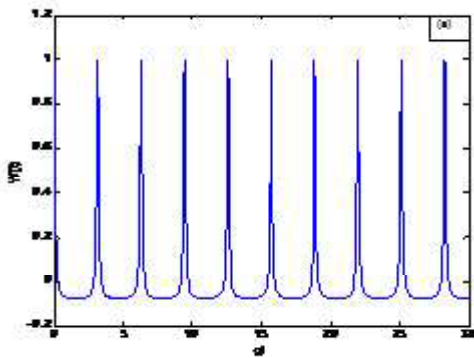


Fig. 2. Time evolutions of atomic inversion for the initial thermal field keeping $\bar{n} = 6$ for
(a) $\chi = 0$
(b) $\chi = 0.2$

Unlike JC model that shows a chaotic behaviour for the initial thermal field here we observe periodic revival and decay in Fig 2 (a) as well as in Fig 2 (b) and the linearity in the energy spectrum is maintained for the thermal field. Presence of kerr non linearity enhances the time averaged value of atomic inversion and decreases the revival time.

4. Mean number of photons in the modes

We study the time evolution of mean number of photons. The mean number of photons in the modes can be calculated as given below:

$$\langle \hat{a}^\dagger(t) \hat{a}(t) \rangle = \langle N(t) \rangle = \sum_{n=0}^{\infty} P_n(\bar{n}) |a_n|^2 + \sum_{n_1=0}^{\infty} \sum_{n_2=0}^{\infty} (n+1) P_n(\bar{n}) |b_{n+1}|^2 \quad (22)$$

$$\langle \hat{a}^\dagger(t) \hat{a}(t) \rangle = \bar{n} + \sum_{n=0}^{\infty} P_n(\bar{n}) |b_{n+1}|^2 \quad (23)$$

Fig. 3.(a) and 3.(b) depicts the time evolution of mean number of photons for the initial coherent field for $\chi = 0$ and $\chi = 0.2g$ respectively. We find that plots are similar to



Fig. 3. Time evolution of the mean number of photons for (a) $\bar{n} = 6$, $\chi = 0$ (b) $\bar{n} = 6$, $\chi = 0.2$.

that of atomic probabilities and the same strict periodicity in collapse revival of mean number of photons is observed as observed in case of atomic probabilities in Fig1(a₁) and Fig(b₁) respectively. This is so because the time evolution of mean number of photons and atomic probabilities are determined by the same harmonic time functions.

CONCLUSION

We have analyzed the dynamics of a two-level atom interacting with intensity dependent single mode field in a cavity filled with a Kerr-like medium. The atom-field system has been described by considering a generalization of the intensity dependent Jaynes-Cummings Model with additional nonlinear interaction term that describes the influence of the Kerr-like medium. Exact solutions using the method given by the first author were obtained¹³. The effect of detuning and Kerr non-linearity on atomic dynamics has also been analysed and we observe that the detuning and Kerr non-linearity have opposite effect on the revival time. Whereas presence of Kerr medium shortens the revival time detuning elongates it.

ACKNOWLEDGEMENT

The authors are thankful to the Head, University Dept. of Physics, Ranchi University, Ranchi for his all round motivation & support.

REFERENCES

1. Jaynes, E. T. and Cummings, F. W. 1963. Comparison of quantum and semiclassical radiation theories with application to the beam maser. *Proc. IEEE* 51:89–109.
2. Narozhny, N. B., Sanchez, J.J. and. Eberly, J.H. 1981. Coherence versus incoherence: Collapse and revival in a simple quantum model *Phys. Rev. A* 23:236.
3. Meystre, P. and Zubairy, M.S. 1982. Squeezed states in the Jaynes-Cummings model. *Physics Letters A*, A89:390.
4. Gerry, C. C. 1988. Two-photon Jaynes-Cummings model interacting with the squeezed Vacuum *Phys. Rev. A* 37: 2683.
5. Raimond, Roy, P., Gross, R. M., and Haroche, M. 1983. Observation of Cavity- Enhanced Single-Atom Spontaneous Emission. *Phys. Rev. Lett.* 50:1903.
6. Rempe, G., F. and Walther, H. and Klein, N. 1987. Observation of quantum collapse and revival in a one-atom maser. *Phys. Rev. Lett.* 26:353-356.
7. Rempe, G., Schmidt-Kaler, F. and Walther, H. 1990. Observation of sub-Poissonian photon statistics in a micromaser. *Phys. Rev. Lett.* 64:2783.
8. Buck, B. and Sukumar, C.V. 1981. Exactly soluble model of atom-phonon coupling showing periodic decay and revival. *Phys. Lett. A* 81:132-135.
9. Buck, B. and Sukumar, C. V. 1984. Some soluble models for periodic decay and revival. *J. Phys. A : Math. Gen.* 17:885-894.
10. Singh, S. 1982. Field statistics in some generalized Jaynes-Cummings models. *Phys. Rev. A* 25:3206.
11. Buzek, V. 1989. Jaynes-Cummings model with intensity- dependent coupling interacting with Holstein-Primakoff SU (1,1) coherent state., *Phys. Rev. A* 39:3196.
12. Sukumar, C.V. and Buck, B. 1981. Multi-phonon generalisation of the Jaynes- Cummings Model. *Physics Letters A* Vol. 83 pp.211-213.
13. Singh, Sudha. 2006. Unitary transformation method for solving generalized Jaynes-Cummings models. *Pramana journal of physics*, Volume 66: Issue 3, pp 615-620.
14. Gerry, C.C. and Knight, P.L. 2005. Introductory Quantum Optics. *Cambridge University Press*, pp-98.
15. Meystre, P. And and Sargent M III. 2003. Elements of Quantum Optics. *Springer- Verlag*, pp-294.



Optical phonon and collective charge fluctuation induced superconductivity in $\text{Mg}_{1-x}\text{Al}_x\text{B}_2$ and $\text{Mg}(\text{B}_{1-y}\text{C}_y)_2$

Roopam Sharma^a, Namita Singh^{a*}, Dinesh Varshney^b & R. Khenata^c

^aDepartment of Physics, Ranchi College, Ranchi University, Ranchi, Jharkhand, India

^bSchool of Physics, Vigyan Bhawan, Devi Ahilya University, Khandwa Road Campus, Indore, India

^cLaboratoire de Physique, Quantique et de Modélisation Mathématique (LPQ3M), Département de Technologie, Université de Mascara, 29000 Mascara, Algeria.

*Corresponding author : Phone : 9431140704 , E-mail : nams1420.ns@gmail.com

Abstract: In Al (C) doped MgB_2 , three square well model is used with three interactions namely, the coulomb, the electron-phonon and the electron-charge fluctuations. It is based on indirect-exchange Cooper pairing of electrons (quasiparticles) via adhoc attractive charge fluctuations apart from phonons. The relevant energy gap expressions in the formalism are solved imposing experimental constraints on their solution (critical temperature T_c and isotope effect- B^{10} replaced by B^{11}). The indirect-exchange formalism provides a unique set of electronic parameters [electron-phonon (I_{ph}^{ss}), electron-charge fluctuations (I_{pl}^{ss}), electron-electron (m^{ss}) and Coulomb screening parameter (m^{ss*})]. Moreover the addition of electron to $\text{Mg}_{1-x}\text{Al}_x\text{B}_2$ [$\text{Mg}(\text{B}_{1-y}\text{C}_y)_2$] through the partial substitution of C for B and Al for Mg results in the loss of superconductivity.

Paper History:

Received

12th May 2017

Revised

28th May 2017

Peer reviewed

10th June 2017

Accepted

22nd June 2017

Keywords: Energy gap equation, substitution effects, optical phonon, collective excitations, transition temperature.

INTRODUCTION

MgB_2 superconductor has highest value of transition temperature T_c . Al doping on the Mg site or C doping on B site results in decrease of T_c . Electron-phonon coupling strengths lead to two distinct superconducting gaps, with the σ band gap having the higher electron-phonon coupling and is a main contributor to the unusually high T_c .

Inelastic neutron scattering for MgB_2 shows an acoustic phonon of about 36 meV and highly dispersive optic branches peaked at 54, 78, 89, and 97 meV¹. Band structure studies identifies four important phonon modes: the E_{1u} (~ 41 meV) corresponds to in plane oscillation of both Mg and B ions, the out of plane oscillation of Mg and B ions is from A_{2u} (~ 50 meV), B_{1g} (~ 87 meV) describe a tilting out of plane oscillation of B ions, the E_{2g} (~ 67

meV), corresponds to in-plane B anharmonic oscillation^{2,3}. The phonon spectrum evidenced the strong coupling of the E_{2g} phonon to the carriers in the B plane^{4,5}. Raman spectra^{6,7} in $\text{Mg}_{1-x}\text{Al}_x\text{B}_2$ shows a sharp peak at around 941 cm^{-1} for the $x = 0.5$ sample, in contrast with the broadened Raman band for parent MgB_2 . On the other hand, C doping in the $\text{Mg}(\text{B}_{1-y}\text{C}_y)_2$ compound with concentrations $y > 0.04$, hardens E_{2g} mode at 580 cm^{-1} only moderately. The increased C doping directly impacts on the B layers, and identifies the competing effects of reduced electron-phonon coupling and increased disorder.

The isotope effect for both B and Mg⁸ shows that, although isotope exponent primarily points B phonons to be involved in superconductivity, the Mg phonons also have a little contribution to the overall pairing.

It has been shown that the anisotropy of electron-phonon interaction on the Fermi surface which consists of σ and π band as well as the anharmonicity of phonon modes yield the high superconducting transition temperature and multiple band structure. Moreover, T_c can be enhanced either by raising the phonon density of states on the σ sheets or by increasing the phonon cut-off frequency^{9,10,11}.

Energy gap equation and transition temperature:

In MgB_2 , boron atoms form honeycomb layers alternate with hexagonal layer of Mg atoms. The Mg atom donates two electrons to the B planes, and the ionic compound $\text{Mg}^{++}(\text{B}^-)_2$ results.

The temperature dependent gap equation is solved within the framework of two-particle mass centre, *Nambu-Eliashberg* approach^{12,13}

$$\Delta_k(\omega_n) = -T \sum_{k'', \omega_n'} V(k, k'; \omega_n, \omega_n') G_k'(\omega_n') G_{-k'}(-\omega_n') \Delta_{k'}(\omega_n') \quad (1)$$

The effective electron-electron interaction is represented as $V(k, k'; \omega_n, \omega_n')$. $G_k(\omega)$ is electron Green's function with momentum k and electron Matsubara frequency^{12,13} $\omega_n = (2n+1)\pi T$. In the potential scattering process, momentum is conserved, but the electron energy ω' are not conserved. At low temperatures ($T < T_c \cong 40$ K) the inelastic scattering in MgB_2 is significant. To solve the scattering problem for strong-scattering limit, all quantities depending on ω' in Eq. (1) are replaced by their averages over the surfaces of constant momentum.

Doping of Al and C in the parent MgB_2 causes disorderness and the electrons under the impurity potential manifests the weak localization effects on electron-phonon interaction.

With these the superconducting gap equation follows

$$\Delta_k^i = -\frac{1}{2} \sum_{k', \omega_n} \frac{V_{kk'}^i}{\sqrt{(\epsilon_{k'}^i)^2 + \Delta_{k'}^i}} \Delta_{k'}^i \tanh \left(\frac{\sqrt{(\epsilon_{k'}^i)^2 + \Delta_{k'}^i}}{2k_B T^i} \right) \quad (2)$$

$i = \pi \text{ or } \sigma \text{ band}$

Here, the interaction of superconductor is characterized by $V_{kk'}$, which physically yields the coupling strength for scattering an electron from k to k'

$$V_{kk} = -V_{ph}^i \text{ for } |\epsilon| < \omega_{ph} \\ = V_c^i \text{ for } \omega_{ph} < |\epsilon| < \epsilon_F \\ = -V_{pl}^i \text{ for } \epsilon_F < |\epsilon| < \omega_{pl} \\ = 0 \text{ otherwise} \quad (3)$$

$i = \pi \text{ or } \sigma \text{ band}$

The result is analysed for cases ω_{ph} corresponding to the Debye cut-off frequency for the phonon V_{ph}^i . The notations V_c^i and V_{pl}^i are the electron-phonon and electron-plasmon interaction respectively. The symbols ϵ_F is the Fermi energy and ω_{pl}^i is plasma frequency. It follows from the form of $V_{kk'}$ that the gap function is¹⁴

$$\epsilon_k^i = \begin{cases} \epsilon_0^i & \text{if } |\epsilon| < \omega_{ph} \\ \epsilon_1^i & \text{if } \omega_{ph} < |\epsilon| < \epsilon_F^i \\ \epsilon_2^i & \text{if } \epsilon_F^i < |\epsilon| < \omega_{pl}^i \\ 0 & \text{if } \omega_{pl}^i < |\epsilon| \end{cases} \quad (4)$$

$i = \pi \text{ or } \sigma \text{ band}$

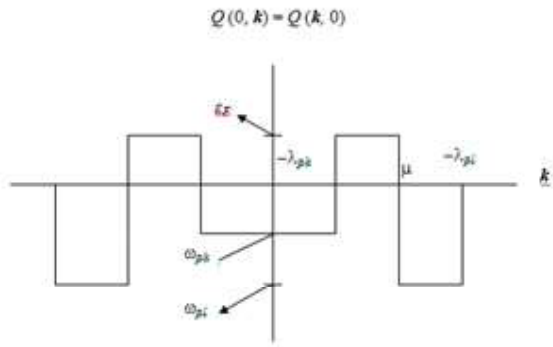


Figure 1. Schematic representation of three square well model $Q(k, k')$ as function of momentum.

Here, the coupling constant $\lambda^i = N^i(\epsilon_F) V^i$ with $N^i(\epsilon_F)$ is the electron density of states at the Fermi level. The product of the gap function Δ_k^i and the frequency range 'ph' and 'pl' of MgB_2 are replaced by square wells of half widths roughly equal to the cut-off energies ω_{ph} and ω_{pl}^i respectively (Figure 1). The coupling strengths λ_{ph}^i , μ^i and λ_{pl}^i with different cut-off energies ω_{ph} , ϵ_F and ω_{pl}^i influence the properties of MgB_2 . Using equation's (3) and (4) in equation (2) one obtains the following set of equation for Δ_0^i , Δ_1^i and Δ_2^i .

$$\left[1 + (-\lambda_{ph}^i + \mu^i - \lambda_{pl}^i)Z^i\right]\Delta^i_0 + (\mu^i - \lambda_{pl}^i)Z^i_2\Delta^i_1 - \lambda_{pl}^i\Delta^i_2Z^i_3 = 0 \quad i = \pi \text{ or } \sigma \text{ band}$$

Here, the effective coupling strength is defined as

$$\frac{1}{\lambda_{eff}^i} = \frac{1}{\lambda_{ph}^i - \lambda_{pl}^i} \quad (11)$$

$$(\mu^i - \lambda_{pl}^i)Z^i_1\Delta^i_0 + [1 + (\mu^i - \lambda_{pl}^i)Z^i_2] \Delta^i_1 - \lambda_{pl}^iZ^i_3\Delta^i_2 = 0$$

$i = \pi \text{ or } \sigma \text{ band}$

The renormalized coupling parameters are

$$\lambda_{pl}^i Z^i_1 \Delta^i_0 + \lambda_{pl}^i Z^i_2 \Delta^i_1 + (-1 + \lambda_{pl}^i Z^i_3) \Delta^i_2 = 0 \quad (12)$$

$i = \pi \text{ or } \sigma \text{ band}$

$i = \pi \text{ or } \sigma \text{ band}$

The notations in Eq.5 follow:

$$\begin{aligned} \lambda_{ph}^i &= N_F^i V_{ph}^i \\ \mu^i &= N_F^i V_c^i \\ \lambda_{pl}^i &= N_F^i V_{pl}^i \end{aligned} \quad (6)$$

$i = \pi \text{ or } \sigma \text{ band}$

and

$$\lambda_{pl}^{i*} = \frac{\lambda_{pl}^i}{1 - \lambda_{pl}^i \ln \left[\frac{\omega_{pl}^i}{\epsilon_F} \right]} \quad (13)$$

$i = \pi \text{ or } \sigma \text{ band}$

The Z integrals appearing in Eq. (5) are evaluated in the logarithmic approximation as

$$\begin{aligned} Z_1^i &= \ln(1.13\omega_{ph}/T_c) \\ Z_2^i &= \ln(\epsilon_F/\omega_{ph}) \\ Z_3^i &= \ln(\omega_{pl}/\epsilon_F) \end{aligned} \quad (7)$$

$i = \pi \text{ or } \sigma \text{ band}$

The superconducting transition temperature T_c is given by the condition that determinant of equation (5) equals to zero.

$$\begin{vmatrix} [1 - (\lambda_{ph}^i + \lambda_{pl}^i - \mu^i)Z_1^i] & (\mu^i - \lambda_{pl}^i)Z_2^i & -\lambda_{pl}^i Z_3^i \\ (\mu^i - \lambda_{pl}^i)Z_1^i & [1 - (\lambda_{pl}^i - \mu^i)Z_2^i] & -\lambda_{pl}^i Z_3^i \\ \lambda_{pl}^i Z_1^i & \lambda_{pl}^i Z_2^i & -1 + \lambda_{pl}^i Z_3^i \end{vmatrix} = 0 \quad (8)$$

$i = \pi \text{ or } \sigma \text{ band}$

Once determinant is evaluated, T_c^i , which is the transition temperature for which Eq. (8) is satisfied, is easily obtained. Eq. (8) reduces algebraically to

$$Z_1^i = \ln \left(\frac{1.13\omega_{ph}}{T_c^i} \right) \quad (9)$$

Rewriting Eq. (9) one finds,

$$T_c^i = 1.13\omega_{ph} \exp \left(-\frac{1}{\lambda_{eff}^i} \right) \quad (10)$$

It is seen that for the narrow band material as MgB_2 the ratio ω_{ph}/ϵ_F is small. The developed three square well model with two-well attractive-attractive version ($\omega_{pl}^i > \epsilon_F > \omega_{ph}^i$) provides an additional constraint for the ratio of characteristic frequency scales ϵ_F/ω_{ph} as $0 < Z_2^i = \ln[\epsilon_F/\omega_{ph}]$, and for the effective coupling constant $\lambda_{ph}^i + \lambda_{pl}^i - \mu^i < \lambda_{eff}^i < \infty$. It is worth commenting that the conventional BCS theory does not impose any constraint on the lower value for ω_{ph} and $\lambda^i - \mu^i > 0$.

Isotope effect exponent

Substitution of constituent elements by their isotopes results shift in T_c . This shift is defined as $\delta = 1 - 2\alpha$ with BCS isotope exponent α is one half. The relation of transition temperature and deviation in isotope exponent is $T_c \approx M^{-0.5(1-\delta)}$ and the mass dependence of phonon frequency as $\omega_{ph} \approx M^{-0.5}$. Since coupling strengths and screening parameter do not depend on the ionic mass M , the shift in isotope effect exponent is obtained from eq. (10) as $\delta = 1 + 2d\ln T_c/d\ln M$.

It is expressed as

$$\delta = 1 + 2 \left\{ \left[\frac{d \ln \omega_{ph}}{d \ln M} \right] - \left[\frac{1}{\lambda_{eff}} \frac{d \lambda_0}{d \ln M} \right] \right\} \quad (14)$$

$$= -\frac{2}{[\lambda_{ph} - \lambda_0]^2} \frac{d \lambda_0}{d \ln M} \quad (15)$$

Finally, the isotope effect exponent shift reduces algebraically to

$$\delta = \left[\frac{\lambda_0}{\lambda_{eff}} \right]^2 = \left[1 - \frac{\lambda_{ph}}{\lambda_{eff}} \right]^2 \quad (16)$$

Based on various coupling strengths, eq. (10) yields the transition temperature and deviation from isotope exponent for MgB_2 .

RESULTS & DISCUSSION

For the calculation more realistic values of some physical parameters are derived from the experimental data. The effective mass of the holes along the conducting boron

plane is obtained using the relation, $m^{\sigma*} = 3\hbar^2\gamma d/\pi k_B^2$. While estimating the effective mass, the interplanar distance $d = 3.525$ (3.338) [3.5164] Å is taken from the structural data^{15,16,17,18} and electronic specific heat coefficient $\gamma = 3.83$ (1.25) [2.8] mJ/mol/K² is taken from the heat capacity measurement^{16,17,18,19} for MgB_2 ($\text{Mg}_{0.5}\text{Al}_{0.5}\text{B}_2$) [$\text{Mg}(\text{B}_{0.9}\text{C}_{0.1})_2$], respectively. Doping dependence of these is further listed in Table 1. Askerzade *et al.* suggest¹⁹ that the effective mass ratio $m^{\sigma*}/m^{\pi*}$ is about 3. Hence, we write $m^{\pi*} = m_e$ for π band electrons. Dielectric constant in MgB_2 is $\epsilon_\infty \cong 3.5$ ²⁰. The obtained values of 3D (2D) plasmon frequency $\omega_{p\pi}$ ($\omega_{p\sigma}$) and the Fermi energy ϵ_F^π (ϵ_F^σ) are listed in Table 1.

Table 1. Estimated values of effective mass and electron parameters

Compounds	Effective mass $m^{\sigma*}$ (in units of m_e)	Effective mass $m^{\pi*}$ (in units of m_e)	Fermi energy (eV)		Plasmon frequency (meV)	
			ϵ_F^σ	ϵ_F^π	$\omega_{p\sigma}$	$\omega_{p\pi}$
MgB_2	3.0	1.0	0.63	2.9	3.25	8.79
$\text{Mg}_{0.9}\text{Al}_{0.1}\text{B}_2$	2.187	0.727	0.89	4.1	4.1	12.2
$\text{Mg}_{0.8}\text{Al}_{0.2}\text{B}_2$	2.16	0.72	0.92	4.2	4.3	12.4
$\text{Mg}_{0.7}\text{Al}_{0.3}\text{B}_2$	2.13	0.71	0.96	4.4	4.4	13.1
$\text{Mg}_{0.6}\text{Al}_{0.4}\text{B}_2$	2.07	0.667	1.01	4.8	4.5	13.6
$\text{Mg}_{0.5}\text{Al}_{0.5}\text{B}_2$	1.957	0.652	1.09	4.9	4.8	14.6
$\text{Mg}(\text{B}_{0.95}\text{C}_{0.05})_2$	2.6	0.867	0.74	3.36	3.6	10.1
$\text{Mg}(\text{B}_{0.925}\text{C}_{0.075})_2$	2.4	0.80	0.80	3.65	3.8	10.9
$\text{Mg}(\text{B}_{0.9}\text{C}_{0.1})_2$	2.2	0.733	0.87	3.99	4.1	11.9
$\text{Mg}(\text{B}_{0.875}\text{C}_{0.125})_2$	2.0	0.667	0.95	4.37	4.3	12.9

Table 2. Estimated values of parameters influencing superconducting state

Compound name	Electron-phonon coupling parameter		Renormalized Coulomb repulsive parameter		Energy gap (meV)		Transition temperature (K)	
	$\lambda_{ph}^{\sigma\sigma}$	$\lambda_{ph}^{\pi\pi}$	$\mu_{\sigma\sigma}^*$	$\mu_{\pi\pi}^*$	$\Delta_\sigma(0)$	$\Delta_\pi(0)$	T_c^σ	T_c^π
MgB_2	0.48	0.35	0.19	0.115	7.2	3.1	41.0	20.9
$\text{Mg}_{0.9}\text{Al}_{0.1}\text{B}_2$	0.43	0.30	0.171	0.102	5.6	2.4	33.0	16.4
$\text{Mg}_{0.8}\text{Al}_{0.2}\text{B}_2$	0.41	0.29	0.17	0.101	4.6	1.7	28.4	14.0
$\text{Mg}_{0.7}\text{Al}_{0.3}\text{B}_2$	0.40	0.26	0.169	0.101	3.8	0.87	23.73	7.8
$\text{Mg}_{0.6}\text{Al}_{0.4}\text{B}_2$	0.36	0.23	0.167	0.099	2.1	0.3	13.37	4.1
$\text{Mg}_{0.5}\text{Al}_{0.5}\text{B}_2$	0.30	0.18	0.164	0.098	0.26	0.05	3.7	0.54
$\text{Mg}(\text{B}_{0.95}\text{C}_{0.05})_2$	0.45	0.32	0.18	0.108	4.76	2.48	31.17	19.98
$\text{Mg}(\text{B}_{0.925}\text{C}_{0.075})_2$	0.42	0.30	0.175	0.105	4.05	1.97	26.52	16.25
$\text{Mg}(\text{B}_{0.9}\text{C}_{0.1})_2$	0.40	0.28	0.17	0.101	2.98	1.515	19.53	12.9
$\text{Mg}(\text{B}_{0.875}\text{C}_{0.125})_2$	0.35	0.20	0.164	0.97	1.46	0.19	9.58	9.92

Sharma *et al.*: Optical phonon and collective charge fluctuation induced superconductivity in $\text{Mg}_{1-x}\text{Al}_x\text{B}_2$ and $\text{Mg}(\text{B}_{1-y}\text{C}_y)_2$

Estimated values of parameters influencing superconducting state is shown in Table 2. In calculations, the dimensionless Coulomb pseudo-potential μ^* is reduced from μ and attributed to the scaling factor $\ln[\epsilon_F/\omega_{ph}]$ appeared in denominator of the expression of μ in Eq.(12). Thus in dealing with MgB_2 superconductors within the present three square well model, the repulsive strength entering in T_c equation is not μ but a renormalized pseudo-potential parameter μ^* by a factor $\ln[\epsilon_F/\omega_{ph}]$.

Mazin and co-workers²¹ report the values of coupling strength $\lambda_{\pi\pi} = 0.21$ and $\lambda_{\sigma\sigma} = 0.78$. Eliashberg formalism and Band structure calculations by Liu *et al.*²² leading to $\lambda_{\pi\pi} = 0.27$ and $\lambda_{\sigma\sigma} = 0.95$. The earlier calculated value of Eliashberg functions for two-band model are $\lambda_{\pi\pi} = 0.448$ and $\lambda_{\sigma\sigma} = 1.017$ (Golubov *et al.*)²³. The different intraband ($\sigma\sigma$ and $\pi\pi$) electron-phonon coupling strength for electron pairing with σ holes and π electrons causes different values of transition temperature. The calculations reveal that as

the Al(C) concentration increases, T_c decreases. Details are tabulated in Table 2 and are consistent with reported value^{24,25,26,27} for $\text{Mg}_{1-x}\text{Al}_x\text{B}_2$ and for $\text{Mg}(\text{B}_{1-y}\text{C}_y)_2$, respectively.

From Eq. (10), it is clear that T_c is strongly influenced by the Coulomb repulsive parameter and is higher for small values of μ . As the value of μ^* increases with increasing value of μ , all the repulsive excitations are predominant compared to the plasmon attractions. This results into suppressed values of T_c .

Figure 2 illustrates T_c as a function of the Al (C) concentration ($0 \leq x \leq 0.5$) ($0 \leq y \leq 0.125$).

In this figure, average result of $T_c(x)$ obtained from various sets of parameter is shown. It is seen that T_c decreases gradually with the increase of C(Al) concentration^{26,27} and giving rise to a decreasing trend of $x(y)$ with T_c . The above physical picture is evident from equation (12).

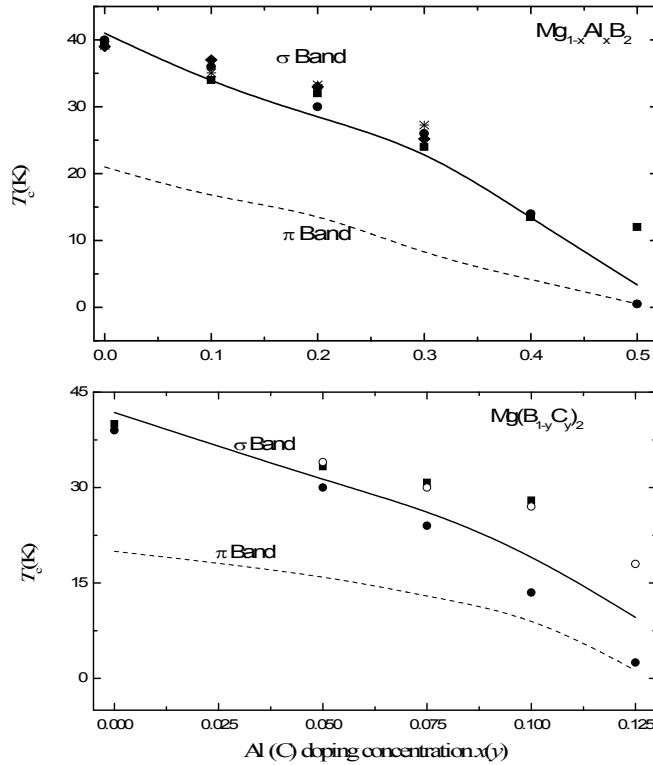


Figure 2 : Variation of Al [C] doping concentration (x) with transition temperature T_c in $\text{Mg}_{1-x}\text{Al}_x\text{B}_2$ [$\text{Mg}(\text{B}_{1-y}\text{C}_y)_2$]. For Al doping, closed circles are the theoretical data from Pena *et al.*²⁸, squares are the experimental data from Liu *et al.*²², diamonds are the experimental data from Park *et al.*²⁴, stars are the experimental data from Birajdar *et al.*²⁷. For C doping, closed circles are the experimental data from Lee *et al.*¹⁷, squares are the experimental data from Kazakov *et al.*¹⁸, open circles are the experimental data from Ummarino *et al.*²⁶.

The isotope effect exponent is given by $T_c \approx M^{0.5(1-\delta)}$, with $\delta = 1 - 2\alpha$ is the deviation from ideal isotope effect exponent. The ratio $\lambda_{eff}/\lambda_{ph}$ is about 1.1. From Equation (13) it is noted that when $\lambda_{eff}/\lambda_{ph}$ is much larger than 1.1, the obtained value of α is 0.4 which is consistent with reported value for the boron isotope effect (α_B). When $\lambda_{eff} \approx 1.1 \lambda_{ph}$, the one half value of α is obtained and when the ratio $\lambda_{eff}/\lambda_{ph}$ is much smaller than 1.1, the present approach explains the null isotope effect in MgB_2 which is consistent with the reported value of α_{Mg} . Thus the cooperative optical phonon-collective excitations model reveals the consistent explanation of observed isotope effect.

CONCLUSIONS

MgB_2 , $Mg_{1-x}Al_xB_2$ & $Mg(B_{1-x}C_x)_2$ are superconductors with ionic, covalent and metallic bonding. Using a three square well model, the attractive pairing mechanism for superconductivity arising from Coulomb interactions, is treated by high energy optical phonons and low energy collective excitations (plasmons). For superconductivity in parent and Al (C) doped MgB_2 , σ band is mainly responsible. A cooperative pairing mechanism is developed, where optical phonons and collective excitations both coexist. Since phonon mechanism alone is insufficient to show the superconducting and normal state, the model is related to physical parameters of the superconducting state, i.e. the transition temperature (T_c) and isotope effect exponent (α).

To account for high- T_c , a three square well model with Coulomb, electron-phonon and electron-plasmon interactions is formulated within the framework of Eliashberg theory^{12,13}, which essentially points to the relative contributions of the various interactions in yielding a high- T_c value in parent MgB_2 as well Al(C) doped MgB_2 . In this respect the dependence of T_c on various coupling strength parameters can be carefully studied and if collective excitations are essential candidate for high- T_c superconductivity then it follows: $\mu^* < \mu$, $\lambda_{ph} < \mu^*$ and $\lambda_{pl} < \lambda_{ph}$, μ^* . The present analysis reveals that T_c strongly depends on the Coulomb repulsive parameter and is higher for small values of μ .

The relevance of the model calculations with both Coulomb, as repulsive well and phonons (collective excitations), as attractive well is noticed from the fact that several experimental facts as concerned with the superconducting state turn out to be explained in this work.

REFERENCES

1. R Osborn, E A Goremychkin, A I Kolesnikov and D G Hinks (2001), "Phonon Density of States in MgB_2 " *Phys. Rev. Lett.* **87**, 017005, 1-4.
2. Dinesh Varshney, Swati Bhatnagar, Meenu Varshney and Namita Singh (2015), "Thermal conductivity of $Mg(B_{0.94}C_{0.06})_2$ superconductors: role of carrier and lattice-impurity Scattering", *Molecular simulation* **41**, 1466-1475.
3. Takahiro Muranaka and Jun Akimitsu, (2011) "Superconductivity in MgB_2 " *Z. Kristallogr.* **226**, 385-394.
4. N.D. Markovsky, J. A. Munoj, M. S. Lucas, Chen W. Li, O.Delaire, M. B. Stone, D. L.Abernathy and B. Fultz, (2011), "Nonharmonic phonons in MgB_2 at elevated temperatures", *Physical Review B* **83**, 174301, 1-7.
5. Jose A. Alarco, Peter C. Talbot and Ian D. R. Mackinnon, (2015), "Phonon anomalies predict superconducting T_c for AlB_2 -type structures", *Phys. Chem. Chem. Phys.*, **17** 25090-25099.
6. D A Tenne, X X Xi, A V Pogrebnnyakov and J M H Redwing, (2005), "Raman scattering in pure and carbon-doped MgB_2 films", *Phys. Rev. B* **71**, 132512, 1-4.
7. S Galambosi, J A Soinenen, A Mattila, S Huotari, S Manninen, Gy Vankó, N D Zhigadlo, J Karpinski, and K Hämäläinen, (2005), "Inelastic x-ray scattering study of collective electron excitations in MgB_2 " *Phys. Rev. B* **71**, 060504 (R), 1-4.
8. D G Hinks, H Claus and J D Jorgensen, (2001), "The complex nature of superconductivity in MgB_2 as revealed by the reduced total isotope effect", *Nature* **411**, 457-460.

9. C P Moca and B Janko, (2003), "Theory of strong electron-phonon superconductivity for MgB_2 in the framework of two-band model", *Physica C*, **387**, 122-130.
10. O V Dolgov, R K Kremer, J Kortus, A A Golubov and S V Shulga, (2005) "Thermodynamics of two-band superconductors: The case of MgB_2 ", *Phys. Rev. B*, **72**, 024504, 1-11
11. H. D. Yang, H. L. Liu, J. Y. Lin, M. X. Kuo, P. L. Ho, J. M. Chen, C. U. Jung, Min-Seok Park, and Sung-Ik Lee, (2003), "X-ray absorption and optical spectroscopy studies of $\text{Mg}_{1-x}\text{Al}_x\text{B}_2$ ", *Phys. Rev. B*, **68**, 092505, 1-4.
12. G M Eliashberg, (1960) , "Interactions between electrons and lattice vibrations in a Superconductor", *sov. Phys. JETP*, **11**, 966-976.
13. V Ivanov and Y Maruyama, (1995), "Disorder and phonon windows for superconductivity in doped fullerenes" *Physica-C*, **247**, 147-155.
14. Dinesh Varshney and M Nagar, (2007), "Optical phonon and collective charge fluctuation induced superconductivity of MgB_2 ", *Supercond. Sci. Technol.* **20**, 930-943.
15. J Nagamatsu, N Nakagawa, T Muranaka, Y Zenitani and J Akimitsu, (2001), "Superconductivity at 39 K in magnesium diboride" *Nature* **410**, 63-64.
16. M. Putti, C. Ferdeghini, M. Monni, I. Pallecchi, C. Tarantini, P. Manfrinetti, A. Palenzona, D. Daghero, R. S. Gonnelli, and V. A. Stepanov, (2005), "Critical field of Al-doped MgB_2 samples: Correlation with the suppression of the s-band gap", *Phys. Rev. B*, **71**, 144505, 1-6.
17. Sergey Lee, Takahiko Masui, Ayako Yamamoto, Hiroshi Uchiyama and Setsuko Tajima, (2004), "Crystal growth of C-doped MgB_2 superconductors: accidental doping and inhomogeneity", *Physica C*, **412-414**, 31-35.
18. S. M Kazakov, R Puzniak, K Rogacki, A. V Mironov, N. D Zhigadlo, J Jun, Ch Soltmann, B Batlogg and J Karpinski, (2005) "Carbon substitution in MgB_2 single crystals: Structural and superconducting properties" *Phys. Rev. B*, **71**, 024533, 1-10.
19. I N Askerzade, A Gencer, N Guclu and A kilic, (2002) "Two band Ginzburg-Landau theory for the lower critical field H_{c2} in MgB_2 ", *Supercond. Sc. and Technol* **15**, L13-L16.
20. V Zelezny, D Chvostova, L Pajasova, A Plecenik, P Kus and L Satrapinsky, (2003), "Infrared studies of superconducting MgB_2 thin films", *Physica C*, **388-389**, 129-130.
21. I I Mazin, O K Anderson, O Jepsen, A A Golubov, O V Dolgov and J Kortus, (2004), "Comment on First-principles calculation of the superconducting transition in MgB_2 within the anisotropic Eliashberg formalism" *Phys. Rev. B*, **69**, 056501, 1-3.
22. A Y Liu, I I Mazin and J Kortus, (2001) "Beyond Eliashberg Superconductivity in MgB_2 : Anharmonicity, Two-Phonon Scattering, and Multiple Gaps" *Phys. Rev. Lett.* **87**, 087005, 1-4.
23. Dinesh Varshney, M. S. Azad and R. K. Singh, (2004), "Superconducting transition temperature, isotope and pressure effect in MgB_2 : phonon and charge fluctuation-mediated pairing mechanism" *Supercond. Sci. Technol.* **17**, 1446-1457.
24. Min-Seok Park, Heon-Jung Kim, Byeongwon Kang and Sung-Ik Lee, (2005), "The upper critical field and two-gap nature in $\text{Mg}_{1-x}\text{Al}_x\text{B}_2$ " *Supercond. Sc. & Technol*, **18**, 183-186.
25. C. H. Cheng, Y. Zhao, X. T. Zhu, J. Nowotny, C. C. Sorrell, T. Finlayson and H. Zhang, (2003), "Chemical doping effect on the crystal structure and superconductivity of MgB_2 " *Physica C* **386**, 588-592.

26. **G. A Ummarino, D Daghero, R. S Gonnelli and A. H Moudden,(2005)**, “Carbon substitutions in MgB₂ within the two-band Eliashberg theory”, *Phys. Rev. B*, **71**, 134511,1-6.
27. **B. Birajdar, T. Wenzel, P. Manfrinetti, A. Palenzona, M. Putti and O. Eibl, (2005)**, “Al-alloyed MgB₂: correlation of superconducting properties, microstructure, and chemical composition” *Supercond. Sc. & Technol.* **18**, 572-581.
28. **O. de la Peña, A. Aguayo, and R. de Coss, (2002)**, “Effects of Al doping on the structural and electronic properties of Mg_{1-x}Al_xB₂” *Phys. Rev. B*, **66**, 012511,1-4.



Effect of dietary chitosan extracted from carapace of freshwater crab *Sartoriana spinigera* on food intake of Albino rats.

Shiny E.C. Kachhap* & Suhasini Besra

Department of Zoology, Ranchi University, Ranchi, Jharkhand, India

*Corresponding author : Phone : 8051188762 , E-mail : shiny.eliza89@gmail.com

Abstract: Chitosan, a biopolysaccharide comprising copolymers of glucosamine and N-acetyl glucosamine, has been shown to have anti-obesity properties that are directly related to satiety and lower food intake in animals fed with chitosan. This study was carried out to investigate the efficacy of chitosan extracted from carapace of freshwater crab *Sartoriana spinigera* on lowering of food intake by albino rats. 20 albino rats were randomly divided into 4 groups fed with different experimental diets: Group A-Basal diet, Group B-High fat diet, Group C-high fat diet+5% chitosan and Group D-High fat diet +5% hypolipidemic drug Ezetimibe. The experiment was conducted for 30 days. It was observed that average food intake in high fat diet group was highest i.e., 9.30±.50 g/day/rat and lowest in group C i.e. 7.30±.91 g/day/rat , 8.54 ± .34 g/day/rat in group A and 8.38 ±.76 g/day/rat in group D. Statistical analysis by Student's t- test showed that in group C, the food intake was significantly decreased at 0.1%,5% and 1% level with group B,D and A respectively ,indicating that chitosan extracted from freshwater crab *Sartoriana spinigera* decreases food intake and help fight obesity and its resultant diseases.

Paper History

Received

17th May 2017

Revised

22nd June 2017

Peer reviewed

29th June 2017

Accepted

5th July 2017

Keywords: Chitosan, *Sartoriana spinigera*, food intake, Student's t- test

INTRODUCTION

Obesity is a chronic disease characterized by accumulation of fat in adipocytes and directly or indirectly leads to various cardiovascular diseases, hypertension and non alcoholic fatty acid liver. Obesity is caused due to overconsumption of high calories of food, particularly high fat diet. Obesity is reported to increase the risk of premature mortality and to affect the quality of life, increasing the cost of healthcare greatly. Therefore, obesity is now considered a disease requiring treatment. Presently, the most effective method for weight loss is bariatric surgery but is associated with various surgical complications. Therefore, natural products are now being reported to help fight obesity. Presently, Zootherapy has become a potent treatment against various health problems. One such zootherapeutic medicine is chitosan. Chitosan, a cationic polysaccharide is produced by the N-deacetylation of chitin under alkaline conditions. It contains a linear sugar

backbone composed of β -1, 4-linked glucosamine units. Chitosan can be obtained by deacetylation of chitin which is found in the shells of invertebrates such as shrimp and crabs (Hirano,1996) and also found in exoskeleton of arthropods and certain fungi (Furda,1983). Several supplementation studies reported a lowering effect of chitosan on lipid absorption ,and lowering of food intake during supplementation. A decrease in food intake may help in decreasing obesity.

In the present study, chitosan has been extracted from a freshwater crab *Sartoriana spinigera* which is a local crab of Jharkhand and consumed not only as a local delicacy but is also of ethno medicinal significance as it is used by the tribals of Jharkhand against many health problems such as microbial infections, gastrointestinal disorders and arthritis.

The aim of this experiment was to determine if dietary chitosan extracted from carapace of freshwater crab *Sartoriana spinigera* could reduce food intake in albino

rats and comparing the efficacy of this effect with hypolipidemic drug Ezetimibe.

MATERIALS & METHODS

Extraction of chitosan

The method of Takiguchi M.(1991) was selected from other methods for extraction of chitosan using minimum chemicals. The 3 processes that involved extraction of chitosan was done as follows-

1. Demineralization- The carapace of *Sartoriana spinigera* was obtained and dried at 60°C until a constant weight was obtained. It was then crushed with motor and pestle to obtain a fine powder. The powder was then soaked in 2N HCl in a beaker for 24 hours with constant stirring. The substance obtained was filtered with filter paper and the residue obtained was washed with distilled water 2-3 times to obtain a constant pH of 7. It was dried again.

2. Deproteinization- The powder was then boiled in 300 ml of 1N NaOH at 80°C-100°C for 24 hours. It was then washed with deionized water and filtered. The residue obtained was again dried into dry powder form. The powder thus obtained was chitin.

3. Deacetylation- Chitin powder was soaked in 300 ml of 50% NaOH and heated in hot water bath at 100°C for 18 hours with 3 intervals. After every 6 hours, NaOH was replaced by fresh quantity and the residue was washed

with distilled water each time. The residue obtained finally was dried and weighed. The powder obtained was Chitosan.

EXPERIMENTAL DESIGN

Animals and diet:

20 albino rats, each measuring about 80 grams were purchased from local rearing laboratory. Rats were divided into 4 groups (A,B,C and D) and housed in metallic cages under healthy condition. Rats were maintained at room temperature. There was 12 hours daytime light between 6AM to 6PM and 12 hours of dark. Water and basal diet were provided *ad-libitum* for 3 days as acclimatization period. Experimental diet was given for 30 days. 10 g of food was given to each rats of all groups at 9 a.m and 9 p.m .On 1st,3rd,5th,7th,14th,21st and 30th day, leftover food was collected at 8 a.m and 8 p.m out of food given and weighed .

4 groups of rats were fed with following experimental diets following Kumar.V *et al* (1999)

Group A-basal diet

Group B-high fat diet

Group C-high fat diet + 5%chitosan

Group D-high fat diet+ 5% hypolipidemic drug (ezetimibe)

Table 1: composition of experimental diet

Component	GROUP A Basal diet g/1000g	GROUP B High fat diet g/1000g	GROUP C High fat diet + chitosan g/1000g	GROUP D High fat diet + Ezetimibe g/1000g
Casein	215	147	147	147
Gram + wheat + maize	450	306.6	306.6	306.6
Sucrose	200	140	140	140
Soyabean oil	50	15	15	15
Vitamin + mineral mixture	35	35	35	35
Cellulose	50	50	-	-
Chitosan	-	-	50	-
Hypolipidemic drug	-	-	-	50
Cholesterol	-	5	5	5
Deoxycholic acid	-	2	2	2
Coconut oil	-	300	300	300

Kachhap & Besra: Effect of dietary chitosan extracted from carapace of freshwater crab *Sartoriana spinigera* on food intake of Albino rats.

Calculation of food intake:-

Total food consumed (g) = Total food given (g) - total leftover food (g).

Statistical analysis

The variability of the results was expressed as mean \pm standard deviation. The significance of the differences between mean values of different groups was determined using Student's t- test.

RESULTS & DISCUSSION

Table 2 showed the effect of chitosan extracted from *Sartoriana spinigera* on reduction in food intake by albino rats in an experiment of 30 days. Water was given *ad libitum* and 10 g of food was given to each rat of all 4 groups. Table 2 showed the average food consumed was $8.54 \pm .34$ g/day/rat, $9.30 \pm .50$ g/day/rat, $7.37 \pm .91$ g/day/rat and $8.38 \pm .76$ g/day/rat in group A, B, C and D respectively. Group B fed with high fat diet showed highest food intake whereas lowest food intake was recorded in group C that was fed with high fat diet and 5% chitosan.

Table 3: Statistical analysis showed that chitosan was able to decrease food intake than group A fed with basal diet at 1% significance level indicating that chitosan can decrease food intake level even in rat fed with normal diet. Statistical analysis also showed that in group C, food intake was significantly decreased at 5 % level than group D, indicating that chitosan is more potent agent for decreasing food intake and thereby reducing obesity than commercially used hypolipidemic drug. Group C fed with HFD and chitosan decreased food intake than group B at 0.1%

significance level, indicating that chitosan was able to cause satiety in the rats causing least amount of food intake. This result corroborates with the experiment conducted by Walsh *et al* (2013), according to which 1200 ppm chitosan decreased dietary intake, which was associated with increased serum leptin concentrations and decreased CRP concentration. High concentration of leptin in blood indicates that lipid and energy store in the body is higher and that the food intake should be reduced. But contrary results were reported by Mohamed M.M (2011) according to which chitosan significantly reduced serum level of leptin.

A number of in vitro studies have demonstrated by Gades M.D and Stern J.S. (2003) and Zeng L *et al* (1998), according to them chitosan dissolves in the stomach, emulsifying fat and forming a gel, which binds with the fat in the intestine, therefore interfering with the absorption of fat in the intestine. This leads to a sense of stomach fullness in animals thereby consuming lesser food. Chitosan is strictly not a dietary fibre, because it does not have a vegetable origin, but it does have the same chemical and physiological properties as have vegetable fibres. (Sumiyoshi, M., and Kimura, Y.,2006)

Obesity is associated with both increased local adipose and more generalized systemic inflammation (Berg A.H. and Scherer P.E.,2005). Walsh *et al* (2013) also observed that CRP is a sensitive marker of inflammation and that chitosan was able to decrease serum CRP concentration thereby decreasing body weight and lower food intake.

Table 2:- Effect of basal diet, high fat diet, chitosan and hypolipidemic drug on food intake(g/day/rat)

Experimental diets	Weight of food consumed (g/day/rat)							
	1 st day (g/day/rat)	3 rd day (g/day/rat)	5 th day (g/day/rat)	7 th day (g/day/rat)	14 th day (g/day/rat)	21 st day (g/day/rat)	30 th day (g/day/rat)	Average (g/day/rat)
Group A Basal diet	8.56	8.55	8.78	8.00	9.10	8.34	8.51	$8.54 \pm .34$
Group B High fat diet(HFD)	10	10	9.70	9.00	9.26	9.04	8.80	$9.30 \pm .50$
Group C High fat diet+ 5%chitosan	8.86	8.85	7.27	7.10	6.80	7.00	7.20	$7.30 \pm .91$
Group D High fat diet +5% Ezetimibe	8.82	8.80	8.55	8.24	8.10	8.12	8.50	$8.38 \pm .76$

Table 3:-Statistical analysis of food intake of different experimental groups.

Experimental group	Average Weight of food consumed (g/day/rat)
Group A vs Group B	8.54±.34**
	9.30±.50
Group B vs Group C	9.30±.50
	7.37±.91***
Group C vs Group D	7.37±.91*
	8.38±.76
Group A vs Group C	8.54±.34
	7.37±.91**

*=5% level of significance, **= 1% level of significance, ***=0.1% level of significance

CONCLUSION

Food intake is a form of behavior that is subject to conscious control. Practical data shows that many obese and weight gaining individuals claim that eating is out of their control. Therefore, there is requirement of biological and environmental forces that could help control food intake. Chitosan extracted from freshwater crab *Sartoriana spinigera* is one such factor that can cause reduction in food consumption, thereby decreasing obesity in people and its resultant diseases. Use of chitosan from a freshwater crab will not only acknowledge the society about its importance but will also enhance its economic importance and will be an encouragement for the farmers to culture *Sartoriana spinigera*.

ACKNOWLEDGEMENT

Authors are thankful to Head, University Department of Zoology, Ranchi University, Ranchi for providing all laboratory facilities & support.

REFERENCES

- Hirano, S., (1996):** Chitin biotechnology applications. *Biotechnol A Rev.*, 2:237-258
- Furda, I., (1983):** Aminopolysaccharides-their potential as dietary fibre. In: Unconventional sources of Dietary fiber (Furda, I., ed.). *ACS Symposium series.*, 214:105-22
- Takiguchi, Y., (1991):** Preparation of chitosan and partially deacetylated chitin. In: *A Otake and M. Yabuki (eds.), Chitin, Chitosan Jikken Manual chapter-2, Gihodou Shupan Kaisha, Japan*, 9-17.
- Kumar V., Singh, P., Chander, R., Mahdi, F., Singh, S., Singh, R., Khanna, A.K., Saxena J.K., Mahdi A.A., Singh, V.K., Singh, R.K., (2009):** Hypolipidemic activity of *Hibiscus rosasinensis* rott in rats. *Indian Journal of Biochemistry and biophysics*, vol 46, December 2009, pp 507-510
- Walsh, A.M., Sweeney, T., Bahar, B., O'Doherty J.V., (2013):** Multi-functional role of chitosan as a potential protective agent against obesity. *PLoS ONE* 8(1): e53828. doi:10.1371/Journal.pone.0053828
- Mohamed, M.M., (2011):** Effects of chitosan and wheat bran on serum leptin, TNF- α , Lipid profile and oxidative status in animal model on non alcoholic fatty liver. *Australian Journal of basic and applied sciences*, 5(10):1478-1488, 2011
- Gades, M.D., Stern J.S. (2003):** Chitosan supplementation and fecal fat excretion in men. *Obesity* 11:683-688
- Zeng, L., Qin C., Wang, W., Chi, W., Li, W., (2008):** absorption and distribution of chitosan in mice after oral administration. *J Carbohydr Polym* 71:435-440
- Sumiyoshi, M., and Kimura, Y. (2006):** Low molecular weight chitosan inhibits obesity induced by feeding a high fat diet long term in mice. *J Pharm Pharmacol* 58:201-207
- Berg, A.H., and Scherer, P.E., (2005):** Adipose tissue, inflammation, and cardiovascular disease. *Nature* 444:875-880



Biochemical composition of leg muscle of freshwater edible crab *Sartoriana spinigera* with special reference to glucose

Kumari Neetu* & Suhasini Besra

Department of Zoology, Ranchi University, Ranchi, Jharkhand, India

*Corresponding author : Phone : 8969497075 , E-mail : kneetu121@gmail.com

Abstract:- Present study deals with estimation of Glucose in the leg muscle of the freshwater edible crab *Sartoriana spinigera*. The result showed the value of average glucose concentration in leg muscle of freshwater crab *S. spinigera* of various weight group (23 – 53.9 g) was 0.1313 ± 0.0130 mg/100mg of muscle and showed a negative correlation between body weight and tissue glucose concentration ($b = -0.000287$, $r = -0.379$, $y = -0.00029x + 0.14246$). The results are plotted and discussed in detail.

Paper History

Received

11th April 2017

Revised

9th May 2017

Peer reviewed

20th May 2017

Accepted

6th June 2017

Keywords: *S. spinigera*, Muscle extract, Glucose content, Correlation coefficient.

INTRODUCTION

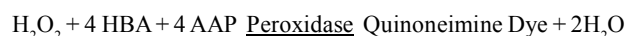
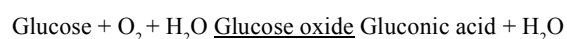
The freshwater crabs are good source of food and medicinal values and are an important role in the food chain of aquatic ecosystems^{1,2}. Recently there is a growing interest for estimating the biochemical components of edible muscle of freshwater crabs which are used as a superb source of high quality nutrients due to its content of essential amino acids, proteins, unsaturated fatty acids, carbohydrate, fat and minerals^{3,4,5}.

Carbohydrate is considered to be the first among the organic nutrients to be utilized to generate required energy⁶. They serve as precursor for the dispensable amino acids and some nutrients, which are metabolic intermediates necessary for growth⁷. *Sartoriana spinigera* an edible freshwater crab which is abundantly found in Jharkhand are regarded as indicator organism and are a potential biological tool for assessing the health of a particular ecosystem. Since little work has been done in the biochemical composition of the freshwater crab,

S. spinigera, the present study was undertaken to estimate the glucose content in the muscle of this freshwater crab, to evaluate its nutritional value.

MATERIALS & METHODS

Live specimens of freshwater crab *S. spinigera* of different weight groups were collected from Patrattu dam brought to Zoology Department Laboratory of Ranchi University. The crabs were then allowed to get acclimatized in the laboratory condition, weighed and leg muscles were taken out and blotted dry with blotting paper and 100 mg of it was homogenized in 1ml of 10% TCA and centrifuged at 2500 rpm for 10 minutes. The glucose analysis was done with the help of glucose kit using Trinder⁸ method as follows:-



4AAP : 4—Amino antipyrine

4 HBA : 4 ———Hydroxy Benzoic Acid

The intensity of pink colour formed is proportional to the glucose concentration. Glucose level was determined with commercially available kit using photometrically between 500 to 540 nm with the help of colorimeter.

Statistical Analysis

Statistical analysis was done to calculate correlation coefficient to show relationship between body weight and glucose concentration in crabs meat.

Table 1- Estimated value muscle Glucose concentration (mg/100mg) in different Weight group of Adult Crabs, *S.spinigera*

Sl.No.	Body Weight (g)	Concentration (mg/100mg)
1	23	0.135
2	30.6	0.132
3	39.4	0.121
4	39.52	0.1419
5	45.75	0.136
6	53.9	0.122
	Mean	0.1313
	Sd	0.0130
	r	-0.379

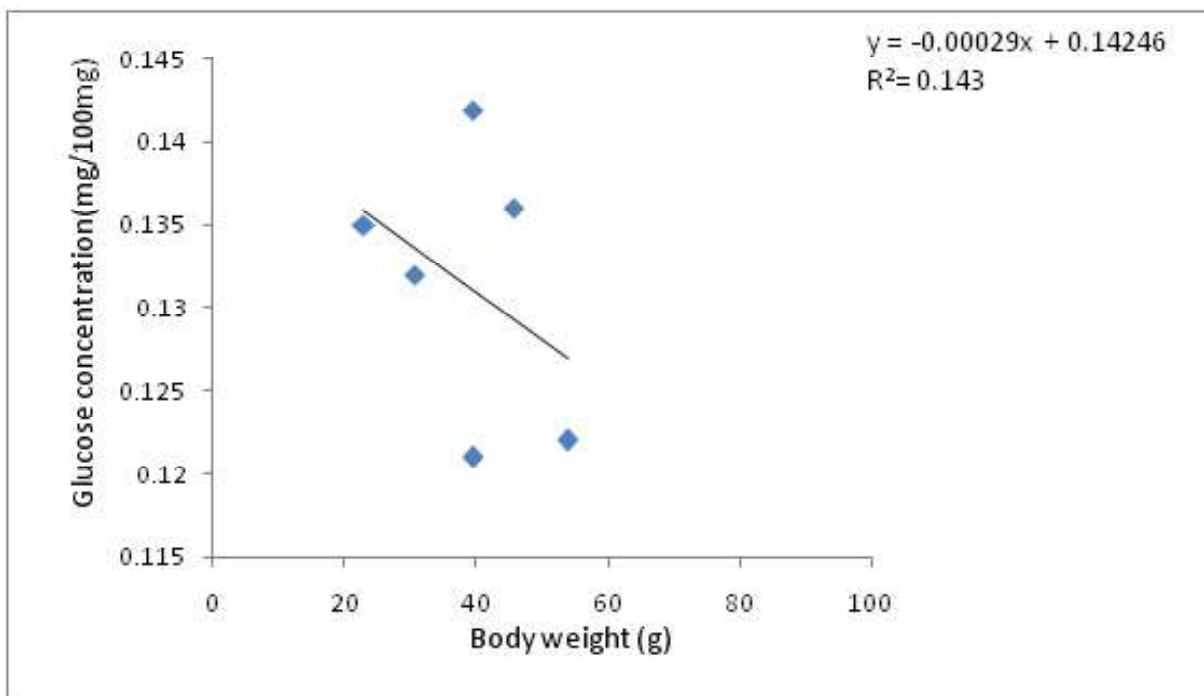


Fig I : Correlation between Body Weight (g) Vs muscle Glucose Concentration (mg/100mg) in different weight groups of Adult Crabs, *S. spinigera*

Kumari & Besra: Biochemical composition of leg muscle of freshwater edible crab *Sartoriana spinigera* with special reference to glucose

RESULTS & DISCUSSION

Table I showed the glucose concentration in the muscle of crab's chelate leg of various weight groups (23 – 53.9 g), Average glucose concentration was 0.1313 ± 0.0130 mg/100mg of wet muscle.

Fig.I showed a negative correlation between body weight and tissue glucose concentration. As the body weight increased glucose concentration decreased with a slope of $b = -0.00028$, $r = -0.379$, $y = -0.00029x + 0.14246$ but this correlation was not significant as the $r = -0.379$.

It has been reported by Babu⁹ that *Scylla serrata* meat contained 2.7% of carbohydrate but in crab, *Chionoecetes opilio* contained negligible amount of carbohydrate i.e. leg and claw meat contained only 0.075% and body meat contained 0.054% of carbohydrate. This finding corroborates the present observation that in case of *S.spinigera* glucose concentration was only $0.1313 \pm 0.0130\%$. Babu⁹ also studied the biochemical composition of the muscles and hepatopancreas in various stages of molting in the crab, *Menippe rumphii* and reported that the animal stores its reserve food materials in the hepatopancreas to a greater extent and in the muscle to a lesser extent during the intermolt period.

Vinagre¹⁰ studied the seasonal variation of energy metabolism in ghost crab, *Ocypode quadrate* and reported that the claw muscle glycogen remained constant in muscle gonads and gills in males, but in females muscle glycogen increased in spring and gonad glycogen decreased in the summer.

In crab, lipids seem to be an important reserve of energy used during reproduction for vitellogenesis in female crab, while glycogen may be used during periods of intense activity or fasting.

Zafar¹¹ studied the biochemical composition in *Scylla serrata* and reported that the highest carbohydrate content was recorded in the male crab during May (0.92%) and in the female crab during September (1.29 %) in the year. He also reported that carbohydrate content varied from 0.31 – 0.92 % in male and 0.29 – 1.29 % in female crab.

Zaitsev¹² found 0.30 to 1.10 % glycogen in the crab meat. Khan¹³ reported 0.13% carbohydrate in the male and 0.86% in female body meat of *S. serrata*.

Srinivasagam¹⁴ studied the nutritive values of the meat of Portunid crabs and observed 0.15 to 0.17 % carbohydrates in *S. serrata*. This observation corroborates the present observation. He also reported that carbohydrate content showed negative correlation with body weight both in male and female *S. serrata* ($r = -0.946$; $t = 9.183$; $df = 10$; $p = 0.0001$) and ($r = -0.850$, $t = 5.092$; $df = 10$; $p = 0.0005$).

The above observation and discussion may be concluded that leg muscle contained meagre amount of glucose and fat which increases its nutritional value.

ACKNOWLEDGEMENT

Authors are thankful to Head, University Department of Zoology, Ranchi University, Ranchi for providing all laboratory facilities.

REFERENCES

1. Cobb BF, Conte FS, Edwards MA (1975). Free Amino Acids and Osmoregulation in Penaeid Shrimp. J Agric Food Chem 23:1172-1174
2. Fang LS, Tang CK, Lee DL, Chen IM (1992). Free Amino Acid Composition in Muscle and Hemolymph of the Prawn *Penaeus Monodon* in Different Salinities. Nippon Suisan Gakkaishi. 58: 1095-1102
3. Adeyeye EI (2002). Determination of the Chemical Composition of the Nutritionally Valuable Parts of Male and Female Common West African Fresh Water Crab *Sudananautes Africanus Africanus*. Int J Food Sci Nut 53: 189-196
4. Celik M, Tureli C, Celik M, Yanar Y, Erdem U, Kucukgulmez A (2004). Fatty Acid Composition of the Blue Crab (*Callinectes sapidus*) in the North Eastern Mediterranean. Food Chem 88: 271-273.
5. Musaiger AO, Al-Rumaidh MJ (2005). Proximate and Mineral Composition of Crab Meat Consumed in Bahrain. Int J Food Sci Nutr 56:231-5
6. Heath, A.G (1987). Water pollution and fish physiology. (Chap. 5), Physiological Energetic (pp. 131-163). CRC Press, Boca Raton, FL.
7. NRC (National Research Council) (1993). Nutrient requirements of fish, Committee on Animal Nutrition.

- Board on Agriculture. National Research Council. National Academy Press. Washington DC, USA pp. 114.
8. **Trinder, P. (1969).** Annals. Clin. Bio Chem. 6, 24.
 9. **BABU, D. Erri (1984).** Biochemical composition of the muscles and hepatopancreas in various stages of moulting in the crab, *Menippe rumphii* (Fabricius). Indian J Comp. Anim. Physiol. Vol 2 No.1 July pp 64-71.
 10. **Vinagre, A.S., Amaral, A.P., Ribarcki, F.P., Silveira, E.F., Perico, E (2007).** Seasonal variation of energy metabolism in ghost crab *Ocypode quadrata* at Siriu Beach (Brazil). Comparative Biochemistry and Physiology, Part A 146, 514-519.
 11. **Zafar, M., Siddiqui, M.Z.H. & Hoque, M.A (2004).** Biochemical composition in *Scylla serrata* (Forsk.) of Chakaria, Sundarban area, Bangladesh. *Pakistan J. Bio. Sci.* 7(12) 2182-2186
 12. **Zaitsev, V., I.Kizevette, L.lagunoy and T.Makarov (1969).** Fish Curing and Processing. MIR Publishers, Moscow, pp.280.
 13. **Khan, P. A (1992).** Biochemical composition, minerals (calcium and iron) and chitin content of two portunid crabs *Scylla serrata* Forskal and *Portunus pelagicus* linnaeus available in and around the coastal regions of Bangladesh. M.Sc. Thesis, Institute of Marine Sciences, Chittagong University, pp: 112.
 14. **Srinivasagam, S (1979).** On the nutritive values of the meat of Portunid crabs. J. Inland Fish Soc. India, 11:128-131.



Biochemical properties of stress secretion of freshwater snail *Bellamya bengalensis* (Jousseau, 1886) with reference to body size.

Kanchan* & Suhasini Besra

Department of Zoology, Ranchi University, Ranchi, Jharkhand, India

*Corresponding author : Phone : 9334523737 , E-mail : kanusri121@gmail.com

Abstract- Freshwater edible snail *Bellamya bengalensis* has potential nutritional as well as medicinal importance. In present work the concentration of total protein, glucose in stress secretion of *B. bengalensis* of different shell size (1-2cm and 2-3.5cm) were analysed. The investigation results have shown that the concentration of the protein in larger size snail (2-3.5cm) was 3.9 ± 0.22 g/dl and in smaller size snail (1-2cm) was 2.6 ± 0.1 g/dl. The concentration of glucose in larger size snail (2-3.5cm) 10.8 ± 1.5 mg/dl and in smaller size snail (1-2cm) was 7.3 ± 0.84 mg/dl in the stress secretion of snails. Statistical analysis were calculated by using student's t-test, it revealed that both protein and glucose concentration were significantly higher in larger snail group at 0.1% level ($p < 0.001$).

Paper History

Received

10th May 2017

Revised

22nd May 2017

Peer reviewed

9th June 2017

Accepted

15th June 2017

Keywords- *Bellamya bengalensis*, Snail stress secretion, Glucose, Protein, Student's t - test

INTRODUCTION

The freshwater edible snail *B. bengalensis* is abundantly found in all types of temporary and permanent water bodies of Jharkhand. Many people belonging under different economic classes of tribal community of Jharkhand depend on *B. bengalensis* since an immemorial time. People consume *B. bengalensis* as their food intake for not only its cheap rate and better taste but also its great nutritional as well as its medicinal value. Especially people suffering with anaemia, malformation of bone structure, treatment of eye problems, consume its meat and soup with belief to restore their health.

People strongly believe about the function of *B. bengalensis* which can cure several diseases such as controlling conjunctivitis, night blindness, diarrhoea, stomach disorder, arthritis, joint pain, rheumatism cardiac diseases controlling blood pressure, asthma, rickets (calcium metabolism) nervousness and giddiness etc. *B. bengalensis*, the common banded pond snail of India was described by Annandale. N. et al¹ and also by Sewell.

et al², who studied the ecology and growth rate of snail. According to P. Srivastava. et al³ it breeds throughout year reaching its peak during April to July. Many works have been done on the reproduction and biochemical studies of some freshwater snail muscle such as *Lymnaea acuminata*. Recently Ethnomedicinal importance of *B. bengalensis* was estimated in terms of analysis of its protein and amino acid composition by Debojit. et al⁴ and also studied proximate fatty acid composition of *B. bengalensis*. The secretion secreted by snails have a powerful antioxidants which protect them from an atmosphere full of oxygen radicals.

It can also enhance the proliferation and functional capability of fibroblast cell. Fibroblasts are responsible for generating all the elements of the skin matrix, including collagen, elastin fibres, glycosaminoglycans and proteoglycans. It provides firmness, strength, suppleness and elasticity for the skin by containing water.

The bodies of snails are characterised by rich mucus which covers their surface. Apparently, the mucus may

serve in preventing the moisture evaporation and it helps in smooth movements by Simkiss and Wilbur⁵. It also protect the body from mechanical injuries. Mucus and stress secretion have antibacterial properties against many pathogenic bacteria. In addition sum unknown biochemical functions may be involved in the stress secretion, though nothing has been reported so far with this respect. Snails are fairly resistant to infection by microorganisms. So, present studies have been done to estimate biochemical composition such as protein and glucose of stress secretion between two sized snails.

MATERIALS & METHODS

Collection of Sample and extraction of secretion:

Snail *B. bengalensis* were purchased from Ranchi market and brought to P.G .Department of Zoology laboratory,

and collected sample were kept in aquarium under laboratory condition. They were thoroughly cleaned with cleaned napkin to remove all the sand and debris on the shell.

The protein content of secretion was done by Biuret method of Henry *et al*⁶, 10µl of secretion was added in 1ml Biuret reagent and left for 10 minutes at room temperature. Violet coloured appeared. Absorbance was read in colorimeter at 540 nm wavelength against blank.

While glucose content was determined by GOD-POD (Colorimetric) method of Trinder.P.⁷, 10µl of secretion mix with 1ml reagent and left for 1 hour at room temperature. Cherry red coloured turned and absorbance was read the extinction at 520 nm against blank.

RESULT

Table1: Protein concentration (g/dL) of stress secretion in different size of *Bellamya bengalensis*.

Snail Size(cm)	Protein concentration (g/dL) (↓)	Av. Concentration of protein (g/dL)	Value of t-test
2-3.5	4.2 4.0 3.5 3.9 4.1 4.1 3.8 3.9 3.6 4.0	3.9±0.22	7.6***
1-2	2.6 2.5 2.5 2.7 2.6 2.9 2.6 2.6 2.8 2.7	2.6±0.1	

***=P<0.001, significant at 0.1%

Table 2: Glucose concentration (mg/dL) of stress secretion in different size of *Bellamya bengalensis*.

Snail Size(cm)	Glucose concentration (mg/dL)	Av. Concentration glucose (mg/dL)	Value of t-test
2-3.5	11.0	10.8±1.5	6.25***
	10.0		
	10.0		
	10.5		
	11.0		
	10.5		
	10.0		
	12.0		
	12.0		
	11.0		
1-2	7.0	7.3±0.84	
	6.0		
	6.2		
	6.3		
	7.0		
	7.1		
	6.2		
	6.8		
	6.7		
	7.0		

***=P<0.001, Significant at 0.1%

DISCUSSION

Table 1, showed that larger sized snail had more protein content (3.9±0.22 g/dl) than smaller size snail (2.6±0.1 g/dl). When these values were statistically analysed with t-test it was observed that larger size snail had significantly higher protein concentration at 0.1% level (P<0.001). In table 2, Glucose concentration of secretion showed that in larger size snail had more glucose concentration (10.8±1.5 mg/dl) than smaller size snail (7.3±0.84 mg/dl). When these values were statistically analysed it was observed that larger sized snail had more significantly higher concentration of glucose 0.1% level (P<0.001). It indicated that protein and glucose of stress secretion of snail increased with increasing snail size.

The result corroborates with the studies done by Admolu .K.O.*et.al*⁸, according to which hemolymph of snail *Archachatina marginata* content of protein 5.4 g/dl

and glucose 35.0 mg/dl. According to Lori. *et. al*⁹ protein concentration in hemolymph of freshwater bivalve *Elliptio complanata* is 73.3 mg/dl. It was observed that the hemolymph of garden snail *Helix Pomotia L* has concentration of protein 4 mg/dl and glucose 14.4 mg/dl by Bislimil. K. *et al*¹⁰. It was also reported by *Journal of Marine biology*¹¹ content of protein in hemolymph of crustaceans *Astacus leptodactylus* and *Carcinus aestuarii* had 3.32±0.25 g/dl and 4.01±0.07 g/dl respectively.

So, from present discussion it concluded present that, stress secretion of *B. bengalensis* had more protein concentration and so it is more protective than hemolymph of *Helix pomotia L* and freshwater bivalve *Elliptio complanata*.

CONCLUSION

Based on the obtained result, it is clear that larger size snail has rich in protein and glucose than smaller size snail and it is beneficial for human being.

ACKNOWLEDGEMENT

Authors are thankful to Head of P. G. Department of Zoology, Ranchi University, for providing all laboratory facilities.

REFERENCES

1. **Annandale.N. (1921):** The bonded pond snail of India (*Vivipara bengalensis*) pt. II systematic. The Edge of a mantle and external ornamentation of the shell. *Rec. Indian Mus.***22**:215-292.
2. **Sewell. R. B. S. (1921):** The banded snail of India, (*Vivipara bengalensis*) pt.1. *Anatomical. Rec. India Mus.*,**22**:529-548.
3. **P. Srivastava, P. Kumar, B. K .Singh and D . K Singh. (2010):** Effect of Piper nigrum and cinnamomum Tamala on biochemical changes in the nervous tissue of freshwater snail *Lymnaea acuminata* *Bioscan*, 1:247-256.
4. **Deojit. Chakraborty, Madhumita. Mukharjee, and Joydev. Maity. (2015):** Estimation of proximate fatty acid composition in ethnomedicinally important viviparous Gastropod, *B.bengalensis* (Lamark, 1822) *International journal of advanced scientific and technical research* .
5. **Simkiss,K. & Wilbur,K.M.(1977).** The molluscan epidermic and its secretion. *Symposium of the Zoological society of London*,**39**: 35-76.
6. **Henry, R.J, Canon, D.C and Winkelman, J.W. (1974).**Clinical Chemistry: Principle and Technique 2nd ed.,*Harper and Row publishers*, New York,Pb 54-56.
7. **Trinder, P.(1969) :** Determination of glucose in blood using glucose oxidase with on alternative oxygen receptor. *Ann Clin.Biochem.***6**:24-27
8. **Ademolu. K. O., Jayeola. O. A., Dedeke. G. A and Idowu, A.B . (2011)** Comparative analysis of the growth performance and hemolymph biochemical properties of normal and land snail –*Archachatina Marginata*. *Ethiopian Journal of Environmental Studies rand Management Vol.4 No.2* 2011.
9. **Lori.L.Gustaison, Michael,K..Stoskopf, William Showers, Thomas.J.Kwak, (2005):** Evaluation of a nonlethal technique for hemolymph collection in *Elliptio Complanata*, a freshwater bivalve (*Mollusca:Unionidae*) .*Diseases of Aquatic Organisms* Vol,**65**:159-165,2005.
10. **Bislimi .k, F .Holili ,I .Elezaj, Q. Selimi &XH.Kamberaj .(2002):** Hepatotoxic and renotoxic effects of ash from K11osova’s Power Plant in hens (*Hisex brown*) Kerkime 10, ASHAK, *Seksioni I shkencave tc Natyres, Prishtine*,f. 131-144.
11. **Journal of Marine Biology ,Volume (2011),**Article ID 153654, 7 : Ecological Relevance of Hemolymph Total Protein Concentration in Seven Crustacean Species.



RUJOST

ISSN : 2319-4227

Instruction to Authors

Scope : The journal aims to publish original peer reviewed/refereed research papers/ reviews on all aspects of pure and applied science and technology.

Categories of Manuscripts : Following categories of manuscripts are accepted for publication.

1. Review articles (not exceeding 5000 words with 6 display items)
2. Research articles (not exceeding 4000 words and 5 display items)
3. Research communication (not exceeding 2000 words and 3 display items)

Submission of Manuscripts : Only original papers are considered for publication. The authors should declare that the manuscript has not been submitted to any another journal for consideration at the same time. Three copies of manuscripts (one original and two photocopies), complete in all aspects including figures and tables, should be submitted to the respective Heads of the Department.

The authors must ensure that the manuscript has been prepared strictly according to the Journal guidelines in all aspects, failing which the manuscripts may not be processed.

Preparation of Manuscripts : The manuscripts should be prepared only in English and should be printed only on A-4 size paper, with double spacing and minimum 2.5 cm margin on all the four sides. First page of manuscripts should be the title page containing full title of the paper, Surname of author(s) and First name(s), Name of the laboratory where the work has been carried out and also the address to which all correspondence concerning the manuscript should be made. E-mail address of the corresponding author should be mentioned in the title page. The title of the manuscript should be brief, specific and amenable to indexing.

A short running title should be given at the end of the title page. The text of the manuscript should run into Abstract, Introduction, Materials and Methods, Results, Discussion, Conclusion, Acknowledgment (if any) and References or other suitable heading in case of reviews and theoretically oriented paper. Short research communications not exceeding 150 words can also be entertained in running format.

Abstract should be followed by keywords which should not exceed six words. The figures should be drawn on MS-Word sheet with the legends provided on the same sheet. Photographs should be black and white or coloured embedded on a MS-Word sheet.

Tables should be typed on separate sheets bearing a short title, preferably in horizontal form. Scanned copies of Table and Photographs will not be entertained.

References should be numbered in superscript serially in the order in which they appear in manuscript. References should not include unpublished source materials. The list of References at the end of the text should be in the following format:

1. Feyissa, T., Welander, M. and Nagesh, L (2005), Plant Cell and Tissue Culture, Vol. 80, pp. 119-127.
2. Rathore, P., Suthar, R. and Purohit, S.D. (2008), Indian Journal of Biotechnology, Vol. 7, pp. 246-249.
3. Crouch, I.J. and Van Staden, J. (1988), African Journal of Botany, Vol. 54, pp. 94-95.

No part of the manuscript should be in Italic except for Latin names of organisms (genus and species), special terms, local names, local terms and names of books and journals in reference section. If abbreviations are absolutely necessary, they should be placed in parentheses after the words/ phrases where they appear first in the text.

Only metric units (SI Units) should be used. Other units may be given in parentheses only if absolutely necessary.

Abbreviations of units are same for the singular and plural. Greek letters and unusual symbols should be identified separately in the margin. Distinction should be made between confusing letters like letter O and zero (0) and between K and kappa (k).

Proofs and Reprints : Page proofs will be sent to the corresponding author. The corrected proofs should be returned to the Editor without delay. Alterations in the proofs, other than those necessitated by the printer's errors, should be kept to the minimum.

A soft copy of corrected manuscript (preferably on CD) in MS-Word/ with PDF should be sent. CD must be labeled with the author's name and address.

Papers should be submitted to the Dean, Faculty of Science, Ranchi University, Ranchi-834001, Jharkhand. India.

RUJOST



I.D. Publishing
print your imagination

Regd. Office : Rai Saheb Nandlal Colony, H. B. Road, Kokar, Ranchi - 834001, Jharkhand
Works : Som Vihar, Near S.R.I. Institute, P.O. RMCH Colony, Bariatu, Ranchi - 834009

Mobile : 94311 82812, 95341 23144 • E-mail : idpublishing2008@gmail.com, ishwar61@gmail.com